Genetic Coordination of Subplate-Dependent Neural Circuit Development

by

Daniel Doyle

A dissertation submitted in partial fulfillment
of the requirements for the degree of
Doctor of Philosophy
(Neuroscience)
in the University of Michigan
2023

Doctoral Committee

Associate Professor Kenneth Y. Kwan, Chair
Professor Anthony Antonellis
Associate Professor Catherine A. Collins, Case Western Reserve University
Assistant Professor Paul M. Jenkins
Associate Professor David L. Turner

Daniel J. Doyle

doyledan@umich.edu

ORCID iD: 0000-0002-8959-5906

Acknowledgements

I have been lucky to be surrounded by people who support me while encouraging me to embrace opportunities that pique my interest. First, thank you to my parents, Jim and Michelle, my sister, Emily, and my brother, Ben, who will be writing one of these himself in a few years. Through my time in college and graduate school I've been privileged to have some of the best friends you could ask for. Steven, Emily, Veena, Drew, and Jenna thank you for everything over the past 8+ years. To the friends I have made in graduate school, Dalia, Ahmed, Lauren, Fred, Marie, Lorraine, Lexi, Millie, Ben, Jenn, Shannon, among others, thank you for always finding ways to get together and have fun, whether that was tailgates, Costco premade family meals for celebrations, etc. Many moved on to the next stage of your lives; I can't wait to see where you wind up.

To my committee, Dr. Tony Antonellis, Dr. Cathy Collins, Dr. Dave Turner, and Dr. Paul Jenkins, thank you for your guidance and patience. While I was not the most frequent scheduler of committee meetings, I am grateful for your feedback, positivity, insights, and support.

I want to thank the Kwan lab. I came in not fully knowing much of what graduate school would require. I never could have imagined how important each lab member was going to be not only in my scientific growth but my personal growth as well. The lab environment is nearly impossible to match, constantly encouraging us enjoy our time in lab and with the lab; new snacks, laser tag, escape rooms, etc. Each day is a pleasure

and I can’t imagine better colleagues and friends, past or present. Jason Keil and Owen Funk, thank you for your friendship. As a young grad student you were the perfect pair to learn from. Adel and Yaman Qalieh, thank you for spending endless hours explaining and helping with essentially every computational analysis. To the newer members of the lab, Rama, Ikenna, Karina, and Viktoria, you all have been great to work with and I’m happy to have had the opportunity before I leave, and Maddie thank you for reading earlier drafts of these chapters and giving feedback.

To Mandy Lam, thank you for everything. Of course, for all the experimental guidance, but for your friendship even more. You and Ken have always made me feel welcome, whether it has been inviting me to dinner when I don’t go home for holidays or just having coffee during work and talking about anything. I am extremely grateful for everything both inside and outside the lab the past 7 years.

To my mentor, Ken Kwan, who has always supported me despite having never responded to the first email I sent inviting him to speak while I was an undergraduate. Thank you for believing and investing in me, pushing me to be my best, and giving me the freedom and opportunities needed to grow as a scientist. I could not have asked for a better person to learn from. You made lab about more than just work, created a nurturing environment where everyone is heard, and gave me both a scientific and personal role model.

And finally, my dog, Maizie, simultaneously a menace and joy, you have made my life endlessly more enjoyable.

Table of Contents

List of Figures

List of Tables

List of Abbreviations

AC	Anterior commissure
aRG	Apical radial glia
ASD	Autism spectrum disorder
BAF	BRG1/BRM associated factor
bRG	Basal radial glia
CC	Corpus callosum
cKO	Conditional knockout
cKO-E	Conditional knockout via *Emx1*^{Cre}
cKO-N	Conditional knockout via *Neurod6* ^{Cre}
cKO-hG	Conditional knockout via Tg(*hGFAP-Cre)*
CP	Cortical plate
CSPG	Chondroitin sulfate proteoglycan
ECM	Extracellular matrix
E*n*	Embryonic day *n*
IPC	Intermediate progenitor cell
IUE	In utero electroporation
IZ	Intermediate zone
L*n*	Cortical layer *n*
NPC	Neural progenitor cell
P*n*	Postnatal day *n*
RG	Radial glia
RNA-seq	RNA-sequencing
SP	Subplate
SPN	Subplate neuron
SVZ	Subventricular zone
TCA	Thalamocortical axon
tRG	Truncated radial glia
UMI	Unique molecular identifier
VZ	Ventricular zone
WM	White matter

Abstract

The mammalian neocortex supports conscious functions through development of carefully coordinated connectivities. Ultimately, proper circuit wiring requires harmonious interplay between cell autonomous and non-cell autonomous events. Disruption of these processes during corticogenesis can cause alterations in brain circuits. Recently, dysfunction of chromatin remodelers has been increasingly associated with neurodevelopmental disorders, often presenting with connectivity changes. Chromatin remodelers mediate processes that occur on DNA, such as DNA replication, transcription, and DNA repair, and each of these facets has the capacity to impact circuit development. Mutations in *ARID1A*, a critical subunit of the BAF chromatin remodeling complex, are associated with the neurodevelopmental disorder Coffin-Siris syndrome. However, how *Arid1a* orchestrates brain development has not been established.

Here, I leveraged a complement of mouse genetic tools to assess spatiotemporal and cell type-specific requirements for ubiquitously expressed *Arid1a* during cortical development. I uncovered surprising cell autonomous and non-cell autonomous *Arid1a* functions to direct cortical circuit formation. Conditional deletion of *Arid1a* from cortical neural progenitors led to widespread misrouting of callosal and thalamocortical connectivities. Surprisingly, disruption of both tracts was due to non-cell autonomous *Arid1a* functions. Putative callosal axons were wrongly directed radially toward the pia,

whereas thalamocortical projections entered the cortex via an aberrant trajectory, failed to pause within the subplate, and did not organize into stereotypical whisker barrels. Using conditional deletion of *Arid1a* from newly postmitotic neurons, I narrowed the potential critical window for *Arid1a*'s circuit wiring influence to encompass progenitors and neurons shortly after their genesis; postmitotic deletion failed to alter brain wiring. Thus, *Arid1a* non-cell autonomously directs the developmental establishment of major cortical circuits.

Arid1a's control over development of cortical connectivity was centered on a surprising cell type-specific role. Underlining its role in transcriptomic regulation, *Arid1a* was necessary to establish neuronal gene expression, largely that of subplate neurons. Subplate neuron gene expression changes were concomitant with pronounced disruption of their organization, morphologies, projections, and extracellular matrix, major proposed contributors to subplate-dependent circuit wiring. To define requirements for subplate *Arid1a*, I introduced a novel approach to assess gene necessity and sufficiency in subplate neurons during corticogenesis. Remarkably, sparing subplate neurons from *Arid1a* deletion was sufficient to enable proper formation of both callosal and thalamocortical connectivity. Therefore, *Arid1a* coordinates developmental brain wiring via cell autonomous and non-cell autonomous influences centered on subplate neurons.

Together, this work identified a multifaceted regulator of subplate neuron-dependent cortical development. Subplate neurons are the firstborn cortical neurons, situated at the interface of cortical grey and white matter and ideally positioned to direct nascent circuitry. I provide empirical support for their relationship with thalamocortical

axon targeting and, despite previous contradicting reports, add strong evidence for their involvement during callosal formation. These findings raise important questions and possibilities for cell type-specific roles of ubiquitous chromatin remodelers, subplate orchestration of corpus callosum development, and consequences of subplate dysfunction in developmental brain disorders.

Chapter 1: Neocortical Origination, Organization, and Optimization

Thesis Overview

The neocortex is the crux of mammalian evolution and exceptional conscious capabilities. Its dysfunction contributes broadly to developmental disorders, including autism spectrum disorder (ASD), intellectual disability, and schizophrenia. While decades of work have focused on mechanisms governing brain development, innumerable intricacies of how the brain is built remain unknown. This thesis aims to understand how *Arid1a*, a DNA-binding subunit of the BAF (BRG1/BRM associated factor) chromatin remodeling complex, orchestrates neuronal function and connectivity in the developing neocortex. In Chapter 1, I focus on our current understanding of emergence of the neocortex, its constituents and connectivities, and molecular mechanisms underpinning these functions. In Chapter 2, I report *Arid1a*'s unique non-cell autonomous contributions during cortical development to direct cortical efferent and afferent circuitry, including major interhemispheric connectivity. In Chapter 3, I describe *Arid1a*'s cell autonomous impact in subplate neuron (SPN) identity, morphology, projections, and extracellular matrix (ECM), factors likely governing non-cell autonomous influences, and subplate (SP) *Arid1a*'s surprising sufficiency in coordinating cortical connectivity. In Chapter 4 this thesis culminates with how my findings factor into our understanding of brain wiring how SPNs orchestrate circuitry, and future studies to uncover connectivity influences of distinct SP features.

Evolutionary emergence of the neocortex

The cerebral cortex underlies mammalian species' conscious thoughts, actions, and perceptions. Although many non-mammalian organisms have brain regions with relative homology to the neocortex, its initial appearance coincides with the divergence of mammals from other chordates: reptiles, amphibians, birds, and fish (1). The neocortex has not remained stagnant since its inception. Instead, stark differences are apparent across mammalian species. While the laminar structure is largely consistent, the primate neocortex, especially in modern-day humans, displays a remarkable increase in not only in general size, but also in complexity and connectivity (2). The complexities of the neocortex leave it extraordinarily susceptible to genomic disruptions that can alter structure, function, and overall brain connectivity. Numerous human developmental disorders including ASD, intellectual disability, and schizophrenia have distinct neocortical phenotypes both in organization and circuitry (3). How distinct genetic mechanisms contribute to developmental disorders remains an active field of research and necessitates consideration of both conserved and human-specific contributions to brain development.

Development and structure of the forebrain

During fetal development, the three primitive germ layers; endoderm, ectoderm, and mesoderm; differentiate to form distinct organs and tissues. Endoderm and mesoderm derivatives include liver and skeletal muscle, respectively, whereas ectoderm generates the central nervous system and neural crest. Early in embryogenesis, the ectoderm-derived neural plate folds, and completion of primary neurulation results in the formation of three primary vesicles; the prosencephalon,

mesencephalon, and rhombencephalon; ultimately becoming forebrain, midbrain, and hindbrain, respectively. The forebrain is further subdivided into two structures that are fused together: telencephalon (cerebral hemispheres and basal ganglia) and diencephalon (thalamus and hypothalamus, as well as some other smaller structures). Each region has distinct neuronal cell types, connectivities, and influences on organismal function.

The cerebral cortex is the outermost portion, the “bark” of the brain. Contained within it is a whole host of neuronal, glial, ependymal, and endothelial cells. They are organized such that, in the mammalian allocortex (archicortex and paleocortex) and neocortex (isocortex), there are up to six unique layers, containing cell bodies (grey matter) sitting directly above efferent and afferent projections (white matter [WM]). The neurons, primarily GABAergic and glutamatergic, transmit signals via electrical activity and release of neurotransmitters for communication both within and outside the brain. The resulting cortical signalling underlies our species’ remarkable conscious capabilities.

Ventromedial to the cerebral cortex sit the basal ganglia, the striatum (caudate putamen in rodents and caudate nucleus and putamen in higher mammals), globus pallidus, substantia nigra, subthalamic nucleus, nucleus accumbens, and ventral pallidum. Together, they contain a neuronal repertoire with vast neurotransmitter capabilities (e.g. GABAergic, glutamatergic, dopaminergic, and cholinergic) that receive input from a variety of brain regions and primarily project within the basal ganglia and to the thalamus (4). These connections mediate processes such as emotion and fine

motor movements, and their dysfunction is associated with degenerative disorders including Parkinson's disease (5).

In contrast to telencephalic structures, the diencephalon largely acts as a hub to pause, refine, and transmit information to its necessary destination. The largest mediator of these functions is the thalamus. The thalamus is a collection of neighboring nuclei across the mediolateral and rostrocaudal axes of the brain, containing mainly GABAergic and glutamatergic neurons (6). These neurons are essential to transmit sensory information to the cerebral cortex where it can be processed. Disruption of thalamic projections may contribute to hypersensitivity in many neurodevelopmental disorders such as ASD (7, 8). Together, the coordinated formation of telencephalic and diencephalic structures from the forebrain is integral for conscious and unconscious actions, emotions, and overall function, the precision and depth of which vary coincident with evolutionary alterations across mammals, reptiles, invertebrates, etc.

Neocortical divergence of mammals

Reptiles and mammals reside together within the amniote clade but are exceptionally distinct from each other in their visual appearances, movements, and importantly, underlying brains. The initial divergence of *Sauropsida* (sauropsids, including reptiles) and *Synapsida* (synapsids, including mammals) occurred during the late Carboniferous and early Permian period; the last common ancestor between the groups was 310-320 million years ago (9-11). Interestingly, this split in the phylogenetic tree was based in part on skull structure and other skeletal features (12, 13). Over the past 310 million years or so, sauropsids have further differentiated into anapsids (extinct, but controversially may include turtles) and diapsids (reptiles and birds) (14).

Synapsids encompass prototherian (monotreme, e.g. platypus), metatherian (marsupial, e.g. koalas), and eutherian (placental, e.g. rodents and primates) mammals (13). Although these organisms have brains of similar relative size based on body mass (15), accompanying millions of years of evolution are robust changes in brain architecture, intermingled with conservation (16).

In both turtles and lizards, the telencephalon contains, among others, medial cortex, dorsomedial cortex, dorsal cortex, lateral cortex, and dorsal ventricular ridge. (**Figure 1.1**). The mammalian telencephalon has many similarities with these structures. For example, medial cortex is similar to mammalian hippocampus and lateral cortex to piriform cortex. However, it also contains a novel structure. The aptly named neocortex (meaning new cortex) is comparable in its location to the reptilian dorsal cortex (16). Although it is thought to contain some evolutionarily conserved cell types, the neocortex is defined by myriad unique features.

The reptilian dorsal cortex is laminated, but only includes three layers compared to the six-layered mammalian neocortex. Single-cell transcriptomics support the notion that the vast repertoire of excitatory, glutamatergic neurons within the mammalian neocortex are grossly unique from those found in reptiles (17). Interestingly, and in stark contrast, although there is tremendous diversity in mammalian GABAergic cortical neurons, many of these subtypes are conserved within dorsal cortex of reptiles based on comparison of single-cell RNA-sequencing (RNA-seq) (17). Recent work uncovered that, while some ventral brain structures and cell types are even further conserved with non-amniotes including amphibians (e.g. salamander, *Pleurodeles waltl*), molecularly the dorsal forebrain is relatively unique (18). Crucially, two of the evolutionarily

emergent layers of neocortical cells contain SP and Cajal-Retzius neurons. While some molecular markers of these neurons are present in dorsal regions of non-mammals, their ultimate arrangement is lacking (19, 20). SP and Cajal-Retzius neurons are among the first neurons born in the fetal neocortex (21), and their appearance and constructive organization likely govern orchestration of neocortical development. Together, the mammalian neocortex depends on an evolutionarily unique set of excitatory neuron subtypes to complement conserved inhibitory neurons. These new neuronal subtypes may support the appearance of mammals, but what molecular programs define excitatory neurons in the mammalian neocortex and enable exceptional cognitive abilities?

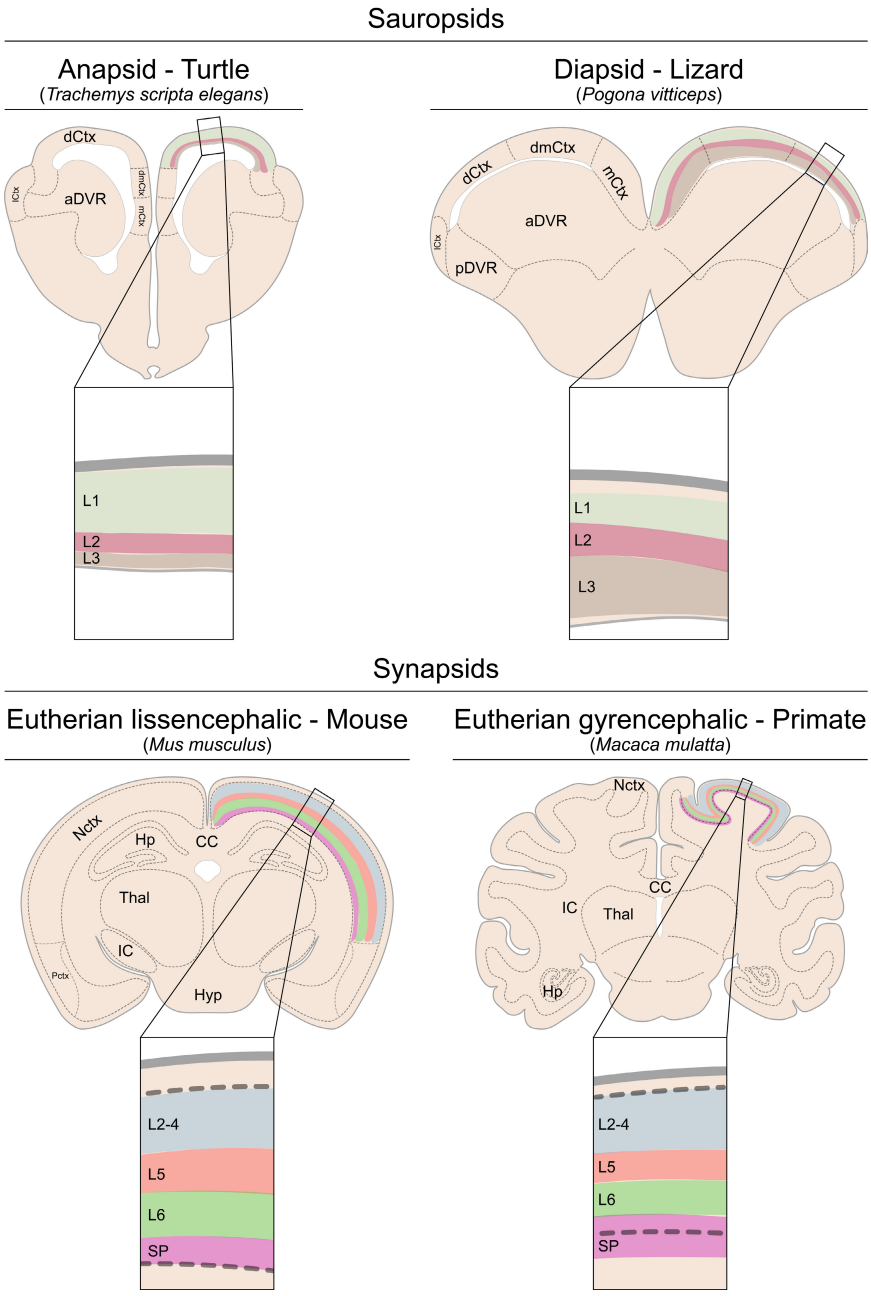

Figure 1.1 Species-specific structure of the dorsal forebrain

Schematic illustrations (not to scale) of Sauropsid and Synapsid forebrain. The reptilian dorsal forebrain contains three distinct, horizontal layers The mammalian neocortex is conserved across lissencephalic and gyrencephalic mammalian species, with six cortical layers and glutamatergic neuron types not found in sauropsids.

aDVR: anterior dorsal ventricular ridge, CC: corpus callosum, dCtx: dorsal cortex, dmCtx: dorsomedial cortex, Hp: hippocampus, Hyp: hypothalamus, IC: internal capsule, lCtx: lateral cortex, mCtx: medial cortex, Nctx: neocortex, Pctx: piriform cortex, pDVR: posterior dorsal ventricular ridge, Thal: thalamus

From mice to men

The mammalian neocortex contains six cytoarchitectonically distinct horizontal layers of neurons with unique identities, projections, and functions. Although this organization is relatively consistent across mammalian species, there is incredible diversity in neocortical cell types and overall structure and connectivity. Mice have a smooth, lissencephalic brain while primates have an extensively folded, gyrencephalic brain with increased area for cells. This folding is due in part to *ARGHAP11B*, which emerges evolutionarily in primates and is absent from rodents. *ARGHAP11B* expression in mice is sufficient to initiate cortical folding (22). In addition to cortical folding, novel connectivity and neuronal subtypes (similar to reptiles versus mammals) may explain, at least in part, the remarkable extent to which the human brain has evolved.

One factor that can contribute to human-specific features is termed “human accelerated regions.” Human accelerated regions are genomic loci largely conserved throughout mammals but with distinct sequence changes in humans (23). These alterations are thought to contribute to human-specific functions. One example of this is *PPP1R17*. Human accelerated regions are proposed to contribute to a human-specific pattern of *PPP1R17*, which coordinates cell cycle length and ultimately regulates neural progenitor cell (NPC) divisions (24). Once progenitors divide, they produce neuronal progeny. Genomic modifications could contribute to human-specific neuronal identities.

Rodents have increased glutamatergic neuron subtypes compared to reptiles, with a relative conservation in GABAergic subtypes (17). Interestingly, GABAergic neurons do appear to ultimately diverge within mammals. The human neocortex is characterized by tyrosine hydroxylase (TH)-positive GABAergic neurons that are born

subcortically and migrate tangentially (25). However, these neurons are not found in neocortex of rhesus macaque (*Macaca mulatta*) or chimpanzee (*Pan troglodytes*), and likely not in rodents (25). Why are these GABAergic neurons specific to humans? Sousa et al. suggest two interesting possibilities in their manuscript (25): 1) “these cells could have been lost due to genetic disruptions affecting interneuron migration, differentiation, or survival” and 2) “A second possibility is that these interneurons are present in the non-human African ape cortex but do not express TH, do so only transiently, or die prior to our ability to detect them." Evolutionary changes don’t only occur at the transcriptomic level. Posttranscriptional mechanisms can contribute to human-specific cortical neuron features (26). Ultimately, emergent neuronal subtypes may support increased control of conscious and unconscious features underlying human function.

From the genome to neuronal identities to brain regions, evolutionary differences become more grossly evident. One prime example of regional expansion is the prefrontal cortex, specifically L4, in humans and other primates versus rodents (27, 28). The prefrontal cortex is associated with cognitive functions and its dysfunction is implicated in developmental disorders including ASD and schizophrenia (29). However, the molecular mechanisms contributing to its relative growth have only recently begun to be unraveled. Interestingly, across primate species but not rodents, retinoic acid and its signalling partners are abundant in mid-fetal prefrontal cortex (30). This signalling is associated with enrichment of *CBLN2* and ultimately an increased synaptic connectivity (31). To control these species-distinct patterns, *Cbln2* expression in mouse is restricted by *Sox5*-mediated repression, but the putative SOX5 binding sites in regulatory regions near *CBLN2* are eliminated in primate (31). Activation of *CBLN2* by retinoic acid

signalling and elimination of repressive regulatory elements can support increased area synaptogenesis of the prefrontal cortex (30, 31), potentially underlying cognitive functions that have arisen in primates and particularly humans. Together, the genomic alterations along with the emergence of cell types, expanded brain regions, and increased connectivity can explain, at least in part, the evolutionary divergence of rodents and primates, specifically humans.

Sequential cortical neurogenesis

The mammalian neocortex is defined by six horizontal layers of neurons, conveniently named L1-6. Of these layers, L2-6 includes a mix of excitatory and inhibitory neurons whereas L1 contains exclusively inhibitory neurons (21). Glutamatergic excitatory neurons encompass a variety of morphological and molecular subtypes that are identifiable in part based on their laminar position. Despite the diversity of their neuronal identities, cortical excitatory neurons are derived from the same pool of NPCs. Conflicting studies have suggested and refuted that, perhaps, in mouse, there may be subgroups within the NPC pool that are lineage-restricted, such that they are only capable of generating certain subtypes of excitatory neurons (32-35). Regardless of the existence of fate-restricted NPCs, it is well-established using clonal analyses that some NPCs produce excitatory neurons spanning L2-6 (36). The production of these neurons occurs in a sequential, inside-out manner (**Figure 1.2**). Disrupting the sequential generation of cortical neurons can contribute to changes in brain circuitry and ultimately function. Thus, the mechanisms regulating NPC neurogenic progression from L6 to L2 have been, and remain, subjects of tremendous interest.

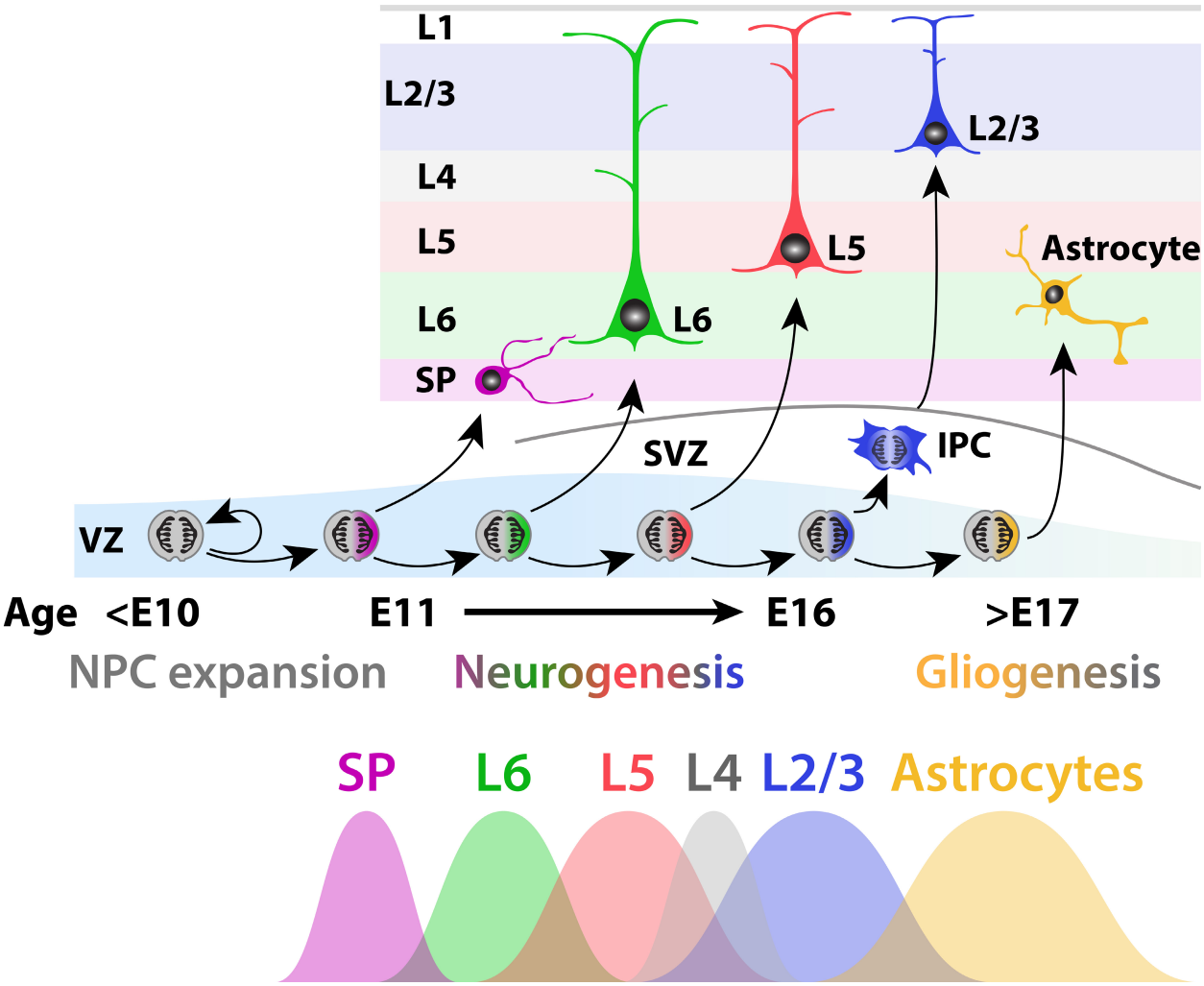

Figure 1.2: Neocortical sequential corticogenesis

Cortical neural progenitors divide symmetrically to expand the pool and enable production of numerous progeny. Starting around E11 in mouse, NPCs divide via asymmetric, neurogenic divisions to generate neurons of the neocortex. Cortical excitatory neurons are produced in a sequential, inside-out fashion such that subplate neurons are born first followed by L6, L5, L4, and L2/3. Progenitors then proceed to gliogenesis around E17, generating astrocytes and other glial cell types which populate the neocortex.

IPC: intermediate progenitor cell, NPC: neural progenitor cell, SVZ: subventricular zone, VZ: ventricular zone

Neurogenic competency and progeny

During nervous system development, multipotent neuroepithelial cells originate from the ectoderm and sit near the ventricular system while contacting both the pial and ventricular surfaces of the developing neocortex. Prior to the genesis of cortical neurons, neuroepithelial cells undergo a state transition by altering their gene expression profiles and reorganizing tight junctions to produce a progenitor type called radial glia (RG) (37-39). RG generate the long-term tenants of the cortex. Their basal process, reaching toward the pia, provides a scaffold by which developing neurons are guided to their ultimate destinations (**Figure 1.3**) (40). The apical process, directed toward the lateral ventricle, receives signalling cues from circulating cerebrospinal fluid, especially via primary cilia extended into the ventricles (41, 42). Precise morphological features of RG are necessary to coordinate cortical organization and function.

RG ultimately produce the entire complement of cortical excitatory neurons, either directly or indirectly, and therefore must be actively cycling throughout corticogenesis. During the RG cell cycle, the nucleus undergoes robust, kinesin-dependent localization changes in a process termed interkinetic nuclear migration (**Figure 1.3 B**) (43-46). As RG progress through G1 phase, the nucleus moves into the upper VZ to go through S-phase and double their DNA. Following replication and during G2 phase, the nucleus descends toward the ventricular surface where RG undergo mitosis and cytokinesis to produce two daughter cells (47). The importance of this process is illustrated by its dysfunction. Disruption of *PAFAH1B1* (*LIS1*), and thus interkinetic nuclear migration (48), is associated with lissencephaly in humans (49). Following S phase and DNA replication, the RG and future daughter cells rely on the

mitotic spindle, spindle assembly checkpoint, and cleavage furrow to appropriately segregate sister chromatids and divide into two daughter cells without producing widespread aneuploidy or exponentially deleterious structural variants. Failure of these processes can lead to widespread apoptosis of RG, clearance of debris by microglia, and the inability to produce additional neurons or glia (50-52).

RG divide both symmetrically, to exponentially expand the progenitor pool, and asymmetrically to generate the necessary neuronal and glial progeny. Expansive self-renewal produces two daughter RG from a single mother RG. This occurs reliant on coordination of RG cell surface proteins and circulating proteins within cerebrospinal fluid. In developing RG, division is influenced by interplay between *Pten* and *Pals1* to display IGF1R on primary cilia at the ventricular surface and enable subsequent binding of IGF2 circulating through cerebrospinal fluid (53). Loss of either *Igf1r* or *Igf2* leads to a reduction in mitotic RG and ultimately microcephaly (53), highlighting the importance of both intrinsic (*Igf1r*) and extrinsic (*Igf2*) coordination to support RG division.

RG transition from symmetric, expansive to asymmetric, neurogenic divisions in a stereotyped manner described by the transverse neurogenetic gradient. This process begins at the rostrolateral and ends in the caudomedial portions of the cortex (54-56). Starting around embryonic day (E) 11 in mouse, the first cortical neurons are generated and migrate to the pial surface to construct the preplate, a transient structure comprised of future subplate and marginal zone/L1 neurons (57). Subsequently, cortical plate (CP) neurons are generated until about E17 in a sequential, inside-out manner, L6 → L5 → L4 → L3 → L2 (**Figure 1.2**) (58, 59). They migrate through the intermediate zone (IZ), split the preplate, and create the CP. Preplate splitting separates the neurons into

marginal zone, abutted to the pial surface, and SP zone, sitting right below L6 and at the interface of cortical grey and white matter. Frequently, RG will give rise to about 8-9 neurons throughout their lifetime, and about 12% of neurogenic RG will eventually produce glia (36). The neurons from a single RG are spread throughout the cortical lamination in a column-like structure. These columns are comparable spatially and genetically and form the basis of the radial unit hypothesis that proposes the neocortex is composed of many repeating cortical columns generated from distinct RG (60, 61).

The transition in RG division mode is highly correlated with alterations in cell cycle dynamics. In comparison to symmetrically dividing RG, neurogenically dividing RG undergo lengthened G1 and M phases, but a decrease in S phase (62, 63). Altering the length of cell cycle phases is sufficient to convert RG to self-renewing or neurogenic states (64, 65). Once RG reach M phase they are partitioned into two daughter cells. The cleavage plane orientation during this process has been linked to division mode in invertebrates (66-68). While some studies associated mammalian RG plane of division with division mode (69-71), mitotic spindle orientation during cleavage is insufficient to differentiate between symmetric proliferative and symmetric neurogenic divisions (69). The transition of RG division mode from symmetric to asymmetric also coincides with ingrowth of cerebral vasculature and altered metabolic state (72-75). Together, various molecular processes contribute to the method by which RG divide.

NPCs in the neocortex, however, are not all equal. In fact, there are multiple spatiotemporally unique subtypes. Apical radial glia (aRG) are housed within the cortical ventricular zone (VZ) and extend a radial, basal process up to the pial surface, thereby creating a consistent scaffold along the cortical wall. During deep-layer (L6/5)

neurogenesis aRG begin producing an alternative progenitor type known as an intermediate progenitor cell (IPC) (21, 76). IPCs are largely housed superficially to the VZ, within the subventricular zone (SVZ), and are clearly delineated from aRG by morphological and molecular identities. While aRG are often bipolar and express high levels of *Sox2*, but not *Eomes* (*Tbr2*), IPCs express *Eomes* and present a variety of morphologies, primarily spherical, short multipolar, and horizontal, but occasionally bipolar (77). Importantly, IPCs primarily undergo symmetric, neurogenic divisions and are thus significant producers of neurons during later neurogenesis. Their disruption is associated with neurodevelopmental disorders and reduced neuronal quantity (78, 79).

Fine-tuning of neuronal generation is based on diverse NPCs. In addition to aRG and IPCs, neurons are generated from basal radial glia (bRG, also known as outer radial glia) and truncated radial glia (tRG) (**Figure 1.3 A**). bRG are housed within the SVZ and extend a process to the pial surface, but in contrast to aRG, they do not send a process to the ventricular surface to receive signalling from circulated cerebrospinal fluid (80, 81). While bRG are substantial contributors in primates, they are present only at low levels in lissencephalic rodents (82). Alternatively, tRG have only been described in gyrencephalic mammals, including humans (*Homo sapiens*) and ferrets (*Mustela putorius furo*) (83-85). They are found in the VZ with a connection to the ventricular surface, but in contrast to aRG and bRG, their basal process does not extend beyond the SVZ. Often, the basal process of tRG terminates on or near developing vasculature (81) and cannot contribute extensively to the RG scaffold utilized by postmitotic neurons after early migration (84, 86). Together, bRG and tRG are thought to contribute to upper-layer neuron expansion in primates compared to their rodent counterparts.

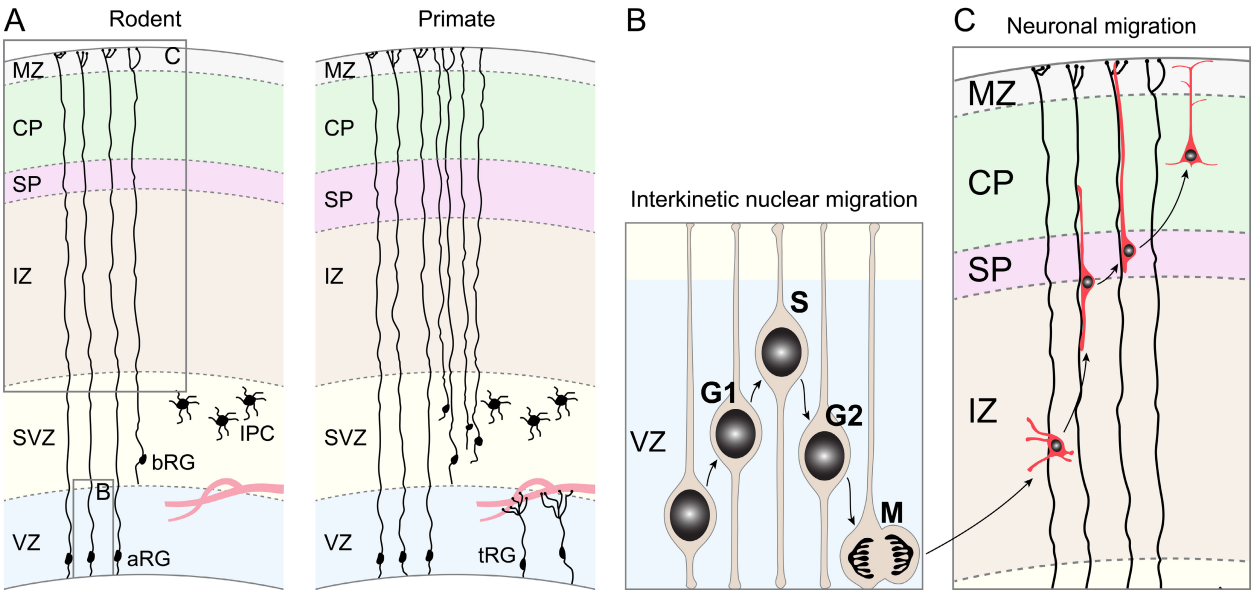

Figure 1.3: Diverse neural progenitors and neuronal migration

(A) The developing neocortex contains a variety of progenitor subtypes. In rodents, these include aRG and IPCs, with modest contributions from bRG. In contrast primate neocortex features a substantial increase in bRG and the appearance of tRG. Based on features in (81).

(B) During aRG cell cycle, the nucleus is positioned in predefined areas based on its phase of the cell cycle, known as interkinetic nuclear migration. Beginning near the ventricular surface, the nucleus ascends to the outer portion of the VZ for S phase and travels back to the ventricular surface to go through M phase and divide. Adapted from (87).

(C) Following its genesis, a neuron exhibits multiple migration states. Initially, cortical excitatory neurons migrate in a multipolar manner, but upon reaching the SP they transition to a bipolar phase. This bipolar phase can include locomotion and somal translocation, and following migration the new excitatory neurons populate CP.

aRG: apical radial glia, bRG: basal radial glia, CP: cortical plate, IPC: intermediate progenitor cell, IZ: intermediate zone, MZ: marginal zone, SP: subplate, SVZ: subventricular zone, tRG: truncated radial glia, VZ: ventricular zone

Regulation of neurogenesis resulting from NPC divisions depends on intrinsic and extrinsic signalling mechanisms to produce the proper neuronal subtypes at the correct time. However, it remains unclear what combination of cell and non-cell autonomous mechanisms orchestrate the temporal and sequential generation of neuronal and glial cell types from NPCs. Early NPCs largely produce deep-layer (L5-6), whereas later NPCs generate upper-layer neurons (L2-4). Pioneering work revealed that subtype-specific production of neurons is not solely based on intrinsic NPC properties, but rather in tandem with the environment (88). Interestingly, even once NPCs have transitioned to neurogenic divisions, they do not always retain their capacity to generate both deep- and upper-layer neurons. Transplantation of early NPCs into a late corticogenic environment shifts output to upper-layer neurons (88, 89). In agreement, late NPCs can produce deep-layer neurons when transplanted into an early environment (89). However, this capacity may be restricted to aRG, as broad pools of late NPCs (88) or specific analysis of IPCs (89) maintain restriction to upper-layer neuron production independent of environment. Interestingly, both the transition from proliferative to neurogenic divisions (90) and the aRG capacity to generate diverse neuronal subtypes (89) are dependent on the Wnt/β-catenin signalling pathway and likely restricted by the cell cycle stage of RG when cues are introduced (91). Altogether, the ability of NPCs to generate widespread neuronal subtypes is progressively restricted, both by intrinsic and extrinsic mechanisms in the developing cortex.

Autonomously, it's thought the epigenomic landscape directs sequential output of deep-layer neurons → upper-layer neurons → glia. In support of this, a variety of epigenetic factors influence neurogenic production in the developing neocortex. In part,

this can be based on deposition and removal of histone modifications. Trimethylation of lysine 27 on histone H3 (H3K27me3) is a repressive mark, disruption of which leads to de-repression (92, 93). In the developing brain, deletion of the histone modifiers *Ezh2* or *Eed*, which are essential for PRC2's (polycomb repressive complex 2's) catalysis and deposition of H3K27me3, alters cortical production of both neurons and astrocytes (94-97) and mutations in *EED* are associated with intellectual disability and Cohen-Gibson syndrome (98). However, some findings suggest that PRC2 may impact cortical neurogenesis at a population level rather than exclusively cell autonomously (97). Alternatively, H3K4me3, a mark of active chromatin, can be deposited by various lysine methyltransferases including KMT2A and KMT2D (MLL1and MLL2) (99). Mutations in *KMT2A* and *KMT2D*, are associated with intellectual disability and developmental disorders including Wiedemann-Steiner syndrome (100) and Kabuki syndrome (101). Interestingly, synergy between H3K27me3 and H3K4me3 is integral for fine-tuning gene expression. Genomic loci coated with both marks are termed bivalent, quite common in stem cells, and resolved over time to activate or repress gene expression (102). The inability to resolve bivalent loci is coincident with unrefined neuronal fates (103). However, the coordination between, and precise necessity of, epigenetic regulation in NPCs and newly born postmitotic neurons to orchestrate sequential corticogenesis remains unclear.

Following generation of cortical excitatory neurons, progenitors transition to gliogenesis, during which they produce various glial cell types and precursors (86). Together, glial cell types support proper neuronal functioning via involvement in synapses, neurotransmitter recycling, and myelination to support action potential

propagation. Together, coordination of RG, IPCs, astrocyte precursors, and oligodendrocyte precursors via intrinsic and extrinsic mechanisms are indispensable for formation of an organized and functional brain.

Neuronal migration

Cortical excitatory neurons are generated by RG and IPCs. Following their birth, these neurons travel radially toward the pial surface to reach their individual destinations underlying cortical function (**Figure 1.3 C**) (21, 40, 60, 104). To traverse the cortical wall and reach the CP, excitatory neurons utilize three distinct modes of movement, multipolar migration, locomotion, and somal translocation, and two major morphological presentations, multipolar and bipolar (76, 105). Shortly after their genesis, neurons are largely situated within the SVZ and IZ. They exhibit multipolar migration and morphology, extend and retract numerous processes that are not closely apposed to RG fibers, and do not necessarily travel in a radial trajectory (76). Upon close proximity with the SP zone, multipolar migrating neurons transition to a bipolar morphology, mediated in part by DCX and FLNA (106-108). This morphological change coincides with an adjustment to locomotion- or somal translocation-based migration. During locomotion, neurons travel up RG fibers and move at incredibly diverse rates; they pause, speed up, and slow down (76). However, in somal translocation, the migrating neuron extends a leading process up to the pial surface and the soma moves ascends at a relatively consistent rate until it has reached its destination (76). Interestingly, it's unclear whether neurons migrating via somal translocation require a state change to locomotion, but neurons beginning with locomotion often switch to somal translocation as they are completing migration (109). Proper migration requires

centrosomal microtubule nucleation and reorganization. In postmitotic neurons, this process couples the nucleus to the soma during somal translocation. Disruption can ultimately impair neuronal migration and thus cortical organization (110, 111). Regulation of neuronal morphology and migratory mode are highly coordinated events which underlie the precise organization of the neocortex.

The cortex also includes a variety of GABAergic interneurons to modulate neuronal activity and circuit function. In contrast to locally generated cortical excitatory neurons, cortical interneurons (CINs) are generated in the subpallium, largely the caudal and medial ganglionic eminences (CGE and MGE, respectively) (112). Being born outside the cortex, CINs travel tangentially to populate the cortex (113, 114). Once CINs are born, they move through the subpallium, cross the pallial-subpallial boundary (PSB), and travel either in the marginal zone and SP zone or through the lower IZ and upper SVZ before pausing and later populating the CP via radial migration (115, 116). This pause, while somewhat shorter, is similar to both thalamocortical axons' (TCAs') "waiting period" in the SP zone and delayed CP invasion by microglia (117-119). Interestingly, although CINs are largely produced in subcortical regions, some evidence suggests cortical RG may also have competency to generate CINs locally (120-122), thus migration strategies may differ.

Neuronal migration is controlled by non-cell autonomous and cell autonomous mechanisms, and disruption of these processes can contribute to altered cortical organization and circuitry associated with neurodevelopmental disorders. Human mutations in *RELN*, an ECM protein secreted by Cajal-Retzius cells, are associated with lissencephaly and epilepsy (123, 124), and disruption of *Reln* non-cell autonomously

alters migration of CP neurons; preplate does not split and CP is inverted (125-128). On the other hand, deletion of *Satb2* delays migration of L2-4 neurons, likely cell autonomously, and impairs their initial axonal projections (129, 130). Mutations in *SATB2*, which regulates transcription and chromatin structure, are associated with Glass syndrome, a developmental disorder with intellectual disability and myriad physical features (131, 132). In contrast to control of cortical excitatory neurons' radial migration, CINs' tangential migration can be influenced as they traverse various brain regions. *NRG1* is a chemoattractive cue expressed in both the striatum and neocortex, mutations in which are associated with schizophrenia (133-135). Developmental deletion of *Nrg1* leads to a reduction of CINs that migrated into the cortex (136). Intrinsically, CINs are directed by transcription factor *Mafb*. It is necessary for proper Martinotti cell migratory route and axonal projections, and mutations in *MAFB* are associated with intellectual disability (137, 138). Together, the extensively regulated radial and tangential migration strategies employed by cortical excitatory and inhibitory neurons support the extravagant organization underlying cortical function.

Regulation and refinement of cortical neuron identity

Cortical neurons display various identities based on location, gene expression, and projections (**Figure 1.4**). Some of this gene expression is realized immediately after a neuron is generated from an NPC. However, cortical neurons are not born in their final fate. They must form connections, adjust them, and slowly adapt over time. Accordingly, neuronal molecular identities are not fully recognized immediately post-mitosis. Rather, they are refined throughout the first few days after neuronal birth. Ultimately, the early

and refined fates of cortical neurons can influence the organization of cortical layers and connections underlying function.

Layer-specific gene expression profiles

Similar neuronal subtypes are generally found in comparable laminar positions within the neocortex. These neurons, produced by NPCs at similar time points, retain somewhat comparable gene expression profiles and connectivities. Deep-layer neurons are easily distinguishable from upper-layer neurons, and laminar subtype distinctions have been unraveled over the last twenty-five years. The importance of these molecular markers, and ultimately the diverse identities of cortical neurons, is highlighted by the implication of many in neurodevelopmental disorders.

SPNs are among the firstborn excitatory neurons of the cortex, generated beginning around E11.5 in mice (21). Although they are distinct physically and morphologically from their CP L6 counterparts, there is extensive overlap in their identified molecular determinants. SP-specific markers are largely underdefined at embryonic ages. Overall, SPNs are characterized in part by expression of *Cplx3*, *Ctgf*, *Nr4a2* (*Nurr1*), *Lpar1*, *Sox5*, and *Kcnab1*, with some variation between subpopulations (139-142). The majority of L6 marker genes, in addition to *Sox5*, including *Tbr1*, *Tle4*, and *Zfpm2* (*Fog2*), are also often expressed by SPNs (141, 143-147). Mutations in *SOX5* and *TBR1* are associated with neurodevelopmental disorders such as Lamb-Shaffer syndrome (148) and intellectual disability and ASD (149). By contrast, L5 neurons are characterized by high expression of *Rbp4*, and *Fezf2* (*Zfp312* and *Fezl), and Bcl11b* (*Ctip2*) (103, 150-154). Corresponding mutations in *BCL11B* are associated with intellectual disability (155).

The superficial layers (L2-4) of the neocortex display expression profiles largely distinct from their deep-layer counterparts. The major input layer, L4, is characterized by *Rorb* (156), and mutations in *RORB* are associated with epilepsy (157). L2-3 neurons express *Cux1*, *Pou3f2* (*Brn2*), and *Satb2* (158-160), which, in humans as previously noted, is associated with altered neurodevelopment. And finally, to complete the organization of the cortical wall, L1 or marginal zone Cajal-Retzius neurons express *Reln*, which is necessary for laminar organization (125-128). Together, unique identities of cortical excitatory neurons support widespread cortical functions.

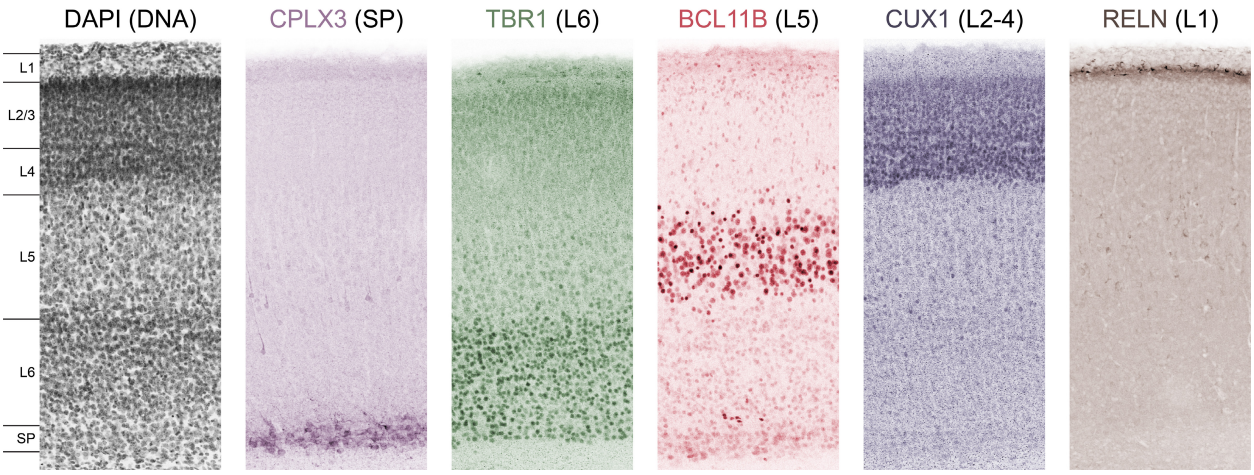

Figure 1.4: Layer-specific expression profiles in postnatal neocortex

DAPI (black) reveals cytoarchitectural differences across cortical laminae in P3 mouse neocortex. Distinct cortical layers are identified by immunostaining of molecular markers including CPLX3 (purple), TBR1 (green), BCL11B (red), CUX1 (blue) and RELN (brown).

Progressive postmitotic refinement of neuronal identities

Immediately after a neuron is born, it displays a transcriptomic state which differs from its mother cell. Neurons must deactivate NPC gene expression programs related to multipotency, division mode, and DNA replication, while initiating programs for migration, neuronal identity, and projections. However, cortical neurons do not immediately adopt their layer-specific identities. Instead, they have broad profiles that are refined over the first postmitotic days to finely regulate their laminar, morphological, and electrophysiological characteristics.

Deep-layer neurons are born and quickly express a plethora of corticofugal markers that eventually resolve into layer-specific or -preferenced profiles. The first few days after genesis of eventual L6 and L5 neurons, the populations are overlapping, expressing TBR1, ZFPM2, BCL11B, and FEZF2 (103, 141). However, during the first week after neuronal birth in mouse neocortex, these factors have largely been refined and are relatively specific to L6 (TBR1 and ZFPM2) or L5 (BCL11B and FEZF2) (**Figure 1.5**). This postmitotic refinement of neuronal identity is dependent on positive and negative interactions with regulatory elements. Future L6 is refined by SOX5 repressing *Fezf2* and TBR1 repressing both *Fezf2* and *Bcl11b* (161-163). Interestingly, later during postnatal development, *Tbr1* expression is increased in L2-4, potentially indicating a role in maintaining the molecular identities of upper-layer neurons (162).

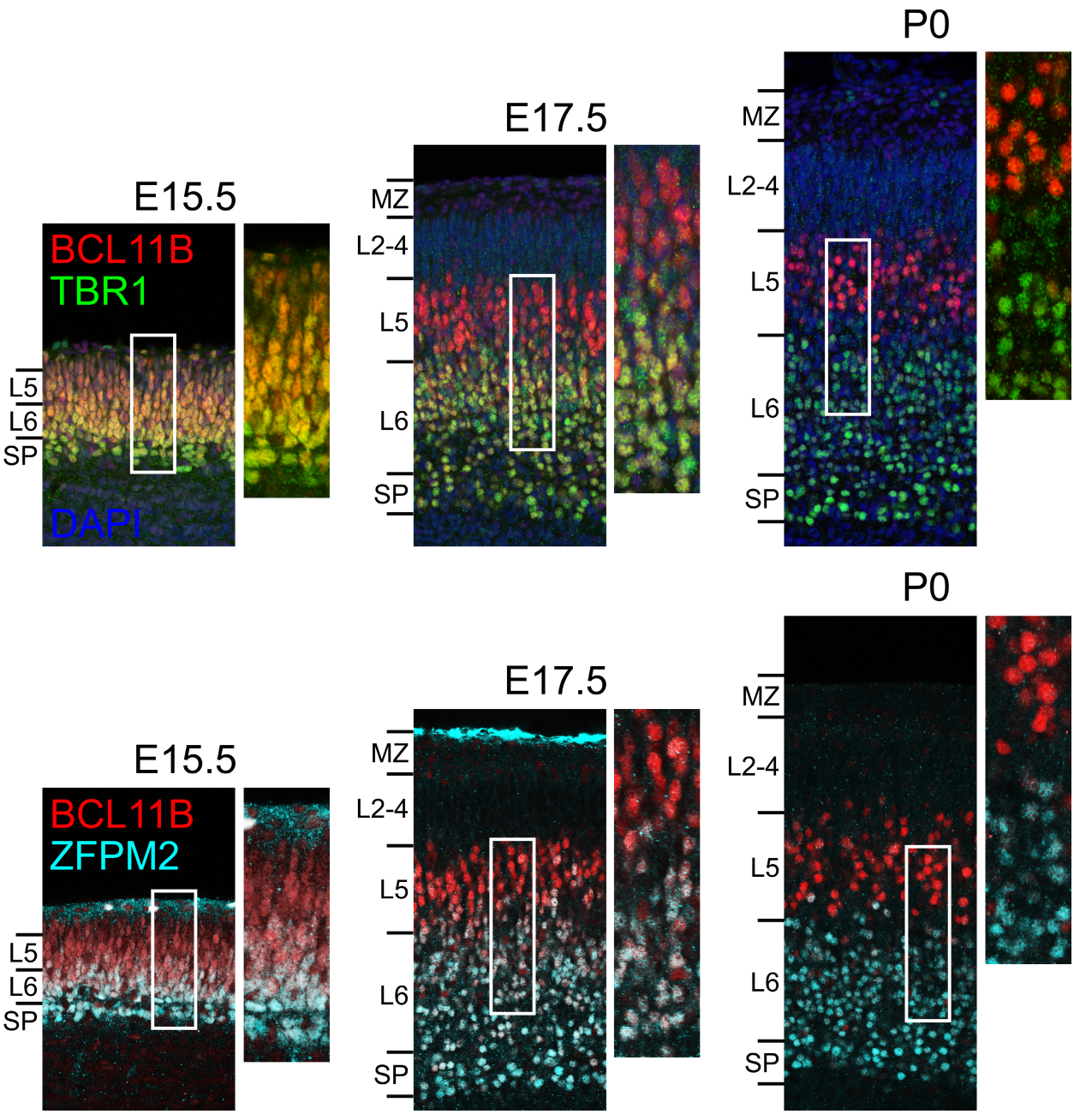

Figure 1.5: Progressive refinement of cortical neuron identities

Soon after neuronal birth, deep-layer neurons simultaneously express L6 (TBR1 [green] and ZFPM2 [cyan]) and L5 (BCL11B [red]) markers. As neurons mature, they progressively restrict these expression patterns. By P0, TBR1+ and ZFPM2+ neurons are largely contained in L6 whereas BCL11B+ neurons are primarily in L5. Adapted from (103).

Within the deep cortical layers, FEZF2 and TLE4 work collaboratively to repress subcerebral and intracortical identities to support development of corticothalamic neurons (164). In contrast, and spanning the layers, *Satb2* regulates intracortical projection fate potentially by repressing *Bcl11b* and a corticofugal fate (129, 130). Interestingly, some work suggests that identity refinement is not solely dependent on intrinsic mechanisms, rather it collaborates with signalling from developing circuitry. Thalamocortical projections may also contribute to postmitotic refinement of cortical neuron identity, in part signalling via VGF (165). Normally, L4 neurons refine their fate such that they transition from POU3F2+ to RORB+ with an intermediate phase of coexpression. In the absence of VGF secretion from thalamocortical projections, potential L4 neurons retain a POU3F2/RORB co-positive fate; they do not completely refine into L4 neurons (165). Without various cell and non-cell autonomous mechanisms, neocortical neurons fail to reach their expected identities and can be impaired in their connectivity.

Unique gene expression intrinsically regulates cell fate reliant on coordination with histone dynamics; improper chromatin structure can preclude transcription factor activity. When a neuron is born, it quickly alters its transcriptomic landscape. However, the DNA is coated with a full complement of nucleosomes thus inhibiting DNA accessibility and the potential for rapid transcriptional control. Therefore, eviction and remodeling of histones is necessary to establish the transcriptomic landscape of a newly postmitotic neuron. However, once histones are evicted, they need to be replaced to once again protect the DNA and package it within the nucleus. A nucleosome is comprised of two copies each of histones H2A, H2B, H3, and H4, but there are multiple

varieties of each. For histone H3, genes encoding canonical variants H3.1 and H3.2 have unique structures that restrict their transcription to S phase, when cells are actively replicating their DNA and must double the number of nucleosomes to protect twice the amount of DNA (166). However, noncanonical variant H3.3 is structured such that H3.3-encoding genes *H3f3a* and *H3f3b* can be expressed at any stage in the cell cycle (167). Thus, when H3 must be replaced in terminally postmitotic cells to remodel chromatin, it does so via H3.3. In previous work led by Owen Funk, we uncovered that *de novo* deposition of H3.3 in terminally postmitotic cortical neurons is essential for defining the neuronal transcriptome. Without it, NPC genes are not downregulated, and neuronal genes remain inactivate (103). Concomitantly, newborn neurons are unable to refine their fates. Instead, postnatal deep-layer neurons broadly co-express both L5 and L6 markers (103). The vague identity is accompanied by alterations in cortical connectivity, with corticofugal tracts properly exiting the cortex but unable to culminate in accurate corticospinal or corticothalamic tracts (103). Haploinsufficiency of H3.3 via mutations in *H3-3A* or *H3-3B* is associated with Bryant-Li-Bhoj neurodevelopmental syndrome, which presents with global developmental delay and intellectual disability (168, 169). Together, transcriptomic orchestration, in tandem with non-cell autonomous signalling from circuitry, is integral for neuronal identity, connectivity, and organismal function.

Assembling cortical connectivity

Organismal function depends on precise connections to process the outside world (e.g. how our food smells) and support bodily control (e.g. when we walk and talk). These circuits require distinct communication with the neocortex. Accompanying the widespread molecular identities of cortical excitatory neurons are axonal projections

to wire the neocortex together with other brain regions such as the spinal cord and thalamus. Any alterations in assembling these circuits can contribute to circuit miswiring in neurodevelopmental disorders.

Targeting of corticofugal projections

Corticofugal projections, those which originate within the cortex and extend to regions outside of it, originate exclusively from SP and deep-layer neurons (**Figure 1.6**). They travel through the developing cortical WM and exit, crossing the PSB. From there, many corticofugal tracts course through the internal capsule, while some contribute to the external capsule. Ultimately, corticofugal projections are comprised by corticothalamic, corticostriatal, corticobulbar, corticopontine, corticotectal, corticorubral, and corticospinal connectivities. These circuits originate from unique cortical neurons and require diverse and extensive cues to guide them to their ultimate targets.

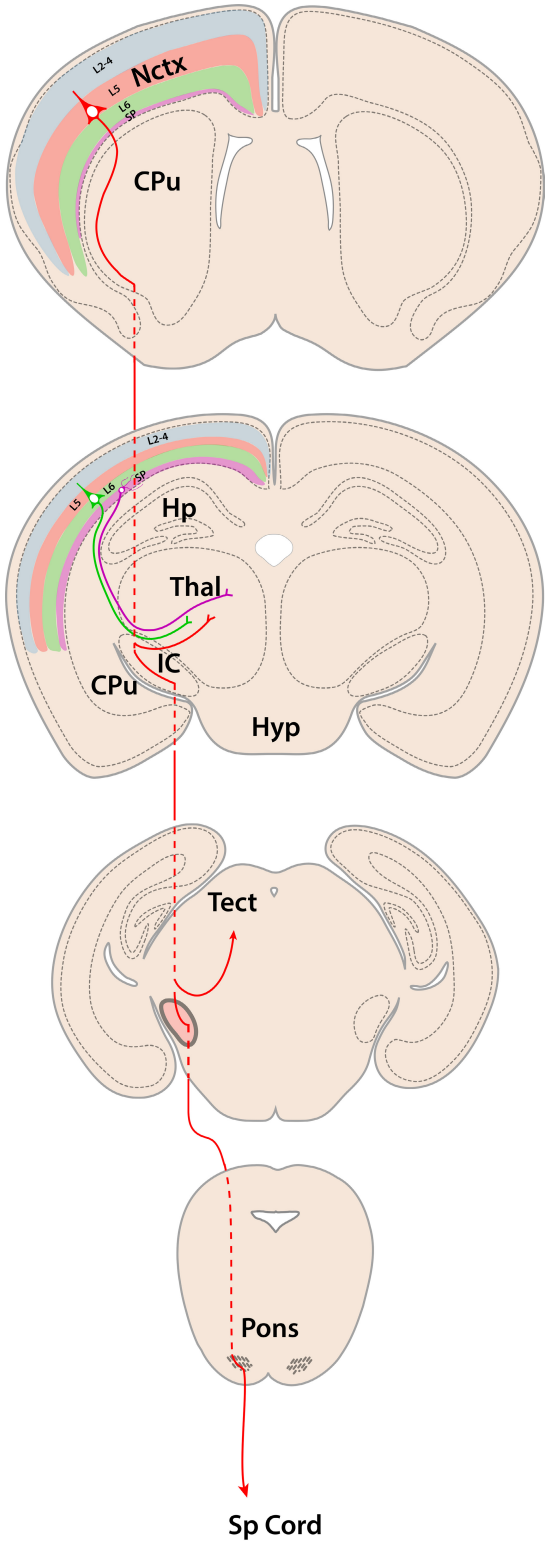

Figure 1.6: Corticofugal projections originate from deep cortical layers

Cortical efferents arise deep in cortical laminae and project to diverse targets. L5 neurons (red) extend descending axons through the internal capsule (IC) to the thalamus (Thal), tectum (Tect), and continuing down through the pons before decussating and entering the spinal cord (sp cod). L6 (green) and SP (purple) neurons follow a similar trajectory exiting the cortex and largely innervate the thalamus. Contributions of L6 or SP to the corticospinal tract have not been identified. In contrast to the deep-layers, L2-4 do not extend their axons to subcortical regions.

CPu: caudate putamen, Hp: hippocampus, Hyp: hypothalamus, IC: internal capsule, Nctx: neocortex, Sp Cord: spinal cord, Tect: tectum, Thal: thalamus

Corticothalamic axons connect the cortex with various thalamic nuclei and are positioned to mediate processing and response aspects of sensory signalling. While neurons from subplate, L6, and L5 contribute to corticothalamic circuitry (170), they are distinct in their precise thalamic innervations. SPNs send axons to high-order thalamic nuclei (171). Similarly, L5 neurons project into high-order thalamic nuclei (172), but with more robust innervation of the posterior nucleus of the thalamus than SPNs (171). By contrast, L6 neurons extend to both higher- and first-order thalamic nuclei (173). While corticothalamic neurons span the laminar distribution of SP and L6, in L5 they are largely confined to the lower portion, L5B (170). Together, corticothalamic neurons coordinate the communication of information from the cortex to various thalamic nuclei. Interestingly, corticothalamic innervation of the dorsal lateral geniculate nucleus by SP and L6 neurons is coordinated and refined dependent on activity, particularly retinal input (174). The extensive corticothalamic connections are controlled in part by *Fezf2*, *Tbr1*, *Tle4*, and *Zfpm2* expression. Disruption of any of these factors alters corticothalamic innervation with distinctive misrouting (145, 162-164, 175-180).

While corticothalamic projections are extensive and vary in their position within neocortical laminae, corticostriatal, corticobulbar, corticopontine, corticotectal, and corticorubral neurons are much more constrained in terms of their somal location. The nuclei of all five of these tracts are housed within cortical L5 (170). Corticostriatal neurons originate in L5A and are involved in regulating decision-making (170, 181, 182). By contrast, corticobulbar, corticopontine, and corticotectal neurons are situated largely in L5B and involved in facial movements, upper limb movements, and visual

input, respectively (170, 183-186). Corticorubral neurons find a happy medium at the interface of L5A and L5B and project to indirectly impact limb movements (170, 187).

The neocortex directly orchestrates conscious movement via the corticospinal tract. Corticospinal neurons reside in L5B neurons with distinctive, large somata (170). Multiple molecular determinants of CST development have been identified. *Fezf2*, *Bcl11b*, and *Sox5* are all necessary for proper extension of corticospinal axons and directly interact with corticothalamic determinants for refine molecular identities and axonal trajectories. Their disruptions lead to a variety of alterations in presumptive corticospinal axon trajectories. Knockdown or deletion of *Fezf2* leads to reduction in corticofugal projections from and loss of corticospinal projections (161-164, 188). By contrast, overexpression of *Fezf2* is sufficient to induce subcortical projections from upper-layer neurons (154). *Fezf2* also activates *Bcl11b*, which is individually necessary for formation of the corticospinal tract. In the absence of *Bcl11b*, supposed corticospinal projections largely fail to extend beyond the pons and do not form the pyramidal decussation (151). However, in the absence of *Fezf2*, overexpression of *Bcl11b* is sufficient to induce subcerebral projections (189). In an interesting complementary fashion, *Sox5* influences corticospinal development by directly repressing *Fezf2* expression and postmitotically refining neuronal fate (141). In *Sox5*'s absence, although *Fezf2* is expanded, axons fail to extend to the pons and beyond; the corticospinal tract is not formed. However, in contrast to *Fezf2*, although *Sox5* is necessary for CST formation, it is not sufficient. Overexpression of *Sox5* does not effectively reprogram neurons to send their axons subcerebrally (141). Together, precise coordination of

multiple molecular mechanisms orchestrates distinct neuronal identities and their corresponding corticofugal projections.

Intracortical projections

Contrasting corticofugal projections, intracortical fibers both originate and terminate within the cortex. These tracts largely integrate and process information and can be subdivided into intrahemispheric and interhemispheric, such that they make connections within the cortical hemisphere they originate or long-range connections with the contralateral hemisphere (**Figure 1.7**). Short-range connections often occur within a cortical column and enable additional processing of information before output. For example, ocular dominance columns are refined over time after receiving visual information from the lateral geniculate nucleus of the thalamus (190-194) and contain intracolumnar connections between neurons in L6 and L4 (195, 196) and L4 and L3 (197). These columns depend on precise gene expression programs and protein secretion (198, 199) and can be disrupted if visual input isn't received (200).

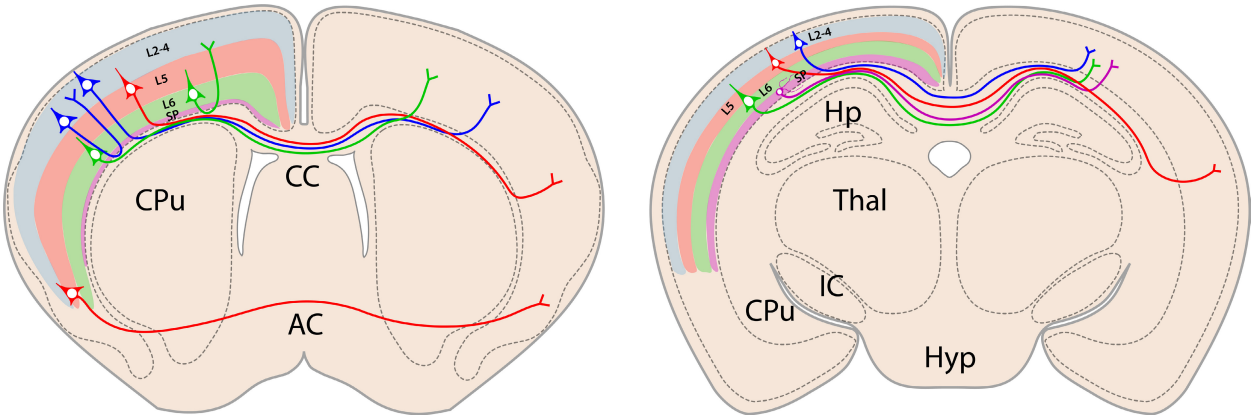

Figure 1.7: Intracortical projections span neocortical layers

Schematic illustrations of intracortical projection neurons. Neurons across cortical laminae project interhemispherically through the CC. Deep-layers and SP largely project significantly to heterotopic areas and upper-layers primarily to homotopic regions. Within the CC, axons are organized dorsal to ventral based on somal position from medial to lateral neocortex. Some projections from L5 contribute to the AC. Intrahemispheric connections arise from multiple layers, and many form synaptic partnerships with other neurons in their cortical column.

AC: anterior commissure, CC: corpus callosum, CPu: caudate putamen, Hp: hippocampus, Hyp: hypothalamus, IC: internal capsule, Thal: thalamus

Complementing local circuitry, cortical excitatory neurons send long-range projections from one cortical hemisphere into the other. The most prominent interhemispheric connection is the corpus callosum (CC), the largest WM tract in eutherian mammals. These connections can be between homotopic or heterotopic regions (201), and contrasting corticofugal projections that originate solely from deep-layers, callosal connections begin in L2, 3, 5, 6, and SP (202). The resultant long path from one hemisphere to another requires not only well-defined neuronal identities, but a multitude of guidance cues and populations along the way.

An intracortical projection fate is dependent on the aggregate of transcripts expressed. While *Bcl11b* directly supports a corticofugal fate, *Satb2* in tandem with *Ski* represses *Bcl11b* to initiate intracortical identities (129, 130, 203). SATB2+ cells are distributed throughout cortical layers, but while deep-layers have a healthy mixture of BCL11B+ versus SATB2+ neurons, L2/3 is nearly exclusively SATB2+. The initial callosal axons traverse the midline and set the stage for elaborate connectivity around E16 in mice and fetal week 11 in humans (204-207). Interestingly, homotopic callosal projections largely originate from upper-layers and heterotopic across layers (208), indicating that there is some layer-based directive of callosal projection types.

Once axons extend toward the midline to form the CC, they are extensively guided into the contralateral hemisphere. Along their growth trajectory, callosal axons receive a variety of attractive and repulsive cues. In particular, *Slit2*, *Robo1*, *Robo2*, *Fzd3*, and *Ntn1* are each necessary for proper callosal formation (209-212). Rather than this signalling being restricted to cortical cells, callosal axons also receive signals from the developing meninges to inhibit aberrant outgrowth (213). These cues are

constructively integrated with midline glial structures to direct axons across the midline. Positioned right at the interface of septum and cortex, are midline zipper glia adjacent to the subcallosal sling, indusium griseum, and glial wedge which guide callosal axons interhemispherically (214-216). Their disruption can lead to partial or complete callosal agenesis, a feature observed in a variety of neurodevelopmental disorders (216-219). In the absence of proper midline formation, likely callosal axons that fail to cross frequently coalesce to form Probst bundles near the midline, unable to reach their target destinations (220).

During initial outgrowth of callosal and other intracortical axons, they reach out to overly broad regions and some are subsequently selectively eliminated or refine their connectivity (221-229). The fine-tuning of intracortical connections depends on a variety of factors, including neuronal activity based on *Kcnj2* (*Kir2.1*) (230), JAK2 signalling (231), and activation of *Kcna1* (*Kv1.1*) and *Kcna3* (*Kv1.3*) mediated by the upper-layer marker *Cux1* (232). Disruption of electrical activity by reducing *Kcna1*/*Kcna3* is sufficient to selectively eliminate contralateral, but not ipsilateral, connections (232). Together, the transmittal of information within the neocortex, relies on coordination of neuronal identities, axon guidance molecules and receptors, midline glial structures, and neuronal activity to direct the initial outgrowth and refinement of circuitry.

Coordination with cortical afferents

Cortical efferents alone are insufficient to support brain function and organismal fitness. Instead, there is an elaborate network of connectivity that extends from subcortical structures into the cortex. Of these cortical afferents, the most prominent are thalamocortical projections, which originate in the thalamus and terminate largely in

neocortical L4. The thalamus receives information from widespread areas in the body, including from the limbs via the spinal cord and from distinct nuclei of cranial nerves, and disseminates those signals for additional processing. Once the signal reaches the neocortex, it gets further integrated and transmitted for any output. Importantly, these connectivities don't develop in a vacuum, they depend on one another to refine.

As described earlier, cortical neurons can have intracolumnar synaptic partners. These circuitries are especially prominent within thalamocortical input areas including somatosensory cortex. Cortical sensory areas organize into distinct structures (e.g. whisker barrels) dependent on thalamocortical activity. Interestingly, while much of sensory map remains unrefined until mid to late in the first postnatal week in mice, it depends on spontaneous activity from thalamocortical neurons as early as E16.5, and interactions with SPNs even earlier. Altering thalamocortical spontaneous activity is sufficient to eliminate the formation of sensory whisker barrels (233) and thus proper processing of sensory information. Disrupting the somatosensory map can contribute to altered responses to sensory stimuli as often seen in neurodevelopmental disorders.

History and influence of subplate neurons in cortical architecture

Over a century of work hinted at the existence of the SP zone and SPNs without truly appreciating the influence they leverage during cortical development. The harmony of the brain depends on rigorous and extensive coordination between neuronal generation, positioning, and axonal growth and targeting. At the center of this orchestration are SPNs. SPNs are the firstborn neurons of the neocortex and originate from various spatial locations (**Figure 1.8**) (59, 234, 235). Seated within the space between cortical L6 and WM, SPNs maintain an intimate relationship not only with CP

neurons but also with interstitial neurons, residents of the WM. During embryogenesis SPNs are able to extend the first cortical axons, both corticofugally and intracortically, and interact with migrating neurons, cortical afferents, and other cortical efferents or intracortical projections. Thus, SPNs are well-positioned to widely influence developmental architecture and connectivity.

SP and interstitial neurons have been described hand-in-hand beginning in the late 1800s, and some SPNs are thought to transition to interstitial after initial development. Fundamental drawings and descriptions of interstitial neurons within the WM of frontal and visual cortex were in the mid 1800s with the term “interstitial” in regards to neurons in the brain beginning near the turn of the 20th century (236); a more comprehensive review than what I can convey is deserving of a read (237). The SP zone, although not yet appropriately named, was finally well-illustrated in fetal cat by Shinkishi Hatai in 1902 (238). Ultimately, the SP zone was not termed until 1974 by Ivica Kostović and Mark Molliver (239).

SPNs sit within the SP zone, whereas interstitial neurons are located amid the WM (240). This crucial distinction supports the presence of interstitial neurons throughout various compartments in the developing nervous system, particularly in the cerebellum and spinal cord, while confining SPNs to the cerebral cortex. However, some SPNs may be eliminated in later stages of development while others can transition to interstitial and likely play integral roles in long-term functions of brain connectivity (240-247). Interestingly, in rodents, although some SPNs are eliminated in the first postnatal week, the SP zone is largely identifiable throughout life, although it is commonly referred to as L6b. By contrast, the SP zone is in fact transient in humans

and primates. While the SP zone goes through a secondary expansion coincident with axonal ingrowth during fetal development (248), some SPNs remain throughout life; many of them are eventually interstitial, whereas others are closely situated along L6 in L6b (249). Some work in human cortical organoids also suggests they may further refine and integrate within deep cortical layers (250, 251). It seems quite likely the expansion of WM within gyrencephalic mammals may lend to the transient nature of the SP zone and relative increase in adult cortical interstitial neurons compared to lissencephalic rodents.

During human fetal development, Kostović and Molliver defined the SP zone by dividing the IZ into two separate parts: 1) the lower portion containing the WM and 2) the upper, SP zone, containing both pyramidal and multipolar neurons with long dendrites (239). Not only did they report mature neurons within the fetal SP zone, but also an extensive number of synapses, suggesting early communication between SPNs and other cells (239). The SP does not only include excitatory neurons. Rather, multiple mammalian species display evidence of GABAergic neurons within the SP (252-254). Interestingly, GABA can play an excitatory function early in development and later transitions to be a largely inhibitory neurotransmitter (255), suggesting GABAergic SPNs could modulate developing and mature circuits within the brain differentially to fine-tune excitatory and inhibitory signalling.

The morphology of SPNs and their interstitial counterparts has been well-documented over the past half century in rodents, cats, and primates including humans. Consistent with the complexity of their molecular identities, their potential morphologies are diverse. The morphological classifications for SP and interstitial neurons vary

dependent on species, age, and research team. In early postnatal rodent, SPN morphologies can be described as horizontal (bitufted and monotufted), multipolar, inverted pyramid, tripolar or pyramid-like, and neurogliaform (256-258). Although rodent SPNs in different morphological groups do not display exceptional variation in their electrical properties (256), their projections appear linked to morphology (257). Specifically looking at pyramidal, neurogliaform, and multipolar SPNs in P2 rat, corticofugal projections are encompassed by pyramidal and multipolar, cortical intrahermispheric represented all three morphologies, and callosal exclusively multipolar (257). In stark contrast, only five days later in P7 rat, all three connectivities are largely represented by multipolar SPNs—pyramidal and neurogliaform are few and far between (257). Interestingly, while many non-pyramidal SPNs appear lost during the early postnatal period, all morphological subtypes are still present in adult L6b, indicating a strong relationship between SP and L6b (258). However, most multipolar and neurogliaform neurons were interstitial after early development (257). Thus, although many studies lack adequate distinctions between SP and interstitial neurons when interrogating structure and function, the two groups display overlapping and divergent primary morphologies.

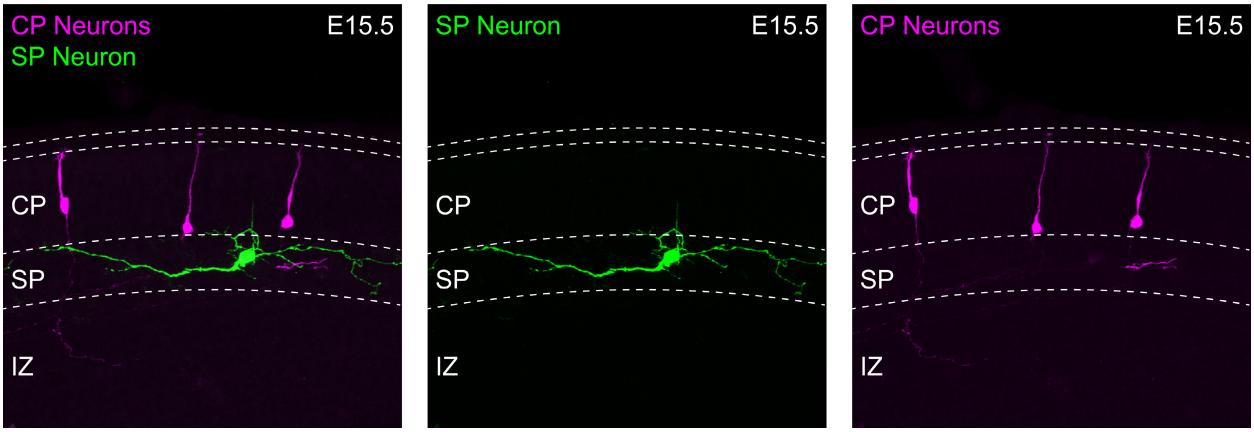

Figure 1.8 Subplate-cortical plate spatial and morphological distinctions

Visualization of a subplate neuron (green) and three cortical plate neurons (magenta) in E15.5 cortex. Subplate neurons display diverse morphologies and often fail to resemble their pyramidal cortical plate counterparts. By sitting between the cortical plate and intermediate zone, subplate neurons are poised to direct developing circuitry and migrating neurons.

CP: cortical plate, IZ: intermediate zone, SP: subplate

In contrast to rodents, the primate SP zone is incredibly transient, and coincident with this, many SPNs that survive into adulthood eventually become interstitial neurons (246). However, similar to rodents, the early human and non-human primate SP zone is characterized by pyramidal, multipolar, fusiform, and polymorphic neurons (246). In primates, many of these morphologies are found during postnatal ages near L6. In comparison, cortical interstitial neurons are more restricted morphologically. Embryonically, they are largely polymorphic whereas during adulthood they are largely, but not exclusively, fusiform (240, 259). These extensive morphological features of SP and interstitial neurons enable informative interactions in various processes, including neuronal migration and cortical efferent and afferent projections.

One way SPNs can influence cortical lamination is via interactions with migrating CP neurons. As CP neurons migrate through the IZ and bypass the SP, they make transient contacts with SPNs and their morphology is altered (106). These contacts could involve synaptic activity. SPNs are electrically active and form synapses early in corticogenesis (239, 246, 260-263). Disrupting electrical activity of or glutamate release from SPNs is sufficient to impair morphological state change of migrating CP neurons and their subsequent laminar organization (106). The first of the migrating CP neurons, L6 neurons, split the preplate (previously referred to as MZ, early MZ, and primordial plexiform layer) into the SP and marginal zones (21, 57, 235, 264-268). Unsuccessful preplate splitting is coincident with disrupted organization of cortical layers and altered cortical circuitry (141, 144, 162, 163, 178, 269-274). However, reduced signalling from MZ by eliminating Cajal-Retzius cells does not elicit such robust alterations (275). Thus,

SPNs exert elaborate non-cell autonomous influence over the overall organization and connectivity of the neocortex.

In combination with SPNs' instruction of neuronal migration, they also extend some of the first axonal projections and can thereby influence subsequent circuitry. Initially it was thought that SPNs send the first axons of the CC across the midline, however, although conflicting reports identified a few SPNs that do project interhemispherically, they collectively found it more likely that the CC is actually pioneered by neurons within cingulate cortex (205, 207, 257, 276-282). Corticofugal projections tell a different story. SPNs are the first to project across the PSB and extend toward the thalamus (283-285). While their status as the first to ultimately reach the thalamus varies dependent on species (286, 287), SP pioneering of corticothalamic circuitry is thought to influence the eventual innervation of distinct thalamic nuclei (285).

The early subcortical extension of SP-derived axons gives them a unique opportunity to convene with primordial cortical afferents. An exemplar is the meeting between SP axons and TCAs within the subpallium (**Figure 1.9**). TCAs bring sensory information to the cortex and enable processing and subsequent responses. The timing of SP-thalamic and thalamocortical outgrowth and innervation is stereotyped and well-coordinated. Around E13.5 in mice, SP axons extend across the PSB and TCAs across the diencephalic-telencephalic boundary. Subsequently, corticothalamic axons and TCAs meet within the internal capsule and begin to interact with one another. Based on the "handshake hypothesis" these thalamic and cortical afferents then travel along one another to form reciprocal connections (288). TCAs, around E14.5, traverse PSB and enter the neocortex, arriving within the SP zone around E15.5. Although TCAs

eventually transmit information to L4 cortical neurons, by E15.5 these target neurons have neither been fully generated nor migrated to their final destinations. To avoid entering the CP prematurely, TCAs exhibit a prolonged “waiting period” within, and dependent on, the SP (117, 118). Their paused trajectory highlights an additional characteristic of SPNs thought to be integral in developmental circuit wiring, the ECM corridor (**Figure 1.9**) (289-295). During mid to late corticogenesis, the SP zone is characterized by an extensive ECM composed of chondroitin sulfate proteoglycans (CSPGs). The CSPG corridor is organized near the initiation of the thalamocortical “waiting period” and is largely dispersed concomitant with CP ingrowth by TCAs (289). It is thought to act as a restrictive signal to guide both developing cortical afferent and efferent axons throughout the cortex on their way to their cortical or subcortical targets (290). It may also work in tandem with other guidance molecules and receptors that display SP-biased patterns during early development, such as *Epha5* (296, 297). As such, it is likely that disrupting the ECM corridor during development can derail cortical circuit formation.

Following the completion of the “waiting period,” around E18.5, TCAs begin to invade the CP and within about a week they organize into distinct sensory compartments, such as whisker barrels (298, 299). In the reverse direction and following “handshake” with TCAs, corticothalamic axons travel through the subpallium and cross the diencephalic-telencephalic boundary around E16. Similar to the TCA “waiting period” in the SP, corticothalamic projections sit within the prethalamus until E17.5 when they begin to invade the thalamus (300). Slowly over the next couple weeks they organize into specific thalamic nuclei. Interestingly, although these close

interactions described in the “handshake hypothesis” can be visualized in multiple species, the necessity for them within the subpallium may differ across species; in primates, TCAs cross the PSB prior to their “handshake” with corticofugal axons (301).

The disruption of SP and interstitial neurons leads to extensive changes in cortical connectivity across multiple species (141, 162, 302-308), and is thought to be a significant factor in multiple developmental disorders (309-315). This idea initially arose in the early 1900s (316) and patients with either ASD and schizophrenia often display an increase in the number of interstitial neurons (309, 310, 317). Changes in SP and interstitial neuron number and characteristics, likely disrupt SP organization, projections, and ECM. These alterations can contribute to circuit miswiring that instigates various phenotypes, including sensory hypersensitivity, identified in many patients with neurodevelopmental disorders like ASD.

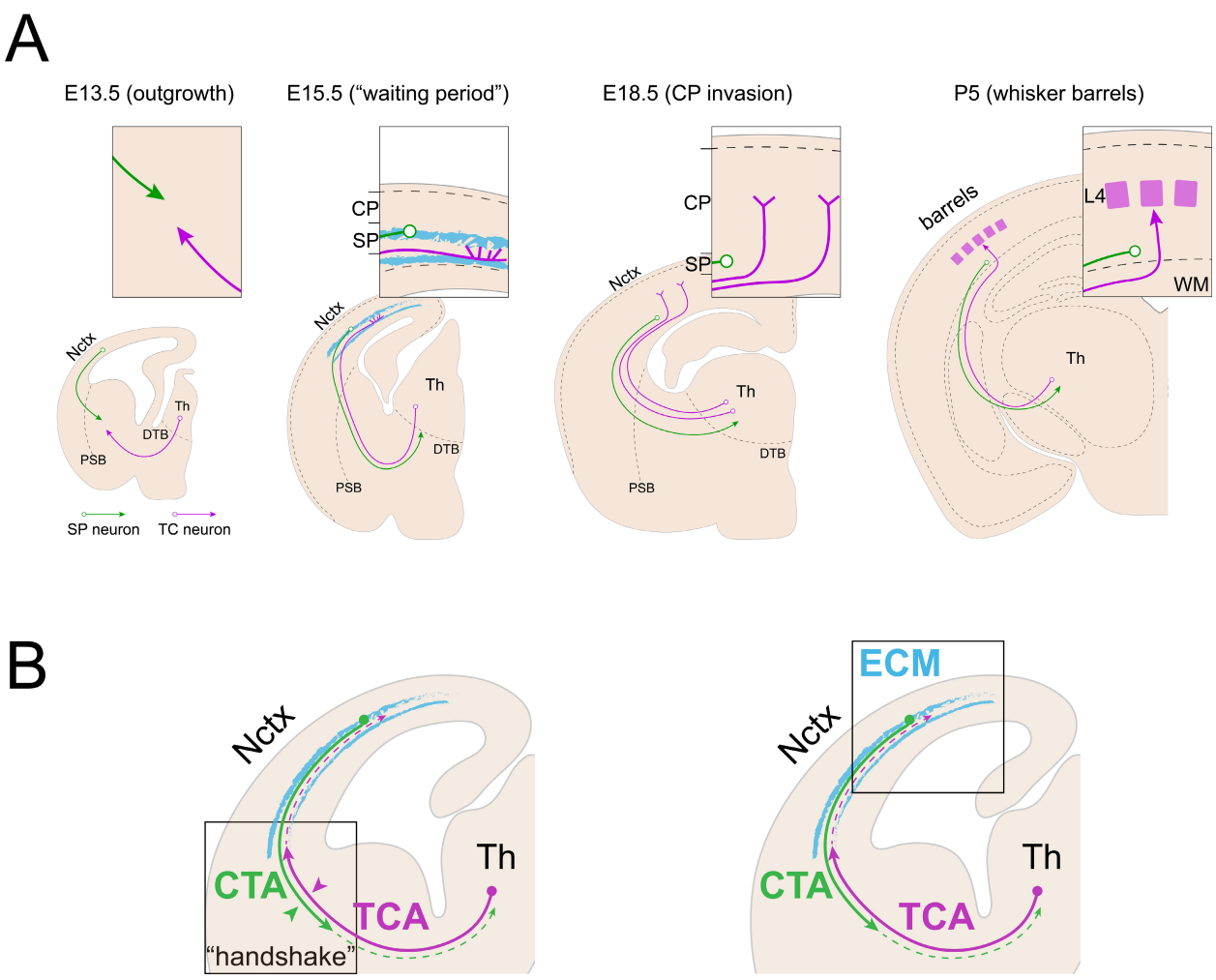

Figure 1.9 Coordination of thalamocortical ingrowth and subplate outgrowth

(A) Thalamocortical axons follow a stereotyped growth trajectory with subplate neurons. By E13.5 in mouse, subplate neurons have crossed the pallial-subpallial boundary (PSB) and TCAs extend across the diencephalic-telencephalic boundary (DTB), reaching close proximity with one another in the subpallium. These axons shake hands, communicate, and travel along one another to form reciprocal connections in thalamus and neocortex. Once TCAs enter the neocortex, by E15.5, their L4 targets are unprepared. TCAs pause in an extensive subplate extracellular matrix corridor (cyan) rich in chondroitin sulfate proteoglycans (CSPGs). Following a brief "waiting period," TCAs begin invade the cortical plate and finally organize into defined whisker barrels.

(B) Two major characteristics of subplate-dependent circuit wiring are the "handshake" in the subplallium and extracellular matrix in the subplate zone.

CP: cortical plate, CTA: corticothalamic axon, DTB: diencephalic-telencephalic boundary IZ: intermediate zone, Nctx: neocortex, PSB: pallial-subpallial boundary, SP: subplate, Thal: thalamus, TC: thalamocortical, WM: white matter

Chromatin remodeling in corticogenesis

Mutations in genes encoding chromatin remodelers have been increasingly implicated in developmental disorders (318-321), but why? To properly function, each neuron utilizes twenty-two pairs of autosomes and two sex chromosomes, each with an elaborate combination of gene bodies, regulatory elements, and other noncoding regions. Together, these components collaboratively add up to about six feet of DNA per nucleus. For scale, the nucleus is about 10 μm in diameter whereas six feet of DNA is nearly 1.8×10^6 μm, 180,000 times greater. To fit the entire complement of DNA into each nucleus, the DNA must be compacted from a linear stretch into a three-dimensional structure. This condensation is accomplished by tightly wrapping DNA around nucleosomes and packaging them together. However, compaction inhibits any processes that need to happen on the DNA, such as DNA replication, transcription, and DNA repair. Remedying this inaccessibility, chromatin remodelers are multi-protein complexes that hydrolyze ATP and harness that energy to slide, evict, or replace nucleosomes, thereby fine-tuning DNA accessibility (**Figure 1.10**) (322). Chromatin remodelers, and thus alterations in chromatin structure, are uniquely positioned to control various aspects of corticogenesis. Disrupting these processes has the potential to widely alter brain development and function.

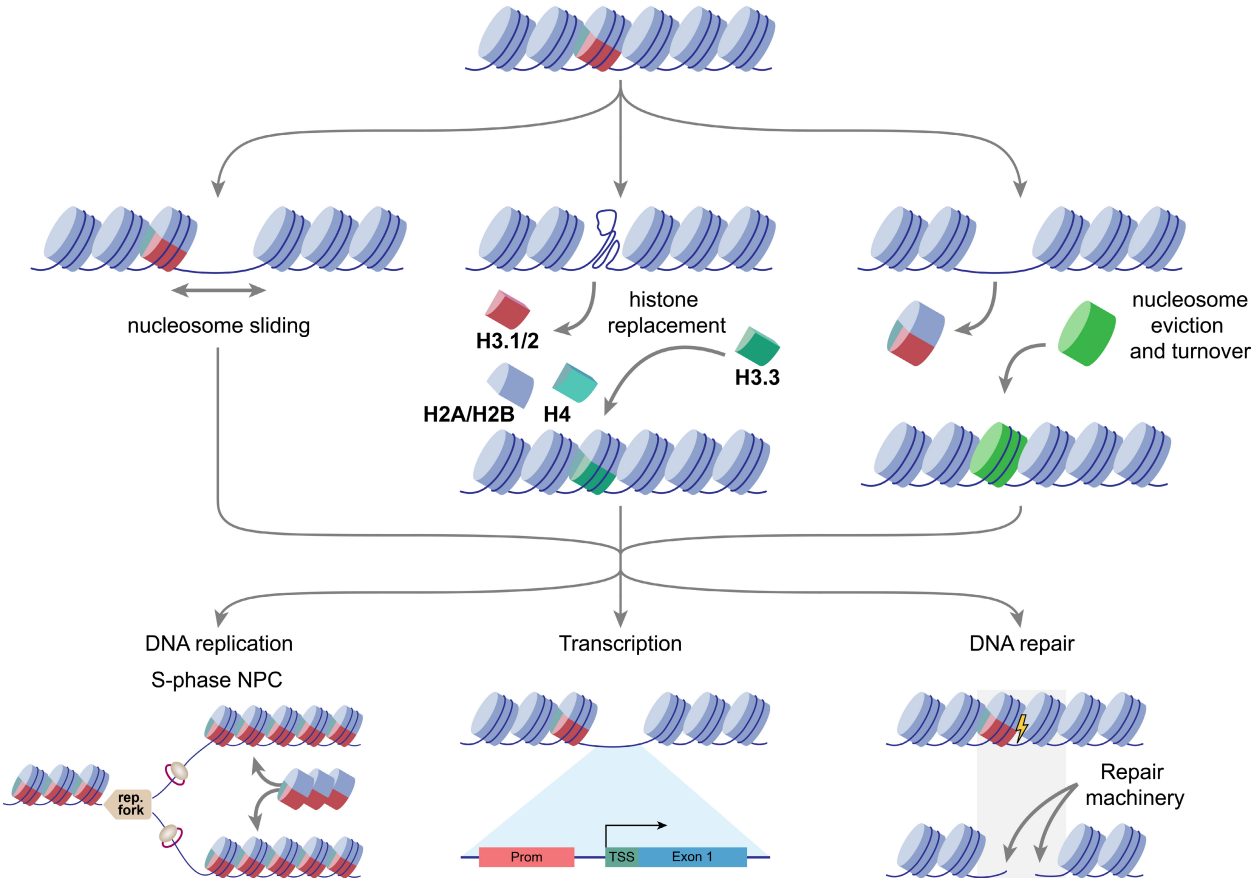

Figure 1.10: Molecular functions of chromatin remodelers

Chromatin structure allows DNA to be compacted but precludes events that occur on the DNA. Chromatin remodelers hydrolyze ATP and use that energy to slide nucleosomes, replace histone subunits, or evict and replace entire nucleosomes. Each of these processes can contribute to DNA accessibility necessary for DNA replication, transcription, and repair of DNA breaks. In replication, chromatin remodeling allows progression of the replication fork and deposition of new nucleosomes to protect nascent DNA. To promote or inhibit transcription, nucleosomes can be altered to reveal genomic regions for transcription factor binding and transcription machinery. Finally, when DNA is undoubtedly damaged, nucleosomes must be evicted or reorganized to allow access to repair machinery, end resection of damaged regions, and ultimately DNA repair.

DSB: double strand break, NPC: neural progenitor cell, Prom: promoter, rep. fork: replication fork

Functions of chromatin remodeling complexes

The entire body develops from a single cell and increases exponentially during embryogenesis. This process requires replication of the entire genome during S phase to enable cell division and pass on a full complement of DNA to two daughter cells. However, the compaction of DNA via nucleosomes precludes its availability for replication. As such, nucleosomes must be removed so parental DNA can be unwound and separated by a helicase complex and DNA polymerase can add complementary nucleotides to each strand, thereby producing two copies of double-stranded DNA. These new DNA molecules, containing one parental and one nascent strand of DNA, are segregated into new daughter cells during M phase and provide the entire genome for each new cell. Impairing the removal of histones and nucleosomes can disable the ability for a cycling cell to synthesize new DNA, and thus is deleterious to any division. Much of the remodeling near the onset of DNA replication may be initiated by the origin recognition complex. The origin recognition complex catalyzes ATP to evict histone H2A/H2B dimers from parental DNA during G1 phase, thereby leaving H3/H4 dimers and potentially preparing for the arrival of replication machinery (323). Disrupting this complex can lead to impaired DNA replication (324), and therefore the inability to produce new cells. Chromatin remodeling is thus the backbone of genomic integrity and cell division in the neocortex.

Distinct from DNA replication, transcription occurs whether a cell is progressing through the cell cycle (e.g. differentiating RG), halted in a quiescent state (e.g. some adult neural stem cells), or active and terminally postmitotic (e.g. active neuron). While DNA is compacted, gene regulatory elements and gene bodies can be obstructed by

nucleosome position, components, or modifications. Therefore, DNA can be made more (or less) accessible for transcription by sliding or evicting nucleosomes, exchanging their subunits, or altering histone tail modifications. Altering the chromatin landscape enables transcription factor binding and influence of gene expression (325). In the absence of genomic accessibility, the transcription initiation complex containing RNA polymerase II is unable to target near the transcription start site and RNA cannot be generated. Gene expression therefore depends on organization of the chromatin landscape by chromatin remodelers.

Both replication and transcription put DNA under immense stress and can cause genomic damage. Interestingly, in dividing cells, there can also be detrimental collaboration between the two by which replication and transcriptional machineries collide and damage the genome, especially on long transcripts (326-328). Any DNA damage can be mutagenic, deleterious, and require rapid repair to reduce any harmful effects. These corrections depend on chromatin remodeling and can occur through a variety of mechanisms. The two major forms of double-strand DNA damage repair are homologous recombination and non-homologous end-joining. Homologous recombination is thought to be the less error-prone method of repair and thus seems more preferred. While often referred to erroneously as “error-free”, it can still lead to extensive rearrangements of the genome, both intrachromomsomal and interchromosomal (329). Additionally, homologous recombination requires a second copy of the DNA as a repair template and therefore usually only occurs in cells later in S or G2 phase that contain sister chromatids. By contrast, non-homologous end-joining can occur in any cell at any time, however, it is thought to have greater mutagenic

potential. Both types of repair require resection of damaged DNA, but nucleosomes may impede the accessibility of these regions to the resection machinery. Chromatin remodelers are essential for sliding or evicting nucleosomes near sites of DNA damage thereby increasing accessibility for repair. The cell type-specific requirements for these repair mechanisms are likely distinct and there is undoubtedly some compromise between repair mode, speed, and potential for deleterious impact. Together, chromatin remodelers meticulously influence DNA replication, transcription, and DNA repair to orchestrate organismal development and function.

Contributions and dysfunction of chromatin remodeling in brain developmental

A large number of chromatin remodeler genes are expressed in a near ubiquitous manner, in most or all cells most or all of the time. However, they do not necessarily perform the same function all the time or even in every cell; chromatin remodelers may have cell type-specific actions. Although there is a plethora of chromatin remodeler complexes, their influence over replication, transcription, and repair and importance during brain development can be easily illustrated with a few examples, namely the INO80, ISWI, and BAF chromatin remodeling complexes.

The INO80 (INOsitol-requiring mutant 80) chromatin remodeling complex is made up of fifteen individual protein subunits. Over the years, the INO80 complex has been well-described in a variety of organisms from yeast to mammals mediating diverse DNA replication, transcription, and DNA damage repair (87, 330-336). Mutations in its catalytic subunit, *INO80*, are associated with an overall reduction in brain size and thus microcephaly (337). In our previous work led by Jason Keil, we uncovered that *Ino80*'s contributions to brain development are not only unique but indispensable for genome

integrity and corticogenesis (87). In transcription, *Ino80* collaborates with transcription factor YY1 to activate gene expression (334). Interestingly, this gene expression is not ultimately necessary for establishment of neuronal identity or connectivity. Separately, *Ino80* is necessary for homologous recombination DNA repair in symmetrically dividing NPCs to coordinate corticogenesis. In its absence, NPCs that have not yet transitioned to neurogenic divisions sustain a normal quantity of double-strand DNA breaks during S phase, however, these breaks are inadequately repaired. Insufficient DNA damage repair leads to widespread p53-dependent NPC apoptosis, an inability to produce neuronal progeny, and severe microcephaly (87). These findings illustrate alternative requirements for DNA damage repair within proliferative versus neurogenic NPCs while highlighting how disruption of chromatin remodelers can potentially lead to genomic mosaicism and altered brain development.

During S phase, nucleosomes must be removed to enable replication of parental DNA strands and subsequently doubled and redeposited to protect nascent DNA. The eviction and deposition of nucleosomes requires precisely controlled chromatin remodeling. Two major contributors, *Baz1a* (*Acf1*) and *Smarca5* (*Snf2h*, *Iswi*), are members of the ISWI (Imitation SWItch) chromatin remodeling complex. They have been implicated in coordinating DNA replication in heterochromatic regions and chromatin structure near the replication fork (338-340). Mutations in *BAZ1A* and *SMARCA5* are each associated with developmental delay (341, 342), with *SMARCA5* also associated with microcephaly (341). These aren't the only chromatin remodelers associated with DNA replication. In fact, ATRX is involved in reducing replication stress that can lead to DNA damage. In its absence, NPCs accumulate more DNA damage,

undergo apoptosis, and generation of upper-layer (late-born) neurons is reduced (343). Disruption of *ATRX* is also associated with intellectual disability (344). These findings are consistent with the necessity for DNA replication and integrity during cell division and illustrate the importance for chromatin remodelers in mediating these processes.

One of the most well-studied protein collectives, and the one central to this thesis, is the BAF chromatin remodeling complex, also known as the SWI/SNF (SWItch/Sucrose Non-Fermentable) complex. The BAF complex has a tremendous variety of ubiquitous and cell type-specific subunit compositions, each with 10-15 components carefully selected from a pool of at least 29 proteins (345, 346). Broadly, these compositions can be classified into canonical BAF (cBAF), non-canonical BAF (ncBAF), and polybromo-associated BAF (pBAF) (347). Together they have the potential to organize into at least 1400 unique complexes (346). BAF complex subunits are both frequently mutated and studied in the context of cancer and play important roles across tissues. Often, germline loss of BAF-associated genes is embryonically lethal, thereby necessitating conditional strategies to effectively study their impact during fetal development. Through a combination of constitutive and conditional knockout models, they have been shown to play diverse roles during brain and widespread nervous system formation. BAF complex subunits play integral roles in neuronal and glial production, neuronal migration neuronal subtype identity, and fine-tuning of cortical connectivity, among others. Each complex includes either SMARCA4 (BRG1) or SMARCA2 (BRM), the catalytic subunits that hydrolyze ATP and harness the energy necessary for remodeling (345). Mutations in either of these genes are associated with various developmental disorders, including ASD, schizophrenia, Coffin-

Siris syndrome, and Nicolaides-Baraitser syndrome (318, 348-350). In mice, deletion of *Smarca4* from early NPCs alters the balance of neurogenesis and gliogenesis, accompanied by microcephaly (351, 352). Although studies have not directly linked *Smarca2* knockout to modified corticogenesis *in vivo*, *SMARCA2* mutations in human embryonic stem cells differentiated into NPCs disrupt the chromatin landscape concomitant with altered neuronal production (353). Together, SMARCA4 and SMARCA2 dysfunction highlight some requirements for BAF in the developing brain, but the intricacies arise from precise coordination of interchangeable subunits.

Outside of the main catalytic components a few BAF proteins have shown robust influences on NPC development and differentiation. Collectively, SMARCC1 (BAF155) and SMARCC2 (BAF170) promote a fine balance between self-renewal and differentiation of NPCs within the developing cortex along with influence on neuronal migration. A decrease in SMARCC2, which is accompanied by an increase in SMARCC1, leads to expanded indirect neurogenesis with an increase in neuronal number and cortical size (354, 355). Alternatively, an increase in SMARCC2 or decrease in SMARCC1, promotes direct neurogenesis and a decrease in overall neuronal production (354, 356). Interestingly, in the absence of both SMARCC1 and SMARCC2 at the onset of neurogenesis, the BAF complex is dissociated and the neocortex remains relatively unformed; many progenitors undergo apoptosis and there is only a negligible layer of cells that remain (357). Whether this apoptosis is due in part to increased or unrepaired DNA damage in NPCs is unknown. However, delaying co-deletion of these two subunits until a couple days after corticogenesis begins restricts the impact to impaired neuronal migration (358). Thus, although BAF complex subunits

can be widely expressed, they can also play precise cell type- and temporal-specific roles during cortical development.

The differentiation of an NPC to a postmitotic neuron is accompanied by the dissolution of neural progenitor-specific BAF complexes (termed npBAF) and assembly of neuron-specific BAF complex (termed nBAF) (359-361). During this transition is the exchange specific subunits within the complex (352). The neural progenitor-specific subunits impact expansive versus neurogenic divisions (352, 362), whereas neuronal components play multiple roles in fine-tuning dendritic and synaptic features (362-364). In addition to neuron-specific BAF subunits, some broader subunits that can be included both in progenitors and neurons, including BCL11A (CTIP1) and BCL11B, are crucial mediators of neuronal identity and function. Deletion of *Bcl11a* from developing cortex leads to impaired neuronal migration, cortical organization of sensory input, and balance between intracortical and corticofugal projections (365-367). *Bcl11a* has also been implicated in the temporal progression of corticogenesis (368). Alternatively, and as mentioned previously, *Bcl11b* is necessary and sufficient for development and extension of corticospinal projections (151, 188). Recent work suggests that *Bcl11a* and *Bcl11b* can work collaboratively and potentially in compensatory fashions to regulate neuronal identity and subsequent connectivity (368).

Chromatin remodeling complexes are unable to properly function without being targeted and bound to genomic regions. In the BAF complex, much of this binding can be performed by ARID1A (BAF250A), ARID1B (BAF250B), or ARID2 (BAF200). These subunits are mutually exclusive, required for complex formation, and ARID1A/ARID1B are associated with canonical and non-canonical BAF compositions while ARID2 is

incorporated in polybromo-BAF complexes (369, 370). Each of these subunits binds to DNA in a relatively sequence-independent manner and has distinct roles in organismal development (370-372). I will point the spotlight at *Arid1a* in the next section, and for large portions of Chapters 2 and 3, and thus will touch on only *Arid1b* and *Arid2* here. *ARID1B* is one of the top risk genes associated with ASD and extensively linked to Coffin-Siris syndrome (318, 373). As such, it has been increasingly studied over the past ten years in the context of brain development and function. Overall, its impact has largely been attributed to interneuron genesis and maturation, callosal projection development, and some slight involvement in cortical neurogenesis (374-376). In the absence or reduction of *Arid1b*, mice display altered behavior along with a significant reduction of cortical NPCs in M phase, IPCs, and cortical GABAergic neurons. These decreases are concomitant with modest increases in progenitor apoptosis, however, DNA damage status is unknown (374, 375, 377, 378). Later in neuronal maturation, *Arid1b* impacts synaptic connectivity (379). While mutations in *ARID2* have also been associated with Coffin-Siris syndrome (380), its role in brain development is uncertain and knockout models have not revealed any gross abnormalities in *Arid2*-deficient cortices (381). Interestingly, although each of these ARID proteins are widely expressed, ARID1A is present at a rate 3.5 times greater than ARID1B across a number of cell lines (370), suggesting it may play a prominent role in cellular function. Together, the INO80, ISWI, and BAF complexes illustrate just a small number of ways by which chromatin remodelers influence DNA replication, transcription, and DNA repair, processes which are indispensable during brain development.

Necessity of ARID1A and consequences of dysfunction

BAF complex subunits are commonly mutated in a variety of cancers. The most frequently mutated subunit, however, is *ARID1A* (382). In some types of cancer (e.g. ovarian clear cell carcinoma), *ARID1A* is mutated in greater than 50% of cases (383). Although *ARID1A*'s role in cancer hasn't been fully fleshed out, it likely includes interactions with *PTEN*, *PIK3CA*, and IL-6 signalling (384). Together, mutations in these genes can lead to increased tumorigenic growth.

Arid1a is not only necessary to curb improper growth; it initiates and guides emergence of the three distinct germ-layers early in embryogenesis. In humans, homozygous mutations in *ARID1A* are not tolerated and heterozygous mutations are deleterious (348). Work in mice revealed that homozygous lethality is likely due to a very early necessity during embryogenesis. In constitutive deletion of *Arid1a*, mice develop until gastrulation begins (near E6.5), but embryos fail to form mesoderm (385). Thus, development is halted, and the embryos are unable to survive. *Arid1a* also plays an important role in ectoderm development. The ectoderm gives rise to the neural crest, and although germline knockout of *Arid1a* precludes study of this process, conditional mouse genetics have revealed a necessity for *Arid1a* in neural crest cell development (385, 386). Neural crest cells contribute to heart development, and in the absence of *Arid1a*, heart formation is not completed coincident with an increase in cell death and embryonic lethality by E14.5 (386). These studies reveal a distinct necessity for *Arid1a* during development.

Some work has illustrated that depletion of ARID1A can elicit an increase of ARID1B with partial rescue (387) whereas conflicting results do not uncover an

upregulation of *ARID1B* or its protein product in *ARID1A*$^{-/-}$ cells (388). Additionally, in *ARID1A* mutant cells, at least one functional copy of *ARID1B* is required for viability in both normal and tumorigenic conditions (389). Although there may some overlap in their functions, the separate necessity for *ARID1A* and *ARID1B* is highlighted in neural crest cells. Without the ability to fully switch back and forth between ARID1A- and ARID1B-containing BAF complexes, human induced pluripotent stem cells are unable to be effectively differentiated into cranial neural crest cells (390). Overall, *Arid1a* and *Arid1b* likely have distinct, redundant, and potentially compensatory roles.

ARID1A's role in chromatin structure is, at least in part, to regulate enhancer activity. One possibility is that ARID1A acts in tandem with the EP300 acetyltransferase, which catalyzes the activating mark H3K27ac, to enable gene expression (391). In both *ARID1A*$^{+/-}$ and *ARID1A*$^{-/-}$ cells there are robust changes in the H3K27ac landscape near enhancers but not promoters (392). ARID1A might impact histone modifications and activation of gene expression with minor or context-dependent changes to chromatin accessibility (387, 388, 393). Interestingly, this may be combined with ARID1A-dependent pausing of RNA polymerase II to regulate gene expression (387). Taken together, both human and mouse *Arid1a* are involved in organismal development and regulation of gene expression. During this thesis I sought to uncover what influence *Arid1a* plays during cortical development considering its implication in ASD and Coffin-Siris syndrome.

Closing Remarks and Overview of Thesis

The overarching objective of this thesis is to deepen our understanding of what it really takes to build the brain. In this pursuit, the experiments presented focus on uncovering the impact of chromatin remodeling during cortical development. Previous work has highlighted the linkage between chromatin remodelers dysfunction and neurodevelopmental disorders. However, the unique influences of distinct chromatin factors are still being unraveled. Efforts have largely described chromatin remodelers in DNA damage repair and transcriptional regulation during brain development. How these might act on a population level, rather than solely autonomously, is unclear. Along these lines, mutations in chromatin remodeler *ARID1A*, part of the BAF chromatin remodeling complex, have been previously associated with altered neurodevelopment. While *Arid1a* has been extensively associated with transcriptional regulation, how it ultimately affects brain development has not been interrogated.

In this dissertation, I leveraged conditional mouse genetics to spatiotemporally identify the global and cell type-specific requirements for *Arid1a* during cortical development. In Chapter 2, *Arid1a* deletion from cortical NPCs induced widespread axonal misrouting of intracortical but not corticofugal connectivities. Complete callosal agenesis mirrored circuit miswiring previously described in *ARID1A* haploinsufficient patients. However, aberrant axonal trajectories were not limited to cortically-derived tracts. Rather, *Arid1a*-proficient TCAs were also misrouted, thereby illustrating a non-cell autonomous necessity for *Arid1a*. To confirm callosal misrouting was also due to non-cell autonomous factors, I designed and utilized a self-excising and self-reporting Cre recombinase construct to manipulate *Arid1a in vivo*. Using a complementary

conditional knockout approach, I identified the critical window for ARID1A to influence circuit wiring encompasses NPCs and/or newborn neurons prior to migratory completion. In Chapter 3 I honed in on the transcriptomic and cell type-specific consequences of *Arid1a* deletion. I uncovered an unexpected necessity for *Arid1a* to establish the neuronal transcriptome, especially that of SPNs. These gene expression alterations are detrimental; SPN organization, morphologies, projections, and ECM depend on *Arid1a*. Introducing a novel approach to assess SP gene necessity and sufficiency during cortical development, I found although *Arid1a* is ubiquitously expressed, its role specifically in the SP is largely sufficient to orchestrate developmental circuit wiring. This finding suggests a more broadly applicable framework by which SP dysfunction can contribute to altered connectivity in neurodevelopmental disorders. Finally, in Chapter 4 I evaluate how this work fits into the current landscape of the field, where we can go next, and the bigger picture questions we are now poised to address.

Chapter 2: *Arid1a* is Essential for Establishing Cortical Circuitry in the Developing Cortex[1]

Abstract

Cortical connectivity underlies mammalian conscious thought, action, and perception. Here, I identified chromatin remodeler *Arid1a* as an essential regulator of elaborate cortical circuit development. Deletion of *Arid1a* from cortical NPCs led to robust axonal mistargeting of intracortical but not corticofugal projections. Remarkably, thalamocortical axons that retain *Arid1a* expression were also misrouted, indicating a non-cell autonomous mechanism. *In vivo* manipulation of *Arid1a* via *in utero* electroporation revealed callosal agenesis was also a result of non-cell autonomous influence. Interestingly, postmitotic deletion of *Arid1a* revealed a critical period for ARID1A in NPCs or prior to completion of neuronal migration to direct brain wiring. Together, this work uncovered a spatiotemporal necessity for *Arid1a* to non-cell autonomously orchestrate cortical circuit development.

Introduction

The brain is the epitome of "the whole is greater than the sum of its parts." Although individual neurons, glia, etc. have distinct functions, the brain is not simply additive. Its collective development relies on meticulous coordination of cell and non-cell

[1]This chapter includes the publication: **Doyle DZ**, Lam MM, Qalieh A, Qalieh Y, Sorel A, Funk OH, & Kwan KY (2021). Chromatin remodeler *Arid1a* regulates subplate neuron identity and wiring of cortical connectivity. *PNAS*. DOI: 10.1073/pnas.2100686118

autonomous mechanisms for overall function. In particular, this is true for developmental brain wiring. Each neocortical neuron intrinsically procures its molecular identity with expression of various factors that also influence initial outgrowth of axonal and dendritic projections. However, along their growth trajectories processes respond to environmental cues originating from other neurons, be they repulsive or attractive signals. Disruption of non-cell autonomous mechanisms can therefore greatly alter brain wiring. Diagnoses of neurodevelopmental disorders are frequently accompanied by changes in brain circuitry, but the mechanistic underpinnings are unclear.

Recent human genetic findings have convergently implicated altered chromatin function in disorders of brain development (318, 320, 321). Chromatin organization can contribute to a variety of cellular functions, including genomic integrity, neuronal identity, and neuronal function (87, 103, 394). Impairments in any of these processes has the potential to negatively influence brain development. Importantly, these events do not exclusively retain cell autonomous impacts. Instead, changes in the chromatin landscape can send new signalling coursing throughout the developing brain and adjust circuit formation (103). Chromatin remodelers control events that need to occur on DNA, and thus are ideally positioned to coordinate brain development.

Here, I focused my studies on the impact of chromatin remodeler gene *Arid1a* during cortical development. ARID1A is an integral member of the BAF chromatin remodeling complex that binds AT-rich regions of DNA to facilitate BAF targeting and ultimately BAF-mediated changes to the chromatin landscape. Over the years, *de novo* mutations in *ARID1A* have been linked to cancer, and more recently Coffin-Siris syndrome (345, 395), a multi-anomoly developmental disorder with brain phenotypes.

Accordingly, *ARID1A* is extremely intolerant to loss-of-function mutations based on the rate of mutation occurrence in a phenotypically unaffected population (gnomAD: observed/expected ratio = 0.02, pLI [Probability of being Loss-of-function Intolerant] = 1) (396). However, the function(s) of ARID1A during brain development, and thus how mutations in *ARID1A* can alter neurodevelopment, have not been unraveled.

Patients with Coffin-Siris syndrome frequently present with incomplete CC development (395), suggesting *ARID1A* might dictate cortical circuit wiring. However, ARID1A is present in both NPCs and postmitotic neurons (**Figure 2.1**) and could wield its influence in either cell type, or both, to direct connectivity. To identify whether, which projections, and via what cell type *Arid1a* might influence developmental brain wiring, I used complementary Cre mouse lines to delete *Arid1a* with spatiotemporal control. Conditional deletion of *Arid1a* from cortical NPCs near the onset of neurogenesis caused widespread misrouting of intracortical, but not corticofugal, axons. Cortical afferents were also disrupted, illustrating an indisputable non-cell autonomous role for *Arid1a*. Interestingly, sparse deletion of *Arid1a* using *in utero* electroporation (IUE) confirmed intracortical misrouting was also the result of non-cell autonomous mechanisms. Deletion of *Arid1a* from NPCs, however, did not distinguish between its necessity in NPCs, neurons, or both during cortical development. To differentiate between the possibilities, I deleted *Arid1a* specifically from postmitotic neurons during early stages of migration. Surprisingly, intracortical and thalamocortical circuit miswiring was largely rescued in deletion of *Arid1a* post-mitosis. Together, these experiments demonstrated *Arid1a* is necessary in NPCs or early in newborn neurons to non-cell autonomously influence circuitry, disruption of which occurs brain disorders.

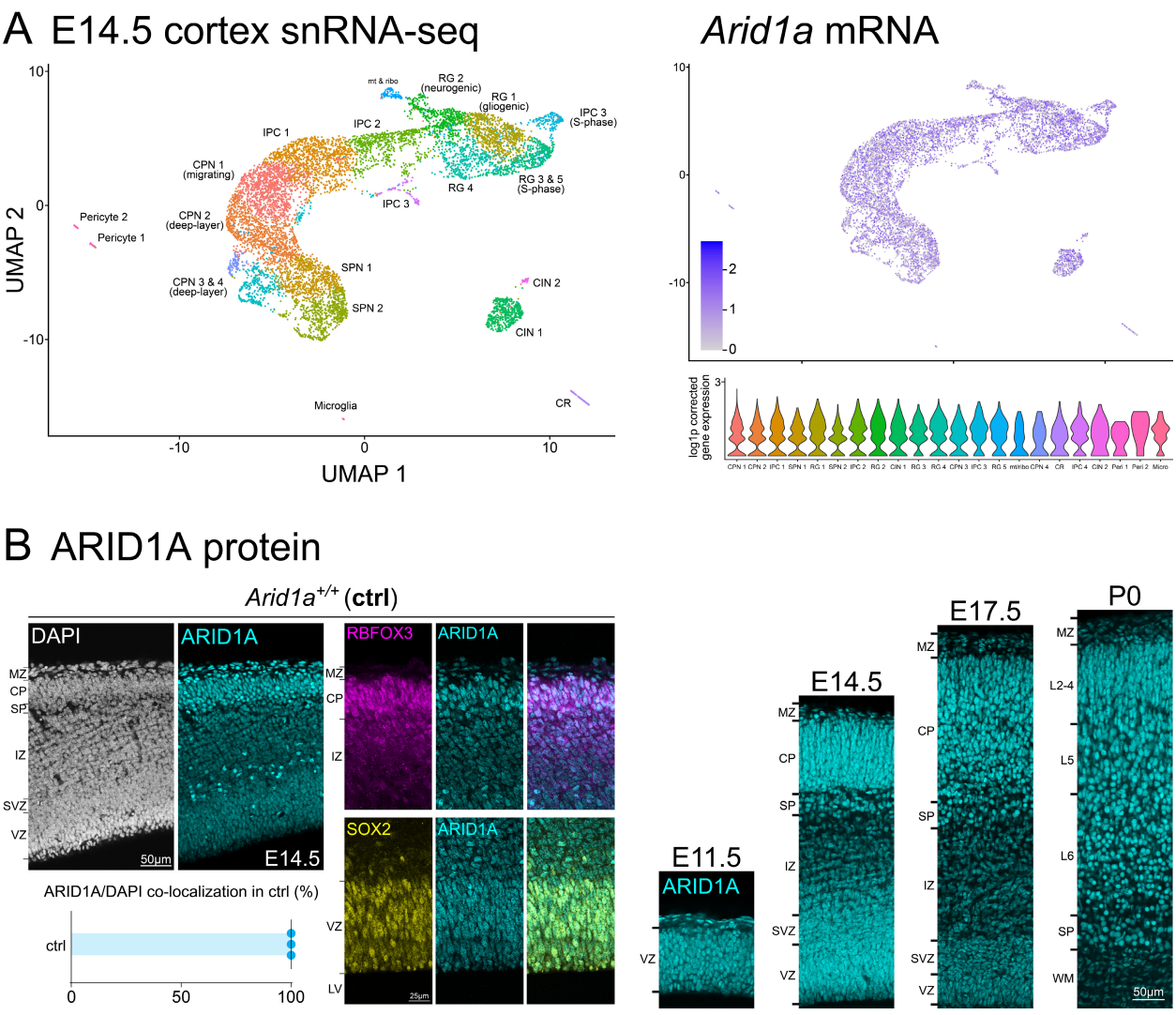

Figure 2.1 *Arid1a* is ubiquitously expressed during cortical development

(A) Visualization of *Arid1a* expression in single-nucleus RNA-seq from E14.5 wildtype cortex (103). *Arid1a* is robustly expressed in all cell types queried.

(B) Spatiotemporal analysis of ARID1A (cyan) during corticogenesis. E14.5 immunostaining of ARID1A in control brains revealed ARID1A expression in SOX2+ NPCs (yellow) and RBFOX3+ (NEUN+) neurons (magenta), and complete ARID1A colocalization with DAPI (white) (n=3 animals), supporting ubiquitous expression of ARID1A during cortical development. E11.5, E14.5, E17.5, and postnatal day P0 brain sections revealed widespread ARID1A expression during cortical development.

CIN: cortical interneuron, CPN: cortical projection neuron, IPC, intermediate progenitor cell, RGC: radial glia cell, SPN: subplate neuron, CP: cortical plate, IZ: intermediate zone, L*n*: layer *n*, LV: lateral ventricle, MZ: marginal zone, SP: subplate, SVZ: subventricular zone, VZ: ventricular zone

Results

Arid1a deletion does not broadly impair cortical layer formation

Mutations in *ARID1A* are associated with Coffin-Siris syndrome, which has nervous system features such as intellectual disability and partial to complete agenesis of the CC (395). Single-nucleus RNA-seq (103) complimented with immunostaining illustrate that *Arid1a* and its protein product are found nearly ubiquitously during corticogenesis and early postnatal development (**Figure 2.1**). At E14.5, *Arid1a* was found in all identified cell types, and ARID1A was present in all DAPI+ cells, robustly co-localized with SOX2 in the VZ, a marker of NPCs, and RBFOX3 (NEUN) in the CP, a marker of postmitotic neurons. Together, the association between *ARID1A* and Coffin-Siris syndrome, and the broad expression of ARID1A suggest a probable role in coordinating brain development. However, constitutive deletion of *Arid1a* in mouse leads to embryonic lethality by E7.5 due to an inability to form mesoderm (385). This is prior to the initial formation of the brain, and thus the function of *Arid1a* in the developing brain had not been studied. To circumvent this premature lethality, I utilized a conditional allele of *Arid1a* (385) to cell type-specifically interrogate its potential influence during brain development.

To first identify whether *Arid1a* does in fact influence cortical development, I used a Cre line which has been well-established to mediate recombination in cortical NPCs near the onset of neurogenesis, about E10.5, $Emx1^{Cre}$ (397). (**Figure 2.2 A**). I utilized a Cre-dependent reporter allele, $ROSA^{mTmG}$ (398), in which Cre-negative cells express a membrane-targeted tdTomato and Cre-positive cells express a membrane-targeted EGFP to enable visualization of where Cre was active and interrogation of gross

anatomical structures. Importantly, immunostaining at E14.5 revealed that deletion of *Arid1a* from cortical NPCs with *Emx1*^{Cre}, *Arid1a*$^{fl/fl}$; *Emx1*$^{Cre/+}$ (**cKO-E**) effectively eliminated ARID1A within the cortex from the *Emx1* lineage, while leaving it intact within *Emx1*-negative cortical endothelial cells and interneurons, and subcortical structures such as the lateral ganglionic eminence (LGE) (**Figure 2.2 B**). Importantly, cKO-E mice were born at Mendelian ratios, did not suffer premature death, and were fertile as adults, in stark contrast to the embryonic lethality of constitutive *Arid1a* deletion. These data confirm the cortical specificity of efficiency of *Emx1*^{Cre} and utility of the *Arid1a* conditional allele.

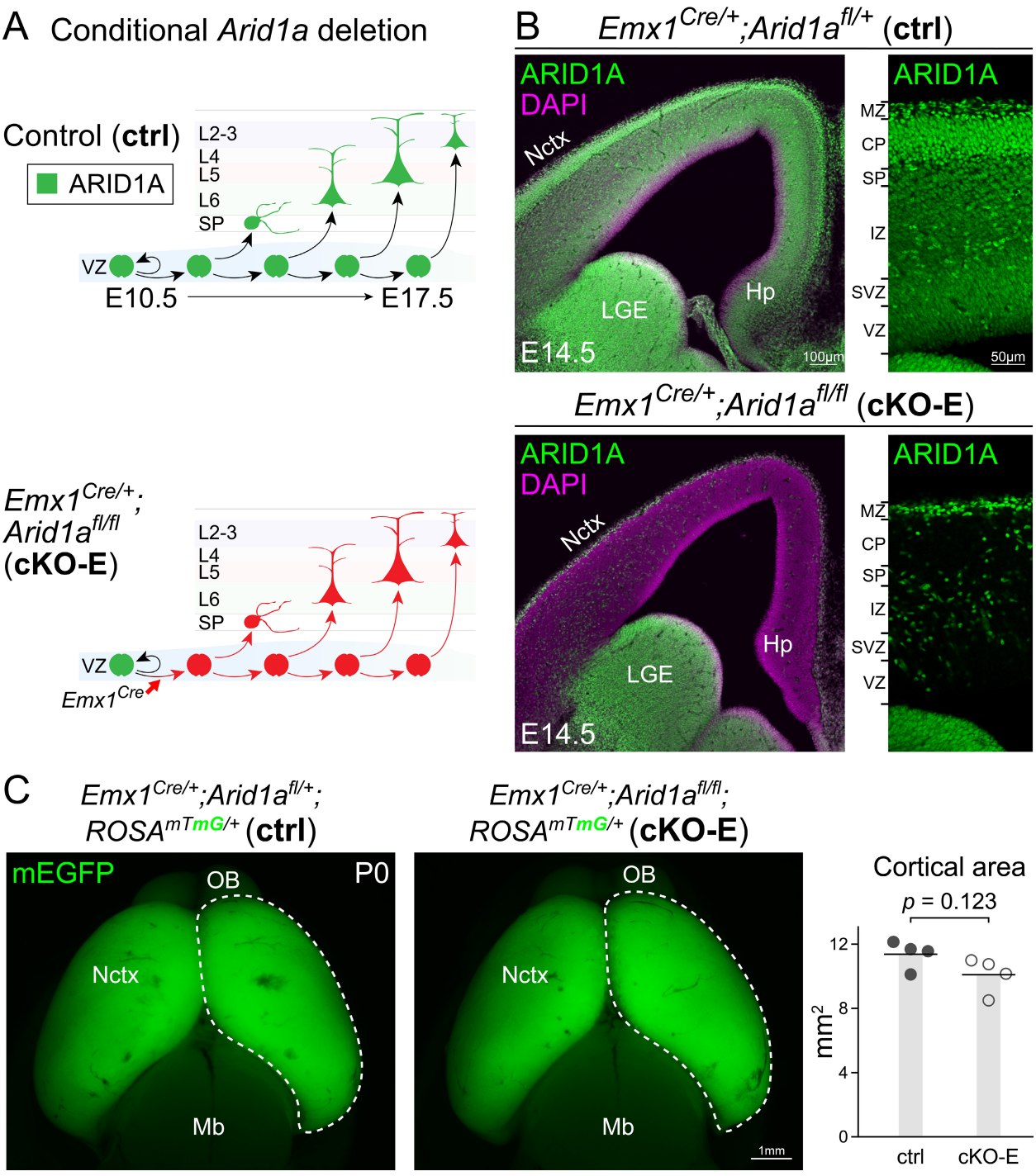

Figure 2.2: Conditional deletion of *Arid1a* in developing cortex

(A) Schematic illustration of conditional *Arid1a* deletion using $Emx1^{Cre}$, which mediates recombination in cortical NPCs at E10.5, near the onset of neurogenesis.

(B) ARID1A (green) and DAPI (magenta) staining of coronal E14.5 $Emx1^{Cre/+};Arid1a^{fl/fl}$ (cKO-E) brain sections revealed loss of ARID1A from VZ and SVZ NPCs and CP

neurons derived from *Emx1* lineage. ARID1A expression was unaffected in ventral forebrain.

(C) Dorsal view of whole mount P0 ctrl and cKO-E brains. Membrane EGFP (mEGFP, green) was expressed Cre-dependently from $ROSA^{mTmG}$. Quantitative analysis of cortical area in P0 cKO-E and ctrl (data are mean, two-tailed unpaired *t* test, n=4 animals/condition).

Nctx: neocortex, Hp: hippocampus, LGE: lateral ganglionic eminence, VZ: ventricular zone, SVZ: subventricular zone, IZ: intermediate zone, SP: subplate, CP: cortical plate, MZ: marginal zone, Mb: midbrain, OB: olfactory bulb

Initial analyses of brain size revealed that *Arid1a* deletion did not impact cortical surface area at P0 (ctrl mean= 11.37 mm^2, cKO-E mean=10.10 mm^2, p=0.123; two-tailed unpaired t test, n=4 animals/condition) **(Figure 2.2 C**). These findings are consistent with a lack of identification of micro or macrocephaly in patients with Coffin-Siris syndrome, and contrasting microcephaly resulting from mutations in chromatin remodelers which extensively regulate DNA damage repair during cortical development (e.g. *INO80*) (87, 337). However, it's possible that ARID1A could instead impact formation and identity of cortical lamination.

The layers of excitatory neurons in the neocortex follow stereotyped laminar positions and neuronal identities. In ctrl mice at P0, TBR1+ layer (L)6, BCL11B+ (CTIP2+) L5, and LHX2+ L2-5 neurons were organized in distinct and complimentary manners and distributed from the cortical white matter (WM) to the marginal zone (MZ) (**Figure 2.3 A**). In cKO-E, TBR1+, BCL11B+, and LHX2+ neurons were present, with location and distribution largely indistinguishable from ctrl. Quantitative comparisons revealed that that were no significant alterations in the number of each of these neurons at P0 in cKO-E compared to ctrl (Marker-positive neurons per 100 μm column, TBR1: ctrl mean=180.7, cKO-E mean=176.7, p=0.806; BCL11B: ctrl mean=246.3, cKO-E mean=244.3, p=0.916; LHX2: ctrl mean=272.7, cKO-E mean=276.3, p=0.875, two-tailed unpaired t test, n=3 animals/condition) (**Figure 2.3 B**). The lack of changes in broad laminar structure and identity suggested that *Arid1a* is not globally necessary for neuronal migration and fate.

Although there were no widespread alterations in cortical lamination, a striking gap appeared to fracture the LHX2+ upper layers in P0 cKO-E but not ctrl. This fissure

had a vast reduction in DAPI+ cells, indicating that it was not a change in neuronal identity within the region, but rather a disruption of the continuous cell bodies found lining the cortical wall. To identify what might be filling this space and displacing the neurons, I performed immunostaining for L1CAM, a cell adhesion molecule present on the surface of developing axons within the nervous system. In ctrl mice, L1CAM+ axons were spread somewhat through the extent of the cortical layers, and slightly enriched within the marginal zone (**Figure 2.3 A**). However, in cKO-E, L1CAM+ axons robustly filled the gap in LHX2+ upper layer neurons, and traveled together tangentially, vastly different from ctrl. Together these data indicate that *Arid1a* plays an integral role in cortical development, potentially by mediating the growth of developing axons. Thus *Arid1a* disruption could lead to altered cortical connectivity, a phenomenon likely related to callosal agenesis identified in patients diagnosed with Coffin-Siris syndrome.

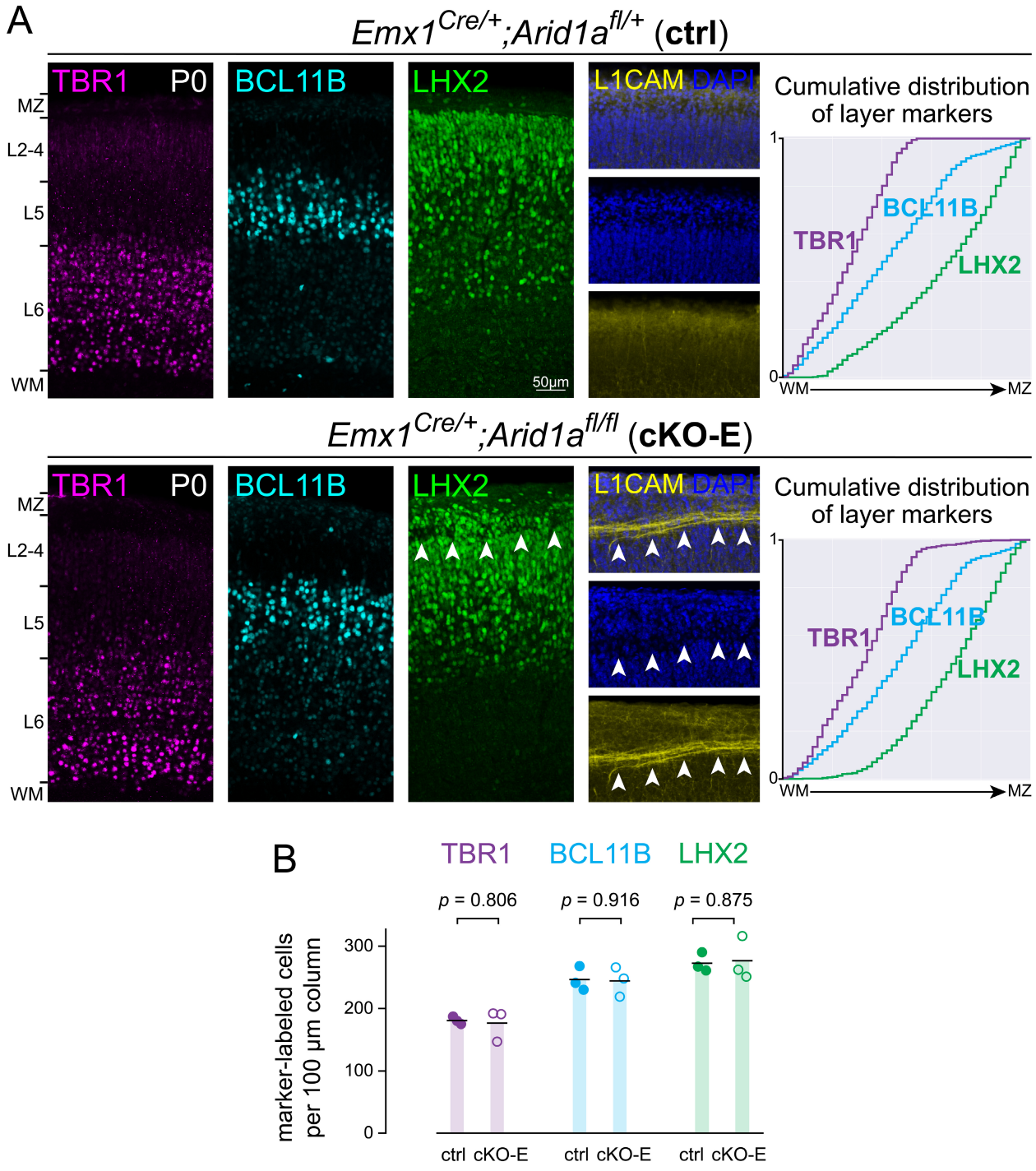

Figure 2.3 Normal cortical lamination but misrouted axons following *Arid1a* deletion

(A) Layer marker immunostaining on coronal P0 brain sections. TBR1+ (L6, magenta), BCL11B+ (L5, cyan), and LHX2+ (L2-5, green) neurons were correctly ordered in cKO-E. Analysis of cumulative distribution of layer marker-expressing neurons through thickness of cortex from white matter (WM) to marginal zone (MZ) revealed no

disruption in cortical lamination in cKO-E (n=3 animals/condition). In all analyzed cKO-E brains (3/3 animals), but none of the littermate control (ctrl) brains (0/3 animals), a stereotyped gap (arrowheads) in the upper cortical layers was observed in LHX2 and DAPI (blue) staining. This gap contained misrouted L1CAM+ (yellow) axons.

(B) Quantification of layer marker immunostaining for TBR1 (L6, magenta), BCL11B (L5, cyan), and LHX2 (L2-5, green) revealed no significant changes in P0 cKO-E compared to ctrl (data are mean, two-tailed unpaired *t* test, n=3 animals/condition).

L*n*: layer *n*, MZ: marginal zone, WM: white matter

Arid1a deletion tract-dependently disrupts cortical axons

Disruption of the LHX2+ upper layers with aberrantly positioned L1CAM+ axons in *Arid1a* cKO-E indicated that *Arid1a* could extensively regulate cortical circuit wiring during development. To examine whether deletion of *Arid1a* in cKO-E led to widespread misrouting of cortical axons, I used the Cre-dependent $ROSA^{mTmG}$ reporter. $Emx1^{Cre}$ coupled with the $ROSA^{mTmG}$ enabled anterograde tracing of all cortical excitatory neurons in ctrl and cKO-E with membrane EGFP (mEGFP), and widespread examination of projections from neurons in which *Arid1a* was deleted in cKO-E. In P0 ctrl, mEGFP beautifully revealed the three major intracortical projections: CC, AC, and hippocampal commissure (**Figure 2.4**). In striking contrast to ctrl, cKO-E had complete agenesis of the CC (CC thickness: ctrl mean=0.283 mm, cKO-E mean=0.00 mm, p=1.0e-4, two-tailed unpaired t test, n=3 animals/condition). The absence of callosal projections was not accompanied by Probst bundles, but rather widespread axonal misrouting. In cKO-E, axons visualized with mEGFP aberrantly traveled tangentially through the upper layers, projected radially through the cortical wall toward the pia and terminated in clusters near the marginal zone, and sometimes appeared to border or break through the pial surface. Furthermore, in cKO-E, presumptive axons of the AC did not cross the midline (AC midline thickness: ctrl mean=0.157 mm, cKO-E mean=0.00 mm, p=9.2e-6, two-tailed unpaired t test, n=3 animals/condition) (**Figure 2.4 B and C**). Instead, they appeared to take an alternative trajectory, diving ventrally and posteriorly toward the hypothalamus. Misrouting of CC and AC was confirmed with L1CAM immunostaining in coronal sections and $ROSA^{mTmG}$ in horizontal sections, highlighting widespread disruption of axonal trajectories (**Figure 2.5**). Accompanying loss of CC and

AC in cKO-E, cortical deletion of *Arid1a* impaired development of the hippocampus (**Figure 2.6**). Not only was the hippocampal commissure disrupted, but the hippocampus itself was hypoplastic and disorganized (hippocampal area: ctrl mean=0.609 mm^2, cKO-E mean=0.342 mm^2, p=7.0e-3, two-tailed unpaired t test, n=3 animals/condition). Axonal trajectories were visibly altered and the fornix, the major output of the hippocampus, was qualitatively reduced. These data identified a severe necessity for *Arid1a* in the initial formation of intracortical axon tracts.

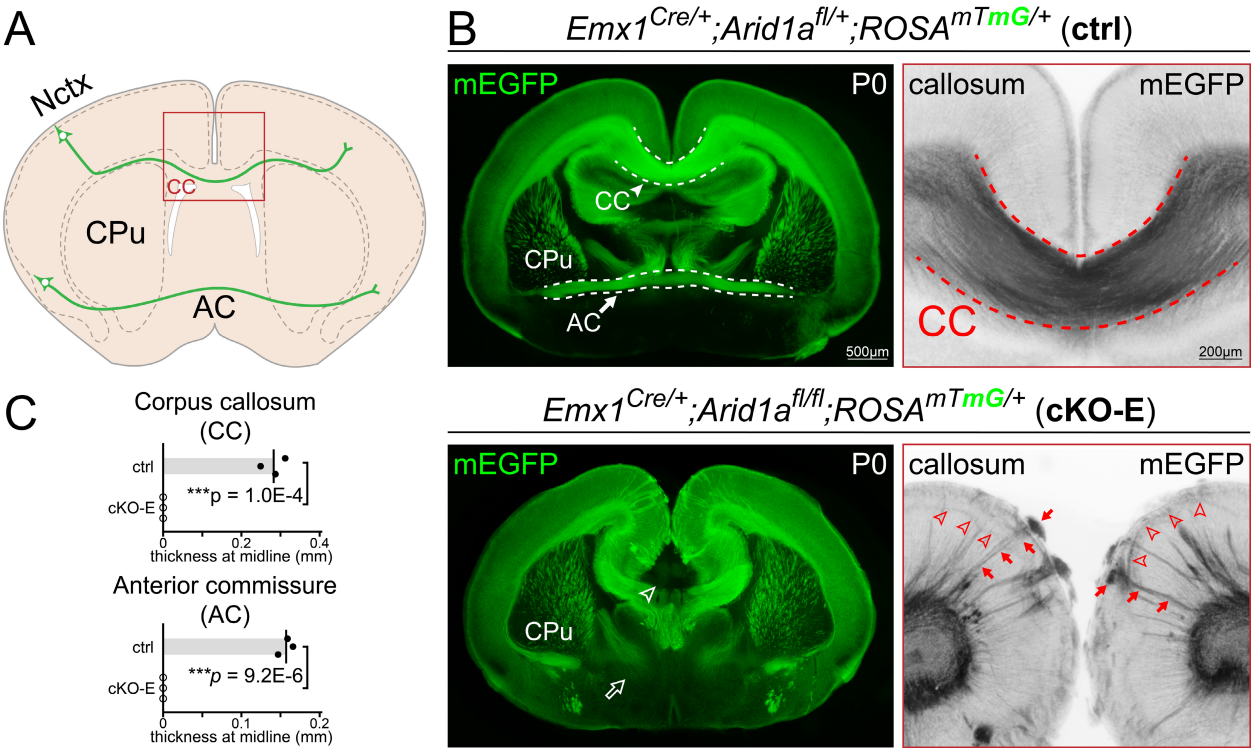

Figure 2.4 Widespread misrouting of intracortical projections in cKO-E

(A) Schematic illustration of interhemispheric intracortical projections on coronal section.

(B) Coronal sections of P0 ctrl and cKO-E brains. Membrane EGFP (mEGFP, green) was expressed Cre-dependently from *ROSA*^{mTmG}, enabling visualization of cortical axons. Agenesis of corpus callosum (open arrowhead) was observed in cKO-E (n=3/3 animals). The anterior commissure also failed to form (open arrow). The cKO-E cortex was characterized by widespread axon misrouting (n=3/3 animals), including radially-directed axons extending to the pia (red arrows) and tangentially-directed axons travelling across the upper layers (red arrowheads).

(C) Quantification of corpus callosum and anterior commissure thickness at midline (data are mean, two-tailed unpaired *t* test, n=3 animals/condition).

AC: anterior commissure, CC: corpus callosum, CPu: caudate putamen, Nctx: neocortex

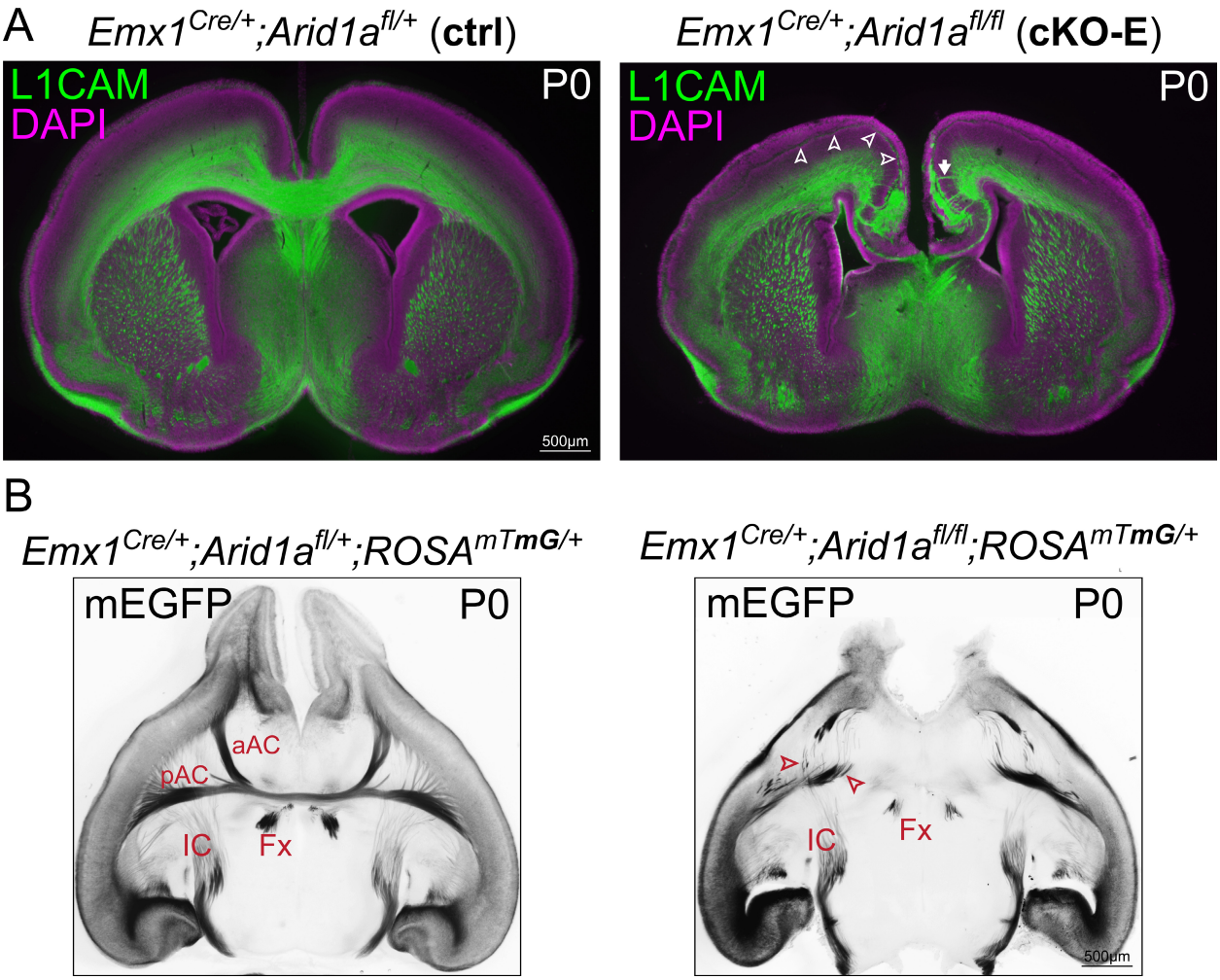

Figure 2.5 Validation of intracortical misrouting following *Arid1a* deletion

(A) Validation of callosal agenesis and misrouting in coronal sections. L1CAM (green) displayed misrouted axons traveling tangentially throughout the upper layers (arrowheads) and radially toward the midline (arrow) in P0 cKO-E but not ctrl.

(B) Horizontal sections of P0 ctrl and cKO-E brains. Visualization of cortical projections by *ROSA*^{mTmG} (black) uncovered in cKO-E misrouting of presumptive anterior commissure axons (arrowheads), which failed to cross the midline. Corticofugal axons, however, innervated the internal capsule (IC) in cKO-E without apparent deficit. Hippocampal axons innervating the fornix (Fx) were present in cKO-E, although that innervation was qualitatively reduced compared to ctrl.

aAC: anterior branch of the anterior commissure, pAC: posterior branch of the anterior commissure, Fx: fornix, IC: internal capsule

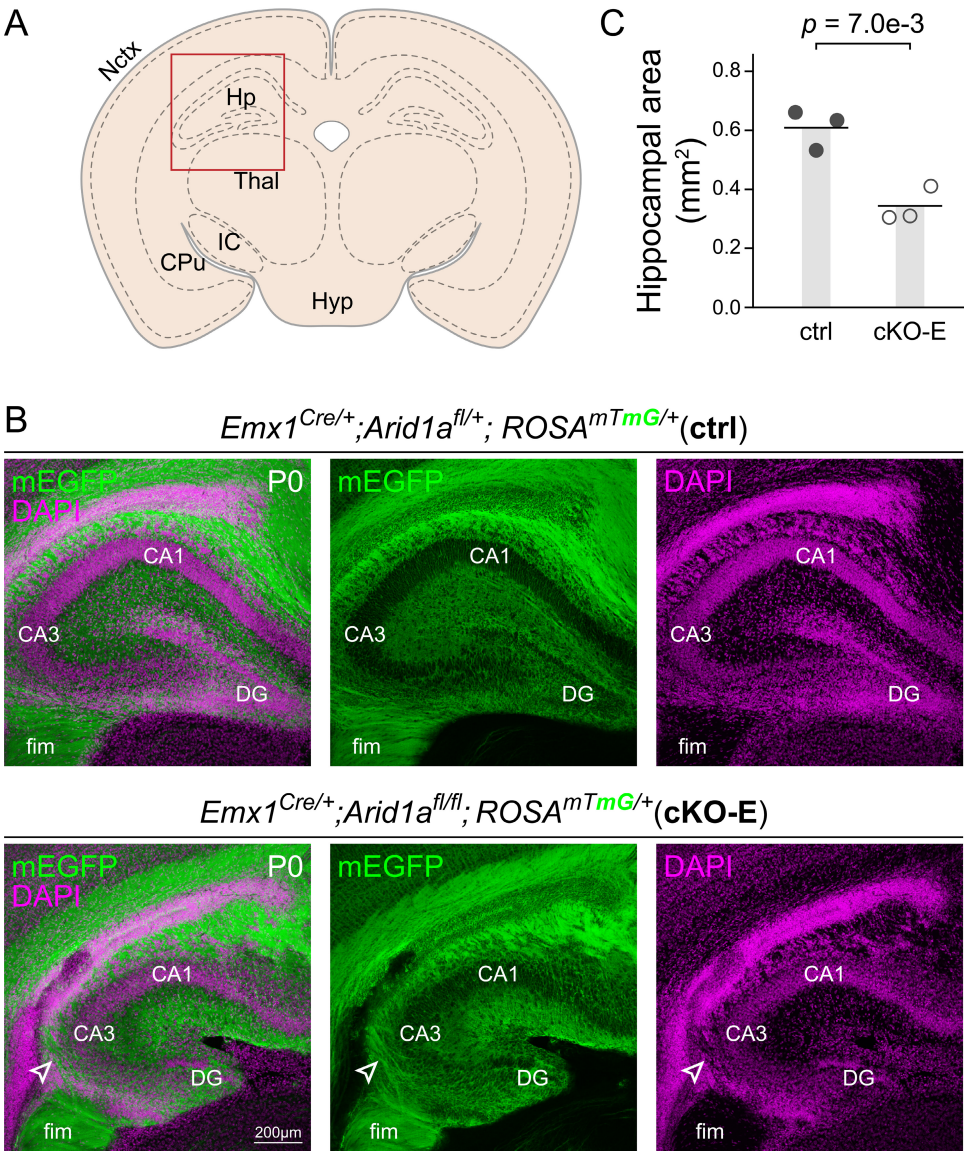

Figure 2.6 Hippocampal agenesis following *Arid1a* deletion

(A) Schematic illustration showing coronal hippocampal inset (red box) in (B).

(B) Coronal sections of P0 ctrl and cKO-E hippocampus. DAPI (magenta) and mEGFP (green) revealed hippocampal hypoplasia and axon misrouting (open arrowhead) in cKO-E.

(C) Quantification of P0 hippocampal area revealed a significant reduction and thus hypoplasia in cKO-E (n=3 animals/condition).

CA: Cornu ammonis, CPu: caudate putamen, DG: dentate gyrus, fim: fimbria, Hp: hippocampus, Hyp: hypothalamus, IC: internal capsule, Thal: thalamus

While upper layer cortical neurons project exclusively intracortically (e.g. CC), deep layer neurons project largely corticofugally, sending information from the cortex to subcortical structures such as the thalamus and spinal cord (21). To examine whether *Arid1a* deletion in cKO-E also impacted the development of corticofugal projections I used the same Cre-dependent anterograde tracing strategy with *ROSA*^{mTmG} (**Figure 2.7**). In sagittal sections of P0 ctrl, mEGFP+ axons could be seen extending out of the cortex and traveling through the internal capsule to their final targets in dorsal thalamus, tectum (inferior and superior colliculi), and spinal cord. In contrast to intracortical misrouting in cKO-E, these corticofugal projections (corticothalamic, corticotectal, and corticospinal) were qualitatively reduced in their strength, but appeared to follow the correct trajectories out of the cortex and to their destinations. Corticothalamic rounded through the internal capsule and turned dorsally into the thalamus, corticotectal extended sufficiently into the midbrain, and corticospinal projected caudally past the pons prior to decussating and entering the spinal cord. Altogether the extensive misrouting of intracortical, but not corticofugal, connectivity supported a tract-dependent and potentially target-based necessity for *Arid1a* in orchestrating cortical circuit wiring.

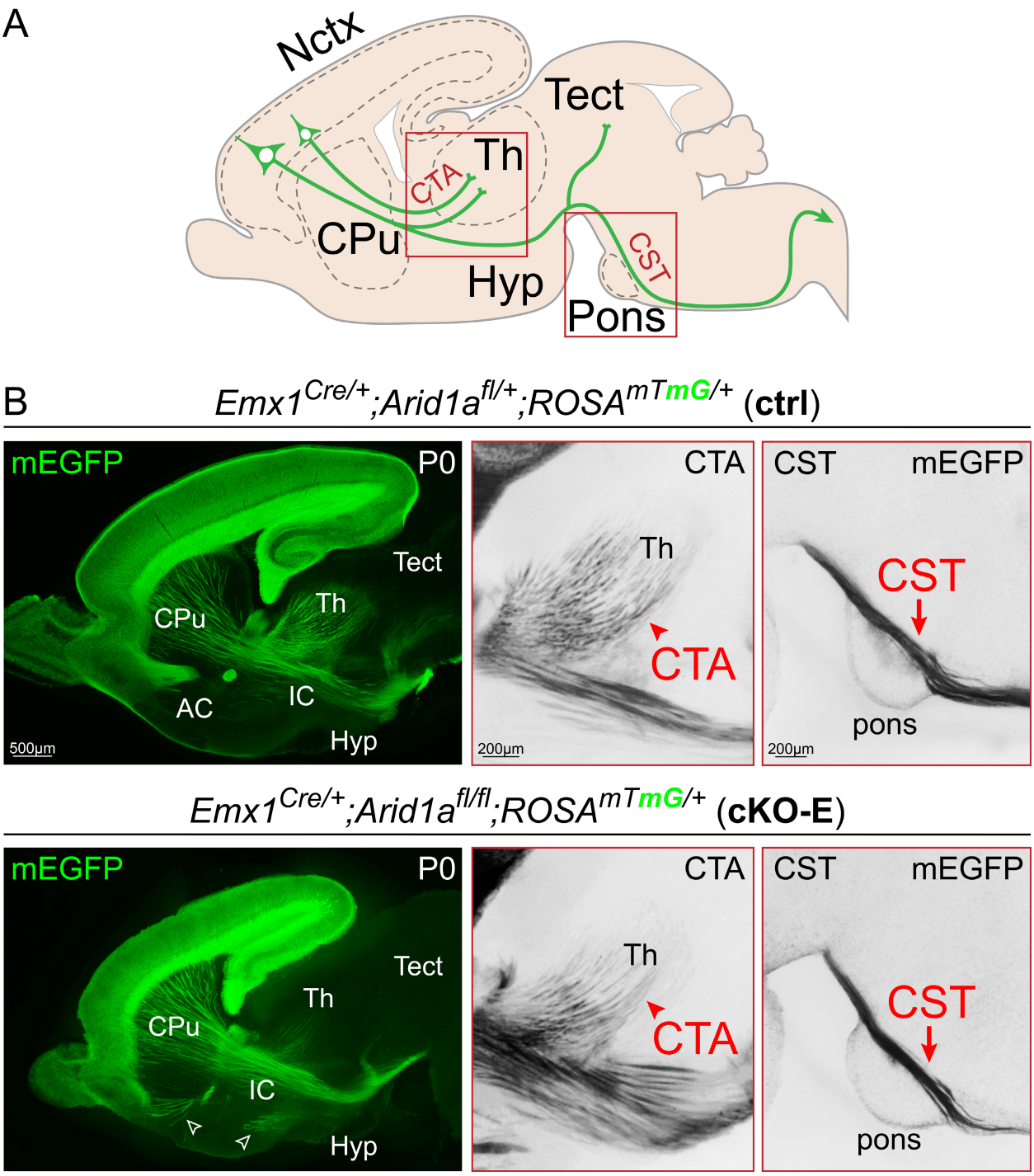

Figure 2.7 Deletion of *Arid1a* did not extensively misroute cortical efferents

(A) Schematic illustration of corticofugal projections.

(B) Sagittal sections of P0 ctrl and cKO-E brains. In cKO-E, corticofugal axons innervated internal capsule (IC) without defect. The trajectories of corticothalamic axons (CTA, red arrowheads), corticotectal axons, and corticospinal tract axons (CST, red

arrows) were unaffected in cKO-E. Axons from anterior commissure (AC) were misrouted to hypothalamus (Hyp, open arrowheads).

AC: anterior commissure, CPu: caudate putamen, CST: corticospinal tract, CTA: corticothalamic axons, Hyp: hypothalamus, IC: internal capsule, Tect: tectum, Th: thalamus

Proper thalamocortical circuit wiring requires cortical Arid1a

The extensive misrouting of intracortical, but not corticofugal axons in *Arid1a* cKO-E illustrated a striking, tract-dependent role for *Arid1a* within the developing cortex. To examine whether *Arid1a* was required in the developing cortex to guide early cortical afferents, those which originate outside the cortex and subsequently travel into it, I examined TCAs (**Figure 2.8**). TCAs bring sensory information from the thalamus into the cortex. Importantly, in cKO-E, Cre expression is restricted to NPCs of the cortex, and thus *Arid1a* is still expressed by thalamocortical neurons.

In ctrl by P7, TCAs robustly innervated the cortex, and organized into stereotypical whisker barrels corresponding to sensory information from each mouse whisker. In cytochrome oxidase (CO) staining of ctrl tangential sections, the overall structure of barrel cortex was consistently observed (n=3 animals) (**Figure 2.8 B** and **Figure 2.9 A**). And in ctrl coronal sections, NTNG1+ TCAs formed discrete, stereotyped, and organized barrels in somatosensory cortex (n=3 animals). However, *Arid1a* cortical deletion led to extensive alterations in barrel formation. At P7 cKO-E TCAs did not form barrel-like structures that could be visualized with either CO or NTNG1 staining. Instead, the TCAs were defasciculated within the developing WM and only formed distorted and disorganized clusters (n=3 animals).

TCAs follow a precise and well-established developmental trajectory in which they travel from the thalamus through the subpallium, cross the PSB into the pallium around E14.5 (298), enter the cortex and wait in the SP around E15.5 while their L4 targets are being born and migrating (246, 263, 399), begin growing into the CP near E18.5 (298), and refine their projections and organize into discrete patterns (e.g.

whisker barrels) by P5 (299). *Arid1a* deletion in cKO-E resulted in loss of TCA organization by P7, but to identify where misrouting or impairments where originating during TCA developmental. In P0 ctrl, NTNG1+ TCAs had begun growing into cortical layers, but largely remained in cortical WM, L6, and MZ (n=3 animals) (**Figure 2.8 C**). However, in P0 cKO-E, NTNG1+ TCAs now traveled dorsally throughout the cortical layers and tangentially traversed through the upper layers toward the midline (n=3 animals). Interestingly, immunostaining for NTNG1 and L1CAM or mEGFP (from $ROSA^{mTmG}$) revealed TCAs did not majorly contribute to radially-directed misrouted axons in cKO-E (**Figure 2.8 C** and **Figure 2.9 B**).

Around E15.5, TCAs have reached the cortex and go through a “waiting period” within the SP. The TCA misrouting in cKO-E at P0 introduced the possibility that following cortical deletion of *Arid1a* in cKO-E, TCAs improperly entered the CP, potentially bypassing the “waiting period” and resulting in the lack of final TCA organization. At E15.5 in ctrl, NTNG1+ TCAs beautifully illustrated the “waiting period” in both medial and lateral compartments of the cortex; after traversing the PSB, they paused their ingrowth within SP and did not enter the CP (n=3 animals) (**Figure 2.8 D**). However, this regulation went largely unnoticed in cKO-E. In E15.5 cKO-E, NTNG1+ axons failed to properly cross the PSB, and instead appeared to take a narrow and more medial, aberrant route (n=3 animals), which could still be seen at E17.5 (**Figure 2.9 C**). Additionally, TCAs in cKO-E bypassed the “waiting period” in SP at E15.5 and prematurely exited WM while prematurely invading CP in both medial and lateral cortex (n=3 animals) (**Figure 2.8 D**). This was even more apparent by E16.5 (**Figure 2.8 E**).

Arid1a cKO-E is characterized by widespread disruption of TCAs beginning during cortical ingrowth and continuing through whisker barrel formation. However, *Emx1*^{Cre} is not active in thalamic neural progenitors or thalamic neurons (397). Thus, TCA misrouting in cKO-E highlights a non-cell autonomous requirement for cortical *Arid1a* in directing development of cortical afferents.

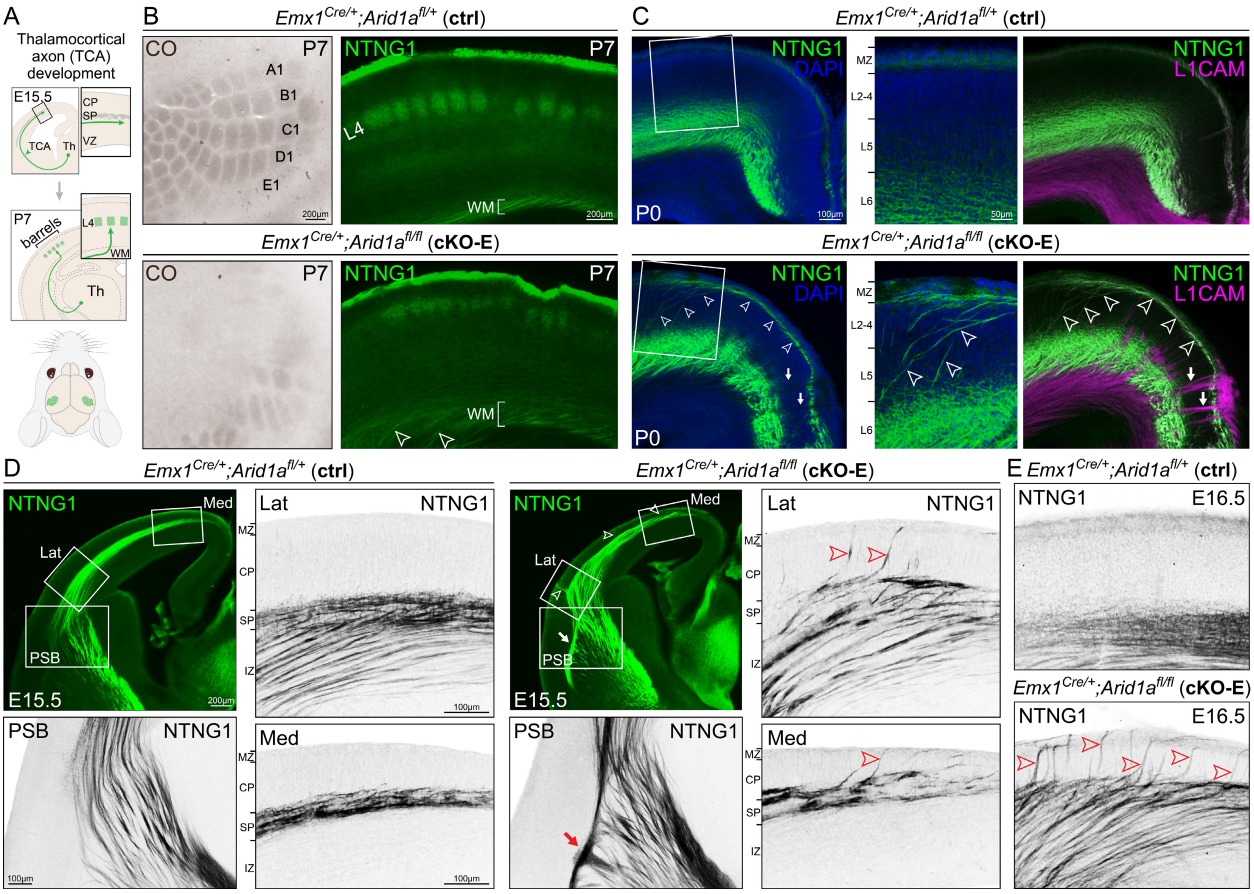

Figure 2.8 Non-cell autonomous disruption of thalamocortical axon pathfinding following *Arid1a* deletion

(A) Schematic illustration of thalamocortical axon (TCA) development.

(B) Whisker barrels in P7 ctrl and cKO-E primary somatosensory cortex were visualized by cytochrome oxidase staining (CO, brown) on flattened cortices and NTNG1 immunostaining (green) on coronal sections. In cKO-E, barrel formation was severely disrupted (n=4/4 animals). Many barrels were missing and the remaining barrels were distorted or disorganized. NTNG1+ thalamocortical axons were defasciculated in cortical white matter (open arrowheads) in cKO-E.

(C) NTNG1 immunostaining (green) on coronal sections of P0 ctrl and cKO-E brains. In ctrl, NTNG1+ thalamocortical axons were present in white matter and L6, as well as marginal zone (MZ). In cKO-E, NTNG1+ thalamocortical axons were markedly misrouted, extending dorsally from white matter through the cortical layers (arrowheads). These aberrant axons then travelled tangentially across the upper layers and toward the midline. NTNG1+ thalamocortical axons did not contribute to the abnormal radially-directed axon bundles labeled by L1CAM (magenta, arrows) in cKO-E.

(D) Analysis of thalamocortical axon development in E15.5 ctrl and cKO-E cortex. In ctrl, NTNG1+ thalamocortical axons extended across the pallial-subpallial boundary (PSB) and were paused within the subplate (SP) during the embryonic “waiting” period. In cKO-E, NTNG1+ thalamocortical axons did not cross the PSB along the normal trajectory (n=3/3 animals). They formed an aberrant bundle of axons parallel to the PSB (red arrow) and entered the cortex via an abnormal dorsal path. Notably, NTNG1+ thalamocortical axons prematurely invaded the cortical plate (CP) in both lateral (Lat) and medial (Med) cortex (red arrowheads) (n=3/3 animals). The trajectory of these axons was similar to that of the misrouted thalamocortical axons in the P0 cKO-E cortex (arrowheads in *C*).

(E) Analysis of E16.5 ctrl and cKO-E cortex revealed an abundance of NTNG1+ thalamocortical axons prematurely invading the cortical plate (red arrowheads).

CP: cortical plate, IZ: intermediate zone, Lat: lateral, L*n*: layer *n*, Med: medial, MZ: marginal zone, PSB: pallial-subpallial boundary, SP: subplate, TCA: thalamocortical axon, Th: thalamus, VZ: ventricular zone, WM: white matter

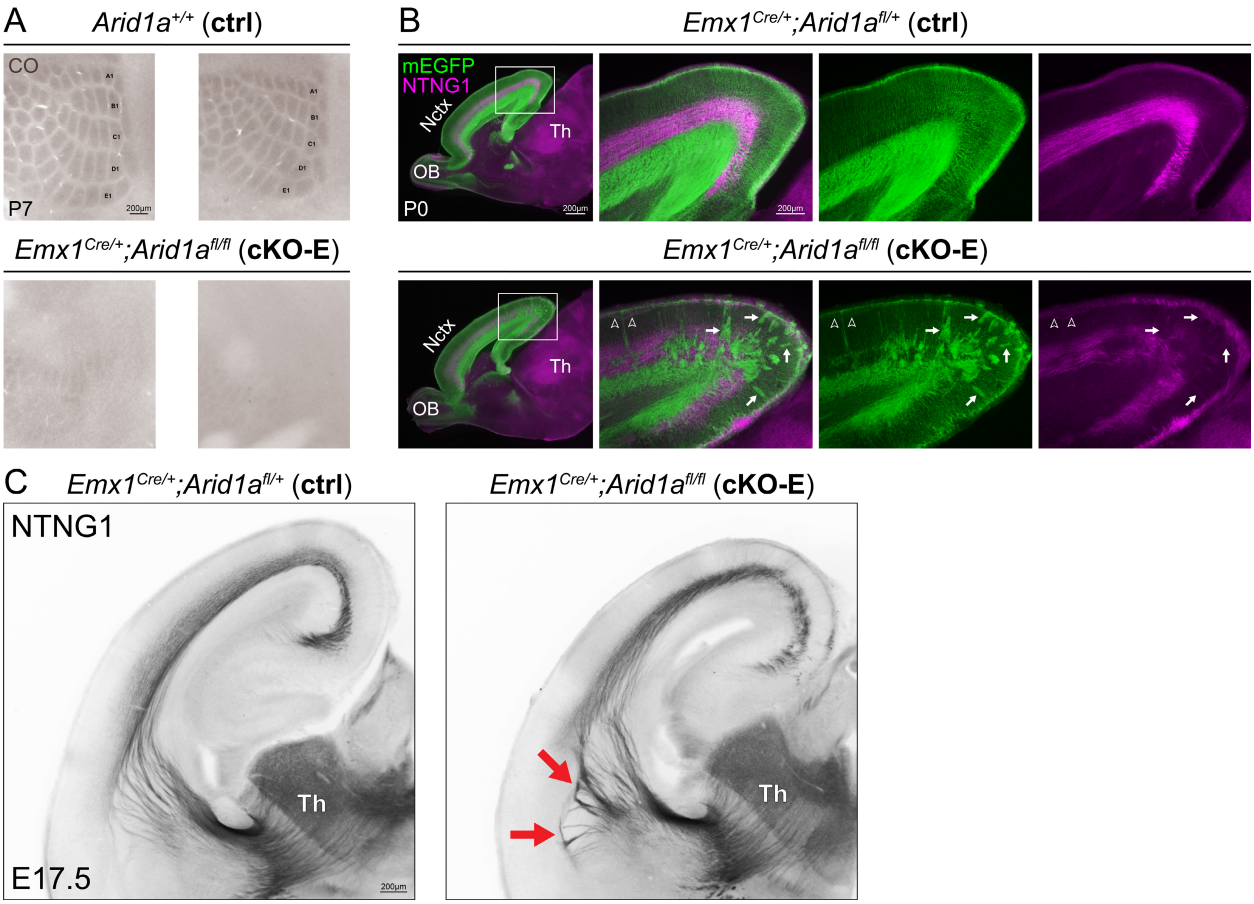

Figure 2.9 Altered thalamocortical innervation following *Arid1a* deletion

(A) Cytochrome oxidase (CO, brown) staining of flattened P7 control and cKO-E cortex. Whisker barrels were stereotypically organized in ctrl but largely absent from cKO-E.

(B) mEGFP (green) and NTNG1 (magenta) immunostaining on sagittal sections of P0 ctrl and cKO-E brains. Both mEGFP+ cortical axons and NTNG1+ thalamocortical axons contributed to the tangentially-directed aberrant axons in the upper layers (open arrowheads) in cKO-E. Only mEGFP+ cortical axons were misrouted into radially-directed bundles toward the pia (arrows).

(C) NTNG1 immunostaining (black) on coronal sections of E17.5 ctrl and cKO-E brains. In cKO-E, NTNG1+ thalamocortical axons failed to correctly cross the pallial-subpallial boundary (PSB), formed dense axon bundles parallel to the PSB (arrows), and entered the cortex via an aberrant medial path.

Nctx: neocortex, OB: olfactory bulb, Th: thalamus

Callosal formation non-cell autonomously requires Arid1a

CC development is a culmination of cell and non-cell autonomous mechanisms by which cortical neurons acquire their identities, extend their axons across the midline, and connect the two cortical hemispheres in both a homotopic and heterotopic fashion. Misrouting of TCAs in *Arid1a* cKO-E introduced the possibility that callosal agenesis and misrouting in cKO-E could also be a result of impaired non-cell autonomous mechanisms. To query whether intracortical misrouting resulted from disruption of non-cell autonomous *Arid1a* functions, I utilized IUE to sparsely delete *Arid1a* from likely callosally-projecting upper-layer neurons. IUE introduces DNA into the lateral ventricles of a developing embryo and use of electric current to transfect NPCs lining the ventricular wall, thereby providing a platform for spatiotemporally controlled manipulation of subsets of NPCs and their subsequent progeny.

To manipulate *Arid1a* via IUE, I first generated a self-excising and self-reporting *Cre* plasmid (CAG-sxiCre-EGFP). The construct was designed in the following order: 1) CAG Promoter for broad, robust expression; 2) loxP-flanked, intron-containing *iCre* with polyA signal for Cre expression in eukaryotic cells and self-removal to avoid Cre toxicity; and 3) *EGFP* with WPRE and polyA to enable strong expression following self-excision of *Cre* (**Figure 2.10 A**). I initially tested the efficacy of CAG-sxiCre-EGFP by transfecting cortical NPCs at E14.5 via IUE and analyzing cortices at P0 (**Figure 2.10 B**). In ctrl mice which have one wildtype allele of *Arid1a* that is unaffected by Cre (*Arid1a*$^{fl/+}$), 100% of EGFP+ cells at P0 still had robust ARID1A immunostaining. However, conditional-ready *Arid1a* mice without genomic *Cre* (sparse deletion by Cre transfection, *Arid1a*$^{fl/fl}$), CAG-sxiCre-EGFP had an *Arid1a* deletion efficacy of 97.67% in EGFP+ cells (proportion of

EGFP+ cells expressing ARID1A: ctrl mean=1.00, sparse deletion mean=0.233, *p*=1.95e-6, two-tailed unpaired *t* test, n=3 animals/condition).

After confirming the efficacy of CAG-sxiCre-EGFP, I performed IUE of *Arid1a*$^{fl/+}$ (ctrl), cKO-E, and *Arid1a*$^{fl/fl}$ (sparse deletion by Cre transfection) mice at E14.5 to target NPCs producing upper layer neurons likely with callosal projections (**Figure 2.11**). In P0 ctrl, EGFP+ cells were located within L2-4 projected robustly interhemispherically. In cKO-E, with pancortical *Arid1a* deletion, EGFP+ cells still migrated to the upper layers but were reduced in their organization qualitatively, likely due to misrouted axons present within the cortex prior to upper layer neurons reaching the cortical plate (e.g. TCAs). Consistent with callosal agenesis revealed by L1CAM and mEGFP (from *ROSA*^{mTmG}) immunostaining, EGFP+ axons in cKO-E completely failed to traverse the midline and instead contributed to the aberrant projections radially toward the pia. Sparse deletion of *Arid1a* did not impair migration of EGFP+ neurons to the upper layers, and in stark contrast to cKO-E, EGFP+ axons abundantly projected into the CC and into the contralateral hemisphere, indistinguishable from ctrl. Together, these data provided strong evidence for *Arid1a* non-cell autonomously directing the development of both thalamocortical and callosal connectivity.

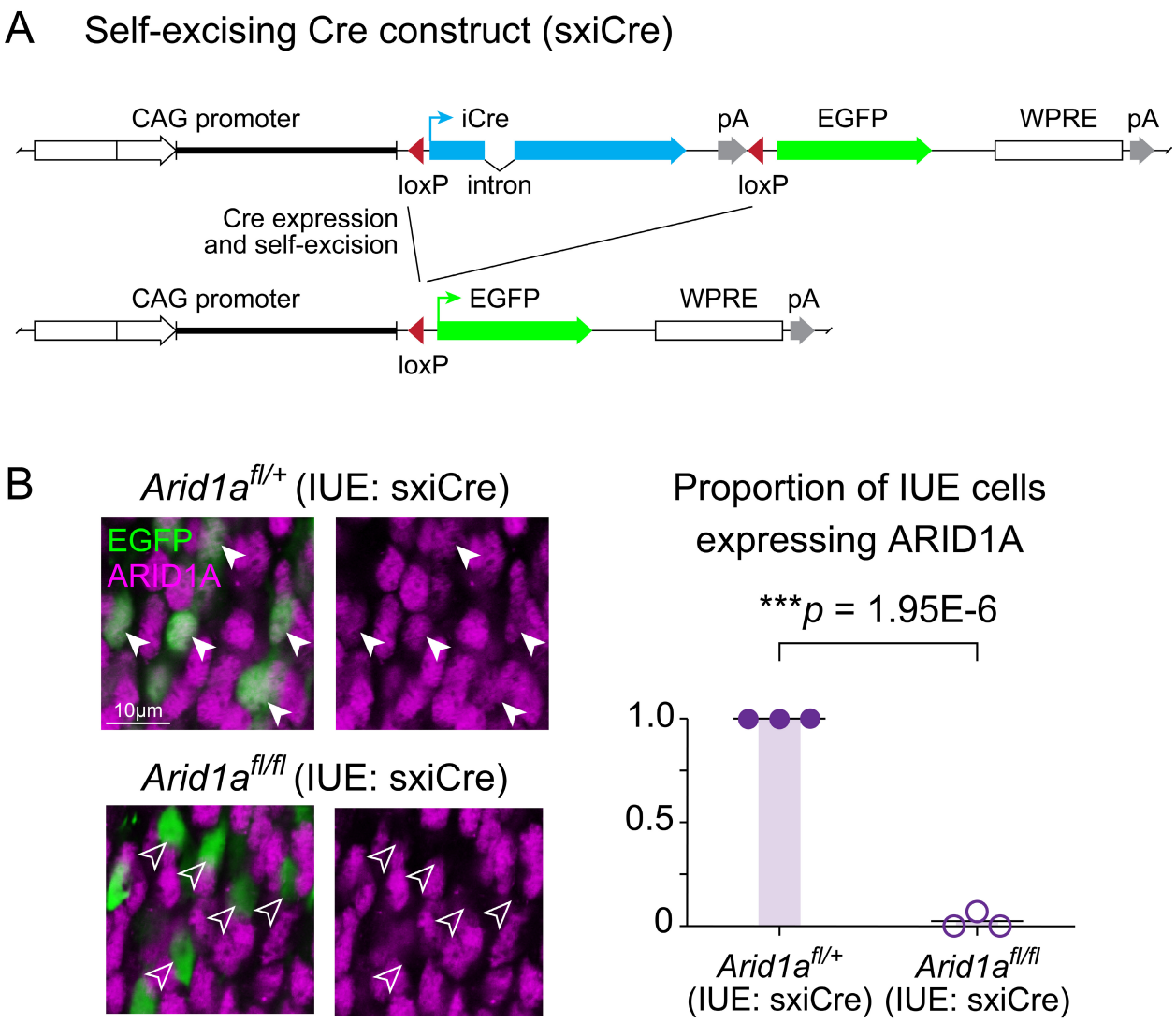

Figure 2.10 Validation of self-excising Cre-mediated *Arid1a* deletion

(A) Schematic illustration of a self-excising Cre expression EGFP reporter construct (sxiCre) used for sparse deletion of *Arid1a* via *in utero* electroporation (IUE).

(B) Successful deletion of *Arid1a* in *Arid1a*$^{fl/fl}$ mice (without genetic Cre) following sxiCre IUE was confirmed by ARID1A (magenta) and EGFP (green) immunostaining. ARID1A was lost (open arrowheads) from 97.67% of EGFP+ transfected cells in *Arid1a*$^{fl/fl}$ mice (data are mean, two-tailed unpaired *t* test, n=3 animals/condition).

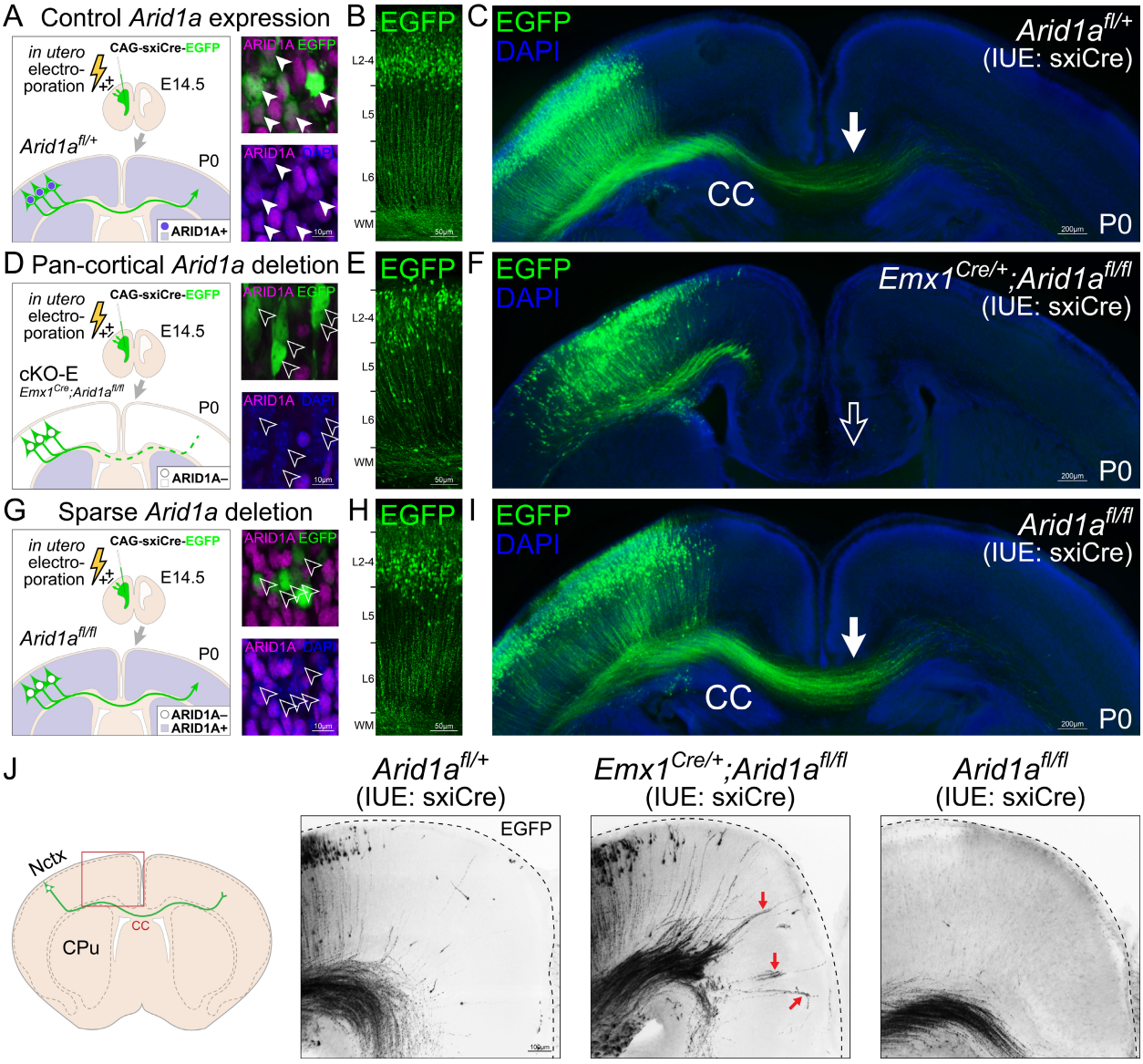

Figure 2.11 Correct callosal axon targeting following sparse deletion of *Arid1a*

A self-excising Cre expression EGFP reporter construct (CAG-sxiCre-EGFP or sxiCre) was transfected into dorsal cortical NPCs of *Arid1a*$^{fl/+}$ (control, A), *Emx1*$^{Cre/+}$*;Arid1a*$^{fl/fl}$ (cKO-E, D), and *Arid1a*$^{fl/fl}$ (without genetic Cre, G) using *in utero* electroporation at E14.5. At P0, ARID1A expression (magenta) was analyzed in EGFP+ transfected cells by immunostaining. ARID1A was present in transfected control EGFP+ cells (solid arrowheads, A), but was lost following pan-cortical genetic *Arid1a* deletion (cKO-E, open arrowheads, D) or sparse *Arid1a* deletion (*Arid1a*$^{fl/fl}$, open arrowheads, G). EGFP+ cells migrated correctly to the upper cortical layers in each condition (B, E, H). EGFP+ axons innervated the corpus callosum (CC) in control (solid arrow, C), but failed to do so following broad *Arid1a* deletion in cKO-E (open arrow, F). Remarkably, sparse deletion of *Arid1a* from *Arid1a*$^{fl/fl}$ EGFP+ cells did not disrupt their innervation of the corpus callosum (solid arrow, I). Loss of ARID1A expression from these cells (open arrowheads, G) following sparse *Arid1a* deletion did not cell autonomously cause a

callosal axon misrouting defect. Dorsally radiating axons could be identified in cKO-E, but not ctrl or sparse *Arid1a* deletion following IUE of sxiCre (red arrows, J).

CC: corpus callosum, L*n*: layer *n*, WM: white matter

Arid1a is not required in postmigratory neurons for circuit formation

Arid1a is expressed ubiquitously during cortical development, in both NPCs and postmitotic neurons. Thus, *Arid1a* could exert its non-cell autonomous influence via a role in NPCs, newborn excitatory neurons, or postmigratory excitatory neurons. To distinguish between these possibilities, I conditionally deleted *Arid1a* from cortical excitatory neurons shortly after their genesis using *Neurod6*^{Cre} (*Nex*^{Cre}), *Neurod6*$^{Cre/+}$; *Arid1a*$^{fl/fl}$ (**cKO-N**) (**Figure 2.12 A**) (400). *Neurod6*^{Cre} activity was confirmed at E14.5 using Cre-dependent tdTomato (*ROSA*^{tdTomato}) (401) within the IZ and CP. In E14.5 cKO-N, ARID1A was intact in SOX2+ NPCs within the VZ, and was present partially during migration through the IZ, but not visible once NEUN+ neurons settled in the CP (**Figure 2.12 B**). Thus, cKO-N could identify whether ARID1A is required post-migration to non-cell autonomously coordinate callosal and thalamocortical development.

In cKO-E, pancortical *Arid1a* deletion led to complete callosal agenesis. To determine whether neuron-specific cortical deletion of *Arid1a* impacted cortical connectivity, I used *ROSA*^{mTmG} in cKO-N to visualize cortical axons (**Figure 2.13 A-D**). In P0 ctrl, mEGFP+ axons extended extensively across the midline and into the contralateral hemisphere. Surprisingly, and contrasting cKO-E, CC mEGFP in P0 cKO-N was indistinguishable from ctrl. It elaborately connected the cortical hemispheres and did not display callosal agenesis (CC thickness: ctrl mean=0.257 mm, cKO-N mean=0.241 mm, p=0.57, two-tailed unpaired t test, n=3 animals/condition). However, AC was not rescued in cKO-N, underlining distinct mechanisms for CC and AC development.

To determine whether this early necessity for cortical *Arid1a* was also true for TCA targeting, I analyzed NTNG1 immunostaining (**Figure 2.13 E**). Although cKO-E displayed disruption of thalamocortical innervation, postmitotic *Arid1a* deletion in cKO-N restored whisker barrel formation. NTNG1+ axons were no longer defasciculated in the WM and barrels were stereotyped and organized. Together, these data suggested *Arid1a* was necessary in NPCs or before migratory completion in postmitotic excitatory neurons to non-cell autonomously direct cortical connectivity.

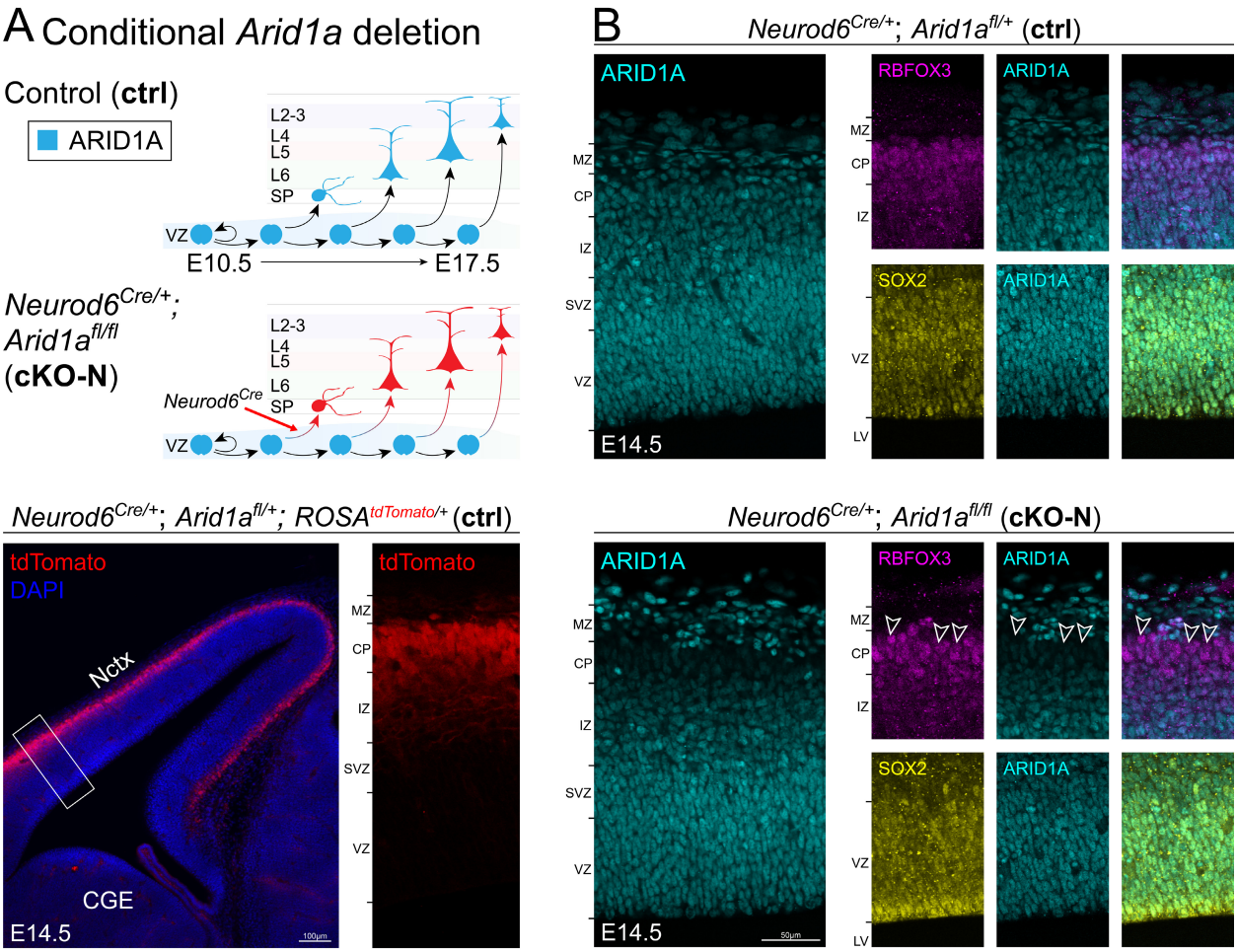

Figure 2.12 *Arid1a* postmitotic neuronal deletion with *Neurod6*^{Cre}

(A) Schematic illustration of conditional *Arid1a* deletion using *Neurod6*^{Cre}, which mediates recombination in cortical excitatory neurons shortly after their genesis. Visualization of Cre activity at E14.5 with *ROSA*^{tdTomato} revealed tdTomato (red) within the IZ and CP but not in the NPC locales of the VZ and SVZ.

(B) At E14.5, ARID1A (cyan) was present throughout ctrl cortex. In cKO-N, ARID1A was still robustly expressed in SOX2+ (yellow) NPCs within the VZ but diminished in a gradient through the IZ. After reaching the CP, RBFOX3+ (magenta) neurons were largely devoid of ARID1A (arrowheads).

CGE: caudal ganglionic eminence, CP: cortical plate, LV: lateral ventricle, IZ: intermediate zone, MZ: marginal zone, Nctx: neocortex, SVZ: subventricular zone, VZ: ventricular zone

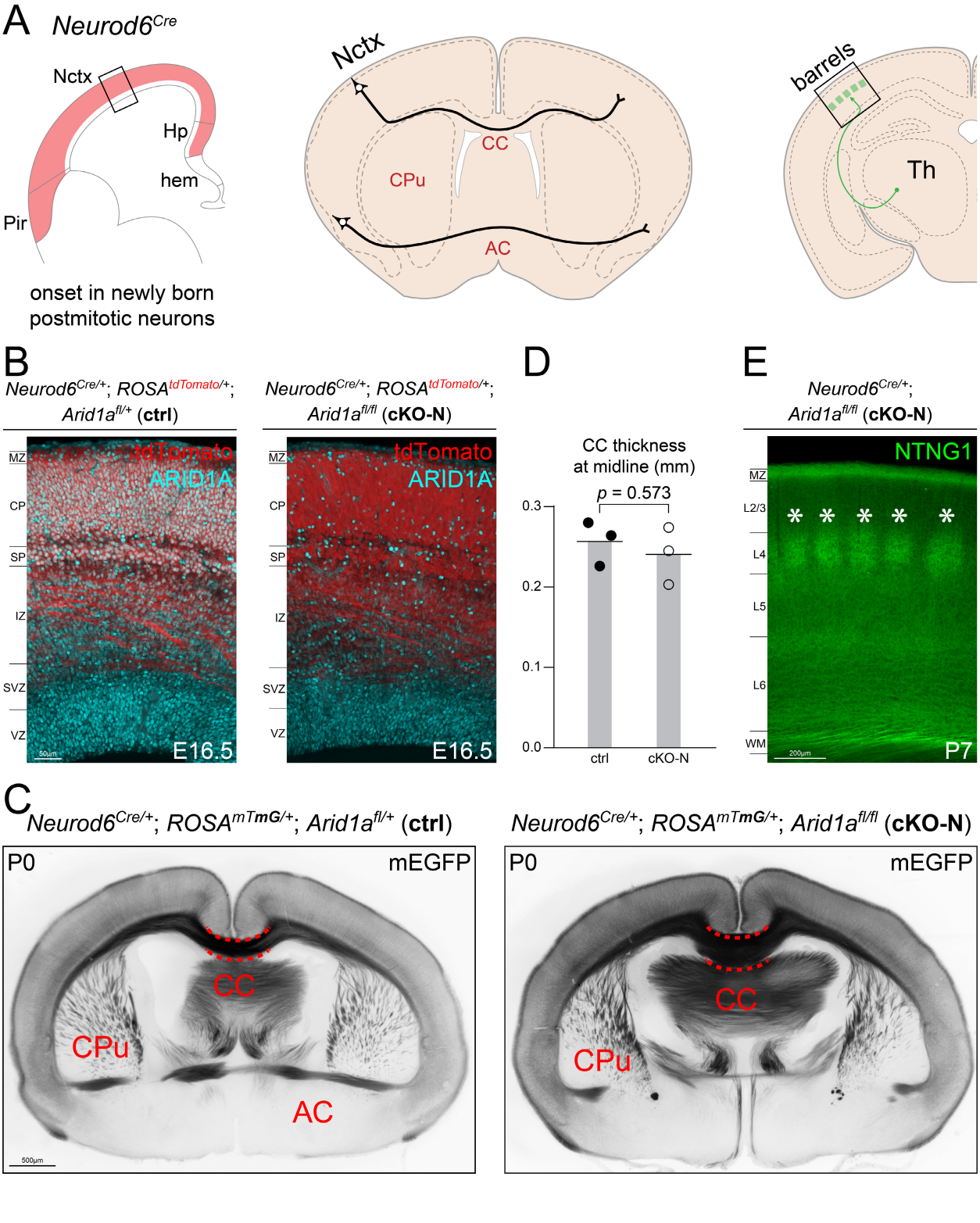

Figure 2.13 Postmitotic neuronal *Arid1a* deletion did not elicit widespread misrouting

(A) Schematic illustrations of *Neurod6*^{Cre} expression (red) throughout the embryonic telencephalon, interhemispheric connectivity (black), and thalamocortical whisker barrels (green) in coronal sections.

(B) *Neurod6*^{Cre} activity during corticogenesis. At E16.5, Cre-dependent *ROSA*^{tdTomato} was apparent throught the IZ, SP, and CP of ctrl and cKO-N. ARID1A (cyan) was broadly expressed throughout the cortical wall of ctrl but absent largely absent from the upper IZ, SP, and CP of cKO-N.

(C) Coronal sections of P0 ctrl and cKO-N brains. Membrane EGFP (mEGFP, black) was expressed Cre-dependently from *ROSA*^{mTmG}. In both ctrl and cKO-N, the corpus callosum formed without defect. In ctrl, the AC crossed the midline, seemingly connecting the two hemispheres. In cKO-N, the posterior branch of the AC failed to form, reminiscent of cKO-E (n=3/3 animals).

(D) Quantification of CC thickness at the midline revealed no significant reduction in cKO-N compared to ctrl (data are mean, two-tailed unpaired *t* test, n=3 animals/condition).

(E) NTNG1+ (green) thalamocortical whisker barrels in P7 cKO-N formed in a stereotypical manner.

AC: anterior commissure, CC: corpus callosum, CP: cortical plate, CPu: caudate putamen, hem: cortical hem, Hp: hippocampus, IZ: intermediate zone, L*n*: layer *n*, MZ: marginal zone, Nctx: neocortex, Pir: piriform cortex, SP: subplate, SVZ: subventricular zone, Th: thalamus, VZ: ventricular zone, WM: white matter

Discussion

Chromatin remodeling during brain development can contribute to various processes, including DNA replication, transcription, and DNA repair. These are nuclear events and are largely considered in the context of cell autonomy. However, autonomous functions can cascade and exert non-cell autonomous influences. *Arid1a*, a central subunit of the BAF chromatin remodeling complex, is consistently linked with transcriptomic regulation. Gene expression broadly influences cellular processes, including by controlling mediators of axon growth and guidance. While many genes have been implicated in brain wiring, how *Arid1a* might leverage influence over cortical connectivity remains unclear.

Clinical findings have implicated *ARID1A* broadly in cortical circuit development. Mutations in *ARID1A* are associated with Coffin-Siris syndrome, a developmental disorder which frequently presents with CC agenesis (395). I found that, in mice, *Arid1a* is integral to direct the initial stages of axon growth and targeting in the developing cortex (**Figure 2.14**). Despite its ubiquitous expression, *Arid1a* leverages surprising non-cell autonomous control over formation of callosal and thalamocortical circuitry broad necessity. These findings highlight the capacity for chromatin-mediated control of brain wiring.

My work hinges on use of a conditional *Arid1a* allele to spatiotemporally delete it from cortical NPCs or only their postmitotic neuronal progeny. Initially, NPC deletion of *Arid1a* in cKO-E resulted in widespread loss of intracortical, but not corticofugal connectivity. While the CC, AC, and hippocampal commissure were all absent, corticothalamic, corticotectal, and corticospinal connectivities appeared correctly routed

with some minor qualitative reduction. The loss of intracortical connectivity did not result from neuronal loss as seen in deletion of other chromatin remodelers. Instead, putative callosal projections diverged from their classical paths and travelled in aberrant trajectories tangentially and radially through cortical laminae. CC misrouting in cKO-E was radically different from classically described Probst bundles, which likely result from unsuccessful midline fusion or disruption of midline glial populations. *Arid1a* likely mediates callosal circuitry via comprehensive guidance of early growth.

The neocortex relies on input from other brain regions to properly coordinate conscious processes. Despite *Arid1a*'s likely autonomous role in chromatin control, aberrant axonal trajectories in cKO-E suggested a potentially broader regulation of connectivity. To assess whether *Arid1a* orchestrated cortical afferents, I examined development of thalamocortical circuits, which ultimately transport sensory information into the cortex. While *Arid1a* was expressed in thalamocortical neurons in cKO-E, they were mistargeted and unable to form stereotypical whisker barrels. To determine whether callosal misrouting was also a result of non-cell autonomous impairments, I designed a self-excising, self-reporting Cre recombinase construct to sparsely delete *Arid1a* from a subset of callosally-projecting neurons. Interestingly, sparse deletion of *Arid1a* from upper-layer neurons revealed callosal misrouting was also a result of non-cell autonomous influence. Together, these findings supported a robust mechanism by which *Arid1a* non-cell autonomously directs callosal and thalamocortical circuitry in the developing cortex.

The ubiquity of *Arid1a* has the capacity to mask its temporal necessity. *Arid1a*'s function could be centered on expression in NPCs, newly born neurons, or

postmigratory neurons. Deletion of *Arid1a* from excitatory neurons shortly after their genesis in cKO-N, although still impairing AC development, surprisingly did not perturb formation of CC or whisker barrels. Importantly, examination of ARID1A in cKO-N enabled clarification of *Arid1a*'s temporal dynamics. ARID1A was still present in neurons migrating through the IZ but largely absent from postmigratory neurons in the CP. Thus, *Arid1a*'s critical window to impact circuit wiring is currently situated to include both NPCs and newly born, perimigratory neurons. It is unlikely the temporal dynamics can be further refined at this time; the available tools are insufficient to completely eliminate ARID1A from neurons as they are born without deleting *Arid1a* from NPCs.

Arid1a has previously been studied in the context of cancer, cardiogenesis, and neural crest development (345, 386). However, it's impact on brain development has been only tentative. It is possible that *Arid1a* impacts cortical NPC proliferation and differentiation as has been reported in other progenitor types (390). Given the lack of robust changes in neuronal quantity or broad subtype specification in cKO-E, this would be a minor effect with far-reaching authority. Alternatively, NPC ARID1A could propagate its influence via mitotic bookmarking. Mitotic bookmarks can include retained genomic binding and histone posttranslational modifications that are passed on from mother to daughter cells (402). As a chromatin remodeler, *Arid1a* could act as a bookmark itself while also having the potential to influence chromatin structure and transcription factors binding. Previously, mitotic bookmarking has been shown to regulate proliferation and lineage commitment. In *Arid1a*'s NPC absence, it is possible that neurons inherit an inadequate chromatin landscape and are unable to properly

function. Partial support for this idea arises as some BAF subunits and factors known to associate with BAF have been suggested as bookmarks (e.g. GATA1) (403, 404).

The lack of gross anatomical and circuit changes in cKO-N does not discount the possibility that *Arid1a* performs an important function in postmigratory neurons. Both cKO-E and cKO-N do not exhibit premature lethality and are able to breed, however, their behavioral and electrophysiological characteristics have not been assessed. If *Arid1a* is unnecessary in postmigratory neurons, it begs the question of why it is expressed in the first place. One potential function for *Arid1a* in mature neurons is in DNA damage repair. While frequently examined in replicating and dividing cells, DNA damage can and does also occur in terminally postmitotic cells. Typically, neuronal DNA damage is attributed to oxidative stress and neuronal activity (405, 406). A potential involvement of *Arid1a* in postmitotic neuron genome integrity is supported by its previous linkage with non-homologous end joining (407).

Overall, it is apparent that *Arid1a* influences cortical circuit development in vital ways. These data strongly support non-cell autonomy; however, the mechanistic underpinnings could be convergent or divergent for callosal and thalamocortical circuitry. While possible that posttranslational mechanisms could contribute, *Arid1a*'s designation as a chromatin remodeler requires careful consideration of transcriptomic regulation. The lack of cell autonomous misrouting of callosal projections raises the intriguing possibility that, although ubiquitously expressed, *Arid1a* may prioritize its contribution through a subset of cortical cells.

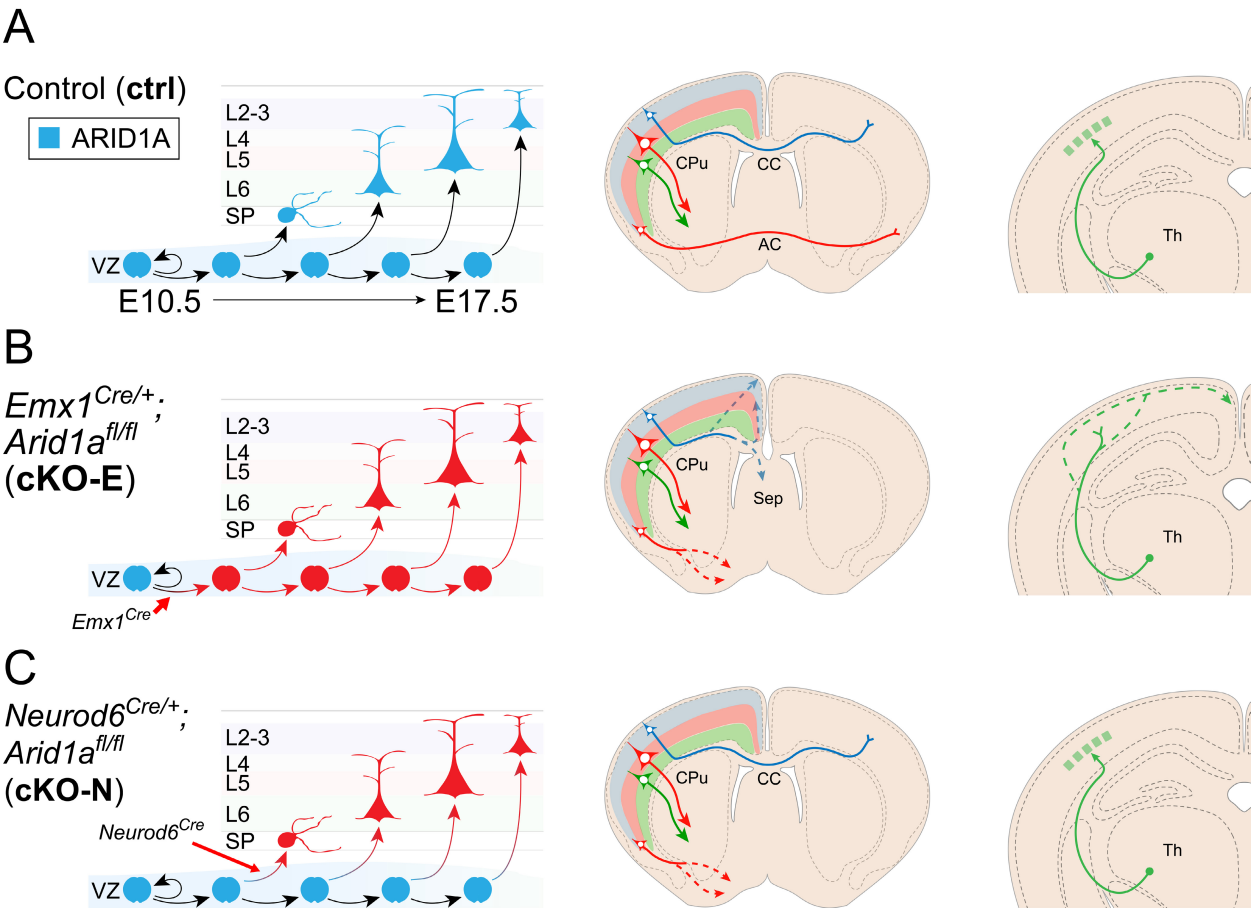

Figure 2.14 Schematic summary of *Arid1a*-dependent cortical circuitry

(A) *Arid1a* is expressed in all cell types throughout corticogenesis. To support brain function, interhemispheric connections including the CC and AC traverse the midline, corticofugal projections exit the cortex to various regions including thalamus and spinal cord, and thalamocortical projections bring sensory information to the cortex.

(B) *Emx1*^{Cre}-mediated deletion of *Arid1a* (cKO-E) occurs near the onset of neurogenesis and affects NPCs and their progeny. In cKO-E, there is complete CC and AC agenesis. Putative CC axons radiate dorsally toward the pia and AC projections dive ventrally toward hypothalamus. In contrast, corticofugal tracts are largely unaffected. Thalamocortical projections, which still express *Arid1a*, are incorrectly targeted; they travel tangentially through upper cortical layers and fail to form distinct whisker barrels.

(C) *Neurod6*^{Cre}-mediated deletion of *Arid1a* (cKO-N) occurs in newly postmitotic neurons. ARID1A is still partially present during neuronal migration and is sufficient to support formation of CC and thalamocortical whisker barrels. In contrast, postmitotic *Arid1a* deletion still elicits misrouting of AC similar to cKO-E.

AC: anterior commissure, CC: corpus callosum, CPu: caudate putamen, L*n*: layer *n*, SP: subplate, Th: thalamus, VZ: ventricular zone

Conclusion

Intricate brain connectivity is the product of precise projection growth and instructions to locate synaptic partners. One method by which to control these events is by intrinsic regulation of chromatin structure and ultimately gene expression. These autonomous acts can influence neighboring cells and projections. Here, I investigated how the chromatin remodeler *Arid1a* mediates cortical development. Consistent with human CC dysgenesis in cases of *ARID1A* mutations, deletion of *Arid1a* from cortical NPCs led to complete callosal agenesis and unexpected radial and tangential misrouting. Surprisingly, corticofugal projections were largely unaffected, but TCAs failed to properly enter the cortex, neglected their "waiting period" in the subplate, and did not organize into identifiable whisker barrels. As thalamocortical neurons still expressed *Arid1a*, their misrouting was undeniably a result of non-cell autonomous mechanisms. To identify whether callosal disruption was also non-cell autonomous, I generated a self-excising, self-reporting Cre recombinase construct that expresses EGFP following Cre activity. Interestingly, deletion of *Arid1a* sparsely from callosal neurons was insufficient to induce misrouting. To identify a critical window, despite its ubiquity, for *Arid1a* to leverage its non-cell autonomous control, I deleted *Arid1a* from postmitotic neurons shortly after their genesis thereby largely eliminating ARID1A by the time migration was completed. Surprisingly, this delayed deletion largely did not affect callosal or thalamocortical circuitry. Together, these analyses illustrate an essential role for *Arid1a* in NPCs or almost immediately after neuronal birth to non-cell autonomously direct major cortical connectivity, disruption of which is associated with neurodevelopmental disorders.

Materials and Methods

Mice and mouse husbandry

All experiments were carried out in compliance with ethical regulations for animal research. The study protocol was reviewed and approved by the University of Michigan Institutional Animal Care & Use Committee. Mice were maintained on 12 hour day:night cycle with food and water *ad libitum*. Mouse strains were previously generated and are listed in **Table 2.1**. Date of vaginal plug was considered embryonic day 0.5. Genotyping was performed with DreamTag Green 2x Master Mix (Thermo Fisher) and primers can be found in **Table 2.2**.

Immunostaining and imaging

Brains were isolated and fixed in 4% PFA overnight at 4° C, embedded in 4% agarose, and vibratome-sectioned at 70 µm. Free-floating sections were blocked and immunostained in blocking solution containing 5% donkey serum, 1% BSA, 0.1% glycine, 0.1% lysine, and 0.3% Triton X-100. Sections were incubated with primary antibodies in blocking solution overnight at 4° C and with secondary antibodies for 1h at RT. Following secondary antibody staining, sections were mounted with VECTASHIELD Antifade Mounting Medium (Vector Laboratories). Images were acquired using an Olympus SZX16 dissecting scope with Olympus U-HGLGPS fluorescent source and Q-Capture Pro 7 software to operate a Q-imaging Regia 6000 camera, an Olympus Fluoview FV1000 confocal microscope with FV10-ASW software, or an Olympus Fluoview FV3000 confocal microscope with FV31S-SW software. Images were processed and quantified in ImageJ and Adobe Photoshop. Primary and secondary antibodies are listed in **Table 2.3**.

Cytochrome oxidase

Brains from P7 mutant and control mice were fixed for 2 h at RT in 4% PFA, and the cortices were dissected off, flattened between two glass slides, and fixed overnight at 4° C. Following fixation, flattened cortices were sectioned on a vibratome at 150 µm. Sections were incubated at 37° C overnight in a solution containing 4 g sucrose, 50 mg DAB (Sigma-Aldrich), 15 mg cytochrome C (Sigma-Aldrich) per 100 mL of PBS. Sections were washed with PBS, and imaged with an Olympus SZX16 dissecting scope.

Plasmid constructs and in utero electroporation

For CAG-sxiCre-EGFP, an iCre sequence followed by polyA and flanked by loxP sites was placed immediately downstream of a CAG promoter. An EGFP sequence, WPRE, and polyA were inserted following the iCre/loxP cassette so that Cre expression will lead to self-excision and EGFP expression. Approximately 2 uL of 1.5 µg/µL CAG-sxiCre-EGFP was injected into lateral ventricles. Plasmids were transferred to NPCs in the VZ by electroporation (five 45-ms pulses of 27 V at 950-ms intervals).

Statistical analyses

Statistical analyses were performed in GraphPad Prism 8 (GraphPad Software). Values were compared using a two-tailed, unpaired Student's *t* test, or ANOVA with Tukey's post hoc test. An α of 0.05 was used to determine statistical significance unless otherwise indicated.

Acknowledgements

The work presented in this chapter is the culmination of a tremendously collaborative and supportive environment in the Kwan lab. Experimentally, Alice Sorel assisted with genotyping, sectioning, and immunostaining. Mandy Lam performed cytochrome oxidase staining and guided me for IUE. Additionally, impromptu conversations with Drs. Jason Keil and Owen Funk were integral in helping me consolidate my ideas regarding *Arid1a*'s spatiotemporal necessity. Finally, the entirety of the Kwan lab contributed beneficial feedback regarding visual appearance and organization of the data.

Table 2.1: Mouse strains used in this study.

Mouse	Description	ID	Citation
STOCK *Arid1a*$^{tm1.1Zhwa}$/J *Arid1a*^{fl}	Floxed exons 8 of *Arid1a*	JAX# 027717	(385)
B6.129(Cg)-*Gt(ROSA)26Sor*$^{tm4(ACTB-tdTomato,-EGFP)Luo}$/J *ROSA*^{mTmG}	Cre-dependent switch from *mtdTomato* to *mEGFP* at ROSA26 locus	JAX# 007676	(398)
B6.Cg-*Gt(ROSA)*$^{26Sortm14(CAG-tdTomato)Hze}$/J *ROSA*^{tdTomato}	Cre-dependent expression of *tdTomato* at ROSA26 locus	JAX# 007914	(401)
B6.129S2-*Emx1*$^{tm1(cre)Krj}$/J *Emx1*$^{IRES-Cre}$	Knock-in of IRES and *Cre* to *Emx1* locus	JAX# 005628	(397)
Neurod6$^{tm1(cre)Kan}$ *Neurod6*^{Cre}	Knock-in of *Cre* to *Neurod6* locus	MGI# 2668659	(400)

Table 2.2: Genotyping oligos used in this study.

Gene Target	Oligo Name	Sequence (5' - 3')	Notes
Cre	Cre-F	TCGATGCAACGAGTGATGAG	500 bp for *Emx1*^{Cre} and *Neurod6*^{Cre}
	Cre-R	TTCGGCTATACGTAACAGGG	
Arid1a^{fl}	Arid1a-F	TGGGCAGGAAAGAGTAATGG	WT = 116 bp Floxed = 170 bp
	Arid1a-R	CACTGACTGGCGTGTTCAGA	

Table 2.3: Primary and secondary antibodies used in this study.

Primary Antibody	Company and product number	Dilution
Rabbit anti-ARID1A	Abcam ab182560	1:1000
Goat anti-SOX2	Santa Cruz Biotechnology sc-17320	1:250
Chicken anti-RBFOX3	Sigma-Aldrich ABN91	1:2000
Rabbit anti-TBR1	Abcam ab31940	1:250
Rat anti-BCL11B	Abcam ab18465	1:500
Rabbit anti-LHX2	Sigma-Aldrich ABE1402	1:2000
Rat anti-L1CAM	Sigma Aldrich MAB5272	1:1000
Chicken anti-GFP	Abcam ab13970	1:2000
Goat anti-Netrin-G1a	R&D Systems AF1166	1:100
Donkey anti-Chicken IgY (H+L), Alexa Fluor 488 AffiniPure	Jackson ImmunoResearch Labs 703-545-155	1:250
Donkey anti-Goat IgG (H+L), Alexa Fluor 488 AffiniPure	Jackson ImmunoResearch Labs 805-545-180	1:250
Donkey anti-Rabbit IgG (H+L), Alexa Fluor 488 AffiniPure	Jackson ImmunoResearch Labs 711-545-152	1:250
Donkey anti-Rat IgG (H+L), Alexa Fluor 488 AffiniPure	Jackson ImmunoResearch Labs 712-545-150	1:250
Donkey anti-Chicken IgY (H+L), Cy3 AffiniPure	Jackson ImmunoResearch Labs 703-165-155	1:250
Donkey anti-Goat IgG (H+L), Cy3 AffiniPure	Jackson ImmunoResearch Labs 705-165-147	1:250
Donkey anti-Rabbit IgG (H+L), Cy3 AffiniPure	Jackson ImmunoResearch Labs 711-165-152	1:250
Donkey anti-Rat IgG (H+L), Cy3 AffiniPure	Jackson ImmunoResearch Labs 712-165-153	1:250
Donkey anti-Chicken IgY (H+L), Alexa Fluor 647 AffiniPure	Jackson ImmunoResearch Labs 703-605-155	1:250
Donkey anti-Rabbit IgG (H+L), Alexa Fluor 647 AffiniPure	Jackson ImmunoResearch Labs 711-605-152	1:250
Donkey anti-Rat IgG (H+L), Cy5 AffiniPure	Jackson ImmunoResearch Labs 712-175-153	1:250

Chapter 3: Subplate *Arid1a* Non-Cell Autonomously Mediates Early Cortical Connectivity[2]

Abstract

Developmental emergence of cortical connectivity can be influenced by pioneering cell types. While distinct cell types have unique gene expression profiles, ubiquitously expressed genes can have cell type-specific influences. Here, I identified *Arid1a* regulates the establishment of the neuronal transcriptome. Rather than broadly affecting neurons, *Arid1a* deletion biasedly impacted subplate neurons. In tandem with gene expression changes, subplate neurons displayed robust changes in organization, morphology, projections, and extracellular matrix. Disruption of these developmental characteristics following *Arid1a* deletion likely contributes to non-cell autonomous circuit miswiring. Sparing *Arid1a* in the subplate was, in fact, sufficient to support brain wiring and ultimately the formation of callosal and thalamocortical connectivities. Altogether, *Arid1a* is a multifaceted regulator of subplate neuron gene expression and accompanying features, ideally positioning subplate neurons to coordinate the formation of essential brain connectivity.

[2]This chapter includes the publication: **Doyle DZ**, Lam MM, Qalieh A, Qalieh Y, Sorel A, Funk OH, & Kwan KY (2021). Chromatin remodeler *Arid1a* regulates subplate neuron identity and wiring of cortical connectivity. *PNAS*. DOI: 10.1073/pnas.2100686118

Introduction

The wiring of cortical circuits requires precise alignment of cell autonomous and non-cell autonomous mechanisms and communication between a variety of cell types. The neocortex is structured such that incoming and outgoing projections sit beneath numerous layers of somata they originated from or are targeting. At the interface of cortical layers and developing connectivity are SPNs, the firstborn neurons of the neocortex.

The SP is a transient layer of the fetal cerebral cortex essential to the developmental wiring of cortical circuits (239, 246, 269, 285, 408-414). During neurogenesis, cortical NPCs generate excitatory neurons following an orderly temporal progression, successively giving rise to SPNs SPNs, then deep layer neurons, then upper layer neurons (21, 59). As the first neurons generated from embryonic cortex, SPNs establish emerging axon tracts and form the earliest synapses (106, 246, 260, 285, 408, 409, 415, 416). Importantly, SPNs, which are strategically positioned at the interface between post-migratory neurons and the developing WM, serve non-cell autonomous wiring functions in the formation of cortical circuits. Experimental SP ablation during fetal development leads to misrouting of TCAs (303-305) and disrupts formation of sensory maps (307, 308), and perturbed SP function has been hypothesized to contribute to circuitry defects in disorders of brain development (311-313). Mechanistically, SPNs non-cell autonomously mediate circuit wiring at least in part by extending the earliest cortical descending axons, which interact with ascending TCAs during pathfinding (as posited by the “handshake hypothesis”) (417, 418) and contribute to their crossing of the PSB (306, 419). SPNs also secrete ECM components that

support axon guidance (246, 289). In addition, SPNs are required for early oscillatory activity (412, 415). In postnatal ages, some SPNs undergo programmed cell death (242), thereby serving a transient role in cortical circuit development.

Despite the central position of SPNs in orchestrating cortical connectivities, the molecular determinants of SP wiring functions have remained largely elusive. Previous studies have focused on genes selectively expressed in SPNs (313, 420). These important studies illuminated the genetic bases of SPN specification, migration, and axon development (141, 142, 144, 162, 163, 274, 421). The severe axon misrouting phenotypes of SP ablation (303-305), however, are not broadly recapitulated in these genetic mutants. And the mechanisms underpinning the axon guidance functions of SP have remained largely mysterious. Here, by cell type-specific dissection of gene function, I identify *Arid1a* as a key regulator of multiple subplate-dependent axon guidance mechanisms indispensable for cortical circuit wiring.

In Chapter 2 I identified *Arid1a*'s necessity for proper targeting of intracortical and thalamocortical circuit development. However, the cell type-mediator of *Arid1a* influence was unclear. Here I use transcriptomics, temporally distinct Cre lines, and cell type-specific reporters to analyze cell type-specific necessity and sufficiency for *Arid1a*. At the transcriptomic level, I unbiasedly find a selective loss of SPN gene expression following *Arid1a* deletion, thus identifying SP as a potential substrate of *Arid1a* phenotypes. Consistent with this, *Arid1a* axon misrouting defects are highly reminiscent of SP ablation (303-305). Furthermore, multiple characteristics of SPNs crucial to their circuit wiring functions, including SP organization and ECM, are disrupted following *Arid1a* deletion. Importantly, descending SP axons are severely attenuated, abrogating

their co-fasciculation with ascending TCAs. This “handshake” interaction with SP axons is essential to TCA pathfinding and whisker barrel formation (417, 418), both of which are disrupted by *Arid1a* deletion. Thus, I find a necessity for *Arid1a* in orchestrating distinct aspects of SP circuit wiring functions. To empirically test *Arid1a* sufficiency in SPNs, I use a genetic approach to generate a CP deletion of *Arid1a* that spares SPNs. In this model, I find that *Arid1a* expression in SPNs is sufficient to support SP organization, “handshake” with TCAs, and ECM. Consistent with these wiring functions, SP *Arid1a* expression sufficiently enables normal TCA targeting, whisker barrel development, and callosum formation. Together, this study identifies *Arid1a* as a central regulator of SP-dependent axon pathfinding, unequivocally establishes SP function as essential to callosal development, and highlights non-cell autonomous mechanisms in circuit development and disorders thereof.

Results

Arid1a establishes the neuronal transcriptome

Mutations in *ARID1A* are associated with Coffin-Siris syndrome, which often presents with callosal agenesis (348). In line with this human phenotype, pancortical deletion of *Arid1a* from NPCs in cKO-E, but not from only postmitotic excitatory neurons in cKO-N, led to robust non-cell autonomous misrouting of callosal and thalamocortical circuitry. Elaborate orchestration of axon growth and guidance programs occurs during development to direct cortical circuit wiring. However, previous studies of axon growth and guidance factors in the developing cortex fail to phenocopy *Arid1a* cKO-E, and thus suggest disruption of one or more novel participants, or combinatorial dysfunction of

multiple known components. As a chromatin remodeler, *Arid1a* is well-positioned to regulate gene expression.

To ascertain whether pancortical *Arid1a* deletion in cKO-E disrupted the transcriptome during corticogenesis, I performed unique molecular identifier (UMI) RNA-seq of E15.5 cortices from littermate ctrl and cKO-E (n=6 animals/condition) (**Figure 3.1 A**). UMI RNA-seq leverages Click chemistry to add a UMI to each initial cDNA molecule to enable deduplication of reads post-sequencing (50, 422). Prior to ctrl versus cKO-E comparisons, analysis of External RNA Controls Consortium (ERCC) RNA standards spike-in revealed reliable quantification over a broad range of expression levels (Pearson correlation coefficient: r=0.7482, Spearman rank correlation coefficient: ρ=0.8109) (**Figure 3.1 B**). Differential expression analysis of ctrl versus cKO-E using edgeR (423) revealed widespread changes in gene expression with a false discover rate (FDR) of <0.01. In E15.5 cKO-E, 103 genes were differentially expressed, with 91 downregulated and 12 upregulated compared to ctrl (**Figure 3.1 C**). Of note, expression-level differences of two downregulated genes (*Tle4* and *Zfpm2*) and two genes without significant changes (*Lhx2* and *Tbr1*) were validated using droplet digital (dd)RT-PCR, a highly sensitive a quantitative technique (Mean Normalized RNA level, *Tle4*: ctrl=0.889, cKO-E=0.458, p=2.9e-4; *Zfpm2*: ctrl=0.730, cKO-E=0.357, p=0.03; *Lhx2*: ctrl=3.67, cKO-E=2.75, p>0.99; *Tbr1*: ctrl=3.84, cKO-E=4.20, p>0.99, two-tailed unpaired t test with Bonferroni correction, *Tle4*, *Zfpm2*, and *Tbr1*: n=6 animals/condition, *Lhx2*: ctrl=6 animals, cKO-E=5 animals) (**Figure 3.1 D**). Importantly, decreased *Tle4* expression was consistent with a reduction in the number of TLE4+ cells in cKO-E

compared to ctrl (Marker-positive cells per 100 μm, ctrl mean=, cKO-E mean=, p=3.9e-3, two-tailed unpaired t test, n=3 animals/condition).

To determine whether axonal misrouting in cKO-E could be due to reduced expression of genes associated with axon extension and guidance, I intersected the 91 downregulated genes in cKO-E with 138 axon extension genes (Gene Ontology [GO]: 0048675) and 253 axon guidance genes (GO: 007411). One axon extension gene (*Myo5b*) and one axon guidance gene (*Ablim1*) were significantly reduced in cKO-E and validated by ddRT-PCR (Mean normalized RNA level, *Myo5b*: ctrl=0.0459, cKO-E=0.0299. p=0.04; *Ablim1*: ctrl=0.483, cKO-E=0.255, p=0.02, two-tailed unpaired t test with Bonferroni correction, n=5 animals/condition) (**Figure 3.1 E**). However, disruption of either gene has not been shown to cause widespread misrouting seen in cKO-E (424). Importantly, neither axon extension nor axon guidance genes were significantly overrepresented in cKO-E downregulated genes compared to chance (axon extension: P_{hyper}=0.3610; axon guidance: P_{hyper}=0.3427, hypergeometric test with Bonferroni correction, α=0.025).

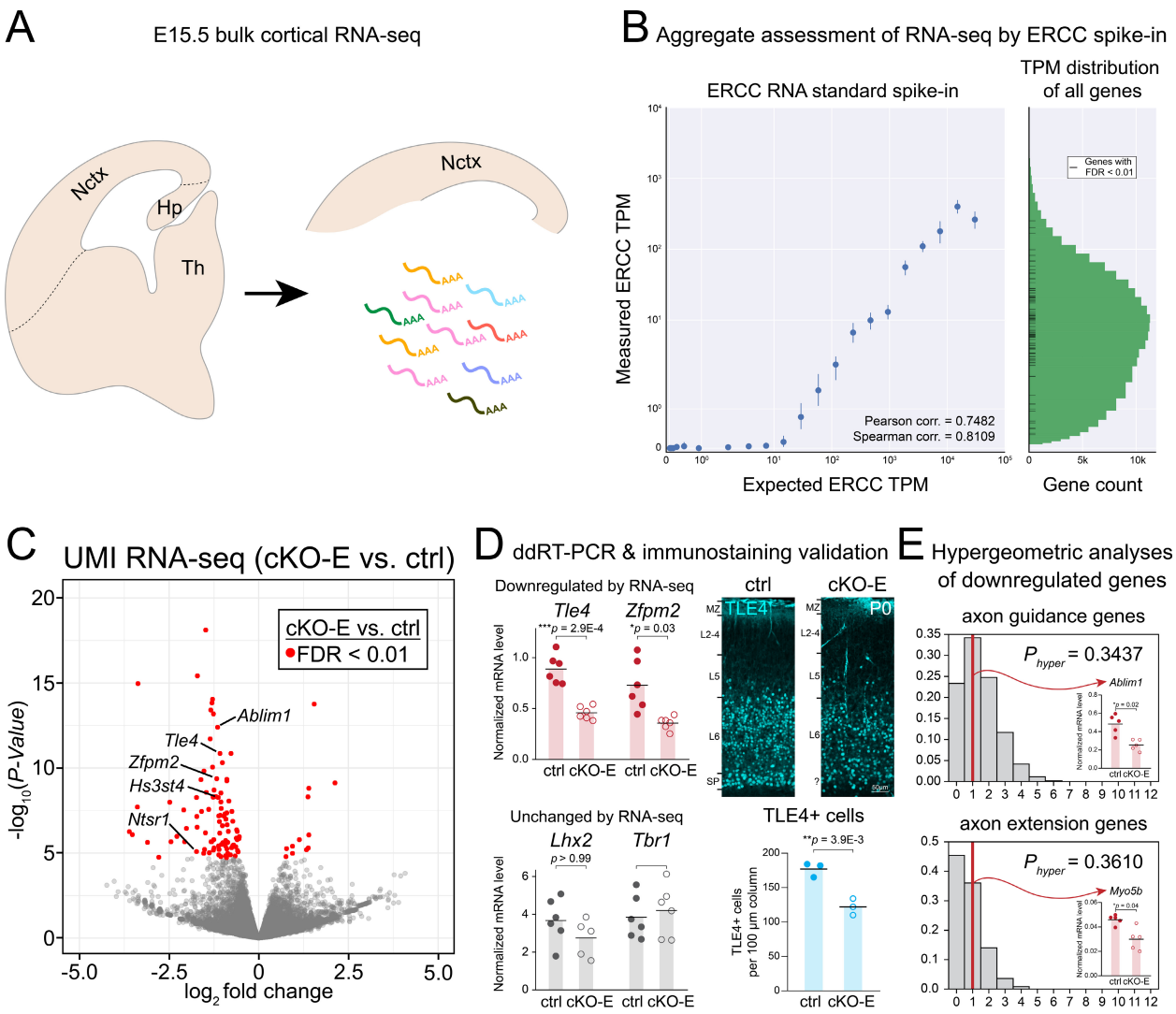

Figure 3.1 Transcriptomic dysregulation following *Arid1a* deletion

(A) Schematic illustration of bulk RNA-seq from microdissected neocortex.

(B) Aggregate assessment of ERCC spike-in standards in UMI RNA-seq revealed excellent quantification over a broad range of expression levels. All differentially expressed genes were within the dynamic range of UMI RNA-seq.

(C) Volcano plot of unique molecular identifier (UMI) RNA-seq data comparing E15.5 cortex of cKO-E (n=6 animals) to ctrl littermates (n=6 animals). For each gene, *P*-value was calculated with likelihood ratio tests and false discovery rate (FDR) was calculated using the Benjamini-Hochberg procedure. Differentially expressed genes (FDR < 0.01) are indicated by red dots. Of the 103 differentially expressed genes, 91 were downregulated and 12 were upregulated in cKO-E.

(D) Droplet digital (dd)RT-PCR validation of two genes that were downregulated in cKO-E based on RNA-seq (*Tle4, Zfpm2*) and two genes unchanged in cKO-E based on RNA-seq (*Lhx2, Tbr1*) (data are mean, two-tailed *t* test with Bonferroni correction, *Tle4*, *Zfpm2*, and *Tbr1*: n=6 animals/condition, *Lhx2*: ctrl n=6, cKO-E n=5 animals). Immunostaining for TLE4 (cyan) in P0 ctrl and cKO-E cortex confirmed a significant loss of TLE4+ cells in cKO-E (data are mean, two-tailed *t* test, n=3 animals/condition).

(E) Hypergeometric analysis of genes significantly downregulated in cKO-E (FDR < 0.01) revealed no significant overrepresentation of axon guidance (GO:0007411) or axon extension (GO:0048675) genes (hypergeometric test, Bonferroni correction, $\alpha = 0.025$). *Ablim1* (axon guidance) and *Myo5b* (axon extension) downregulation in E15.5 cKO-E cortex was confirmed by ddRT-PCR (data are mean, two-tailed *t* test with Bonferroni correction, n=5 animals/condition).

Hp: hippocampus, Nctx: neocortex, Th: thalamus, TPM: transcripts per million, UMI: unique molecular identifier

In cKO-E, *Arid1a* is deleted from NPCs near the onset of neurogenesis, eliminating ARID1A from NPCs and their subsequent progeny. Thus, loss of *Arid1a* could directly impact the transcriptome of NPCs, postmitotic neurons, or both at E15.5. To distinguish between these possibilities, I examined previously generated RNA-seq from laser microdissection of E14.5 VZ, SVZ/IZ, and CP to identify NPC genes (VZ-enriched) and neuronal genes (CP-enriched) (**Figure 3.2 A**) (425). In total, 1262 VZ-enriched and 866 CP-enriched genes were identified (VZ:CP p_{adj}<0.001). In E15.5 cKO-E compared to ctrl, 5 VZ-enriched and 35 CP-enriched genes were significantly downregulated (ctrl:cKO-E FDR<0.01) (**Figure 3.2 B**). Hypergeometric analyses revealed that neuronal (CP-enriched), but not NPC (VZ-enriched), genes were significantly overrepresented in cKO-E versus ctrl downregulated genes (CP-enriched: P_{hyper}=7.16e-21; VZ-enriched: P_{hyper}=0.113, hypergeometric test with Bonferroni correction, α=0.025). Together, these data suggested *Arid1a* plays a significant role in activating the neuronal transcriptome.

Deletion of *Arid1a* only from postmitotic cortical excitatory neurons in cKO-N eliminated ARID1A near completion of neuronal migration. However, cKO-N did not display the callosal agenesis and TCA misrouting of cKO-E, suggesting a necessity for ARID1A in NPCs or newborn postmitotic neurons for circuit wiring. Thus, to differentiate between neuronal gene expression changes that could contribute to circuit miswiring in cKO-E and those unlikely to contribute, I performed UMI RNA-seq on E15.5 ctrl and cKO-N cortices (ctrl n=4, cKO-N: n=6 animals) (**Figure 3.2 C** and **D**). Surprisingly, cKO-N had relatively minimal transcriptional effect; only two genes were differentially expressed (*Lmo3* and *Sema3e*, FDR<0.01), neither of which were altered in cKO-E.

Additionally, the fold changes of cKO-E differentially expressed genes largely collapsed and did not differ from ctrl in cKO-N (**Figure 3.2 E**). Transcriptome data from both cKO-E and cKO-N revealed that ARID1A was required in NPCs or early in postmitotic neurons to establish neuronal gene expression but is unnecessary for neuronal transcriptome maintenance.

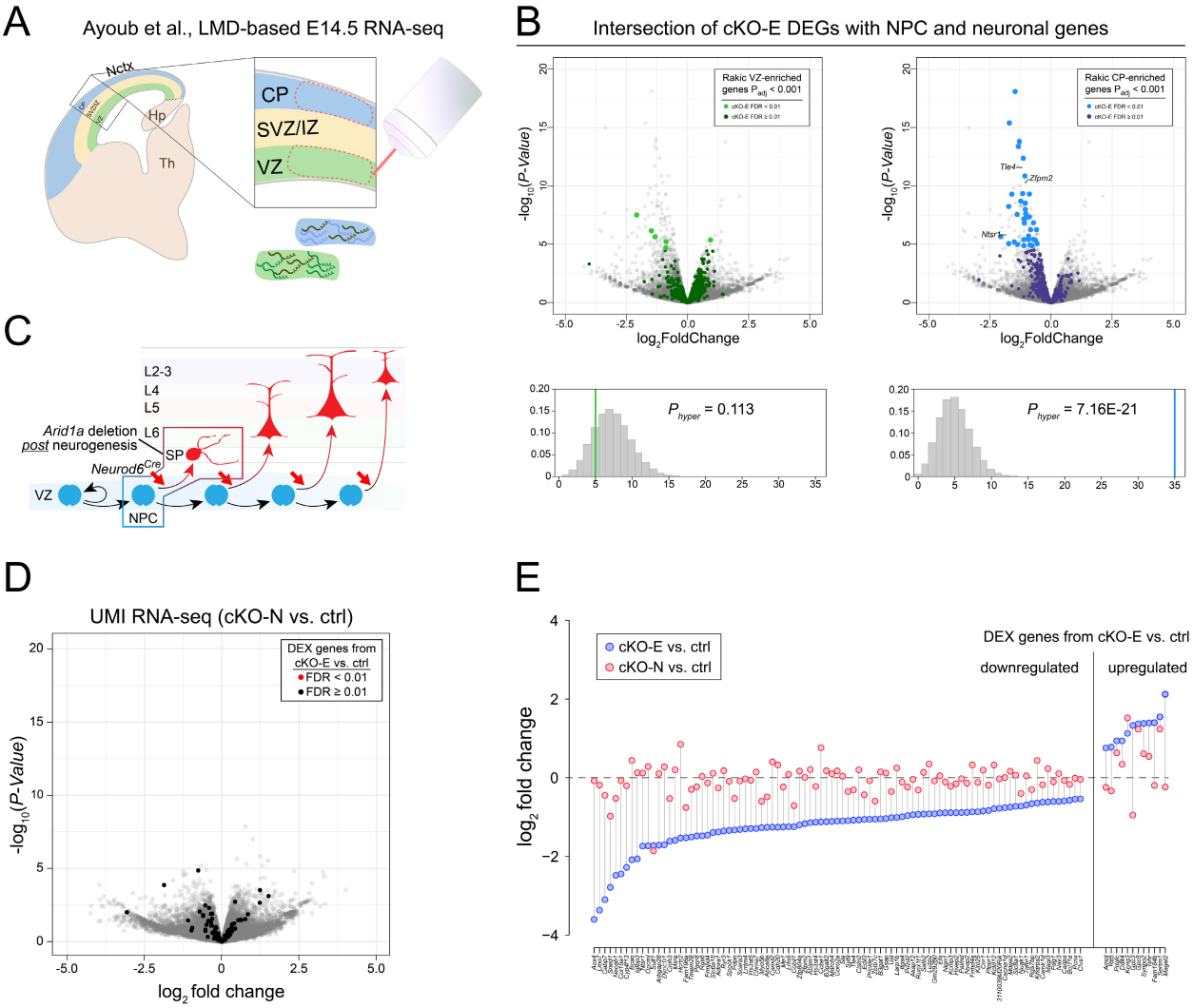

Figure 3.2 *Arid1a* deletion disrupts establishment the neuronal transcriptome

(A) Schematic illustration of laser microdissection (LMD) identifying NPC and neuronal genes based on VZ and CP expression in (425).

(B) Intersectional analyses of cKO-E differentially expressed genes with VZ- and CP-enriched genes. 5 NPC-enriched genes (green) were significantly altered in cKO-E compared to control. In contrast, 35 CP-enriched genes (blue) significantly downregulated in cKO-E. Hypergeometric analysis revealed that NPC genes were not affected at a rate higher than chance whereas neuronal genes were differentially expressed at a rate inconsistent with random likelihood (hypergeometric test, Bonferroni correction, α = 0.025).

(C) Schematic illustration of neuronal deletion of *Arid1a* mediated by *Neurod6*^{Cre}.

(D) Volcano plot of unique molecular identifier (UMI) RNA-seq data comparing E15.5 cortex of cKO-N (n=6 animals) to ctrl littermates (n=4 animals). Although cKO-E

displayed dysregulation of neuronal genes, none of the cKO-E differentially expressed genes were altered in cKO-N. All were reduced to insignificance and are illustrated by black dots.

(E) Visualization of cKO-E differentially expressed genes fold change in cKO-E versus ctrl (blue) and cKO-N versus ctrl (red). The fold-change of the vast majority of cKO-E differentially expressed genes was rescued in cKO-N. Of the few genes that don't show a restoration to a $\log_2$(fold change) near 0, none were significantly altered in cKO-N versus ctrl based on false discovery rate (FDR) calculation using the Benjamini-Hochberg procedure.

CP: cortical plate, DEX: differentially expressed, Hp: hippocampus, IZ: intermediate zone, LMD: laser microdissection, L*n*: layer *n*, Nctx, neocortex, NPC: neural progenitor cell, SP: subplate, SVZ: subventricular zone, UMI: unique molecular identifier, VZ: ventricular zone

NPC deletion of Arid1a selectively disrupts subplate neuron transcriptome

Deletion of *Arid1a* from NPCs in cKO-E disrupted the establishment of neuronal transcriptome. *Arid1a* is ubiquitously expressed and could therefore be impacting all neuronal types. Alternatively, *Arid1a* in cKO-E could play a surprising cell type-specific role in neuronal gene expression. The bulk RNA-seq performed on ctrl and cKO-E cortices does not directly enable uncoupling of the two possibilities. To circumvent this limitation, I intersected downregulated genes in cKO-E with existing single-cell RNA-seq (scRNA-seq) from E14.5 wildtype cortex (426) and examined gene expression at the level of single cells. Unsupervised hierarchical clustering of gene expression profiles revealed that of the 91 downregulated genes in cKO-E, 46 were highly co-expressed at the level of single cells (cluster 1) (**Figure 3.3 A**). Importantly, this highly correlated pattern of gene expression was confirmed using an orthogonal scRNA-seq dataset from E14.5 wildtype cortex (427). Remarkably, this additional dataset revealed strong coexpression of 56/91 cKO-E downregulated genes (cluster A), including all 46 previously identified in cluster 1 (**Figure 3.3 D**). These data strongly suggest that *Arid1a* deletion in cKO-E selectively disrupted the transcriptome of a specific cell type.

To unbiasedly determine what cell type was selectively affected by *Arid1a* deletion in cKO-E, I sought to investigate spatiotemporal gene expression in various brain regions. To this end, I utilized a rich data set from the Allen Brain Atlas which contains gene expression information from 1,200 different brain subregions (428). I intersected the 46 genes in cluster 1 with these 1,200 areas using Enrichr (429). Surprisingly, cluster 1 genes were only significantly overrepresented in six different groups (P_{adj}<0.01): 1) Layer 6b of dorsal anterior cingulate; 2) Layer 6b of prelimbic

area; 3) Layer 6b of ventral anterior cingulate; 4) superficial stratum (CP/MZ) of presubiculum; 5) superficial stratum (CP/MZ) of cerebral cortex; and 6) Layer 6b of cerebral cortex (**Figure 3.3 B**). Surprisingly, of these six, four were layer 6b, alternative nomenclature for SP. Four additional datasets were used for orthogonal validation of cluster 1 gene expression in SP: microdissection and microarray of E15.5 wildtype SP (420), Genepaint E14.5 RNA in situ hybridization (430), Gene Expression Nervous System Atlas (GENSAT) E15.5 EGFP transgene expression data (431), and Projection type-specific RNA-seq from E15-P1 (432) (**Figure 3.3 C**, **D**, and **F**).

In E15.5 wildtype, 17/46 cluster 1 genes were selectively expressed in SP based on microarray (420). E14.5 in situ and E15.5 transgene data from Genepaint and GENSAT, respectively, further confirmed subplate-specific or subplate-preferenced expression of multiple cluster 1 genes (430, 431). Cluster 1 genes were also significantly enriched in neurons projecting in a corticothalamic (CTA) or broader corticofugal manner (CTA group 6, P_{hyper}=3.01e-9; corticofugal group 11, P_{hyper}=4.42e-12, Hypergeometric test with Bonferroni correction, α=0.00238), but not in other cell types (e.g. callosal projection neuron [CPN] and corticospinal tract neuron [CST]) (432). Additionally, genes in clusters 2 and 3 were not significantly enriched in any cell types. Although SPNs were not directly identified in this dataset, SP marker expression in these CTA group 6 and corticofugal group 11 consistently overlapped with E15.5 wildtype microarray data. Together, these analyses uncovered a cell type-specific and -selective alteration to SPN transcriptome following *Arid1a* in cKO-E.

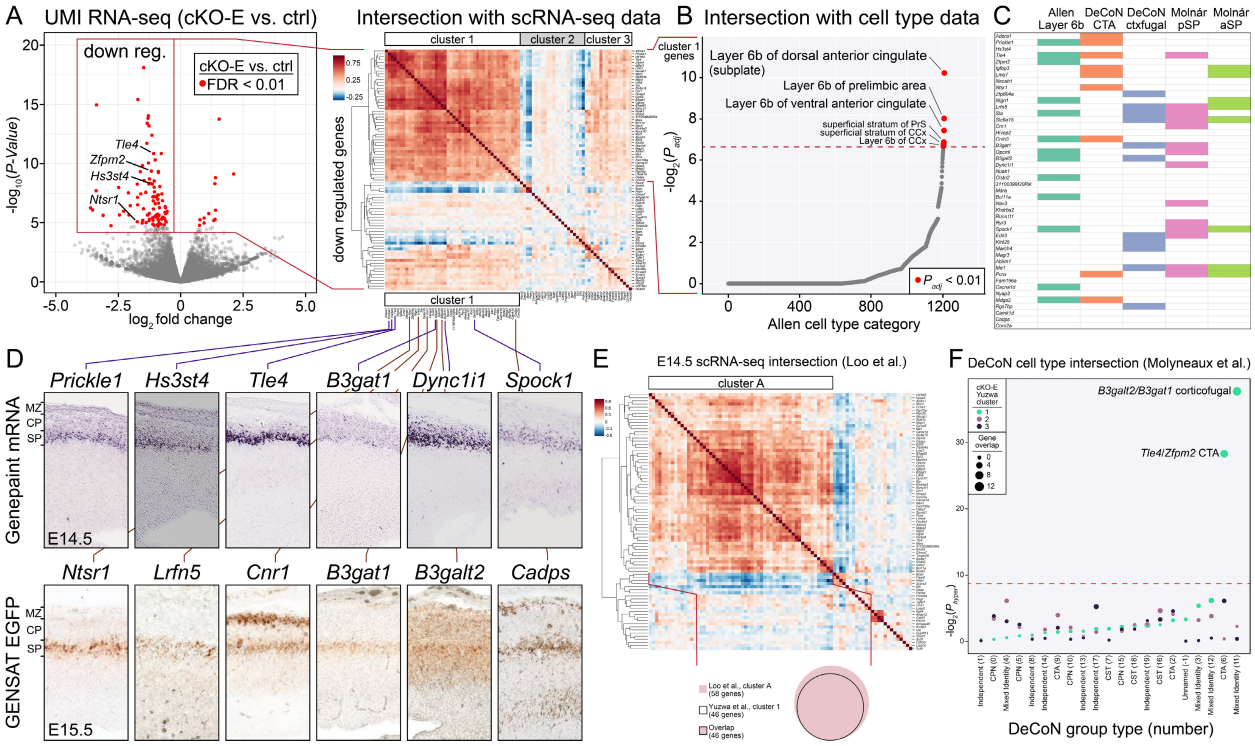

Figure 3.3 Selective disruption of subplate neuron gene expression following *Arid1a* deletion

(A) Intersectional analysis of cKO-E significantly downregulated genes with single cell (sc)RNA-seq data from wildtype embryonic forebrain (426). Unsupervised hierarchical clustering revealed a cluster of 46 downregulated genes (cluster 1) that are highly co-expressed at the level of single cells, suggesting that they may be expressed from one cell type.

(B) Intersectional analysis of the 46 genes in cluster 1 with a spatiotemporal gene expression dataset covering over 1200 brain subregions (428). Cluster 1 showed a significant overrepresentation of genes selectively expressed in cortical layer 6b. Layer 6b is alternative nomenclature for subplate.

(C) Subplate expression of cluster 1 genes was further confirmed by E14.5 *in situ* hybridization data from the Genepaint database and E15.5 EGFP transgene expression data from the GENSAT consortium (430, 431).

(D) Intersectional analysis of cKO-E downregulated genes (FDR < 0.01) with single-cell RNA-seq from wildtype E14.5 cortex (427) revealed a cluster of 58 genes highly co-expressed in single cells (cluster A). Cluster A encompassed all 46 genes from cluster 1 (426), providing orthogonal support that gene expression was preferentially affected within a specific cell type in cKO-E.

(D) Intersection of cKO-E downregulated genes in cluster 1 (426) with cell type-specific RNA-seq data (432) revealed overrepresentation of corticothalamic group 6 and corticofugal group 11, which likely comprise subplate neurons based on marker membership, but no overrepresentation of other cell types (e.g. CPN, CST). Intersectional analyses of cluster 2 and 3 genes revealed no overrepresentation of any cell type (hypergeometric test, Bonferroni correction, $\alpha = 0.00238$).

(E) Intersectional analyses with orthogonal datasets (428, 432, 433) confirmed subplate expression of genes in cluster 1.

CP: cortical plate, CPN: callosal projection neuron, CST: corticospinal tract, CTA, corticothalamic, ctxfugal: corticofugal, MZ: marginal zone, SP: subplate

Arid1a is necessary for subplate neuron organization and morphology

Alterations in SPN gene expression in cKO-E likely lead to changes in SP structure and/or function. To directly investigate the consequences of disrupted gene expression on SPNs, I tested SP organization. The SP forms a dense band of neurons situated below L6 in the cortex, abutted up against cortical WM. In P0 ctrl, the SP can be confidently differentiated with the neuronal marker RBFOX3 (NEUN), which revealed SPNs organized in a distinct, tight band below L6 (**Figure 3.4 A**). However, in cKO-E, RBFOX3+ SPNs appeared disorganized and comingled with L6 neurons. Additional investigation of SPN-specific marker CPLX3 (140), revealed a striking difference between ctrl and cKO-E SPNs (**Figure 3.4 B**). In P0 ctrl, CPLX3+ SPNs were continuous and formed a clean border between L6 and cortical WM. In cKO-E, there were gaps in CPLX3+ SP and some CPLX3+ neurons were found residing within the WM. Overall, cKO-E the CPLX3+ SPNs were more radially dispersed and scattered (Mean CPLX3+ neuron radial dispersion: ctrl=59.20 μm, cKO-E=86.53 μm, p=0.032, two-tailed unpaired t test, n=3 animals/condition; Mean CPLX3+ neurons per 100 μm^2: ctrl=0.1676, cKO-E=0.09774, p=0.027, two-tailed unpaired t test, n=3 animals/condition). These data strongly supported that, in cKO-E, disruption of SP organization is coincident with alterations in SPN gene expression.

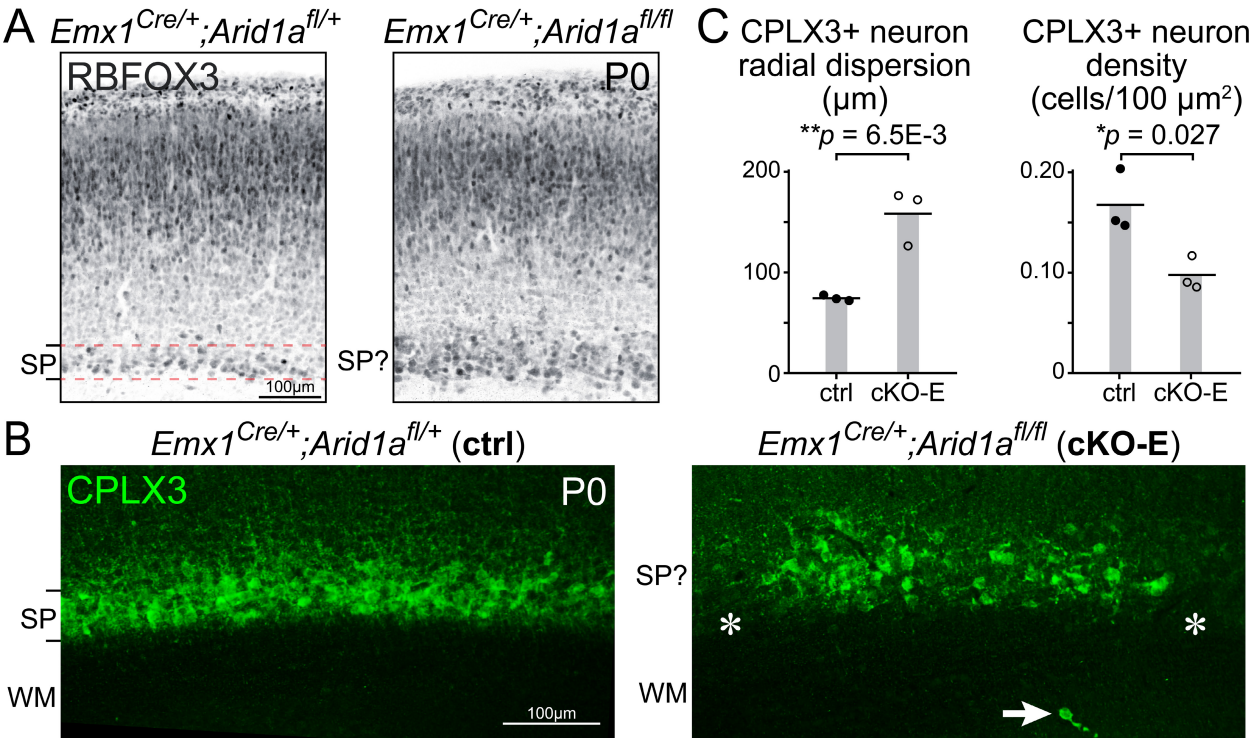

Figure 3.4 Disrupted subplate organization following *Arid1a* deletion

(A) RBFOX3 immunostaining (black) on coronal sections of P0 ctrl revealed a distinct and organized subplate band positioned just beneath the cortical layers. In cKO-E, the subplate band was less clearly defined and not distinct from cortical layers.

(B) CPLX3 immunostaining (green) on coronal sections of P0 ctrl and cKO-E brains. In ctrl, CPLX3+ subplate neurons were organized into a discrete, continuous band. In cKO-E, the band of CPLX3+ subplate neurons was more dispersed and characterized by gaps (asterisks). Some CPLX3+ cells were aberrantly positioned in white matter (WM, arrow).

(C) Quantification of CPLX3+ subplate neuron radial dispersion revealed significant subplate distribution in cKO-E (data are mean, two-tailed unpaired *t* test, n=3 animals/condition). (*I*) Quantification revealed a significant decrease in CPLX3+ subplate neuron density in cKO-E (data are mean, two-tailed unpaired *t* test, n=3 animals/condition).

SP: subplate, WM: white matter

Impaired SP development and function can contribute to disruption of cortical connectivity. Although CPLX3 immunostaining identified changes in P0 SP, it cannot be visualized until P0, thus precluding its utility to study embryonic SP. SP gene expression changes and widespread axonal misrouting are present in cKO-E by E15.5. To assess potential changes in embryonic SP organization that could impact cortical circuit wiring I immunostained TUBB3 (TUJ1), a cytoskeletal marker that reveals neuronal layers (**Figure 3.5 A**). In E14.5 ctrl cortex, strongly-labeled TUBB3+ cells were situated within the SP, and processes were positioned horizontally within the IZ. In cKO-E, however, TUBB3+ cells and processes extended into the CP, no longer providing clear delineation of cortical grey and white matter. Additionally, during embryogenesis, L6 and SPNs are both labeled by NR4A2 (NURR1) and SPNs express high levels of the somatodendritic marker MAP2 in comparison to their CP counterparts (434). In E14.5 ctrl, NR4A2+/MAP2-high neurons were positioned in a distinct band between CP and WM (**Figure 3.5 B**). MAP2+ dendrites projected apically, toward the pial surface in an organized fashion. However, consistent with P0 CPLX3 and RBFOX3, NR4A2+/MAP2-high neurons in E14.5 cKO-E displayed abnormal clustering and gaps while appearing to be intermixed with L6 neurons. Remarkably, although some MAP2+ dendrites extended toward the pia in cKO-E, a multitude reached aberrantly back into the IZ toward the ventricular surface.

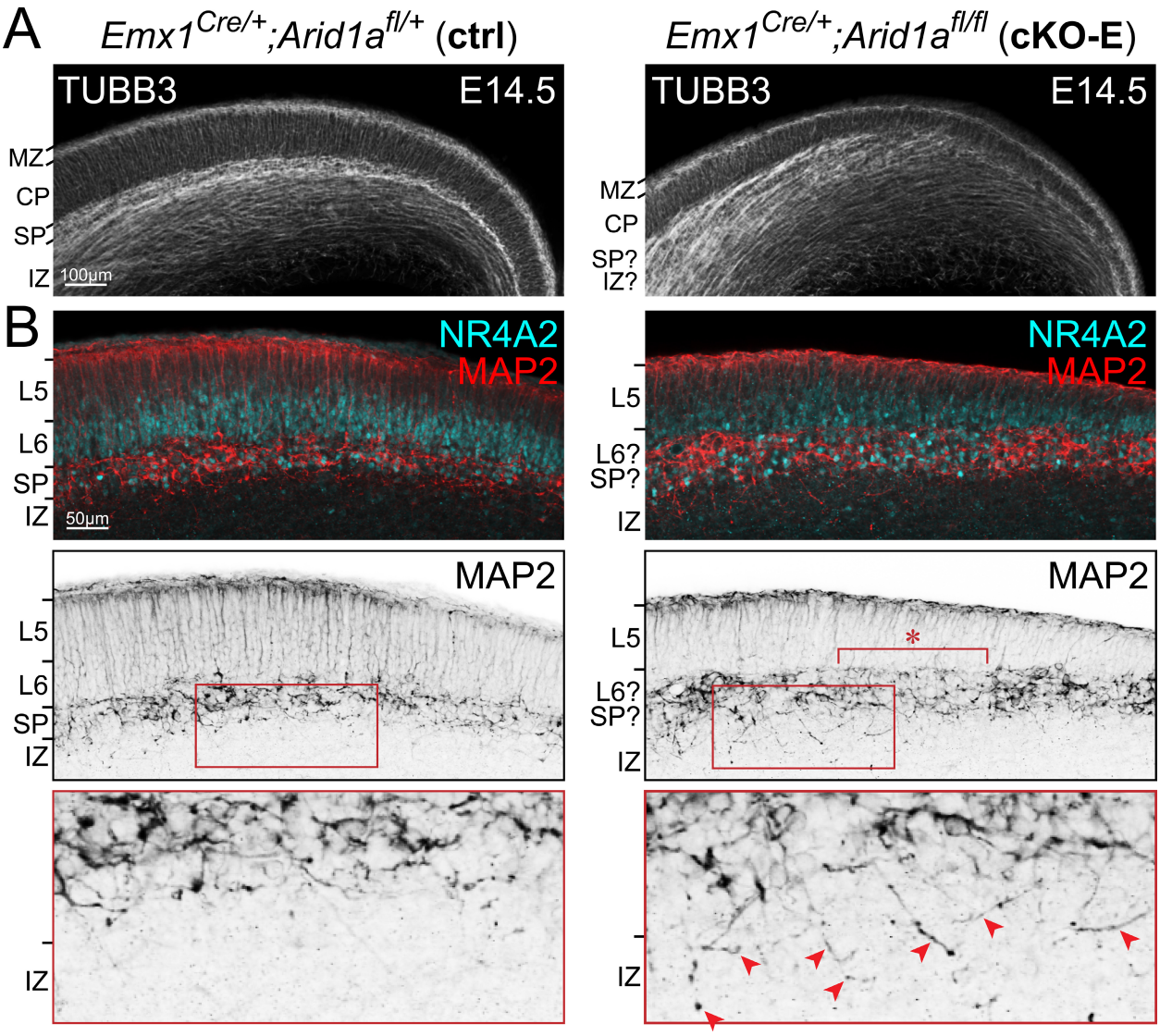

Figure 3.5 Embryonic subplate disruption in *Arid1a* cKO-E

(A) TUBB3 (TUJ1) immunostaining (white) on E14.5 ctrl and cKO-E sections. In ctrl, TUBB3+ processes were horizontally organized in intermediate zone (IZ) and subplate, and radially organized in cortical plate (CP). In cKO-E, TUBB3+ axons became defasciculated in intermediate zone, and invaded cortical plate diagonally.

(B) MAP2 (red, black) and NR4A2 (cyan) immunostaining on E14.5 ctrl and cKO-E sections. In ctrl, MAP2+/NR4A2+ subplate neurons were organized within a clearly delineated layer below cortical plate. In cKO-E, subplate neurons were characterized by abnormal clustering and cell-sparse gaps (asterisk). In cKO-E, misoriented MAP2+ dendrites aberrantly projected ventrally into intermediate zone (red arrowheads, inset).

CP: cortical plate, IZ: intermediate zone, L*n*: layer *n*, MZ: marginal zone, SP: subplate

To unequivocally confirm that these defects were present in embryonic SPNs, I generated ctrl and cKO-E mice containing the *Tg*(*Lpar1-EGFP*) transgene, which expresses EGFP specifically in a subset of SPNs beginning around E15.5 (139, 431). Importantly, at both E16.5 and P0, Lpar1-EGFP-labeled SPNs were altered in cKO-E (**Figure 3.6 A** and **B**). Not only were there gaps and clusters of SPNs, but many were present within the developing WM. Alterations were also apparent in P0 cKO-E SP; Lpar1-EGFP-positive neurons were consistently found outside the presumed SP in WM as interstitial neurons. These deficits are likely broadly applicable to SPNs, as two subtypes of SPNs (CPLX3-positive and Lpar1-EGFP-positive) were disrupted and ARID1A is found in comparable levels in Lpar1-EGFP-positive and surrounding Lpar1-EGFP-negative SPNs (**Figure 3.6 C**). Thus, *Arid1a* deletion in cKO-E not only impacted SPN transcriptome, but also SP organization beginning during corticogenesis.

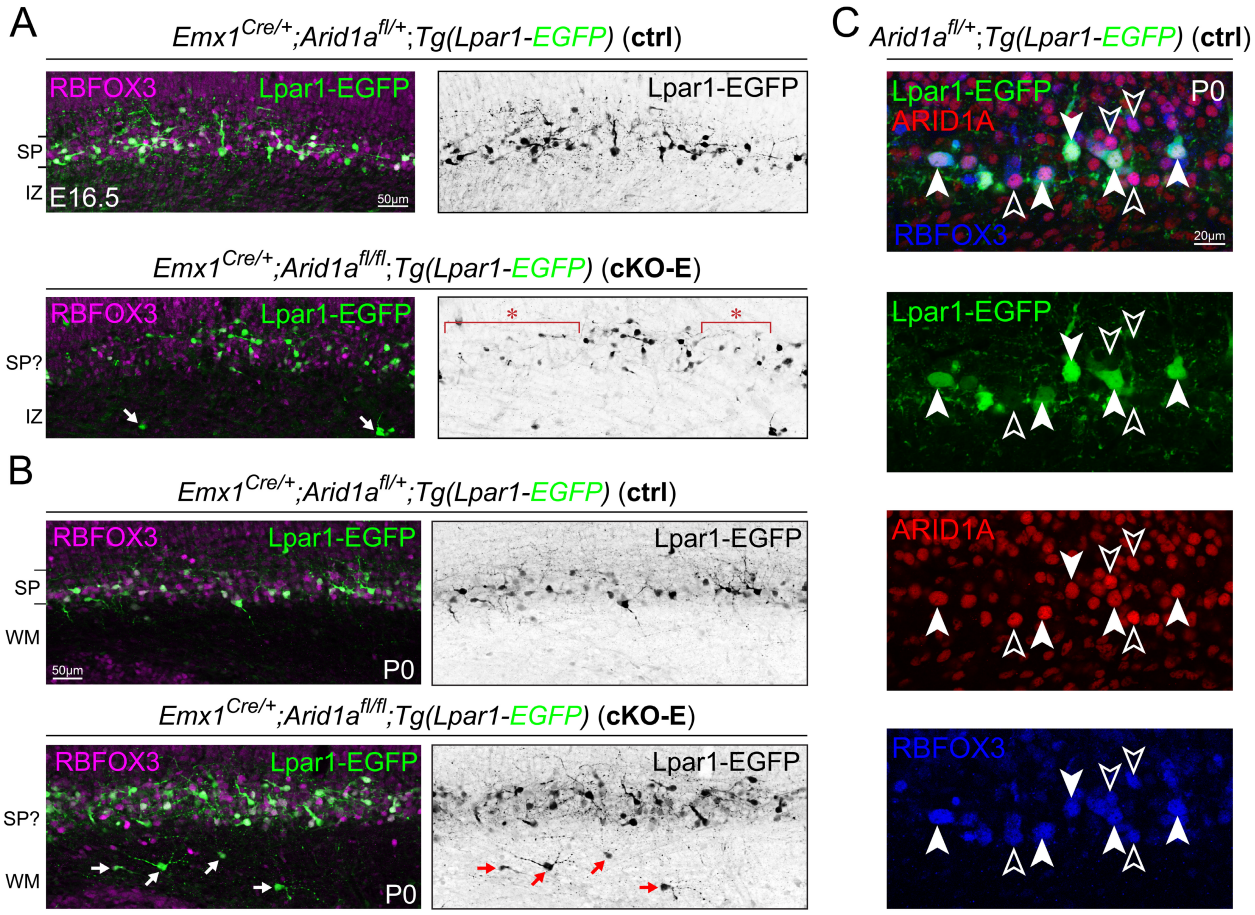

Figure 3.6 Loss of subplate organization following *Arid1a* deletion

(A) RBFOX3 (NEUN) immunostaining (magenta) on E16.5 ctrl and cKO-E brains carrying the *Lpar1-EGFP* transgene. In cKO-E, Lpar1-EGFP+ subplate neurons (green, black) were characterized by cell-sparse gaps (asterisks) and a few Lpar1-EGFP+ neurons were aberrantly positioned in the intermediate zone (arrows).

(B) RBFOX3 (NEUN) immunostaining on P0 ctrl and cKO-E brains carrying the *Lpar1-EGFP* transgene. In cKO-E, RBFOX3+ (magenta) and Lpar1-EGFP+ (green, black) neurons were not tightly organized into a discreet, continuous subplate band beneath the cortical plate. Lpar1-EGFP+ neurons were positioned in white matter (WM, arrows).

(C) ARID1A (red) immunostaining of subplate P0 ctrl with Tg(*Lpar1-EGFP*). ARID1A was present in Lpar1-EGFP+ (green) and surrounding RBFOX3+ (blue) subplate neurons in indistinguishable levels.

IZ: intermediate zone, SP: subplate, WM: white matter

Broad identification of SPNs established impaired SP organization in cKO-E. I sought to assess the development of SPN morphology at a single-neuron resolution. To achieve this, I utilized a CRISPR-Cas9-strategy to produce a double-strand DNA break at the C-terminus of the cytoskeletal gene *Actb* while providing a repair template containing a 3xHA epitope tag flanked by gRNA target sequences (87). Successful cleavage by Cas9 in tandem with non-homologous end joining repair incorporation of the repair template in the forward orientation and in-frame with *Actb* results in expression of ACTB-3xHA. Notably, non-homologous end joining is an imperfect repair method, and thus provides the potential for out-of-frame and/or reversed integration of 3xHA, thereby supporting an optimal approach for sparse, whole-neuron morphological analyses. To utilize this assay and label SPNs *in vivo*, I used IUE to introduce CRISPR-Cas9, repair template, and CAG-mTagBFP2 to NPCS at E11.5, during the peak of SP genesis (**Figure 3.7 A**). By E16.5, SPNs were precisely- and extensively labeled with mTagBFP2. In ctrl mTagBFP2+ neurons formed a distinctive SP band at the base of the CP (**Figure 3.7 B**). However, in cKO-E, SPNs were aberrantly clustered and disorganized similar to what was observed with CPLX3, MAP2/NR4A2, and Lpar1-EGFP.

SPNs have diverse morphologies which have been well-described in over the past 50 years, although embryonic morphologies are less characterized (256-258, 435). In E16.5 ctrl, ACTB-3xHA labeled SPNs were optimally sparse and displayed a variety of morphologies, including pyramidal, bipolar, and multipolar (**Figure 3.7 C**). They had numerous projections and many presented with lengthy axonal extensions. By contrast, HA+ SPNs in cKO-E also took on disparate morphologies, however, they largely did not

resemble the classical pyramidal, bipolar, and multipolar classifications (**Figure 3.7 D**). In addition, the axonal outgrowth was visibly minimized and some HA-labeled SPNs extended ventrally-directed dendrites, reminiscent of MAP2 immunostaining. Although SPNs diverged in cKO-E compared to ctrl, pyramidal neurons were largely indistinguishable. Both control and cKO-E HA-labeled pyramidal neurons had consistent orientation of apically-oriented dendrites, they were not significantly different from one another (Mean absolute value of apical dendrite orientation angle: ctrl=4.47°, cKO-E=4.81°, p=0.742, two-tailed unpaired t test, n=14 neurons/condition) (**Figure 3.8**). Together broad and sparse analyses of neuronal organization and morphology, in tandem with transcriptomic analyses revealed a cell type-dependent function for *Arid1a* during cortical development.

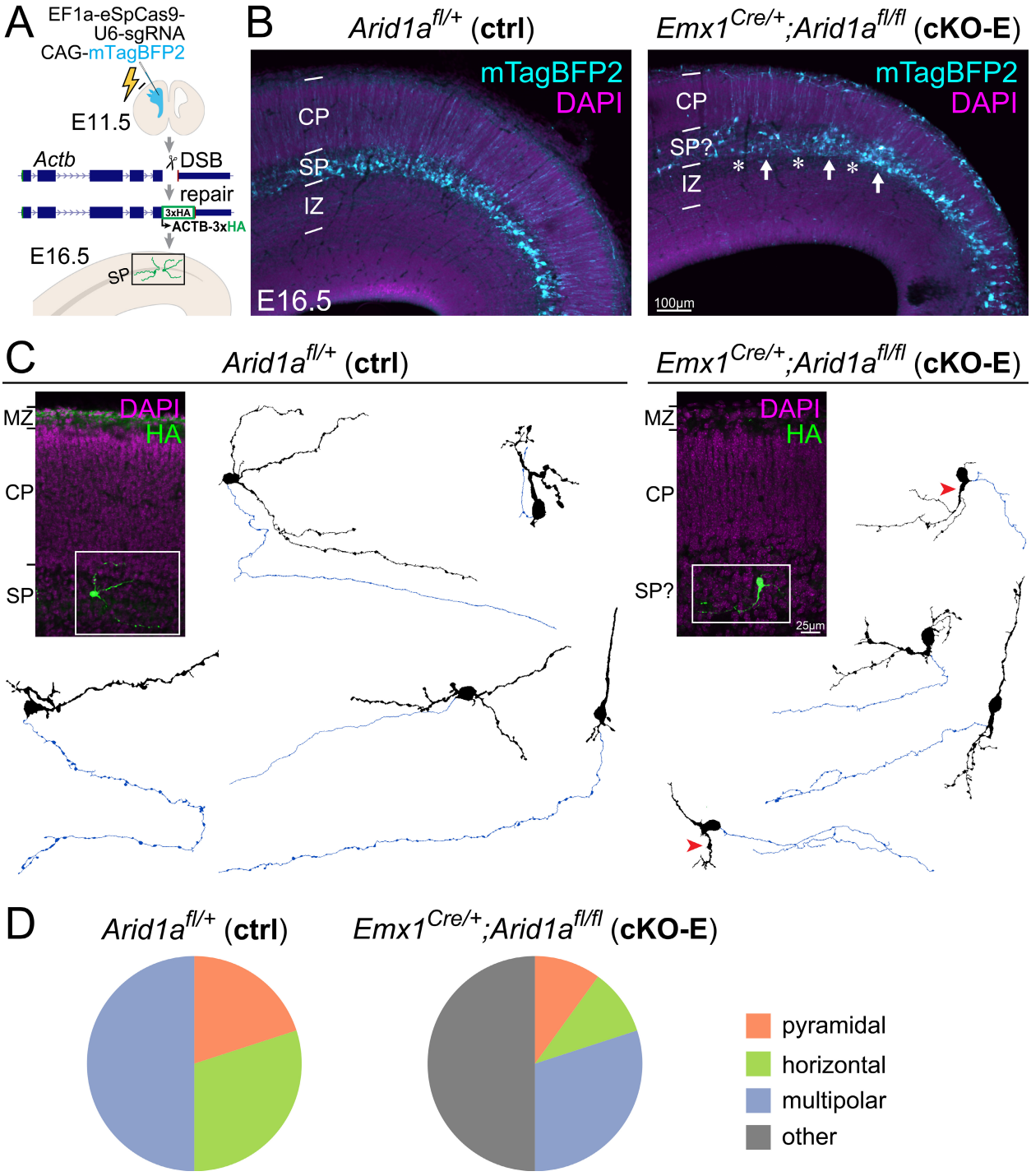

Figure 3.7 *Arid1a* deletion drastically disrupts subplate neuron morphology

(A) Schematic illustration of sparse subplate neuron labeling by *in utero* genome editing. A DNA break was induced by CRISPR-Cas9 within the coding region of *Actb* near the C-terminus. A reporter repair template was designed such that correct DNA repair would lead to expression of ACTB-3xHA. CRISPR-Cas9, reporter repair, and

mTagBFP2 expression constructs were co-transfected into cortical NPCs at E11.5 by *in utero* electroporation (IUE). Electroporated brains were analyzed at E16.5.

(B) In electroporated E16.5 brains, mTagBFP2 (cyan) was successfully targeted to subplate neurons. In cKO-E, labeled subplate neurons showed disorganization with abnormal cell clusters (arrows) and cell-sparse gaps (asterisks).

(C) HA immunostaining (green) revealed the complete morphology of sparsely-labeled subplate neurons. Neurons were reconstructed based on confocal Z-stacks. Dendrites are indicated in black. Axons are indicated in blue. In cKO-E, some neurons were characterized by a dendrite ventrally directed into the intermediate zone (red arrowheads).

(D) Quantification of subplate neuron morphological subclasses.

CP: cortical plate, IZ: intermediate zone, MZ: marginal zone, SP: subplate

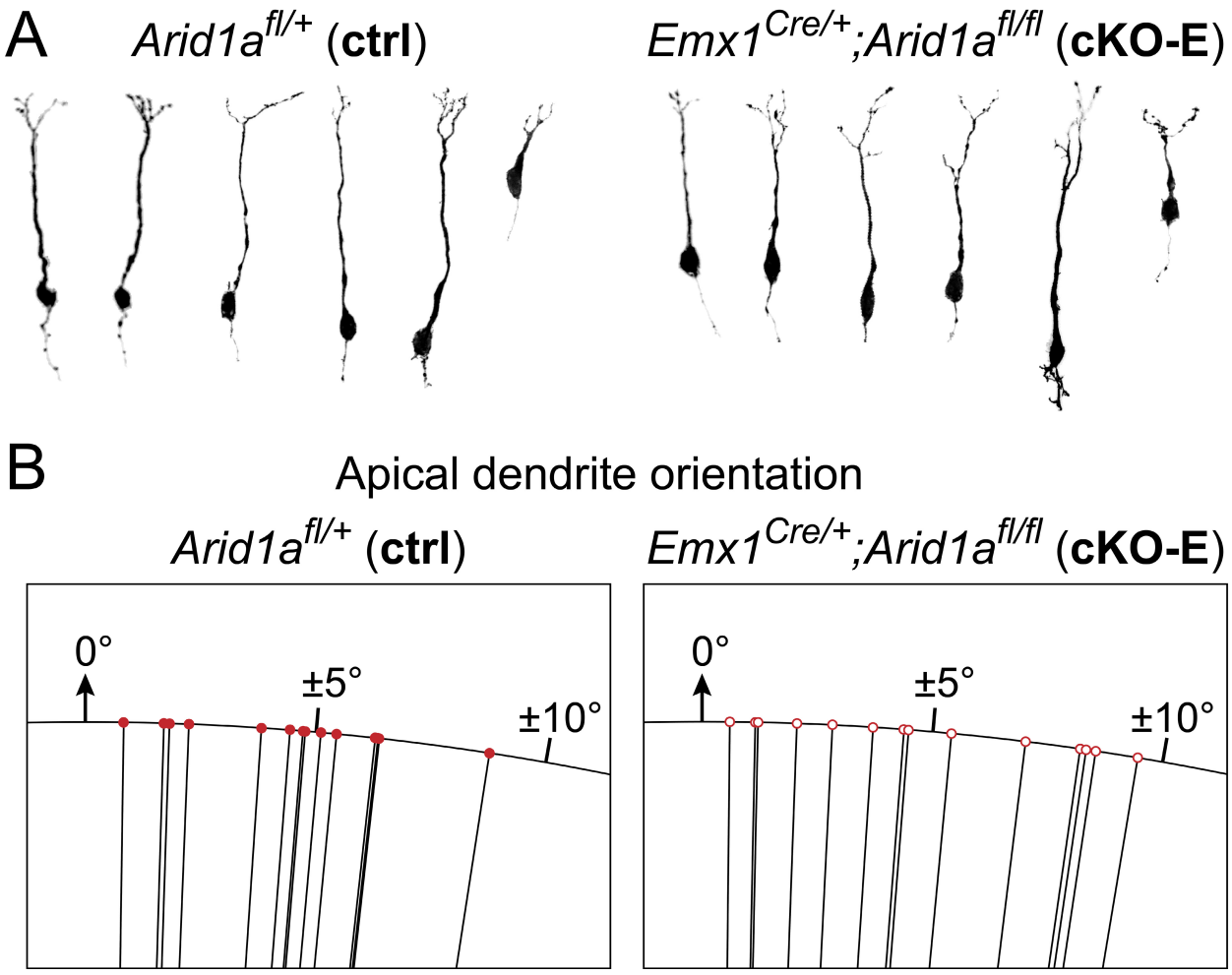

Figure 3.8 Unaltered pyramidal neuron morphology following *Arid1a* deletion

(A) Morphological analysis of ACTB-3xHA-tagged pyramidal neurons at E16.5. No robust morphological differences were found between cKO-E and ctrl pyramidal neurons.

(B) Quantitative analysis of pyramidal neuron apical dendrite orientation at E16.5. No significant difference in apical dendrite orientation was found between cKO-E and ctrl (p = 0.74, two-tailed unpaired t test, n=14 neurons/condition).

Impaired subplate neuron projections and extracellular matrix following Arid1a deletion

SPNs extend the first axons corticofugally and can exert non-cell autonomous influence while communicating with other developing circuitry. Once descending SP axons extend across the PSB, they convene with ascending TCAs within the subpallium, shake hands and cofasciculate, and guide each other to form reciprocal connections as posited in the "handshake hypothesis" (417, 436, 437). In cKO-E, SPNs were disrupted in their transcriptome, organization, and morphology, coincident with disruption of disruption of thalamocortical circuitry, specifically improper crossing of the PSB, premature invasion of the CP, and loss of sensory whisker barrels. Pioneering work ablating the developing SP in fetal cat with kainic acid-mediated excitotoxic lesion revealed impairment of thalamocortical connectivity (303-305).

To visualize SP axons and their potential interactions with cortical afferents, I used Tg(*Golli-tau-EGFP*) transgene which expresses TAU (τ)EGFP in SP and L6 neurons (438, 439). In E15.5 ctrl, an abundance of τEGFP+ axons had already extended across the PSB and were situated within the internal capsule (**Figure 3.9**). These τEGFP+ corticofugal projections were closely apposed to NTNG1+ TCAs, which had extended out of the thalamus and across the telencephalic-diencephalic boundary into the striatum, consistent with previously described cofasciculation. In striking contrast, in cKO-E, τEGFP+ innervation of the subpallium was severely attenuated and there was a near complete lack of cofasciculation with NTNG1+ TCAs. By E17.5, the distinction between ctrl and cKO-E was even more evident. There was extensive cofasciculation of τEGFP+ and NTNG1+ axons in ctrl, but still minimal close interactions in the subpallium of cKO-E. Notably, in P0 cKO-E, some NTNG1+ TCAs appeared to

follow aberrant trajectories laid down by τEGFP+ SP axons and NTNG1+ axons lacking close interaction with τEGFP+ projections were misrouted. Misrouted TCAs were unable to cross the PSB at their normal location, appeared to hit a wall and instead took a more medial route into the cortex, became defasciculated in the IZ, and prematurely invaded the CP. Importantly, TCA disruption was not observed in cKO-E at E13.5, prior to PSB crossing (**Figure 3.10**). These data were in agreement with the "handshake hypothesis," and strongly suggested that the "handshake" directs reciprocal SP/thalamocortical growth.

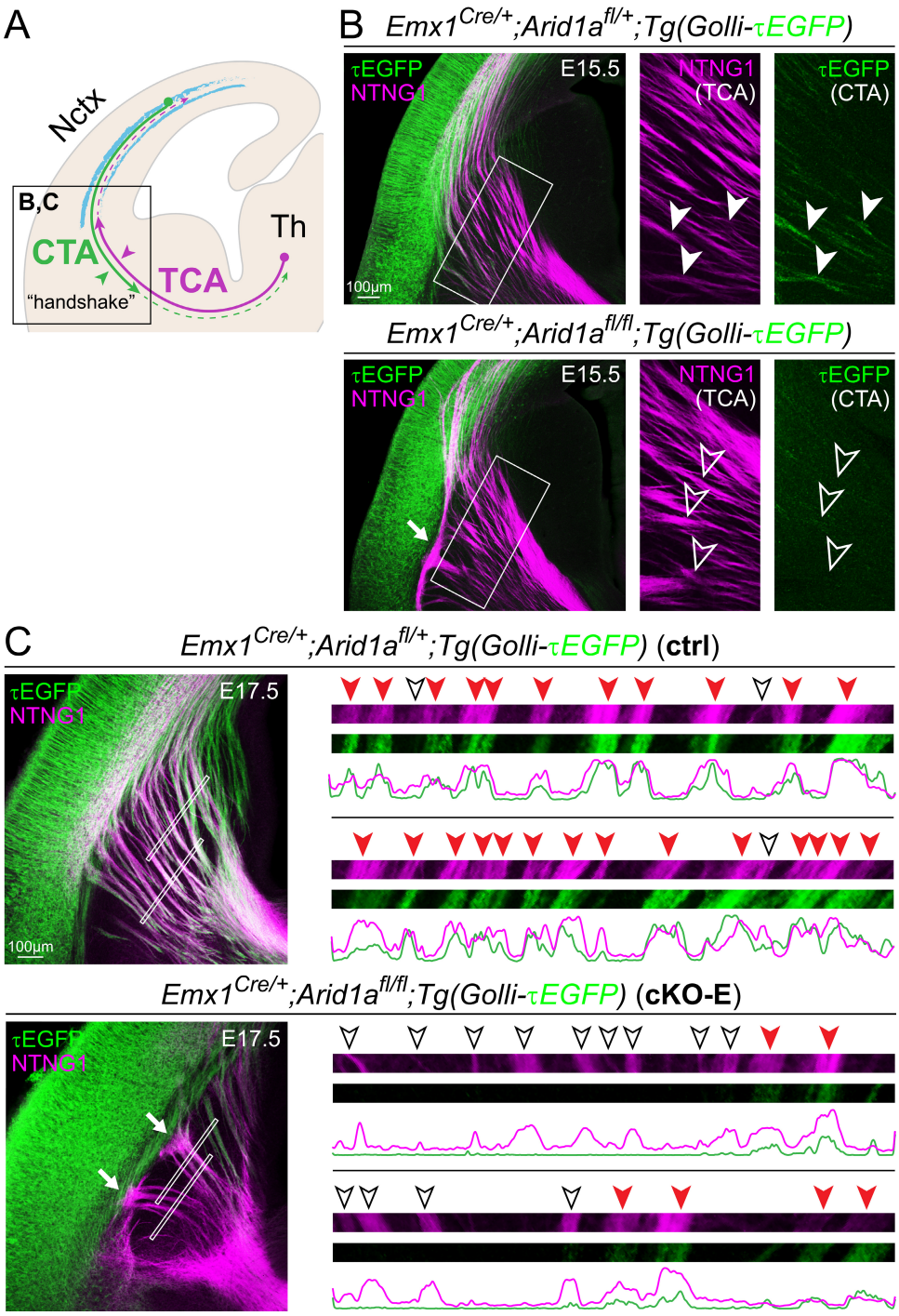

Figure 3.9 *Arid1a* deletion attenuates subplate-thalamocortical "handshake"

(A) Schematic illustration of subplate-thalamocortical interaction in the subpallium.

(B) NTNG1 immunostaining (magenta) on E15.5 (*B*) and E17.5 (*C*) ctrl and cKO-E brains carrying the *Golli-τEGFP* transgene. In E15.5 ctrl, τEGFP+ (green) descending axons from subplate neurons closely co-fasciculated (solid arrowheads) with ascending

NTNG1+ thalamocortical axons (magenta). In E15.5 cKO-E, τEGFP+ axons largely have not crossed the pallial-subpallial boundary (PSB). NTNG1+ thalamocortical axons, without co-fasciculation with τEGFP+ axons (open arrowheads), did not cross the PSB along the normal trajectory and formed an aberrant bundle parallel to the boundary (solid arrow) in cKO-E.

(C) In E17.5 ctrl, analysis of co-fasciculation (insets) revealed frequent co-fasciculation (red arrowheads) of τEGFP+ and NTNG1+ axons, which is consistent with the “handshake hypothesis”. In E17.5 cKO-E, most NTNG1+ thalamocortical axons did not co-fasciculate with τEGFP+ corticothalamic axons (open arrowheads) and were unable to cross the PSB (solid arrows).

Nctx: neocortex, Th: thalamus

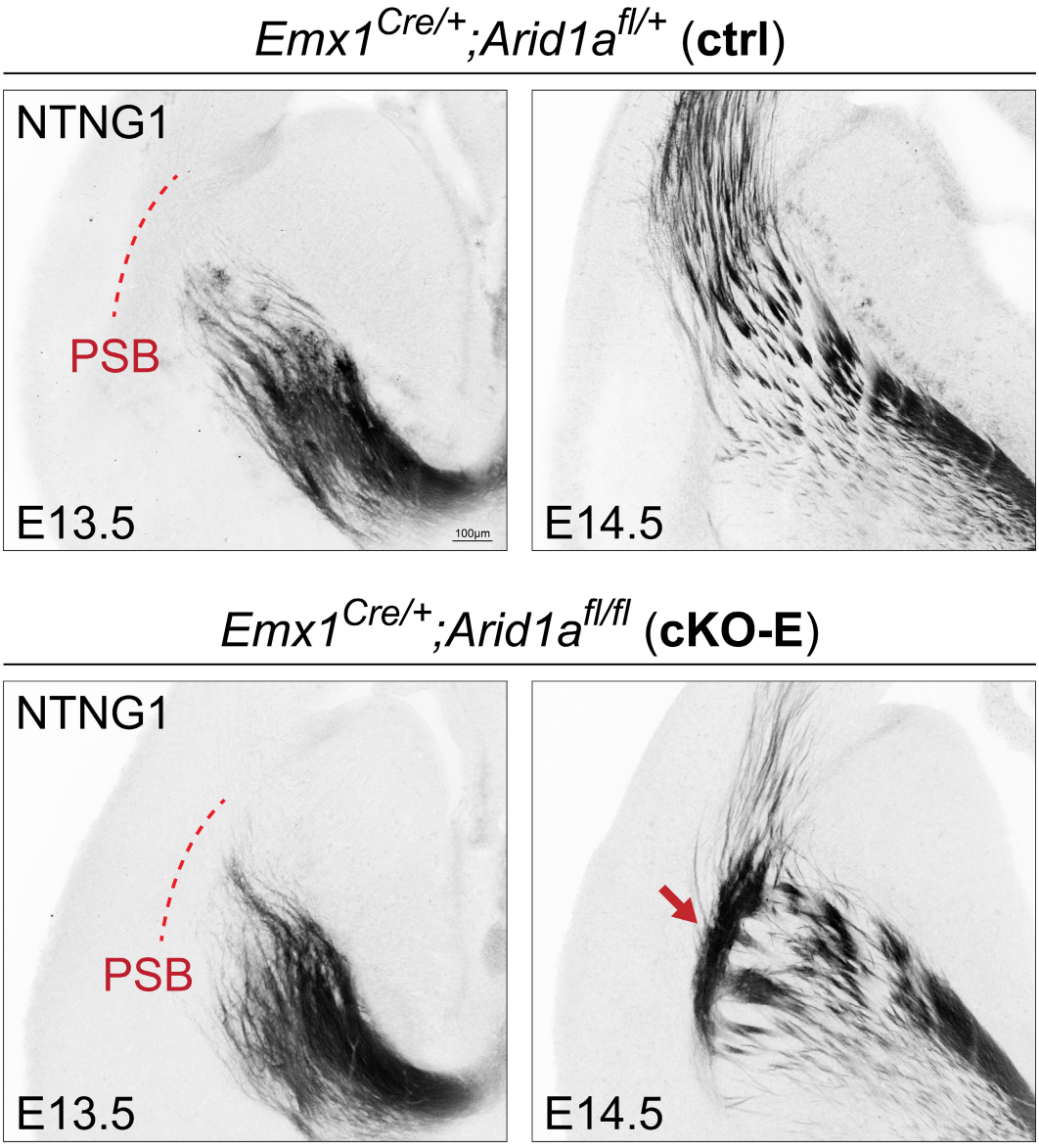

Figure 3.10 Temporal onset of thalamocortical misrouting following *Arid1a* deletion

NTNG1 immunostaining (black) on coronal sections of ctrl and cKO-E. At E13.5, NTNG1+ thalamocortical axons had not crossed the PSB in ctrl. In cKO-E, thalamocortical axons had not shown any misrouting deficits. At E14.5, thalamocortical axons abundantly crossed the PSB in ctrl. In cKO-E, thalamocortical axons had started to show characteristic misrouting and defective crossing of the PSB (arrow).

PSB: pallial-subpallial boundary

One of the main non-cell autonomous influences of SPNs in circuit wiring is via axon-axon interactions with thalamocortical neurons put forward in the “handshake hypothesis” (417). SPNs also secrete various ECM proteins that coalesce form a discrete corridor housing growing axons and migrating GABAergic interneurons (289, 292, 440). The CSPG-rich SP ECM is thought to guide developing axons, and TCAs pause within this corridor during their “waiting period” before extending into the CP at E18.5, around the same time the ECM corridor is diminished. In E15.5 and 16.5 ctrl, the CSPG+ ECM corridor is clearly delineated throughout the mediolateral extent of the SP and filled with NTNG1+ TCAs (**Figure 3.11**). However, in cKO-E, CSPG was reduced and the corridor appeared to collapse, it no longer created a continuous and apparent trajectory for developing axons. Concomitant with ECM corridor disruption in cKO-E, NTNG1+ TCAs were longer confined to the cortical WM and instead deviated from their trajectory and prematurely invaded the CP. Together, analyses revealed deficits in SPN morphogenesis, SP axon cofasciculation with TCAs, and SP ECM after *Arid1a* deletion.

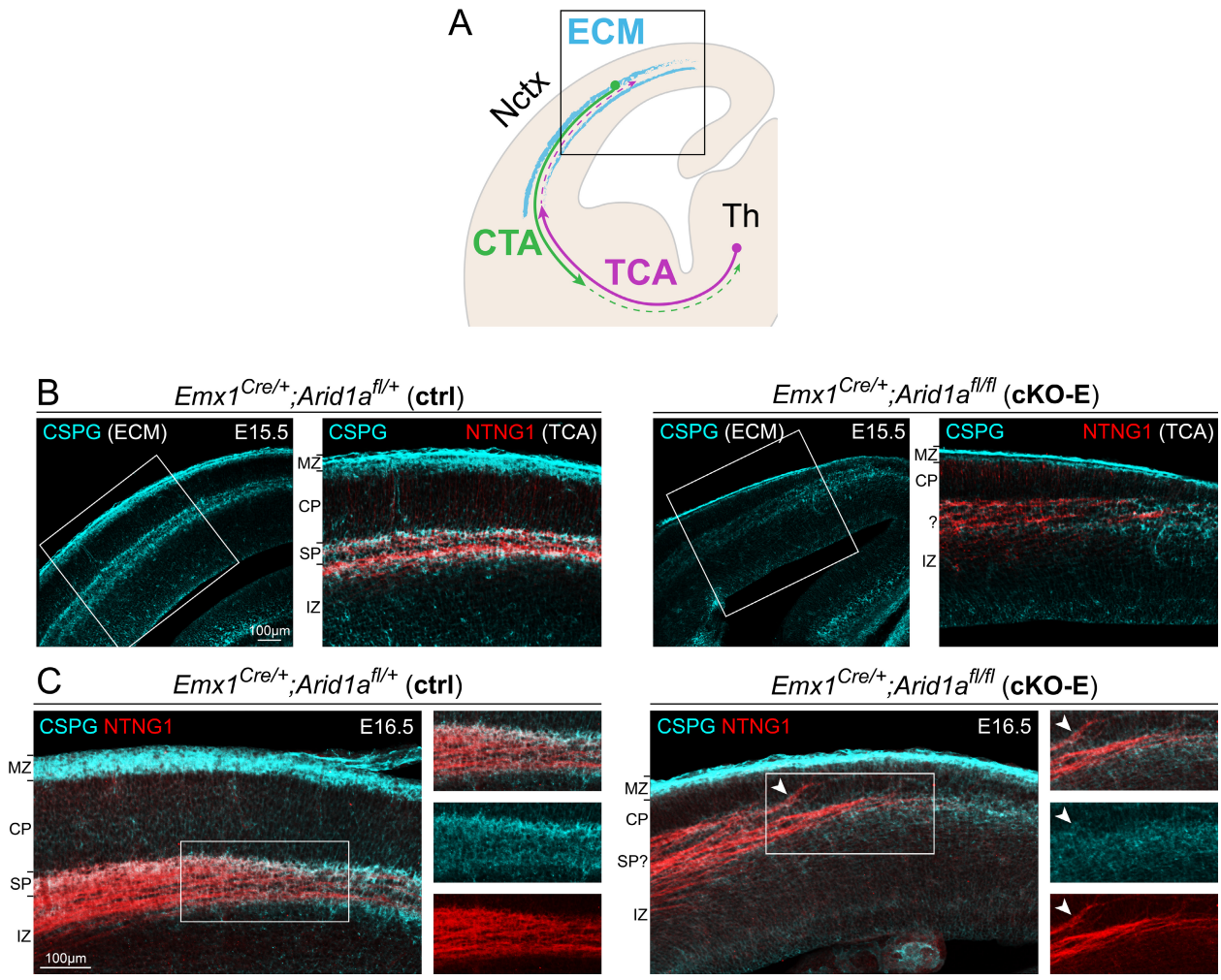

Figure 3.11 Disrupted subplate extracellular matrix following *Arid1a* deletion

(A) Schematic illustration of subplate ECM and thalamocortical ingrowth.

(B and C) CSPG (cyan) and NTNG1 (red) immunostaining on E15.5 (B) and E16.5 (C) ctrl and cKO-E brain sections. In ctrl, NTNG1+ thalamocortical axons tangentially traversed the embryonic cortex within a subplate/intermediate zone corridor neatly delineated by the extracellular matrix component CSPG. In cKO-E, CSPG expression was reduced and the CSPG corridor had collapsed. NTNG1+ thalamocortical axons were not confined within the subplate/intermediate zone, deviated from their normal trajectory, and prematurely invaded cortical plate (arrowhead).

CP: cortical plate, CTA: corticothalamic axon, ECM: extracellular matrix, IZ: intermediate zone, MZ: marginal zone, Nctx: neocortex, SP: subplate, TCA: thalamocortical axon, Th: thalamus

Sparing Arid1a expression in subplate neurons is sufficient to restore callosal and thalamocortical circuitry

My data revealed deletion of *Arid1a* altered SPN transcriptome, organization, morphology, axonal projections, and ECM while simultaneously non-cell autonomously disrupting callosal and thalamocortical circuitry. To empirically test the hypothesis that SPNs mediate the axon guidance functions of *Arid1a*, I sought to determine whether *Arid1a* expression in SPNs was sufficient to support axon pathfinding from cortical neurons that lacked *Arid1a*. I therefore generated an *Arid1a* cKO using Tg(*hGFAP-Cre*) (441). Tg(*hGFAP-Cre*) leverages the human *GFAP* promoter to express Cre specifically in murine cortical NPCs beginning around E12.5 (441), after the majority of SPN have been generated (**Figure 3.12** and **Figure 3.13**). Therefore, *Arid1a* would be deleted from NPCs and CP neurons, but SPNs would be spared. SP-spared cortical deletion of *Arid1a* was confirmed by ARID1A immunostaining at E15.5 in Tg(*hGFAP-Cre*); $Arid1a^{fl/fl}$ (cKO-hG) (**Figure 3.12 B**). Importantly, Tg(*hGFAP-Cre*) mediated recombination deletion from L6 neurons by E13.5, prior to their arrival in the CP, thus largely uncoupling the effects of SPNs from their closely related L6 counterparts (**Figure 3.13 C**). By P0, ARID1A immunostaining across layers in cKO-E versus cKO-hG only differed in SP (Mean ARID1A+ cells normalized to ctrl: SP: cKO-E=0.225, cKO-hG=0.857, p=1.0e-4; L6: cKO-E=0.0797, cKO-hG=0.0775, p=0.88; L5: cKO-E=0.163, cKO-hG=0.133, p=0.28; L2-4: cKO-E=0.227, cKO-hG=0.219; p=0.78, MZ: cKO-E=0.889, cKO-hG=0.796, p=0.28, two-tailed unpaired t test, n=3 animals/condition), confirming the utility of the *Arid1a* SP-spared model for testing *Arid1a* sufficiency in circuit wiring (**Figure 3.13 D**).

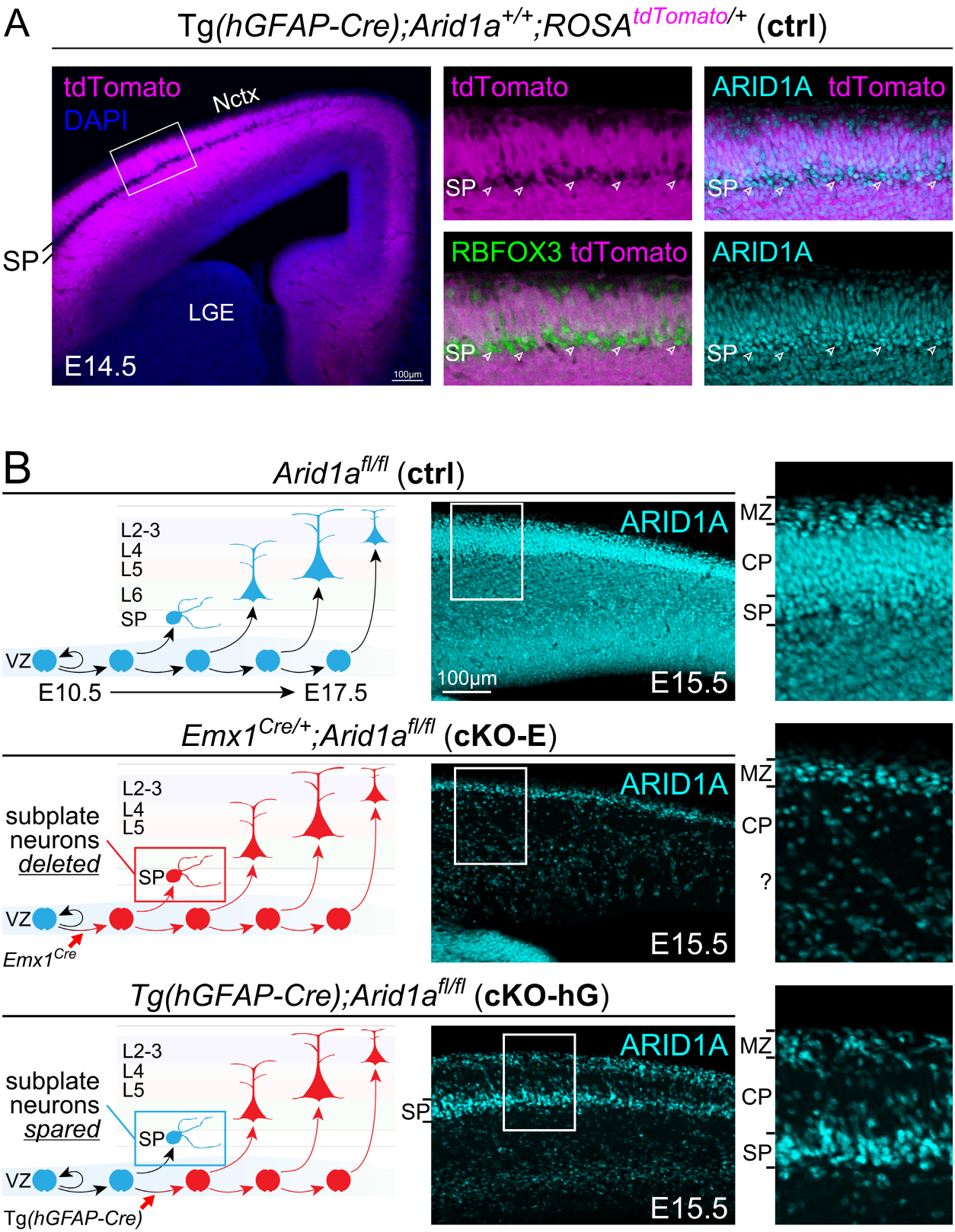

Figure 3.12 Subplate-spared deletion of *Arid1a* with Tg(*hGFAP-Cre*)

(A) Analysis of Tg(*hGFAP-Cre*)-mediated recombination. In E14.5 Tg(*hGFAP-Cre*), analysis using the Cre-dependent reporter *ROSA*^{tdTomato} revealed an absence of tdTomato (magenta) from the subplate (SP) band. Co-immunostaining revealed an absence of tdTomato from RBFOX3+ (green) subplate neurons (arrowheads, inset), which expressed ARID1A (cyan).

(B) Schematic illustration of subplate-spared cortical plate deletion of *Arid1a*. *Emx1*^{Cre} mediates Cre recombination in cortical NPCs starting at E10.5, prior to subplate neurogenesis. ARID1A immunostaining (cyan) in E15.5 *Emx1*$^{Cre/+}$*;Arid1a*$^{fl/fl}$ (cKO-E) revealed loss of ARID1A from subplate and cortical plate neurons. Tg(*hGFAP-Cre*) mediates Cre recombination in cortical NPCs starting at E12.5, after the majority of subplate neurons have been generated. In E15.5 Tg(*hGFAP-Cre*);*Arid1a*$^{fl/fl}$ (cKO-hG), ARID1A was lost from cortical plate neurons, but present in subplate neurons.

CP: cortical plate, LGE: lateral ganglionic eminence, L*n*: layer *n*, MZ: marginal zone, Nctx: neocortex, SP: subplate, VZ: ventricular zone

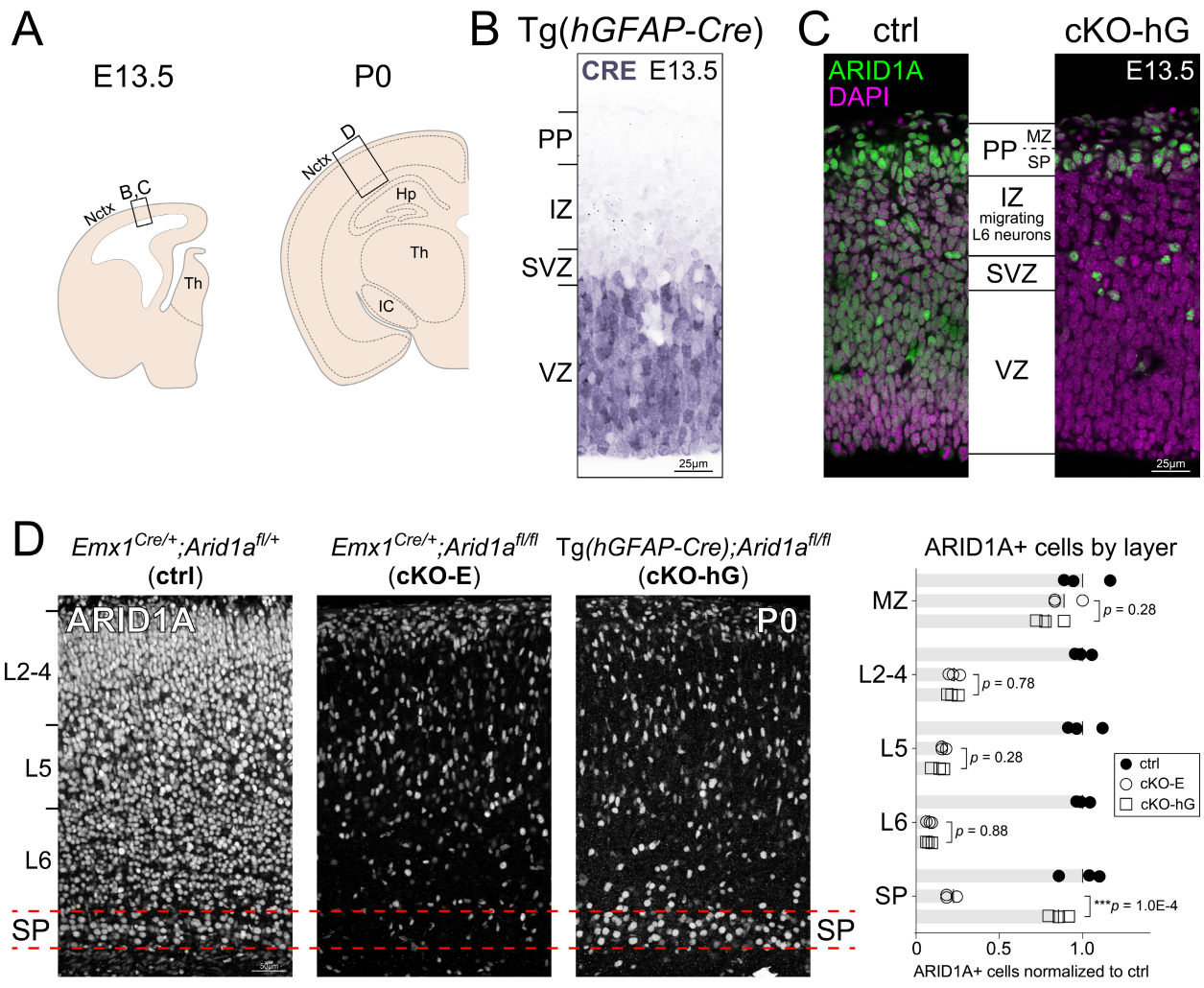

Figure 3.13 Spatiotemporal dynamics of *Arid1a* deletion with Tg(*hGFAP-Cre*)

(A) Schematic illustration of E13.5 and P0 coronal sections with neocortical insets for (B-D).

(B) In Tg(*hGFAP-Cre*) at E13.5, CRE (blue) was abundant in VZ NPCs, but not in postmitotic neurons in IZ or PP.

(C) At E13.5, ARID1A (green) was widely expressed in ctrl cortex. In cKO-hG, ARID1A was present in the PP, where future subplate neurons were located, consistent with a sparing of subplate neurons by Tg(*hGFAP-Cre*). In contrast, ARID1A was absent from migrating L6 neurons in IZ and from NPCs in VZ.

(D) ARID1A immunostaining (white) on coronal sections of P0 ctrl, cKO-E, and cKO-hG brains. ARID1A was present in subplate (red lines) in ctrl and absent from subplate in cKO-E. In cKO-hG, ARID1A expression was present in subplate, confirming sparing of subplate neurons from *Arid1a* deletion. The loss of ARID1A expression from L2-6

neurons, however, was not significantly different between cKO-E and cKO-hG (data are mean, two-tailed unpaired *t* test, n=3 animals/condition).

Hp: hippocampus, IC: internal capsule, IZ: intermediate zone, L*n*: layer *n*, MZ: marginal zone, Nctx: neocortex, PP: preplate, SP: subplate, SVZ: subventricular zone, Th, thalamus, VZ: ventricular zone

Pancortical deletion of *Arid1a* in cKO-E disrupted SP organization. In P0 cKO-hG, sparing *Arid1a* from deletion selectively in SPNs was sufficient to restore the stereotyped RBFOX3+ SP band, and radial dispersion of CPLX3+ SPNs returned to levels comparable to ctrl (Mean CPLX3+ radial dispersion: ctrl=74.5 μm, cKO-E=158.4 μm, cKO-hG=72.6 μm, ctrl:cKO-E p=1.77e-3, ctrl:cKO-hG p=0.988, cKO-E:cKO-hG p=1.57e-3, one-way ANOVA with Tukey's multiple comparisons test, n=3 animals/condition) (**Figure 3.14 A** and **B**). Thus, in cKO-hG, sparing SPNs from *Arid1a* deletion led to correct anatomical formation of the SP band.

To determine whether SP-sparing in cKO-hG aided in restoration of cortical axon tracts, I used the Cre-dependent fluorescent reporter $ROSA^{tdTomato}$ (**Figure 3.14 B**). Remarkably, in cKO-hG, axons arising from tdTomato-labeled, *Arid1a*-deleted, CP neurons correctly formed the CC and projected into the contralateral hemisphere (Mean CC thickess mm, ctrl=0.269, cKO-E=0.000, cKO-hG=0.263, ctrl:cKO-E p=3.53e-7, ctrl:cKO-hG p=0.223, cKO-E:cKO-hG p=3.59e-6, one-way ANOVA with Tukey's multiple comparisons test, n=3 animals/condition). *Arid1a* expression in cKO-hG SPNs was therefore sufficient for normal SP organization and rescue of callosal agenesis observed in cKO-E.

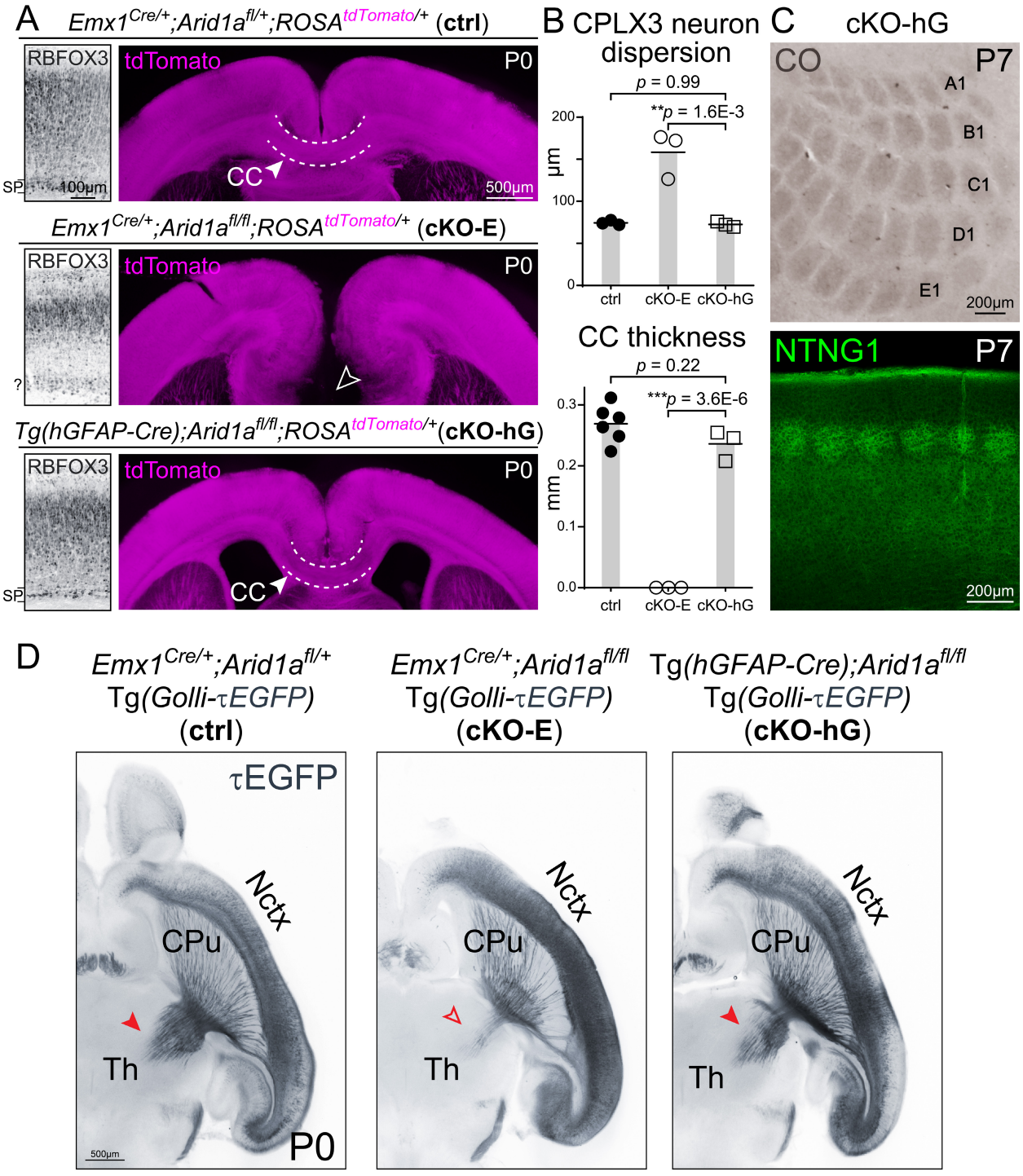

Figure 3.14 Subplate-spared *Arid1a* is sufficient for callosal and thalamocortical formation

(A) Subplate and axon tract analyses on P0 ctrl, cKO-E, and cKO-hG brain sections. RBFOX3 immunostaining revealed in cKO-hG an organized, distinct subplate band positioned just beneath the cortical layers that was indistinguishable from ctrl. tdTomato (magenta) was expressed Cre-dependently from *ROSA*^{tdTomato}, enabling visualization of

cortical axons. Agenesis of corpus callosum (open arrowhead) was observed in cKO-E. However, the corpus callosum (CC) was formed without gross defect in cKO-hG (solid arrowhead, n=3/3 animals/condition).

(B) Quantitative analyses revealed no significant changes in subplate thickness or corpus callosum thickness at midline in cKO-hG compared to ctrl (data are mean, ANOVA with Tukey's post hoc test, n≥3 animals/condition).

(C) Whisker barrels in cKO-hG primary somatosensory cortex were visualized by cytochrome oxidase staining (CO, brown) on flattened cortices and NTNG1 immunostaining (green) on coronal sections. Whisker barrels were formed without defect in cKO-hG (n=3/3 animals).

(D) Horizontal sections of P0 ctrl, cKO-E, and cKO-hG brains carrying the *Golli-τEGFP* transgene. Compared to ctrl, innervation of thalamus (Th) by τEGFP+ axons were qualitatively reduced in cKO-E (open arrowhead), but not in cKO-hG (solid arrowhead).

CPu: caudate putamen, Nctx: neocortex, SP: subplate, Th: thalamus

SP involvement in thalamocortical circuit wiring has been extensively described over the past three decades. Concomitant with disrupted SP features in cKO-E, TCAs were misrouted and sensory whisker barrel formation impaired. Remarkably, SP-sparing of *Arid1a* in cKO-hG was sufficient to rescue SP projections to thalamus and restore thalamocortical refinement. At P7, both CO staining on flattened cKO-hG cortices and immunostaining of NTNG1 on coronal sections revealed typical organization of barrel cortex, largely indistinguishable from ctrl, and extensive innervation of thalamus by τEGFP-positive SP axons (**Figure 3.14 C** and **D**). Thus, *Arid1a* expression in SPNs was sufficient for non-cell autonomous guidance of callosal and thalamocortical targeting.

Although whisker barrels were restored in cKO-hG, I sought determine if this was coincident with normal SP wiring functions. At E15.5 MAP2 immunostaining revealed typical organization of SPNs mid-corticogenesis in both ctrl and cKO-hG (**Figure 3.15 A**). NTNG1+ TCAs extended through the subpallium and traversed the PSB to enter the cortex while properly waiting within SP and not prematurely invading the CP. Correct initial targeting of TCAs was coincident with extensive emergence of τEGFP+ across the PSB and into the subpallium while thoroughly cofasciculating with NTNG1-labeled TCAs in E15.5 ctrl and cKO-hG (**Figure 3.15 B**). The *Arid1a*-proficient SP in cKO-hG also produced an elaborate CSPG-rich corridor, delineating a path for TCAs during their “waiting period” below the CP (**Figure 3.15 C**). Therefore, despite absence of *Arid1a* from CP neurons, SP *Arid1a* was sufficient for normal SP organization, SP axon-TCA cofasciculation, and ECM. Consistent with these wiring functions, SP *Arid1a* sufficiently enabled normal callosum formation, TCA targeting, and whisker barrel development.

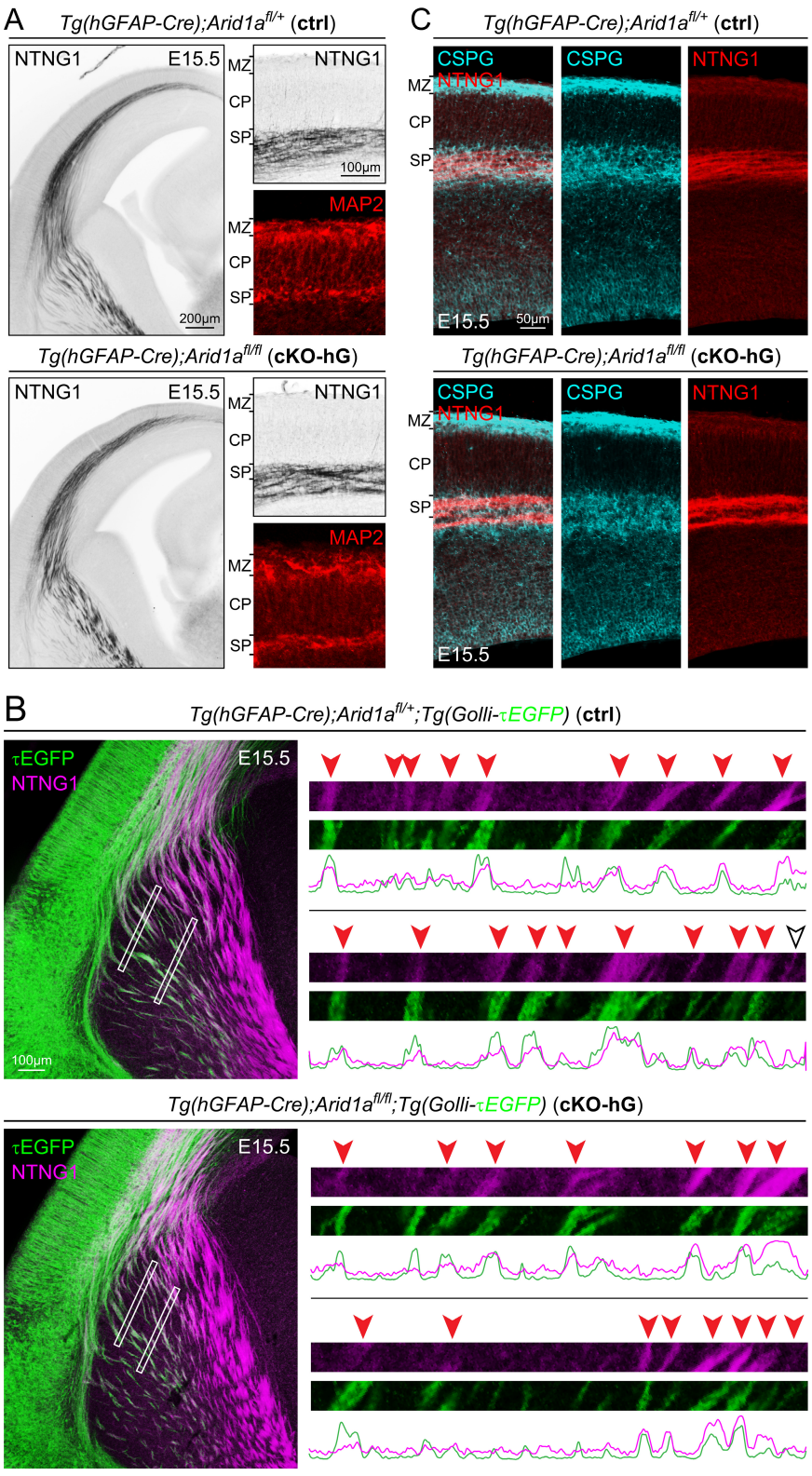

Figure 3.15 Restoration of subplate organization, projections, and extracellular matrix in subplate-spared *Arid1a* deletion

(A) Analysis of thalamocortical axons and subplate neurons in E15.5 ctrl and cKO-hG cortex. In cKO-hG, NTNG1+ thalamocortical axons extended along a normal trajectory across the PSB, without forming an aberrant bundle parallel to the boundary. Upon reaching the cortex, NTNG1+ axons were correctly paused within subplate and did not prematurely invade cortical plate in cKO-hG. MAP2 immunostaining (red) revealed in cKO-hG subplate neurons that were organized within a continuous and clearly delineated layer below cortical plate.

(B) NTNG1 immunostaining (magenta) on E15.5 ctrl and cKO-hG brains carrying the *Golli-τEGFP* transgene. In cKO-hG, τEGFP+ (green) descending axons from subplate neurons closely co-fasciculated (red arrowheads) with ascending NTNG1+ thalamocortical axons (magenta).

(C) CSPG (cyan) and NTNG1 (red) immunostaining on E15.5 ctrl and cKO-hG brain sections. In cKO-hG, NTNG1+ thalamocortical axons travelled within a subplate/intermediate zone corridor neatly delineated by the extracellular matrix component CSPG in a manner indistinguishable from ctrl.

CP: cortical plate, MZ: marginal zone, SP: subplate

Together, *Arid1a* cKO-E and cKO-hG supported identification of cell and non-cell autonomous *Arid1a* functions during cortical development. In SPNs, *Arid1a* cell autonomously established the transcription of SPN identity, thus giving rise to correct SPN morphology, subpallial axons, and ECM. By regulating development of SPNs, *Arid1a* non-cell autonomously controlled the wiring of callosal and thalamocortical connectivities via the axon guidance roles of SP. *Arid1a* is thus a central regulator of multiple SP-dependent axon guidance mechanisms essential to cortical circuit assembly.

Discussion

Despite the central role of SPNs in cortical circuit assembly and their potential contribution to neurodevelopmental disorders (311, 312, 442), they are relatively understudied compared to their CP counterparts. Previous studies have focused on SP-enriched genes (313, 433). Together, these studies have characterized important molecular determinants of SPN specification, migration, and axon projection (141, 142, 144, 162, 163, 273, 421, 443), highlighting the complex genetic regulation required for SP development. The severe axon misrouting phenotypes of SP ablation (303-305) however, are not broadly recapitulated in these genetic mutants. And the mechanistic underpinnings of the diverse circuit wiring functions of SPNs have remained largely mysterious. Here, I leveraged cortical *Arid1a* deletion, which causes multiple axon misrouting defects strikingly reminiscent of SP ablation, to gain mechanistic insights into the non-cell autonomous wiring functions of SPNs in the assembly of cortical connectivities.

Cortical *Arid1a* deletion and previous experimental SP ablation (303-305, 308) phenotypically converge on misrouted TCAs, which prematurely invade the cortical plate and ultimately fail to innervate their L4 targets with correct topology. Disruption of SP function is also known to cause defects in TCA crossing of the PSB (306, 419), an impairment I observe following *Arid1a* deletion. Several aspects of SP function may contribute to correct TCA pathfinding (444). First, the “handshake hypothesis” posits that close co-fasciculation between the earliest descending SP axons and ascending TCAs is important for guidance of both tracts and formation of reciprocal connectivity (177, 288, 445). Following *Arid1a* deletion in cKO-E, SP corticofugal axons are markedly reduced, and their co-fasciculation with TCAs is lost. Consistent with the “handshake hypothesis”, TCAs, in the absence of co-fasciculation, are impaired in their crossing of the PSB, enter the cortex via a narrow medial path, and become defasciculated and misrouted after entering the cortex. Second, SP is characterized by a remarkably rich ECM (290, 446, 447), which can contribute to axon guidance by interacting with growth cones and supporting guidance molecule signalling (442, 448-451). During circuit formation, cortical afferent and efferent axons extend along a WM corridor delineated by matrix component CSPG (289). Following cortical *Arid1a* deletion, CSPG expression is reduced and the corridor collapses. Concomitantly, TCAs become defasciculated in WM and prematurely invade cortical plate without waiting in SP, a phenotype reminiscent of SP ablation (305). Notably, the sparing of SPNs from *Arid1a* deletion in cKO-hG is sufficient to support both SP-TCA co-fasciculation and the CSPG corridor and enables correct TCA pathfinding to their cortical targets. These findings thus provide support that the roles of *Arid1a* in thalamocortical tract formation

are centered on SPNs, and *Arid1a*-dependent SP CSPG and axon co-fasciculation mediate TCA pathfinding. Interestingly, corticothalamic axons from cortical plate neurons are largely intact following *Arid1a* deletion in cKO-E, despite reduction and misrouting of SP-thalamic axons. Thus, I do not find an *Arid1a*-dependent pioneering role for SP axons in guiding corticothalamic axons from subsequent cortical plate neurons.

In addition to TCAs, intracortical axons are also markedly misrouted following cortical *Arid1a* deletion in cKO-E. Unlike the better-known roles of SPNs in TCA guidance, SP contribution to intracortical tract development is less established. Early studies suggest that SPNs pioneer the CC formation by extending the first callosal axons (257, 277, 278, 282). Some subsequent studies, however, find this possibility to be unlikely (205, 276). In my study, I find that pan-cortical *Arid1a* leads to CC agenesis and widespread mistargeting of intracortical axons. Sparse *Arid1a* deletion, however, does not autonomously misroute callosal axons, indicating that callosal agenesis is a non-cell autonomous consequence of pan-cortical *Arid1a* deletion. Remarkably, SP expression of *Arid1a*, following SP-spared deletion in cKO-hG, is sufficient for formation of the CC. Thus, I unequivocally establish that SP function is essential to callosum development. I note that Tg(*hGFAP-Cre*) is active in indusium griseum and glial wedge (217, 452). Thus, it is unlikely that *Arid1a* expression in these structures could contribute to callosum formation in cKO-hG. Diverse developmental disorders are characterized by agenesis or dysgenesis of CC (216). This study highlights a potential contribution of SP dysfunction to callosal defects in disease.

One barrier to molecular study of SP function is the lack of specific genetic access to embryonic SPNs during critical stages of circuit wiring. Although several published Cre lines show SPN specificity, the onset of Cre expression occurs too late for study of circuit development (171). Here, I describe a genetic strategy to target SPNs. *Emx1*^{Cre} mediates gene deletion from all cortical NPCs, including those that give rise to SPNs, whereas Tg(*hGFAP-Cre*) mediates deletion from NPCs after SPNs have been generated. Importantly, Tg(*hGFAP-Cre*) mediates recombination in a majority of L6 neurons, thereby enabling potential effects of SPNs to be uncoupled from closely-related L6 neurons. By comparing "pan-cortical deletion" (*Emx1*^{Cre}) versus "SP-spared deletion" (Tg[*hGFAP-Cre*]), this approach enables interrogation of gene necessity and sufficiency in SP-mediated circuit wiring.

Loss-of-function mutations in *ARID1A* are frequently found in human cancers and the molecular functions of ARID1A in cancer cells are being unraveled (345). ARID1A has been proposed to maintain transcriptional activity by recruiting EP300 acetyltransferase to enhancers (392) or by controlling chromatin accessibility (388). A recent study, however, found that ARID1A depletion only modestly altered accessibility and proposed that ARID1A maintains RNA polymerase pausing to enable robust transcription during homeostasis (387). In cortical NPCs, I find that *Arid1a* deletion does not confer a carcinogenic growth advantage. Instead, it leads to a selective disruption in SPN gene expression. Despite ubiquitous ARID1A expression during cortical development, the effects of *Arid1a* deletion is surprisingly cell type-dependent. A recent study showed that *Arid1b* expression following *Arid1a* depletion is sufficient to partially support BAF complex function (387). In cKO-E, the expression of *Arid1b* may have

attenuated the effects of *Arid1a* loss from cortical plate neurons, thus contributing to SP-selective deficits.

Recent human genetic findings have convergently implicated altered chromatin function in disorders of brain development (318, 320, 321, 453). These studies have identified loss-of-function mutations in *ARID1A* in intellectual disability, autism spectrum disorder, and Coffin-Siris syndrome, a developmental disorder characterized by callosal dysgenesis (395). The mechanisms by which chromatin dysregulation contribute to brain disorders are an active field of study. An important implication of this work is that deficits in SPNs may be an underappreciated contributor to neural circuit miswiring in brain disorders associated with chromatin dysregulation. Like *ARID1A*, many chromatin genes implicated in neurodevelopmental disorders are also broadly expressed (454). I find a surprisingly cell type selective role for *Arid1a* in cortical development, underscoring the potential for cell type-specific functions by other broadly expressed genes. In addition, I discover *Arid1a*-dependent, non-cell autonomous mechanisms in the wiring of cortical circuits (**Figure 3.16**). This study thus highlights the possibility that chromatin regulation can non-cell autonomously contribute to neural circuit development and disorders thereof.

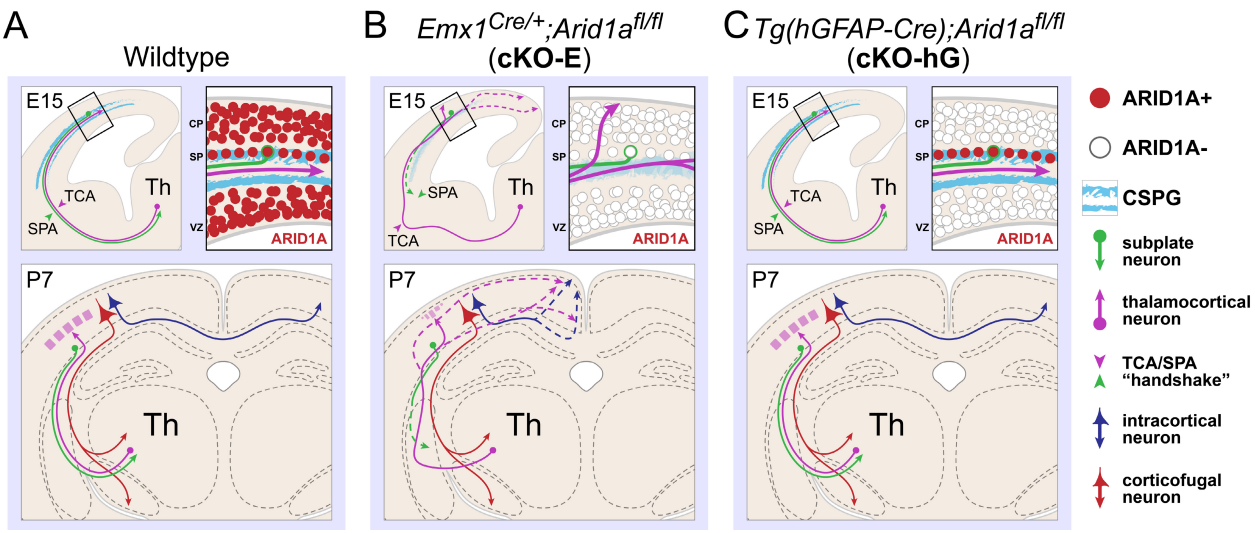

Figure 3.16 Schematic summary of *Arid1a*-dependent cortical connectivity

(A) During embryonic cortical development, *Arid1a* is ubiquitously expressed. Descending subplate axons (SPA, green) co-fasciculate with ascending thalamocortical axons (TCA, magenta), a "handshake" interaction proposed to be crucial for reciprocal connectivity between cortex and thalamus (Th). Subplate neurons secrete extracellular matrix (ECM) components, including CSPG (cyan), which form a corridor for the pathfinding of efferent and afferent axons. Upon reaching the subplate, TCAs undergo a "waiting period" prior to invading cortical plate. During the first postnatal week, TCAs extend into cortical layer 4 and form whisker barrels in somatosensory cortex.

(B) Following pan-cortical *Arid1a* deletion, TCAs (magenta) and callosal axons (blue) are misrouted, and whisker barrel formation is disrupted. Descending subplate axons are attenuated and their co-fasciculation with TCAs is absent. Without the "handshake" interaction, TCAs are impaired in their crossing of the pallial-subpallial boundary. In addition, the subplate CSPG corridor collapses and TCAs, upon reaching the cortex, prematurely invade cortical plate without "waiting" in subplate. Thus, disruption of subplate functions is concomitant with widespread axon misrouting in *Arid1a* cKO-E.

(C) Following subplate-spared cortical plate deletion of *Arid1a* in cKO-hG, subplate expression of ARID1A is sufficient to support subplate axon co-fasciculation with TCAs and subplate CSPG corridor formation. Remarkably, despite loss of ARID1A from cortical plate neurons, the corpus callosum, and thalamocortical axons and whisker barrels developed without defect. Thus, *Arid1a* plays crucial, non-cell autonomous roles in cortical circuit wiring that are centered on the subplate.

Conclusion

Here, I uncover precise genetic sufficiency in SPNs to direct cortical connectivity. *Arid1a*-dependent cortical circuit wiring is based on a temporal necessity to establish the neuronal transcriptome. This role is particularly intensified in SPNs and is correlated with widespread control of features integral to broadly direct cortical connectivity. SP characteristics historically tied to thalamocortical development, including “handshake” and ECM, are dependent on *Arid1a*. *Arid1a*’s circuit wiring influence in corticogenesis is centered on the SP. I introduce a new approach to assess genetic requirements and sufficiency and established that SP *Arid1a* is sufficient to non-cell autonomously orchestrate the formation of callosal and thalamocortical circuitry. Altogether, this work suggests ubiquitous chromatin remodelers likely play underappreciated cell type-specific roles in cortical development, and altered SP development has the potential to be the crux of numerous developmental disorders.

Materials and Methods

Mice and mouse husbandry

All experiments were carried out in compliance with ethical regulations for animal research. The study protocol was reviewed and approved by the University of Michigan Institutional Animal Care & Use Committee. Mice were maintained on 12 hour day:night cycle with food and water *ad libitum*. Mouse strains were previously generated and are listed in **Table 3.1**. Date of vaginal plug was considered embryonic day 0.5. Genotyping was performed with DreamTag Green 2x Master Mix (Thermo Fisher) and primers can be found in **Table 3.2**.

Immunostaining and imaging

Brains were isolated and fixed in 4% PFA overnight at 4° C, embedded in 4% agarose, and vibratome-sectioned at 70 µm. Free-floating sections were blocked and immunostained in blocking solution containing 5% donkey serum, 1% BSA, 0.1% glycine, 0.1% lysine, and 0.3% Triton X-100 (Triton X-100 was excluded from blocking solution when immunostaining for CSPG). Sections were incubated with primary antibodies in blocking solution overnight at 4° C and with secondary antibodies for 1h at RT. Following secondary antibody staining, sections were mounted with VECTASHIELD Antifade Mounting Medium (Vector Laboratories). Images were acquired using an Olympus SZX16 dissecting scope with Olympus U-HGLGPS fluorescent source and Q-Capture Pro 7 software to operate a Q-imaging Regia 6000 camera, an Olympus Fluoview FV1000 confocal microscope with FV10-ASW software, or an Olympus Fluoview FV3000 confocal microscope with FV31S-SW software. Images were processed and quantified in ImageJ and Adobe Photoshop. Primary and secondary antibodies are listed in **Table 3.3**.

ClickSeq

RNA-seq libraries were generated by Click-Seq (422) from 600 ng of purified neocortical RNA. Ribosomal RNA was removed from total RNA using NEBNext rRNA Depletion Kit (NEB). ERCC RNA spike-in was included for library quality assessment (Thermo Fisher). SuperScript II (Invitrogen) was used for reverse transcription with 1:30 5 mM AzdNTP:dNTP and 3′ Genomic Adapter-6N RT primer (GTGACTGGAGTTCAGACGTGTGCTCTTCCGATCTNNNNNN). RNaseH treatment was used to remove RNA template and DNA was purified with DNA Clean and

Concentrator Kit (Zymo Research). Azido-terminated cDNA was combined with the click adaptor oligo (/5Hexynyl/NNNNNNNNAGATCGGAAGAGCGTCGTGTAGGGAAAGAGTGTAGATCTCGGTGGTCGCCGTATCATT) and click reaction was catalyzed by addition of ascorbic acid and Cu^{2+}, with subsequent purification with DNA Clean and Concentrator Kit. Library amplification was performed using Illumina universal primer (AATGATACGGCGACCACCGAG), Illumina indexing primer (CAAGCAGAAGACGGCATACGAGATNNNNNNGTGACTGGAGTTCAGACGTGT) and the manufacturer's protocols from the 2× One Taq Hot Start Mastermix (NEB). To enrich for amplification products larger than 200 bp, PCR products were purified using Ampure XP (Beckman) magnetic beads at 1.25× ratio. Libraries were analyzed on TapeStation (Agilent) for appropriate quality and distribution and were sequenced at the University of Michigan sequencing core on the Illumina NextSeq 550 platform (75 cycle, high output).

RNA purification and droplet digital PCR (ddPCR)

Neocortical tissue was microdissected from E15.5 mice. RNA was isolated by resuspending the tissue in TRIzol, homogenizing with metal beads in a bullet blender, isolating the aqueous phase following addition of chloroform and centrifugation for 15 min at >20,000g at 4°C, and eluting purified RNA with DNase/RNase-free water from a Zymo Research Zymo-Spin IC column. Purified RNA was quantified using a Qubit fluorometer. 1 µg of RNA was reverse transcribed using SuperScript II (Invitrogen). Probe sets (PrimeTime qPCR Probe Assays) from Integrated DNA Technologies were utilized with diluted cDNA and the QX200 Droplet Digital PCR System (Bio-Rad) for gene expression level analyses. The ddPCR reaction mixture contained template cDNA, 2xddPCR Supermix (No dUTP) (Bio-Rad), target probes with HEX fluorescence, and

control probe against the house-keeping gene *Srp72* with FAM fluorescence. Droplets were generated with the QX200 droplet generator (Bio-Rad), thermocycled, and analyzed using the QX200 droplet reader (Bio-Rad). Primers and probes for ddPCR can be found in **Table 3.4**.

RNA sequencing data analysis

RNA-seq data were subject to quality-control check using FastQC v0.11.5 (https://www.bioinformatics.babraham.ac.uk/projects/download.html#fastqc). Adapters were trimmed using cutadapt version 1.13 (http://cutadapt.readthedocs.io/en/stable/guide.html). Processed reads were aligned to GENCODE GRCm38/mm10 reference genome (https://www.gencodegenes.org/mouse/) with STAR(455) (v2.5.2a) and deduplicated according to UMI using UMI-tools (456) (v0.5.3). Read counts were obtained with htseq-count (v0.6.1p1) with intersection-nonempty mode (457). Differential expression was determined with edgeR (423). The *P* value was calculated with likelihood ratio tests and the adjusted *P* value for multiple tested was calculated using the Benjamini-Hochberg procedure, which controls false discovery rate (FDR). Sequencing results were confirmed for 6 genes and normalized to the housekeeping gene *Srp72* using droplet digital PCR with primers and probes in **Table 3.4**.

Single-cell RNA-seq intersectional analysis

Single cell RNA-seq data were obtained (426, 427). To ensure consistency between methods, unclustered data were clustered using standard t-SNE cell-based clustering (458). Raw counts were normalized with K-nearest neighbor smoothing and a Freeman-Tukey transform to improve the signal-to-noise ratio (459). Pearson product-

moment correlation coefficients for gene expression were calculated using NumPy (460) and plotted using seaborn (461).

Plasmid constructs and in utero electroporation

CAG-mTagBFP2 was generated by subcloning mTagBFP2 from mTagBFP2-Lifeact-7 (462) (a gift from Michael Davidson, Addgene plasmid #54602) into pCAGEN (463) (a gift from Connie Cepko, Addgene plasmid #11160). To make eSpCas9opt1.1-Actb_gRNA (87), a gRNA sequence targeting the c-terminus of the *Actb* coding sequence (5′-AGTCCGCCTAGAAGCACTTG) was cloned into eSpCas9Opt1.1, which expresses enhanced-specificity Cas9 and an optimized gRNA scaffold. To construct Actb_NHEJ_3xHA (87), tandem HA tag sequences were cloned between 2 *Actb* gRNA recognition sequences, to enable 3xHA insertion into the *Actb* gene following cutting of the endogenous gene and the plasmid by Cas9. a mix of Actb_NHEJ_3xHA, eSpCas9opt1.1-Actb_gRNA, and CAG-mTagBFP2 each at 1 μg/μL was injected into lateral ventricles. Plasmids were transferred to NPCs in the VZ by electroporation (five 45-ms pulses of 27 V at 950-ms intervals).

Cytochrome oxidase

Brains from P7 mutant and control mice were fixed for 2 h at RT in 4% PFA, and the cortices were dissected off, flattened between two glass slides, and fixed overnight at 4° C. Following fixation, flattened cortices were sectioned on a vibratome at 150 μm. Sections were incubated at 37° C overnight in a solution containing 4 g sucrose, 50 mg DAB (Sigma-Aldrich), 15 mg cytochrome C (Sigma-Aldrich) per 100 mL of PBS. Sections were washed with PBS and imaged with an Olympus SZX16 dissecting scope.

Statistical analyses

Statistical analyses were performed in GraphPad Prism 8 (GraphPad Software). Values were compared using a two-tailed, unpaired Student's *t* test, ANOVA with Tukey's post hoc test, or hypergeometric test with Bonferroni correction. An α of 0.05 was used to determine statistical significance unless otherwise indicated.

Acknowledgements

This work would not have been possible without many Kwan lab members' experimental and computational expertise. First and foremost, Mandy Lam built Click-seq libraries, performed IUE, and cytochrome oxidase staining. Computationally, Adel and Yaman Qalieh were invaluable in the processing and analyses of sequencing results, especially intersectional approaches incorporating previously published single-cell RNA-seq. Dr. Owen Funk also assisted in bioinformatics analyses, Finally, current and former Kwan lab members have each provided unique insights and thoughtful questions that consistently improved the quality and presentation of my findings.

Table 3.1: Mouse strains used in this study.

Mouse	Description	ID	Citation
STOCK *Arid1a*$^{tm1.1Zhwa}$/J *Arid1a*^{fl}	Floxed exon 8 of *Arid1a*	JAX# 027717	(385)
B6.129S2-*Emx1*$^{tm1(cre)Krj}$/J *Emx1*$^{IRES-Cre}$	Knock-in of IRES and *Cre* to *Emx1* locus	JAX# 005628	(397)
Neurod6$^{tm1(cre)Kan}$ *Neurod6*^{Cre}	Knock-in of *Cre* to *Neurod6* locus	MGI# 2668659	(400)
FVB-Tg*(GFAP-cre)25Mes/J* Tg*(hGFAP-Cre)*	Transgenic line with *hGFAP* promoter driving *Cre*	JAX# 004600	(464)
STOCK Tg(*Lpar1-EGFP*)GX193Gsat Tg*(Lpar1-EGFP)*	Transgenic line *EGFP* inserted following the *Lpar1* start codon	MGI# 4847204	(431)
Tg(Mbp-MAPT/EGFP)#Eja *Tg(Golli-tau-EGFP)*	Transgenic line with Golli promoter driving *tau-EGFP*	MGI# 5433179	(438)
B6.Cg-*Gt(ROSA)*$^{26Sortm14(CAG-tdTomato)Hze}$/J *ROSA*^{tdTomato}	Cre-dependent expression of *tdTomato* at ROSA26 locus	JAX# 007914	(401)

Table 3.2: Genotyping oligos used in this study.

Gene Target	Oligo Name	Sequence (5' - 3')	Notes
Cre	Cre-F	TCGATGCAACGAGTGATGAG	500 bp for all Cre lines used
	Cre-R	TTCGGCTATACGTAACAGGG	
Arid1a^{fl}	Arid1a-F	TGGGCAGGAAAGAGTAATGG	WT = 116 bp Floxed = 170 bp
	Arid1a-R	CACTGACTGGCGTGTTCAGA	
Golli-tau-EGFP	Golli-F	AACATAGTATCCGCGCCCC	Estimated about 350 bp
	Golli-R	CCCCTGAGCATGATCTTCCA	

Table 3.3: Primary and secondary antibodies used in this study.

Primary Antibody	Company and product number	Dilution
Mouse anti-TLE4	Santa Cruz Biotechnology sc-365406	1:250
Chicken anti-RBFOX3	Sigma-Aldrich ABN91	1:2000
Rabbit anti-CPLX3	Synaptic Systems 122 302	1:1000
Chicken anti-GFP	Abcam ab13970	1:2000
Rabbit anti-GFP	Invitrogen A-11122	1:1000
Sheep anti-GFP	Bio-Rad 4745-1051	1:500
Mouse anti-TUBB3	Covance MMS-435P	1:1000
Rabbit anti-NR4A2	Santa Cruz Biotechnology sc-990	1:500
Chicken anti-MAP2	Novus Biologicals NB300-213	1:2000
Rabbit anti-tRFP	Evrogen AB233	1:2000
Rat anti-HA	Roche 11867423001	1:1000
Goat anti-Netrin-G1a	R&D Systems AF1166	1:100
Mouse anti-Chondroitin Sulfate	Sigma-Aldrich C8035	1:100
Rat anti-L1CAM	Sigma-Aldrich MAB5272	1:1000
Guinea Pig anti-Cre-recombinase	Synaptic Systems 257 004	1:500
Rabbit anti-ARID1A	Abcam ab182560	1:1000
Donkey anti-Chicken IgY (H+L), Alexa Fluor 488 AffiniPure	Jackson ImmunoResearch Labs 703-545-155	1:250
Donkey anti-Goat IgG (H+L), Alexa Fluor 488 AffiniPure	Jackson ImmunoResearch Labs 805-545-180	1:250
Donkey anti-Mouse IgG (H+L), Alexa Fluor 488 Affinipure	Jackson ImmunoResearch Labs 715-545-150	1:250
Donkey anti-Mouse IgM, μ chain specific, Alexa Fluor 488 Affinipure	Jackson ImmunoResearch Labs 715-545-020	1:250
Donkey anti-Rabbit IgG (H+L), Alexa Fluor 488 AffiniPure	Jackson ImmunoResearch Labs 711-545-152	1:250
Donkey anti-Rat IgG (H+L), Alexa Fluor 488 AffiniPure	Jackson ImmunoResearch Labs 712-545-150	1:250
Donkey anti-Chicken IgY (H+L), Cy3 AffiniPure	Jackson ImmunoResearch Labs 703-165-155	1:250
Donkey anti-Goat IgG (H+L), Cy3 AffiniPure	Jackson ImmunoResearch Labs 705-165-147	1:250
Donkey anti-Rabbit IgG (H+L), Cy3 AffiniPure	Jackson ImmunoResearch Labs 711-165-152	1:250
Donkey anti-Rat IgG (H+L), Cy3 AffiniPure	Jackson ImmunoResearch Labs 712-165-153	1:250
Donkey anti-Chicken IgY (H+L), Alexa Fluor 647 AffiniPure	Jackson ImmunoResearch Labs 703-605-155	1:250
Donkey anti-Rabbit IgG (H+L), Alexa Fluor 647 AffiniPure	Jackson ImmunoResearch Labs 711-605-152	1:250
Donkey anti-Rat IgG (H+L), Cy5 AffiniPure	Jackson ImmunoResearch Labs 712-175-153	1:250

Table 3.4: Droplet digital PCR primers used in this study.

Gene Target	Primer_1/Primer_2 (5' – 3')	Probe (5' – 3')
Ablim1	ACAGACTTCGCTCAGTACAAC	/56-FAM/ACTACCAGA/ZEN/ CCCTCCCAGATGGC/3IABkFQ/
	CCTCTGTCCATTCTCACTGC	
Myo5b	GTGACTCTTAACAACCTACTCCTG	/56-FAM/ACAGGCATG/ZEN/ CAACTCAGGTACAACA/3IABFQ/
	AAGCCACTCTTCCAGTTGAC	
Lhx2	GCATCTGACGTCTTGTCCAC	/56-FAM/TTTCCTGCC/ZEN/ GTAAAAGGTTGCGC/3IABkFQ/
	CTCACCAAGAGAGTCCTCCA	
Tbr1	CCCGTGTAGATCGTGTCATAG	/56-FAM/TTTAGTTGT/ZEN/ GTAATATCCGTGTTCTGGTAGGC/ 3IABkFQ/
	AGACTCAGTTCATCGCTGTC	
Tle4	ACTGACGTGAAAGGAGTATGC	/56-FAM/ACATGCGAG/ZEN/ TGCCAGCAATACCT/3IABkFQ/
	AGCCTATGGAAGATCACCTGT	
Zfpm2	TGGTTTGTCTGAATGGCTGT	/56-FAM/CATCTGATT/ZEN/ CTGCTGGCTCCTGGAT/3IABkFQ/
	GAAGACGTGGAGTTCTTTTGTAAC	
Srp72	CTCTCCTCATCATAGTCGTCCT	/5HEX/CCAAGCACT/ZEN/ CATCGTAGCGTTCCA/3IABkFQ/
	CTGAAGGAGCTTTATGGACAAGT	

Chapter 4: Discussion

Overview

Wiring of cortical circuits depends on coordination of cell autonomous and non-cell autonomous mechanisms. Disruption of these processes is associated with neurodevelopment disorders, which have been increasingly linked to alterations in chromatin remodeler function. Mutations in the chromatin remodeler *ARID1A* have been associated with intellectual disability and erroneous circuitry. My dissertation work sought to illuminate the mechanistic underpinnings by which *Arid1a* impacts the fundamental establishment of brain circuitry. Importantly, I have also addressed cell type-specific orchestration of developmental wiring. In Chapter 2, I uncovered contrasting phenotypes resulting from conditional deletion of *Arid1a* from NPCs in the developing cortex versus newly born postmitotic neurons. NPC deletion caused widespread misrouting of callosal and cortical afferent projections in a surprising non-cell autonomous way while corticofugal tracts were largely intact. However, neuronal deletion was insufficient to recapitulate these aberrant trajectories. These analyses narrowed the critical window for ARID1A necessity to include NPCs or extremely early in postmitotic neurons to direct circuit formation. The non-cell autonomous nature of these phenotypes suggested an attractive possibility that the ubiquitous *Arid1a* might exert its influence in a cell type-specific way.

Chromatin remodelers are often considered correlative to their contributions in autonomous events, such as transcription and DNA repair. In Chapter 3, I established

that *Arid1a* was necessary for the establishment of the neuronal transcriptome, specifically that of SPNs. Remarkably, SP gene expression changes were coincident with broader changes in SP organization, morphology, projections, and ECM. SPNs have long-standing links not only to cortical connectivity, but also to developmental disorders, but the mechanisms are not fully understood. I introduced an original, intersectional approach to assess SPN gene necessity and sufficiency. In doing so, I revealed that despite *Arid1a* expression in all cortical cell types, its expression in SPNs alone was sufficient to support both callosal and thalamocortical development. Together, my work has identified a multi-faceted regulator of SPN functions in *Arid1a*, provided additional support for SP involvement in thalamocortical targeting, identified a surprising non-cell autonomous role for SPNs in callosal development, and established a new method by which to broadly assess gene function in SPNs.

In Chapter 4, I build on each of these findings, putting them into the context of our current understanding of brain development and considering the best steps forward.

***Arid1a*'s surprising cell type-specific role**

Expression of *Arid1a* and its protein product is cellularly indiscriminate. Both are widely, likely ubiquitously, expressed across tissues and cell types. My finding that *Arid1a* exerts its major influences through a particular cell type, SPNs, during cortical development may introduce more questions than it answers. In this section I will recognize some of the remaining and new questions while speculating on possible explanations.

First and foremost, in humans, heterozygous mutations in *ARID1A* are coincident with neurodevelopmental phenotypes. Notably, these phenotypes often include partial

to complete agenesis of the CC (465). However, in mice there were not clear anatomical differences between conditional heterozygous and wild-type control mice. This dose-dependent distinction between humans and mice when studying gene knockouts is not restricted to *Arid1a*. Rather, studies of gene function during brain development frequently necessitate homozygous conditional deletion in mice whereas haploinsufficiency occurs in humans. There are many potential explanations for this phenomenon that are worthy of further study. Briefly, not all mutations are equivalent. Conditional deletion of *Arid1a* eliminates exon 8 and introduces a premature stop codon (385). In this scenario, there could be nonsense-mediated decay or production and stabilization of a truncated ARID1A. The antibody used in this study targets downstream of the *Arid1a* deleted exon and will therefore not bind to truncated ARID1A. This leaves room for partial function, potentially reducing the disruptive effects of *Arid1a* deletion. However, this possibility is unlikely to contribute to species differences as human mutations in *ARID1A* associated with Coffin-Siris syndrome are present from nearly the N- to C-terminal extent (395). Thus, the dominant versus recessive variation in humans versus mice may simply be a result of neocortical expansion and increased reliance on chromatin control during corticogenesis. Importantly, *ARID1A* has orthologs spanning vertebrate and invertebrate species, including those without SPNs (466). One way to assess whether phenotypes are truly species-dependent is by generating mouse lines harboring mutations found in *ARID1A* Coffin-Siris syndrome patients or replacement with non-mammalian *Arid1a* orthologs (e.g. *osa* in *Drosophila melanogaster*) and examining circuitry deficits.

The second and third questions I will address go hand-in-hand: how is *Arid1a*'s autonomous role largely restricted to SPNs and what makes *Arid1a* dispensable after the first few hours following neuronal birth? ARID1A is a DNA-binding subunit critical for BAF function, but it is not the only protein capable of performing this role. Instead, both ARID1A and ARID1B are incorporated into BAF in a mutually exclusive manner such that canonical or noncanonical BAF has either ARID1A or ARID1B. While both *Arid1a* and *Arid1b* are expressed ubiquitously, their levels vary. Overall, ARID1A is present at relatively higher levels than ARID1B in embryonic stem cells (467). During the cell cycle ARID1A is rapidly accumulated early on, particularly in G0 phase, and slowly reduced, whereas ARID1B does not undergo robust changes in levels (467). Previous work described *Arid1b* partially compensating in the absence of *Arid1a*. It's possible that this same phenomenon occurs during brain development. One option is that, in response to *Arid1a* deletion, ARID1B is upregulated and eventually sufficient. While RNA-sequencing of E15.5 cortex in cKO-E versus control did not show a significant increase in *Arid1b*, it is possible that the mechanism is transient earlier in corticogenesis or based on posttranscriptional regulation. However, a compensatory increase in ARID1B may not be quick enough to spare SPNs, the first progeny after *Arid1a* deletion from NPCs in cKO-E. The half-life of nuclear ARID1A is around 75 minutes (468) and coupled with the relatively low amount of ARID1B typically in stem cells (467), feedback and ultimately production of sufficient ARID1B to support SP neurogenesis may be insurmountable. Alternatively, while *Arid1a* is ubiquitous, it may have cell type-specific binding partners directing BAF to the appropriate targets and supporting distinct influences in SP versus cortical plate neurons. Additionally, *Arid1a* has previously

shown a relationship with DNA topoisomerase *Top2b* (469), deletion of which also impairs SPN development (470). Together, while it seems plausible that ARID1B may partially compensate in the absence of *Arid1a* during brain development, it is not unlikely that *Arid1a* has distinct roles and cell type-specific partners.

How might this relate to *Arid1a*'s seemingly unnecessary presence in postmitotic neurons? In cKO-N, *Arid1a* deletion is mediated by *Neurod6*^{Cre}, which is initially active in preplate neurons by E12.5, within one day of their genesis (400). Although I did not identify widespread gross abnormalities in cKO-N cortices, that does not preclude the possibility that cKO-N may have deficits in synaptic connectivity like dendritic spines. Alternatively, *Arid1a*'s neuronal expression may be unnecessary and simultaneously not deleterious, with *Arid1b* leveraging more robust control.

Multiple questions remain regarding ARID1A function during brain development. However, here I will focus one additional line of inquiry: what distinguishes *Arid1a*'s postmitotic influence on callosal versus AC wiring? In cKO-E, both the CC and AC were lost. By contrast, postmitotic deletion of *Arid1a* in cKO-N restored the CC and while the AC was still notably absent. The CC originates largely from the neocortex with some contribution from cingulate cortex and claustrum while the AC consists of three branches, two particularly notable in this context: 1) the anterior branch, which has projections connecting the anterior olfactory nucleus and the olfactory bulb; and 2) the posterior branch, which originates from the piriform, entorhinal, ectorhinal, and temporal cortices (471). The piriform cortex highlights an evolutionary distinction between the CC and AC. In contrast to the six-layered neocortex, the piriform cortex is a three-layered structure lateral to the neocortex and part of the evolutionarily ancient paleocortex

present in reptiles. Interestingly, the AC is present across various mammalian and non-mammalian species lacking a CC (471). Thus, while cortical NPCs give rise to neurons in both the neocortex and piriform cortex, it is possible that *Arid1a* plays evolutionarily divergent roles in paleocortical neurons compared to their neocortical counterparts thereby influencing commissural circuit development by diverse mechanisms.

Dissecting temporal necessity for *Arid1a*

Ubiquitously expressed genes can perform diverse functions in distinct cell types. In the developing cortex, we aim to differentiate contributions in NPCs versus postmitotic neurons. My work utilized *Emx1*^{Cre} to delete *Arid1a* from cortical NPCs near the onset of neurogenesis (cKO-E), thereby affecting NPCs and their progeny. In doing so, and by comparing with sparse deletion via IUE, I revealed a necessity for *Arid1a* in non-cell autonomous orchestration of callosal and thalamocortical circuitry. However, this method alone did not distinguish at what stage *Arid1a* was exerting its influence, in NPCs or neurons.

Frequently, studies of cortical development rely on various Cre recombinase lines to differentiate the gene requirements in NPCs versus postmitotic neurons. While *Emx1*^{Cre} is commonly used for NPC deletion, *Neurod6*^{Cre} (*Nex*^{Cre}) is the field's standard for early postmitotic deletion in cortical excitatory neurons. Commonly, there is occurrence of a phenotype in *Emx1*^{Cre}-mediated deletion and its subsequent rescue in *Neurod6*^{Cre}-mediated deletion. This, in fact, is what I uncovered in *Arid1a* cKO-N; the CC and thalamocortical whisker barrels formed properly and the transcriptome was largely unchanged following postmitotic *Arid1a* deletion. Although this would suggest a role for *Arid1a* in NPCs but not postmitotic neurons during cortical development, and

this has often been the conclusion reported, the explanation is not so cut and dried. While *Neurod6*^{Cre} is expressed shortly after neuronal birth, that does not mean that the gene of interest is immediately absent and has no autonomous influence within neurons. There are three additional considerations: 1) any protein retained by the daughter neuron during cell division; 2) neuronal mRNA and associated protein produced prior to Cre activity; and 3) protein half-life.

In the case of rescue in *Arid1a* cKO-N, these confounding factors can have tremendous impact. First, while I have not directly identified ARID1A transference from mother to daughter cells, ARID1A is present in M phase cells and thus may be initially retained by daughter neurons following cytokinesis. The second and third considerations can be addressed concurrently. *Neurod6* is expressed quickly after neuronal birth, and Cre activity occurs sufficiently early that neurons within the IZ display Cre-dependent fluorescent reporters. However, between the time of neuronal birth and Cre activity, *Arid1a* can be transcribed. This provides a neuronal pool of mRNA and subsequent protein to support function. Similar in embryonic stem cells, ARID1A may be rapidly accumulated in newly postmitotic neurons as they enter a terminal G0 state. Coupled with its half-life previously mentioned (75 minutes in the nucleus), this may allow ARID1A to stick around long enough to establish the chromatin landscape in cKO-N neurons. This possibility is supported by ARID1A's presence in some neurons migrating through the IZ, prior to their entrance into the CP. The currently available tools do not enable us to discern between gene necessity in NPCs versus very early in postmitotic neurons. Thus, suggestions of widely-expressed genes having NPC-

specific roles during cortical development when using *Neurod6*^{Cre} to differentiate neuronal effects should be interpreted with caution.

Distinct influences of chromatin remodeling during brain development

Studies of brain neuronal and circuit development over the last twenty-five years have largely focused on transcription factors. However, transcription factors are unable to properly function without access to DNA. Recently, chromatin organization and remodeling has deservedly entered the spotlight. Much of this work is centered on transcriptional regulation and DNA double-strand break repair. *Arid1a* provides a window into the extremes to which chromatin remodelers influence developmental gene expression and ultimately brain wiring. Our previous work with *Ino80* exemplifies the importance for chromatin remodelers in DNA damage repair to support genome integrity and ultimately neuronal production (87). However, it is important to remember that each of these functions does not occur in isolation. *Ino80* affects both DNA damage repair and transcription. The major driver of developmental phenotypes is a lack of repair, and thus apoptosis and microcephaly. *Arid1a*, however, is crucial for transcriptional regulation that underlies cortical circuit development. Although *Arid1a* cKO-E did not display microcephaly or *Trp53* upregulation, it is important to consider that it may still participate in DNA damage response. Consistent with this, ARID1A has been reported to help recruit non-homologous end joining factors KU70 and KU80 (407) and is extensively linked to cancer. While I did not identify any obvious cell death or tumorigenic growths in *Arid1a* cKO-E, it is possible that disrupted DNA damage repair could contribute to transcriptional dysregulation.

Subplate-dependent wiring of brain circuitry

SPNs have been considered for prominent roles in development of intracortical, corticothalamic, and thalamocortical connectivities for over fifty years. During pathfinding of nascent circuits, SPNs are proposed to influence circuit development via pioneering of corticofugal trajectories, “handshake” with TCAs, extensive ECM, and transient synaptic connections. Although these interactions have been confirmed numerous times, studying their contributions to brain development has proved challenging.

SPNs send the first descending projections across the PSB, making them an ideal candidate to participate in pioneering developing corticofugal circuits. As such, it was previously thought they may be necessary for the formation of cortical efferent tracts. However, developmental SP ablation does not lead to universal disruption of corticofugal tracts (285). Rather, SP pioneering may be required to refine corticothalamic projections into the lateral geniculate nucleus as well as corticotectal axons (285). In my work, I did not find a necessity for *Arid1a* in broad targeting of corticothalamic or corticotectal circuits. However, I did not examine the nuclei specificity of corticothalamic projections or in depth the corticotectal tract. Differences between my findings and SP ablation studies in cats could be a result of distinct molecular influences of *Arid1a* or species differences in axonal trajectories.

SPNs contribute to the corticothalamic tract, which has reciprocity with ascending TCAs. Thalamocortical circuits are thought to depend on early interactions with SP axons. Nearing thirty-five years since its first publication, the “handshake hypothesis” posits that descending SP axons and ascending thalamic axons meet in the subpallium,

shake hands, and travel along one another to form reciprocal corticothalamic and thalamocortical connections (417). Notably, while this “handshake” commences in the subpallium of rodents, in primates TCAs cross the PSB prior to interacting with SP axons (301). Numerous studies have identified defects in SP axon growth concomitant with thalamocortical miswiring. For example, *Lhx2* conditional knockout from either the cortex or thalamus leads to a thalamocortical misrouting similar to *Arid1a* cKO-E (472, 473). While it has been suggested its cortical influence is based in NPCs, the data also support the alternative interpretation that *Lhx2* functions early in postmitotic neurons, prior to effective protein loss after *Neurod6*^{Cre} onset (473). Interestingly, while the thalamocortical phenotypes are convergent, *Lhx2* and *Arid1a* do not directly regulate one another based on RNA-seq in conditional knockouts of each (302, 473). Despite consistent implications, it is difficult to isolate the influence of SP axons as opposed to other features, such as their organization and ECM, on thalamocortical circuit development. In the same vein, although my findings clearly illustrate disrupted subpallial interactions between SP and TCAs, there are also alterations in SP organization and ECM. While convenient, it would be reductive to regard the “handshake” as the central tenant of thalamocortical innervation without adequately decoupling the influences of individual SP characteristics.

Separate from their long-range connections, SPNs generate an elaborate ECM composed of interconnected proteins including CSPGs (289, 291, 295, 408, 413, 474). CSPGs are secreted from SPNs beginning early during fetal development to form a corridor which cortical efferent and afferent projections grow through; the corridor can be visualized by E13.5 in mice and gestational week 11 in humans (291, 292, 475).

During brain development, it has been proposed that SP and its ECM are involved in formation of sulci and gyri (246, 476) and axonal growth. CSPGs likely inhibit growth of developing axons (477). Coincident with localization of the CSPG corridor, short-range intracortical projections, callosal fibers (focused on in the next section), and TCAs display potential “waiting periods” within the SP (263, 281, 294, 478, 479). Eventually, projections enter the CP and form functional synapses or are selectively eliminated. Although the SP ECM is thought to be crucial for the developmental wiring of cortical circuits, its necessity has not been properly interrogated; specific elimination of SP CSPGs has not yet been achieved. Additionally, the collaboration between the “handshake” and ECM during thalamocortical development is unclear. Disruption of SPNs often affects both components, as in *Arid1a* cKO-E, and thus their influences have not been decoupled. It is possible that, at least in rodents, SP-thalamocortical “handshake” is necessary for ascension across the PSB whereas the SP ECM curbs premature invasion of the CP by TCAs.

During the arrival of thalamocortical fibers in the neocortex, they pause within the embryonic SP. However, this period is not devoid of progress. In fact, SPNs have numerous synaptic contacts and altering SP location is also sufficient to relocate the initial thalamocortical synapses, supporting their importance during development (240, 260, 480, 481). Thalamocortical neurons require electrical activity during their “waiting period” in the SP to innervate the proper cortical areas (482). While my work has established multiple roles for *Arid1a* in SP features, its importance in their electrophysiological characteristics is unknown. Together, SPNs orchestrate cortical circuitry via carefully curated projections, ECM, localization, and synaptic contacts, each

of which is likely necessary to mediate distinct aspects of incoming and outgoing fiber growth.

Subplate contributions to callosal development

The largest WM tract within the brain is the CC, connecting the left and right cerebral hemispheres. The neurons comprising the CC come largely from L2-3, with some contribution from L5-6 and minor additions from the SP. While callosally-projecting SPNs are present across lissencephalic and gyrencephalic placental mammals, how they influence callosal development is unclear. Many studies have supported the notion that the callosum is pioneered by deep cortical, but not SP, neurons within the cingulate cortex. However, I uncovered a surprising influence of SP *Arid1a* on callosal formation. In the absence of *Arid1a* the CC did not form, and instead, presumptive callosal axons radiated dorsally toward the pia and did not form Probst bundles. Sparing SP *Arid1a* was sufficient for midline crossing of callosal axons, suggesting that while it may not interhemispherically pioneer, the SP non-cell autonomously directs callosal circuitry. The mechanisms underlying this, however, remain elusive. So how might SP support midline crossing of callosal axons?

One possibility is that, while SP axons may not be the first to cross the midline, they extend pioneering axons toward the midline. Subsequent CP neurons then follow them and utilize the glial scaffold to traverse. In the absence of early SP axons, CP-derived projections may have no pathway to follow, and instead fail to round toward the midline near the cingulum bundle. Rather, as seen in *Arid1a* cKO-E, they diverge from their normal trajectories and invade the ipsilateral cingulate and retrosplenial areas with radiating projections. Interestingly, this differs from oft described Probst bundles (220),

which likely result from failed midline fusion or dysregulated midline glial structures. Live-imaging studies may be poised to identify the neuronal identities of early projections toward the midline rather than just those traversing the midline.

Alternatively, SP influence during CC formation might not be directly linked to SP axons. Instead, callosal development may depend on SP-derived ECM for guidance. While some work has shown a “waiting period” for callosal projections in the contralateral SP, it’s possible that the ipsilateral SP retains influence. Callosal axons descend from neuronal somata and travel within the developing fiber tracts. During early circuit wiring, these pathways are held within the CSPG-rich ECM as they travel toward the midline. Given the inhibitory function of CSPGs, it is quite possible that the ipsilateral ECM corridor restricts presumptive callosal axons from aberrantly exiting the WM and guides it toward the midline. In the dissolution of the CSPG corridor (e.g. *Arid1a* cKO-E), callosal projections may exit their normal appropriate paths and take the road less traveled, aberrantly disrupting ipsilateral cortex. Altogether, and not exclusively, SPNs may influence CC formation via early projections and ECM, both of which are disrupted in *Arid1a* cKO-E. However, it may be difficult to distinguish between the two possibilities as they often go hand in hand.

Molecular determinants of subplate function

SPNs play essential roles during cortical development and alterations have been identified in ASD and schizophrenia. While they’re often easily distinguished by their locations and morphologies, SPNs share similar gene expression profiles, especially during fetal development, with their L6 neighbors. As a result, it has been difficult to understand the molecular mechanisms underlying specific SPN functions. In *Arid1a* I

uncovered a multifaceted regulator of multiple SPN features. At this stage, it is unclear the mechanism by which *Arid1a* mediates SPN development. One possibility is that *Arid1a* activates or acts in tandem with SP-specific genes.

In postnatal ages, SPNs can be clearly identified by their specific expression of *Ctgf* and *Cplx3* as well as some biased expression of *Nr4a2* (*Nurr1*). Additionally, Tg(*Lpar1-EGFP*) shows strong labeling of SPNs. Combinatorial analyses of these markers in P1 and P8 mouse cortex has revealed a wide diversity of SPNs (139), consistent with decades-old findings of distinct neuronal subtypes within the SP. Interestingly, some of these neurons undergo apoptosis during the first postnatal week in mice, and this appears to have at least some link to their gene expression profiles. However, while these genes are often used to enable identification of SPNs, they are largely not expressed sufficiently early to assess SPNs during early corticogenesis.

Tg(*Lpar1-EGFP*) begins to be expressed by SPNs around E14.5 in mice while *Nr4a2*-positive cells span SP and L6. To further identify SP-specific or SP-biased genes during embryogenesis, Oeschger et al. performed laser capture microdissection of the SP zone at E15.5 and compared it to lower CP using microarray (420). Interestingly, the embryonic SP is rich in four different cadherin genes (*Cdh9*, *Cdh10*, *Cdh12*, *Cdh18*) and two protocadherins (*Pcdh10* and *Pcdh18*). *CDH12* also shows a SP-biased expression pattern in embryonic marmoset (483), suggesting this expression pattern and potential function may be conserved. Classical cadherins and protocadherins have been previously linked to neuronal migration and identity (484-486). SP-specific expression of cadherins and protocadherins could help direct early SP positioning and gene expression. However, by E15.5, SPNs have already begun secreting their ECM,

extending their projections, and making transient contacts with ingrowing axons. At this point it is unclear whether SP gene expression at E15.5 is consistent with earlier ages and if other transiently expressed factors may contribute to the most critical facets of nascent SPNs.

Gene necessity and sufficiency in SPNs has also proved challenging to study. Historically, multiple Cre lines have been identified for conditional deletion during different stages from cortical NPCs (e.g. *Emx1*^{Cre}), broad excitatory neurons (*Neurod6*^{Cre} and Tg[*Camk2a-Cre*]), and specific neuronal subtypes (Tg[*Ntsr1-Cre*] [L6], Tg[*Rbp4-Cre*] [L5], and *Rorb*^{Cre} [L4]) (397, 400, 487-489). And while a couple Cre lines have been identified that target SPNs with relative specificity, their onset occurs largely during postnatal ages and is thus insufficient to study SPNs during corticogenesis. In postnatal SPNs, Tg(*Drd1-Cre*) (also referred to as Tg[*Drd1a-Cre*]) colocalizes with both CTGF-positive and CPLX3-positive neurons (171, 490). The Tg(*Drd1-Cre*) population collectively projects to higher-order thalamic nuclei. Interestingly, this population does not include Tg(*Lpar1-EGFP*)-positive SPNs. Unfortunately, Tg(*Drd1-Cre*) is not active in the neocortex until postnatal ages, so although it shows SP specificity, it is unable to contribute to embryonic study. Alternatively, Tg(*Ctgf-Cre*) has been thought a possibility to study SPNs. And while *Ctgf* is used as a marker postnatally, Tg(*Ctgf-Cre*) appears to be expressed more broadly during fetal development and thus is active in many more cells than just SPNs (491). So how do we study genetic influence of SPNs during embryonic development?

There is no current available tool to conditionally delete a gene only from SPNs within hours of their birth. To circumvent this obstacle, I utilized a new approach; rather

than testing gene necessity specifically in SP, an accessible alternative is to test cortical gene necessity side-by-side with sufficiency in SPNs. Genetic deletion with *Emx1*^{Cre} enables gene knockout from cortical NPCs and the entirety of their progeny, including SPNs and starting by E10.5, thereby testing gene necessity in the cortex. Frequently, studies of cortical development also use an alternative Cre line. Tg(*hGFAP-Cre*), similar to *Emx1*^{Cre}, is active in cortical NPCs, but its activity onset occurs later, beginning near E12.5. This delay coincidently precludes Tg(*hGFAP-Cre*) from affecting SPNs, but subsequent NPCs and CP neurons are still impacted. Comparing conditional knockouts using *Emx1*^{Cre} and Tg(*hGFAP-Cre*) supports identification not only of cortical gene necessity, but also of SP gene sufficiency, in brain development. This distinction is clear in *Arid1a* cKO-E and cKO-hG. In *Arid1a* I leveraged this strategy to uncover a necessity for cortical *Arid1a* in callosal and thalamocortical development, and a SP *Arid1a*-sufficiency to support that circuit wiring. While some studies have utilized tamoxifen-inducible Tg(*Emx1-CreER*^{T2}) (492) with induction following SPN genesis, this strategy is can be problematic. *Emx1* is expressed in postmitotic neurons in addition to NPCs, and thus SPNs may still be affected even with delayed activation (493). As such, SP-dependent mechanisms may still contribute to phenotypes in Tg(*Emx1-CreER*^{T2})-mediated deletion even when tamoxifen is introduced after SPN generation. With the currently available tools, the ideal strategy for testing SPN gene expression is likely via sufficiency using Tg(*hGFAP-Cre*) compared to cortical necessity using *Emx1*^{Cre}.

Future investigations

Overall, this work has yielded foundational insights into *Arid1a* function during cortical development, and more broadly identified genetic mechanisms underlying SP

development, SP-dependent circuit wiring, and support for longstanding hypotheses. Along the way have arisen novel questions and technical considerations to dive further into the phenomena orchestrating brain development and function.

In *Arid1a* I uncovered widespread alterations to the SPN transcriptome, coincident with disruption of morphology, projections, and ECM. Molecularly, there are numerous questions that remain unanswered. First, it is currently unclear whether gene expression changes in cKO-E are primary or secondary effects of *Arid1a* deletion. SPNs are generated beginning at E11.5, therefore, RNA-seq at E15.5 may have missed the inception of transcriptional dysregulation and rather featured changes indirectly related to *Arid1a*. This question can and should be addressed in two orthogonal manners. Earlier sequencing of cKO-E may provide evidence of initiation of transcriptomic changes. Alternatively, the possibility remains that it will reveal compatible changes with E15.5. In addition, continuous methodological advances have enabled more precise and accessible mapping of DNA binding by proteins. ARID1A largely binds to AT-rich regions, but its location profile in the developing cortex is unknown. To determine whether ARID1A directly coordinates transcription of cKO-E differentially expressed genes, CUT&Tag or CUT&RUN can be performed during early and mid corticogenesis. Importantly, ARID1A CUT&RUN has been performed in other cell types highlighting the feasibility (494). These experiments performed alongside the same in cKO-hG can provide an intersectional approach to identify subplate-specific *Arid1a* dysregulation and prioritize candidate genes downstream of *Arid1a* directing cortical development.

In addition, while *Arid1a* deletion clearly altered SPN transcriptome, bulk RNA-seq was incompatible with specific examination of SPNs. The increased accessibility of

single-nucleus RNA-seq tools provides an avenue to unbiasedly assess SPN transcriptome without obstruction from similar gene expression profiles of their cortical plate neighbors. Importantly, this methodology will also support distinction of transcriptomic alteration onset in NPCs versus early postmitotic neurons. Collectively, single-nucleus RNA-seq across multiple embryonic ages in control, cKO-E, and cKO-hG mice can distinguish the onset and importance of *Arid1a*-dependent differential gene expression contributing to altered SP development and cortical circuit wiring.

Importantly, ARID1A is not a requisite subunit of the BAF complex per se. While each BAF composition includes an AT-rich binding protein, ARID1B can be incorporated instead of ARID1A. The two have seemingly divergent roles, however, in some scenarios it has been reported that their functions can be partially overlapping. Mutations in *ARID1B* have also been increasingly implicated in neurodevelopmental disorders including ASD and Coffin-Siris syndrome (318, 373), and linked to callosal disruption (376), suggesting a critical role in brain development. While *Arid1b* has largely been studied in interneuron development, it is possible that it can act as a safeguard in the absence of *Arid1a* to support excitatory neuron development. Although I do not find upregulation of *Arid1b* in *Arid1a* cKO-E, it remains a possibility that *Arid1b* may compensate for its absence. Combinatorial investigation of *Arid1b* conditional knockouts and *Arid1a*/*Arid1b* double mutants may reveal their overlapping and unique necessities during neurodevelopment, and particularly any cell type-specific roles.

Numerous genes have been implicated in SPN development. Often, these studies have utilized either constitutive or *Emx1*^{Cre}-mediated gene deletion. As none of these genes have shown SP-specific expression, the resulting changes in cortical

organization and/or connectivity cannot be conclusively dependent on SP function. Importantly, use of cKO-hG highlights an opportunity to examine SP sufficiency of each of these genes and should be considered for further study. As an example, *Sox5*$^{-/-}$ mice show disrupted preplate splitting, changes in SPN identities, impaired neuronal identity refinement, and altered cortical connectivity (141, 273). SOX5 is present in subplate, L6, and L5 early in embryogenesis. Whether SP *Sox5* is sufficient to correct any of these defects would provide additional support for its influence being centered on the SP. This experimental design is broadly applicable to knockout of SP-expressed genes and has the potential to refine our understanding of SPN development and mechanistic coordination of brain circuits.

Deletion of *Arid1a* led to miswiring of thalamocortical and callosal circuitry, concomitant with disorganized SPNs, ECM, and projections. These phenotypes highlight multiple aspects of SP development that can contribute to circuit wiring, while also failing to address others. The importance of each, however, remains unclear. Going forward, *Arid1a* cKO-E and cKO-hG can serve as tools to assess SP-dependent development, but underlying SP functions should be the focus in the immediate future.

First, TCAs interact in three distinct ways during early development: “handshake hypothesis” with SP axons, “waiting period” with SP ECM, and transient synapses with SPNs (413). In *Arid1a* cKO-E, both “handshake” and ECM are disrupted, with the status of transient synapses unknown. Both features are corrected in cKO-hG and thus the importance of each were not distinguished in this study. Second, non-SP callosal projections travel in close proximity to interhemispheric SP axons. While SP axons are not considered callosal pioneers, they may still influence its overall formation.

Additionally, callosal axons travel within the SP ECM in the ipsilateral and contralateral hemispheres. Thus, SP projections and ECM have the potential to influence thalamocortical and callosal circuitry, so how do we distinguish the two?

Many studies have identified altered SP projections but, unfortunately, the ECM is not frequently examined. While it is unclear how to impact SP axon growth while leaving the ECM intact, the most prescient method to further define SP function in circuit wiring is through ECM disruption. The SP ECM is rich in CSPGs, which have been implicated as a repulsive force in axon growth, especially regeneration. As a result, repeated progress has been made in optimizing chondroitinase ABC constructs that are able to digest CSPGs thereby eliminating their influence (495, 496). Interestingly, a recent preprint utilized chondroitinase ABC on E16.5 ex vivo slices to examine the ECM's influence on neuronal migration (497). However, CSPGs are not exclusive to the SP. Instead, they are expressed throughout the cortical wall and enriched in the SP. Thus, widespread application of chondroitinase ABC is insufficient to directly assess SP ECM influence. To prioritize SP ECM and examine its influence on thalamocortical and callosal circuit wiring, creative SP-specific expression of chondroitinase ABC can be achieved with IUE with conditional genetics or generation of novel mouse lines. Regardless, eliminating the SP ECM will enable the first steps toward identifying and distinguishing the contributions of SP projections and ECM individually to brain wiring. Together, these studies can be combined with evolutionary analyses to understand conserved and species-specific features of SP neurons more adequately and how they can coordinate corticogenesis and connectivity. Overall, a more in-depth analysis of SP

features, even in the absence of genetic regulators, is necessary to make major progress in understanding the bases of brain development and disorders thereof.

Concluding remarks

My dissertation work uncovered a surprising cell type-specific requirement for chromatin remodeler *Arid1a* in directing cortical circuit formation. Ultimately, I highlighted the frequently neglected SPNs as a major vessel for *Arid1a*'s developmental influence in the formation of both thalamocortical and callosal connectivity. Importantly, IUE for sparse *Arid1a* deletion confirmed the non-cell autonomous nature of *Arid1a*'s circuit wiring influences. I uncovered a robust transcriptional role particularly in SPNs with major impacts on SP organization, projections, and ECM. To reveal a SP sufficiency for *Arid1a* in directing cortical connectivity, I presented a novel approach using Tg(*hGFAP-Cre*) to compare *Arid1a* deletion from NPCs and CP neurons, sparing SPNs, with pancortical deletion in cKO-E. Sparing *Arid1a* specifically in SPNs was sufficient to non-cell autonomously restore both thalamocortical and callosal circuits, while also autonomously enabling proper SP organization, projections, and ECM. Together, this work unequivocally revealed a multifaceted regulator of SP features and function in *Arid1a*, provide strong evidence for SP-dependent coordination of cortical connectivity, and introduce a method by which to query SPN gene necessity and sufficiency during cortical development. These findings raise further questions of which aspects of SPNs direct distinct connectivities and how SP disruptions can contribute to miswiring in developmental disorders.

References

1. H. J. Jerison, "Fossil Evidence on the Evolution of the Neocortex" in Comparative Structure and Evolution of Cerebral Cortex, Part I, E. G. Jones, A. Peters, Eds. (Springer US, Boston, MA, 1990), pp. 285-309.

2. P. Rakic, Evolution of the neocortex: a perspective from developmental biology. *Nat Rev Neurosci* **10**, 724-735 (2009).

3. J. L. Rubenstein, Annual Research Review: Development of the cerebral cortex: implications for neurodevelopmental disorders. *J Child Psychol Psychiatry* **52**, 339-355 (2011).

4. J. L. Lanciego, N. Luquin, J. A. Obeso, Functional neuroanatomy of the basal ganglia. *Cold Spring Harb Perspect Med* **2**, a009621 (2012).

5. P. Calabresi, B. Picconi, A. Tozzi, V. Ghiglieri, M. Di Filippo, Direct and indirect pathways of basal ganglia: a critical reappraisal. *Nat Neurosci* **17**, 1022-1030 (2014).

6. W. M. Usrey, S. M. Sherman, "Cell Types in the Thalamus and Cortex" in Exploring Thalamocortical Interactions: Circuitry for Sensation, Action, and Cognition. (Oxford University Press, 2021), pp. 11-24.

7. A. Nair, J. M. Treiber, D. K. Shukla, P. Shih, R. A. Müller, Impaired thalamocortical connectivity in autism spectrum disorder: a study of functional and anatomical connectivity. *Brain* **136**, 1942-1955 (2013).

8. L. Cerliani *et al.*, Increased Functional Connectivity Between Subcortical and Cortical Resting-State Networks in Autism Spectrum Disorder. *JAMA Psychiatry* **72**, 767-777 (2015).

9. D. P. Ford, R. B. J. Benson, The phylogeny of early amniotes and the affinities of Parareptilia and Varanopidae. *Nat Ecol Evol* **4**, 57-65 (2020).

10. M. J. Benton *et al.*, Constraints on the timescale of animal evolutionary history. *Palaeontologia Electronica* **18**, 1-106 (2015).

11. J. E. Blair, S. B. Hedges, Molecular phylogeny and divergence times of deuterostome animals. *Molecular biology and evolution* **22**, 2275-2284 (2005).

12. E. S. Goodrich, On the classification of the Reptilia. *Proceedings of the Royal Society of London. Series B, Containing Papers of a Biological Character* **89**, 261-276 (1916).

13. T. Rowe, Definition, Diagnosis, and Origin of Mammalia. *Journal of Vertebrate Paleontology* **8**, 241-264 (1988).

14. M. J. Benton, Phylogeny of the major tetrapod groups: morphological data and divergence dates. *J Mol Evol* **30**, 409-424 (1990).

15. R. G. Northcutt, Understanding vertebrate brain evolution. *Integrative and comparative biology* **42**, 743-756 (2002).

16. G. F. Striedter, The telencephalon of tetrapods in evolution. *Brain Behav Evol* **49**, 179-213 (1997).

17. M. A. Tosches *et al.*, Evolution of pallium, hippocampus, and cortical cell types revealed by single-cell transcriptomics in reptiles. *Science* **360**, 881-888 (2018).

18. J. Woych *et al.*, Cell-type profiling in salamanders identifies innovations in vertebrate forebrain evolution. *Science* **377**, eabp9186 (2022).

19. J. F. Montiel *et al.*, Hypothesis on the dual origin of the Mammalian subplate. *Front Neuroanat* **5**, 25 (2011).

20. W. Z. Wang *et al.*, Comparative aspects of subplate zone studied with gene expression in sauropsids and mammals. *Cereb Cortex* **21**, 2187-2203 (2011).

21. K. Y. Kwan, N. Sestan, E. S. Anton, Transcriptional co-regulation of neuronal migration and laminar identity in the neocortex. *Development* **139**, 1535-1546 (2012).

22. M. Florio *et al.*, Human-specific gene ARHGAP11B promotes basal progenitor amplification and neocortex expansion. *Science* **347**, 1465-1470 (2015).

23. K. S. Pollard *et al.*, An RNA gene expressed during cortical development evolved rapidly in humans. *Nature* **443**, 167-172 (2006).

24. K. M. Girskis *et al.*, Rewiring of human neurodevelopmental gene regulatory programs by human accelerated regions. *Neuron* **109**, 3239-3251.e3237 (2021).

25. A. M. M. Sousa *et al.*, Molecular and cellular reorganization of neural circuits in the human lineage. *Science* **358**, 1027-1032 (2017).

26. K. Y. Kwan *et al.*, Species-dependent posttranscriptional regulation of NOS1 by FMRP in the developing cerebral cortex. *Cell* **149**, 899-911 (2012).

27. K. Semendeferi *et al.*, Spatial organization of neurons in the frontal pole sets humans apart from great apes. *Cereb Cortex* **21**, 1485-1497 (2011).

28. T. M. Preuss, Do rats have prefrontal cortex? The rose-woolsey-akert program reconsidered. *J Cogn Neurosci* **7**, 1-24 (1995).

29. M. W. State, N. Šestan, Neuroscience. The emerging biology of autism spectrum disorders. *Science* **337**, 1301-1303 (2012).

30. M. Shibata *et al.*, Regulation of prefrontal patterning and connectivity by retinoic acid. *Nature* **598**, 483-488 (2021).

31. M. Shibata *et al.*, Hominini-specific regulation of CBLN2 increases prefrontal spinogenesis. *Nature* **598**, 489-494 (2021).

32. S. J. Franco *et al.*, Fate-restricted neural progenitors in the mammalian cerebral cortex. *Science* **337**, 746-749 (2012).

33. C. Guo *et al.*, Fezf2 expression identifies a multipotent progenitor for neocortical projection neurons, astrocytes, and oligodendrocytes. *Neuron* **80**, 1167-1174 (2013).

34. C. Gil-Sanz *et al.*, Lineage Tracing Using Cux2-Cre and Cux2-CreERT2 Mice. *Neuron* **86**, 1091-1099 (2015).

35. M. J. Eckler *et al.*, Cux2-positive radial glial cells generate diverse subtypes of neocortical projection neurons and macroglia. *Neuron* **86**, 1100-1108 (2015).

36. P. Gao *et al.*, Deterministic progenitor behavior and unitary production of neurons in the neocortex. *Cell* **159**, 775-788 (2014).

37. E. Aaku-Saraste, A. Hellwig, W. B. Huttner, Loss of occludin and functional tight junctions, but not ZO-1, during neural tube closure--remodeling of the neuroepithelium prior to neurogenesis. *Dev Biol* **180**, 664-679 (1996).

38. T. E. Anthony, C. Klein, G. Fishell, N. Heintz, Radial glia serve as neuronal progenitors in all regions of the central nervous system. *Neuron* **41**, 881-890 (2004).

39. U. C. Eze, A. Bhaduri, M. Haeussler, T. J. Nowakowski, A. R. Kriegstein, Single-cell atlas of early human brain development highlights heterogeneity of human neuroepithelial cells and early radial glia. *Nat Neurosci* **24**, 584-594 (2021).

40. P. Rakic, Mode of cell migration to the superficial layers of fetal monkey neocortex. *J Comp Neurol* **145**, 61-83 (1972).

41. S. Kim *et al.*, The apical complex couples cell fate and cell survival to cerebral cortical development. *Neuron* **66**, 69-84 (2010).

42. S. Liu, M. X. Trupiano, J. Simon, J. Guo, E. S. Anton, The essential role of primary cilia in cerebral cortical development and disorders. *Curr Top Dev Biol* **142**, 99-146 (2021).

43. F. C. Sauer, Mitosis in the neural tube. *Journal of Comparative Neurology* **62**, 377-405 (1935).

44. T. Takahashi, R. S. Nowakowski, V. S. Caviness, Jr., Interkinetic and migratory behavior of a cohort of neocortical neurons arising in the early embryonic murine cerebral wall. *J Neurosci* **16**, 5762-5776 (1996).

45. R. L. Sidman, I. L. Miale, N. Feder, Cell proliferation and migration in the primitive ependymal zone: an autoradiographic study of histogenesis in the nervous system. *Exp Neurol* **1**, 322-333 (1959).

46. J. W. Tsai, W. N. Lian, S. Kemal, A. R. Kriegstein, R. B. Vallee, Kinesin 3 and cytoplasmic dynein mediate interkinetic nuclear migration in neural stem cells. *Nat Neurosci* **13**, 1463-1471 (2010).

47. T. Takahashi, R. S. Nowakowski, V. S. Caviness, Jr., Cell cycle parameters and patterns of nuclear movement in the neocortical proliferative zone of the fetal mouse. *J Neurosci* **13**, 820-833 (1993).

48. J. W. Tsai, Y. Chen, A. R. Kriegstein, R. B. Vallee, LIS1 RNA interference blocks neural stem cell division, morphogenesis, and motility at multiple stages. *J Cell Biol* **170**, 935-945 (2005).

49. O. Reiner *et al.*, Isolation of a Miller-Dieker lissencephaly gene containing G protein beta-subunit-like repeats. *Nature* **364**, 717-721 (1993).

50. L. Shi, A. Qalieh, M. M. Lam, J. M. Keil, K. Y. Kwan, Robust elimination of genome-damaged cells safeguards against brain somatic aneuploidy following Knl1 deletion. *Nat Commun* **10**, 2588 (2019).

51. Y. Feng, C. A. Walsh, Mitotic spindle regulation by Nde1 controls cerebral cortical size. *Neuron* **44**, 279-293 (2004).

52. J. N. Little *et al.*, Loss of Coiled-Coil Protein Cep55 Impairs Neural Stem Cell Abscission and Results in p53-Dependent Apoptosis in Developing Cortex. *J Neurosci* **41**, 3344-3365 (2021).

53. M. K. Lehtinen *et al.*, The cerebrospinal fluid provides a proliferative niche for neural progenitor cells. *Neuron* **69**, 893-905 (2011).

54. W. Richter, D. Kranz, [Autoradiography of neurogenesis and morphogenesis of the regio cingularis of the rat. IV. Quantitative studies on the times of cell origins in the cortical lamina]. *J Hirnforsch* **20**, 581-629 (1979).

55. G. M. McSherry, I. H. Smart, Cell production gradients in the developing ferret isocortex. *J Anat* **144**, 1-14 (1986).

56. S. P. Hicks, C. J. D'Amato, Cell migrations to the isocortex in the rat. *Anat Rec* **160**, 619-634 (1968).

57. T. B. Committee, Embryonic vertebrate central nervous system: revised terminology. The Boulder Committee. *Anat Rec* **166**, 257-261 (1970).

58. J. B. Angevine, Jr., R. L. Sidman, Autoradiographic study of cell migration during histogenesis of cerebral cortex in the mouse. *Nature* **192**, 766-768 (1961).

59. P. Rakic, Neurons in rhesus monkey visual cortex: systematic relation between time of origin and eventual disposition. *Science* **183**, 425-427 (1974).

60. P. Rakic, Specification of cerebral cortical areas. *Science* **241**, 170-176 (1988).

61. V. B. Mountcastle, The columnar organization of the neocortex. *Brain* **120 (Pt 4)**, 701-722 (1997).

62. T. Takahashi, R. S. Nowakowski, V. S. Caviness, Jr., The cell cycle of the pseudostratified ventricular epithelium of the embryonic murine cerebral wall. *J Neurosci* **15**, 6046-6057 (1995).

63. Y. Arai *et al.*, Neural stem and progenitor cells shorten S-phase on commitment to neuron production. *Nat Commun* **2**, 154 (2011).

64. L. J. Pilaz *et al.*, Forced G1-phase reduction alters mode of division, neuron number, and laminar phenotype in the cerebral cortex. *Proc Natl Acad Sci U S A* **106**, 21924-21929 (2009).

65. C. Lange, W. B. Huttner, F. Calegari, Cdk4/cyclinD1 overexpression in neural stem cells shortens G1, delays neurogenesis, and promotes the generation and expansion of basal progenitors. *Cell Stem Cell* **5**, 320-331 (2009).

66. H. R. Horvitz, I. Herskowitz, Mechanisms of asymmetric cell division: two Bs or not two Bs, that is the question. *Cell* **68**, 237-255 (1992).

67. A. R. Skop, J. G. White, The dynactin complex is required for cleavage plane specification in early Caenorhabditis elegans embryos. *Curr Biol* **8**, 1110-1116 (1998).

68. J. A. Kaltschmidt, C. M. Davidson, N. H. Brown, A. H. Brand, Rotation and asymmetry of the mitotic spindle direct asymmetric cell division in the developing central nervous system. *Nat Cell Biol* **2**, 7-12 (2000).

69. T. F. Haydar, E. Ang, P. Rakic, Mitotic spindle rotation and mode of cell division in the developing telencephalon. *Proc Natl Acad Sci U S A* **100**, 2890-2895 (2003).

70. A. Chenn, S. K. McConnell, Cleavage orientation and the asymmetric inheritance of Notch1 immunoreactivity in mammalian neurogenesis. *Cell* **82**, 631-641 (1995).

71. I. H. Smart, Proliferative characteristics of the ependymal layer during the early development of the mouse neocortex: a pilot study based on recording the number, location and plane of cleavage of mitotic figures. *J Anat* **116**, 67-91 (1973).

72. X. Dong *et al.*, Metabolic lactate production coordinates vasculature development and progenitor behavior in the developing mouse neocortex. *Nat Neurosci* **25**, 865-875 (2022).

73. D. Z. Doyle, K. Y. Kwan, Neurogenic-angiogenic synchrony via lactate. *Nat Neurosci* **25**, 839-840 (2022).

74. R. M. Fame, M. L. Shannon, K. F. Chau, J. P. Head, M. K. Lehtinen, A concerted metabolic shift in early forebrain alters the CSF proteome and depends on MYC downregulation for mitochondrial maturation. *Development* **146** (2019).

75. A. Vasudevan, J. E. Long, J. E. Crandall, J. L. Rubenstein, P. G. Bhide, Compartment-specific transcription factors orchestrate angiogenesis gradients in the embryonic brain. *Nat Neurosci* **11**, 429-439 (2008).

76. S. C. Noctor, V. Martinez-Cerdeno, L. Ivic, A. R. Kriegstein, Cortical neurons arise in symmetric and asymmetric division zones and migrate through specific phases. *Nat Neurosci* **7**, 136-144 (2004).

77. M. P. Pebworth, J. Ross, M. Andrews, A. Bhaduri, A. R. Kriegstein, Human intermediate progenitor diversity during cortical development. *Proc Natl Acad Sci U S A* **118** (2021).

78. L. Baala *et al.*, Homozygous silencing of T-box transcription factor EOMES leads to microcephaly with polymicrogyria and corpus callosum agenesis. *Nat Genet* **39**, 454-456 (2007).

79. S. J. Arnold *et al.*, The T-box transcription factor Eomes/Tbr2 regulates neurogenesis in the cortical subventricular zone. *Genes Dev* **22**, 2479-2484 (2008).

80. D. V. Hansen, J. H. Lui, P. R. Parker, A. R. Kriegstein, Neurogenic radial glia in the outer subventricular zone of human neocortex. *Nature* **464**, 554-561 (2010).

81. P. Rakic, "Emergence of Neuronal and Glial Cell Lineages in Primate Brain" in Cellular and Molecular Biology of Neuronal Development, I. B. Black, Ed. (Springer US, Boston, MA, 1984), pp. 29-50.

82. X. Wang, J. W. Tsai, B. LaMonica, A. R. Kriegstein, A new subtype of progenitor cell in the mouse embryonic neocortex. *Nat Neurosci* **14**, 555-561 (2011).

83. M. Bilgic *et al.*, Truncated radial glia as a common precursor in the late corticogenesis of gyrencephalic mammals. *bioRxiv*, 2022.2005.2005.490846 (2023).

84. T. J. Nowakowski, A. A. Pollen, C. Sandoval-Espinosa, A. R. Kriegstein, Transformation of the Radial Glia Scaffold Demarcates Two Stages of Human Cerebral Cortex Development. *Neuron* **91**, 1219-1227 (2016).

85. D. E. Allen *et al.*, Fate mapping of neural stem cell niches reveals distinct origins of human cortical astrocytes. *Science* **376**, 1441-1446 (2022).

86. D. E. Schmechel, P. Rakic, A Golgi study of radial glial cells in developing monkey telencephalon: morphogenesis and transformation into astrocytes. *Anat Embryol (Berl)* **156**, 115-152 (1979).

87. J. M. Keil *et al.*, Symmetric neural progenitor divisions require chromatin-mediated homologous recombination DNA repair by Ino80. *Nat Commun* **11**, 3839 (2020).

88. G. D. Frantz, S. K. McConnell, Restriction of late cerebral cortical progenitors to an upper-layer fate. *Neuron* **17**, 55-61 (1996).

89. P. Oberst *et al.*, Temporal plasticity of apical progenitors in the developing mouse neocortex. *Nature* **573**, 370-374 (2019).

90. A. Chenn, C. A. Walsh, Regulation of cerebral cortical size by control of cell cycle exit in neural precursors. *Science* **297**, 365-369 (2002).

91. S. K. McConnell, C. E. Kaznowski, Cell cycle dependence of laminar determination in developing neocortex. *Science* **254**, 282-285 (1991).

92. R. Margueron, D. Reinberg, The Polycomb complex PRC2 and its mark in life. *Nature* **469**, 343-349 (2011).

93. K. Ohno, D. McCabe, B. Czermin, A. Imhof, V. Pirrotta, ESC, ESCL and their roles in Polycomb Group mechanisms. *Mech Dev* **125**, 527-541 (2008).

94. J. D. Pereira *et al.*, Ezh2, the histone methyltransferase of PRC2, regulates the balance between self-renewal and differentiation in the cerebral cortex. *Proc Natl Acad Sci U S A* **107**, 15957-15962 (2010).

95. Y. Hirabayashi *et al.*, Polycomb limits the neurogenic competence of neural precursor cells to promote astrogenic fate transition. *Neuron* **63**, 600-613 (2009).

96. L. Telley *et al.*, Temporal patterning of apical progenitors and their daughter neurons in the developing neocortex. *Science* **364** (2019).

97. N. Amberg, F. M. Pauler, C. Streicher, S. Hippenmeyer, Tissue-wide genetic and cellular landscape shapes the execution of sequential PRC2 functions in neural stem cell lineage progression. *Sci Adv* **8**, eabq1263 (2022).

98. A. S. Cohen *et al.*, A novel mutation in EED associated with overgrowth. *J Hum Genet* **60**, 339-342 (2015).

99. P. B. Talbert, S. Henikoff, The Yin and Yang of Histone Marks in Transcription. *Annu Rev Genomics Hum Genet* **22**, 147-170 (2021).

100. W. D. Jones *et al.*, De novo mutations in MLL cause Wiedemann-Steiner syndrome. *Am J Hum Genet* **91**, 358-364 (2012).

101. S. B. Ng *et al.*, Exome sequencing identifies MLL2 mutations as a cause of Kabuki syndrome. *Nat Genet* **42**, 790-793 (2010).

102. B. E. Bernstein *et al.*, A bivalent chromatin structure marks key developmental genes in embryonic stem cells. *Cell* **125**, 315-326 (2006).

103. O. H. Funk, Y. Qalieh, D. Z. Doyle, M. M. Lam, K. Y. Kwan, Postmitotic accumulation of histone variant H3.3 in new cortical neurons establishes neuronal chromatin, transcriptome, and identity. *Proc Natl Acad Sci U S A* **119**, e2116956119 (2022).

104. C. Walsh, C. L. Cepko, Clonally related cortical cells show several migration patterns. *Science* **241**, 1342-1345 (1988).

105. A. R. Kriegstein, S. C. Noctor, Patterns of neuronal migration in the embryonic cortex. *Trends Neurosci* **27**, 392-399 (2004).

106. C. Ohtaka-Maruyama *et al.*, Synaptic transmission from subplate neurons controls radial migration of neocortical neurons. *Science* **360**, 313-317 (2018).

107. J. Bai *et al.*, RNAi reveals doublecortin is required for radial migration in rat neocortex. *Nat Neurosci* **6**, 1277-1283 (2003).

108. T. Nagano, S. Morikubo, M. Sato, Filamin A and FILIP (Filamin A-Interacting Protein) regulate cell polarity and motility in neocortical subventricular and intermediate zones during radial migration. *J Neurosci* **24**, 9648-9657 (2004).

109. B. Nadarajah, J. E. Brunstrom, J. Grutzendler, R. O. Wong, A. L. Pearlman, Two modes of radial migration in early development of the cerebral cortex. *Nat Neurosci* **4**, 143-150 (2001).

110. S. Vinopal *et al.*, Centrosomal microtubule nucleation regulates radial migration of projection neurons independently of polarization in the developing brain. *Neuron* (2023).

111. I. P. Njoku, K. Y. Kwan, Distinct microtubule networks mediate neuronal migration and polarization. *Neuron* **111**, 1168-1170 (2023).

112. Q. Xu, I. Cobos, E. De La Cruz, J. L. Rubenstein, S. A. Anderson, Origins of cortical interneuron subtypes. *J Neurosci* **24**, 2612-2622 (2004).

113. S. A. Anderson, D. D. Eisenstat, L. Shi, J. L. Rubenstein, Interneuron migration from basal forebrain to neocortex: dependence on Dlx genes. *Science* **278**, 474-476 (1997).

114. B. Nadarajah, J. G. Parnavelas, Modes of neuronal migration in the developing cerebral cortex. *Nat Rev Neurosci* **3**, 423-432 (2002).

115. O. Marín, Cellular and molecular mechanisms controlling the migration of neocortical interneurons. *Eur J Neurosci* **38**, 2019-2029 (2013).

116. F. Polleux, K. L. Whitford, P. A. Dijkhuizen, T. Vitalis, A. Ghosh, Control of cortical interneuron migration by neurotrophins and PI3-kinase signaling. *Development* **129**, 3147-3160 (2002).

117. R. D. Lund, M. J. Mustari, Development of the geniculocortical pathway in rats. *J Comp Neurol* **173**, 289-306 (1977).

118. S. P. Wise, E. G. Jones, Developmental studies of thalamocortical and commissural connections in the rat somatic sensory cortex. *J Comp Neurol* **178**, 187-208 (1978).

119. N. Swinnen *et al.*, Complex invasion pattern of the cerebral cortex bymicroglial cells during development of the mouse embryo. *Glia* **61**, 150-163 (2013).

120. R. N. Delgado *et al.*, Individual human cortical progenitors can produce excitatory and inhibitory neurons. *Nature* **601**, 397-403 (2022).

121. K. Letinic, R. Zoncu, P. Rakic, Origin of GABAergic neurons in the human neocortex. *Nature* **417**, 645-649 (2002).

122. X. Yu, N. Zecevic, Dorsal radial glial cells have the potential to generate cortical interneurons in human but not in mouse brain. *J Neurosci* **31**, 2413-2420 (2011).

123. S. E. Hong *et al.*, Autosomal recessive lissencephaly with cerebellar hypoplasia is associated with human RELN mutations. *Nat Genet* **26**, 93-96 (2000).

124. E. Dazzo *et al.*, Heterozygous reelin mutations cause autosomal-dominant lateral temporal epilepsy. *Am J Hum Genet* **96**, 992-1000 (2015).

125. V. S. Caviness, Jr., R. L. Sidman, Time of origin or corresponding cell classes in the cerebral cortex of normal and reeler mutant mice: an autoradiographic analysis. *J Comp Neurol* **148**, 141-151 (1973).

126. V. S. Caviness, Jr., Neocortical histogenesis in normal and reeler mice: a developmental study based upon [3H]thymidine autoradiography. *Brain Res* **256**, 293-302 (1982).

127. D. Rice, T. Curran, Role of the reelin signaling pathway in central nervous system development. *Annu Rev Neurosci* **24**, 1005-1039 (2001).

128. F. Tissir, A. M. Goffinet, Reelin and brain development. *Nat Rev Neurosci* **4**, 496-505 (2003).

129. E. Alcamo *et al.*, Satb2 regulates callosal projection neuron identity in the developing cerebral cortex. *Neuron* **57**, 364-377 (2008).

130. O. Britanova *et al.*, Satb2 is a postmitotic determinant for upper-layer neuron specification in the neocortex. *Neuron* **57**, 378-392 (2008).

131. I. A. Glass, C. A. Swindlehurst, D. A. Aitken, W. McCrea, E. Boyd, Interstitial deletion of the long arm of chromosome 2 with normal levels of isocitrate dehydrogenase. *J Med Genet* **26**, 127-130 (1989).

132. P. Leoyklang *et al.*, Heterozygous nonsense mutation SATB2 associated with cleft palate, osteoporosis, and cognitive defects. *Hum Mutat* **28**, 732-738 (2007).

133. L. W. Harris *et al.*, Gene expression in the prefrontal cortex during adolescence: implications for the onset of schizophrenia. *BMC Med Genomics* **2**, 28 (2009).

134. H. Jaaro-Peled *et al.*, Neurodevelopmental mechanisms of schizophrenia: understanding disturbed postnatal brain maturation through neuregulin-1-ErbB4 and DISC1. *Trends Neurosci* **32**, 485-495 (2009).

135. D. P. Leone *et al.*, Satb2 Regulates the Differentiation of Both Callosal and Subcerebral Projection Neurons in the Developing Cerebral Cortex. *Cereb Cortex* (2014).

136. N. Flames *et al.*, Short- and long-range attraction of cortical GABAergic interneurons by neuregulin-1. *Neuron* **44**, 251-261 (2004).

137. L. Lim *et al.*, Optimization of interneuron function by direct coupling of cell migration and axonal targeting. *Nat Neurosci* **21**, 920-931 (2018).

138. G. S. Pai, R. I. Macpherson, Idiopathic multicentric osteolysis: report of two new cases and a review of the literature. *Am J Med Genet* **29**, 929-936 (1988).

139. A. Hoerder-Suabedissen, Z. Molnár, Molecular diversity of early-born subplate neurons. *Cereb Cortex* **23**, 1473-1483 (2013).

140. A. Hoerder-Suabedissen *et al.*, Novel markers reveal subpopulations of subplate neurons in the murine cerebral cortex. *Cereb Cortex* **19**, 1738-1750 (2009).

141. K. Y. Kwan *et al.*, SOX5 postmitotically regulates migration, postmigratory differentiation, and projections of subplate and deep-layer neocortical neurons. *Proc Natl Acad Sci U S A* **105**, 16021-16026 (2008).

142. S. Y. X. Tiong *et al.*, Kcnab1 Is Expressed in Subplate Neurons With Unilateral Long-Range Inter-Areal Projections. *Front Neuroanat* **13**, 39 (2019).

143. A. Bulfone *et al.*, T-brain-1: a homolog of Brachyury whose expression defines molecularly distinct domains within the cerebral cortex. *Neuron* **15**, 63-78 (1995).

144. R. Hevner *et al.*, Tbr1 regulates differentiation of the preplate and layer 6. *Neuron* **29**, 353-366 (2001).

145. C. Zhou *et al.*, The nuclear orphan receptor COUP-TFI is required for differentiation of subplate neurons and guidance of thalamocortical axons. *Neuron* **24**, 847-859 (1999).

146. A. Junaković *et al.*, Laminar dynamics of deep projection neurons and mode of subplate formation are hallmarks of histogenetic subdivisions of the human cingulate cortex before onset of arealization. *Brain Struct Funct* **228**, 613-633 (2023).

147. J. Kopić *et al.*, Early Regional Patterning in the Human Prefrontal Cortex Revealed by Laminar Dynamics of Deep Projection Neuron Markers. *Cells* **12** (2023).

148. A. N. Lamb *et al.*, Haploinsufficiency of SOX5 at 12p12.1 is associated with developmental delays with prominent language delay, behavior problems, and mild dysmorphic features. *Hum Mutat* **33**, 728-740 (2012).

149. P. Deriziotis *et al.*, De novo TBR1 mutations in sporadic autism disrupt protein functions. *Nat Commun* **5**, 4954 (2014).

150. M. Leid *et al.*, CTIP1 and CTIP2 are differentially expressed during mouse embryogenesis. *Gene Expr Patterns* **4**, 733-739 (2004).

151. P. Arlotta *et al.*, Neuronal subtype-specific genes that control corticospinal motor neuron development in vivo. *Neuron* **45**, 207-221 (2005).

152. K. Inoue, T. Terashima, T. Nishikawa, T. Takumi, Fez1 is layer-specifically expressed in the adult mouse neocortex. *Eur J Neurosci* **20**, 2909-2916 (2004).

153. B. Chen, L. Schaevitz, S. McConnell, Fezl regulates the differentiation and axon targeting of layer 5 subcortical projection neurons in cerebral cortex. *Proc Natl Acad Sci U S A* **102**, 17184-17189 (2005).

154. J. Chen, M. Rasin, K. Kwan, N. Sestan, Zfp312 is required for subcortical axonal projections and dendritic morphology of deep-layer pyramidal neurons of the cerebral cortex. *Proc Natl Acad Sci U S A* **102**, 17792-17797 (2005).

155. D. Lessel *et al.*, BCL11B mutations in patients affected by a neurodevelopmental disorder with reduced type 2 innate lymphoid cells. *Brain* **141**, 2299-2311 (2018).

156. N. Schaeren-Wiemers, E. André, J. P. Kapfhammer, M. Becker-André, The expression pattern of the orphan nuclear receptor RORbeta in the developing and adult rat nervous system suggests a role in the processing of sensory information and in circadian rhythm. *Eur J Neurosci* **9**, 2687-2701 (1997).

157. G. Rudolf *et al.*, Loss of function of the retinoid-related nuclear receptor (RORB) gene and epilepsy. *Eur J Hum Genet* **24**, 1761-1770 (2016).

158. M. Nieto *et al.*, Expression of Cux-1 and Cux-2 in the subventricular zone and upper layers II-IV of the cerebral cortex. *J Comp Neurol* **479**, 168-180 (2004).

159. X. He *et al.*, Expression of a large family of POU-domain regulatory genes in mammalian brain development. *Nature* **340**, 35-41 (1989).

160. O. Britanova, S. Akopov, S. Lukyanov, P. Gruss, V. Tarabykin, Novel transcription factor Satb2 interacts with matrix attachment region DNA elements in a tissue-specific manner and demonstrates cell-type-dependent expression in the developing mouse CNS. *Eur J Neurosci* **21**, 658-668 (2005).

161. S. Shim, K. Y. Kwan, M. Li, V. Lefebvre, N. Sestan, Cis-regulatory control of corticospinal system development and evolution. *Nature* **486**, 74-79 (2012).

162. W. Han *et al.*, TBR1 directly represses Fezf2 to control the laminar origin and development of the corticospinal tract. *Proc Natl Acad Sci U S A* **108**, 3041-3046 (2011).

163. W. L. McKenna *et al.*, Tbr1 and Fezf2 regulate alternate corticofugal neuronal identities during neocortical development. *J Neurosci* **31**, 549-564 (2011).

164. J. Tsyporin *et al.*, Transcriptional repression by FEZF2 restricts alternative identities of cortical projection neurons. *Cell Rep* **35**, 109269 (2021).

165. T. Monko, J. Rebertus, J. Stolley, S. R. Salton, Y. Nakagawa, Thalamocortical axons regulate neurogenesis and laminar fates in the early sensory cortex. *Proc Natl Acad Sci U S A* **119**, e2201355119 (2022).

166. W. F. Marzluff, E. J. Wagner, R. J. Duronio, Metabolism and regulation of canonical histone mRNAs: life without a poly(A) tail. *Nature reviews. Genetics* **9** (2008).

167. R. S. Wu, S. Tsai, W. M. Bonner, Patterns of histone variant synthesis can distinguish G0 from G1 cells. *Cell* **31** (1982).

168. L. Bryant *et al.*, Histone H3.3 beyond cancer: Germline mutations in Histone 3 Family 3A and 3B cause a previously unidentified neurodegenerative disorder in 46 patients. *Sci Adv* **6** (2020).

169. V. Okur *et al.*, De novo variants in H3-3A and H3-3B are associated with neurodevelopmental delay, dysmorphic features, and structural brain abnormalities. *NPJ Genom Med* **6**, 104 (2021).

170. E. G. Jones, S. P. Wise, Size, laminar and columnar distribution of efferent cells in the sensory-motor cortex of monkeys. *J Comp Neurol* **175**, 391-438 (1977).

171. A. Hoerder-Suabedissen *et al.*, Subset of Cortical Layer 6b Neurons Selectively Innervates Higher Order Thalamic Nuclei in Mice. *Cereb Cortex* **28**, 1882-1897 (2018).

172. M. Deschênes, J. Bourassa, D. Pinault, Corticothalamic projections from layer V cells in rat are collaterals of long-range corticofugal axons. *Brain Res* **664**, 215-219 (1994).

173. I. Reichova, S. M. Sherman, Somatosensory corticothalamic projections: distinguishing drivers from modulators. *J Neurophysiol* **92**, 2185-2197 (2004).

174. T. A. Seabrook, R. N. El-Danaf, T. E. Krahe, M. A. Fox, W. Guido, Retinal input regulates the timing of corticogeniculate innervation. *J Neurosci* **33**, 10085-10097 (2013).

175. M. J. Galazo, D. Sweetser, J. D. Macklis, *Tle4* controls both developmental acquisition and postnatal maintenance of corticothalamic projection neuron identity. *bioRxiv*, 2022.2005.2009.491192 (2022).

176. M. J. Galazo, J. G. Emsley, J. D. Macklis, Corticothalamic Projection Neuron Development beyond Subtype Specification: Fog2 and Intersectional Controls Regulate Intraclass Neuronal Diversity. *Neuron* **91**, 90-106 (2016).

177. R. F. Hevner, E. Miyashita-Lin, J. L. Rubenstein, Cortical and thalamic axon pathfinding defects in Tbr1, Gbx2, and Pax6 mutant mice: evidence that cortical and thalamic axons interact and guide each other. *J Comp Neurol* **447**, 8-17 (2002).

178. F. Bedogni *et al.*, Tbr1 regulates regional and laminar identity of postmitotic neurons in developing neocortex. *Proc Natl Acad Sci U S A* **107**, 13129-13134 (2010).

179. T. Hirata *et al.*, Zinc finger gene fez-like functions in the formation of subplate neurons and thalamocortical axons. *Dev Dyn* **230**, 546-556 (2004).

180. Y. Komuta, M. Hibi, T. Arai, S. Nakamura, H. Kawano, Defects in reciprocal projections between the thalamus and cerebral cortex in the early development of Fezl-deficient mice. *J Comp Neurol* **503**, 454-465 (2007).

181. E. G. Jones, J. D. Coulter, H. Burton, R. Porter, Cells of origin and terminal distribution of corticostriatal fibers arising in the sensory-motor cortex of monkeys. *J Comp Neurol* **173**, 53-80 (1977).

182. A. S. Kayser, D. C. Allen, A. Navarro-Cebrian, J. M. Mitchell, H. L. Fields, Dopamine, corticostriatal connectivity, and intertemporal choice. *J Neurosci* **32**, 9402-9409 (2012).

183. H. G. Kuypers, Corticobular connexions to the pons and lower brain-stem in man: an anatomical study. *Brain* **81**, 364-388 (1958).

184. M. Glickstein, J. Stein, R. A. King, Visual input to the pontine nuclei. *Science* **178**, 1110-1111 (1972).

185. J. Park *et al.*, Motor cortical output for skilled forelimb movement is selectively distributed across projection neuron classes. *Sci Adv* **8**, eabj5167 (2022).

186. K. P. Hoffmann, M. Straschill, Influences of cortico-tectal and intertectal connections on visual responses in the cat's superior colliculus. *Exp Brain Res* **12**, 120-131 (1971).

187. N. Tsukahara, Y. Oda, T. Notsu, Classical conditioning mediated by the red nucleus in the cat. *J Neurosci* **1**, 72-79 (1981).

188. B. Chen *et al.*, The Fezf2-Ctip2 genetic pathway regulates the fate choice of subcortical projection neurons in the developing cerebral cortex. *Proc Natl Acad Sci U S A* **105**, 11382-11387 (2008).

189. B. Chen *et al.*, The Fezf2-Ctip2 genetic pathway regulates the fate choice of subcortical projection neurons in the developing cerebral cortex. *Proc Natl Acad Sci U S A* **105**, 11382-11387 (2008).

190. D. H. Hubel, T. N. Wiesel, Anatomical demonstration of columns in the monkey striate cortex. *Nature* **221**, 747-750 (1969).

191. D. H. Hubel, T. N. Wiesel, Receptive fields, binocular interaction and functional architecture in the cat's visual cortex. *J Physiol* **160**, 106-154 (1962).

192. D. H. Hubel, T. N. Wiesel, Binocular interaction in striate cortex of kittens reared with artificial squint. *J Neurophysiol* **28**, 1041-1059 (1965).

193. P. Rakic, Prenatal genesis of connections subserving ocular dominance in the rhesus monkey. *Nature* **261**, 467-471 (1976).

194. S. LeVay, M. P. Stryker, C. J. Shatz, Ocular dominance columns and their development in layer IV of the cat's visual cortex: a quantitative study. *J Comp Neurol* **179**, 223-244 (1978).

195. A. K. Wiser, E. M. Callaway, Ocular dominance columns and local projections of layer 6 pyramidal neurons in macaque primary visual cortex. *Vis Neurosci* **14**, 241-251 (1997).

196. A. K. Wiser, E. M. Callaway, Contributions of individual layer 6 pyramidal neurons to local circuitry in macaque primary visual cortex. *J Neurosci* **16**, 2724-2739 (1996).

197. L. C. Katz, C. D. Gilbert, T. N. Wiesel, Local circuits and ocular dominance columns in monkey striate cortex. *J Neurosci* **9**, 1389-1399 (1989).

198. J. Syken, T. Grandpre, P. O. Kanold, C. J. Shatz, PirB restricts ocular-dominance plasticity in visual cortex. *Science* **313**, 1795-1800 (2006).

199. R. J. Cabelli, A. Hohn, C. J. Shatz, Inhibition of ocular dominance column formation by infusion of NT-4/5 or BDNF. *Science* **267**, 1662-1666 (1995).

200. T. N. Wiesel, D. H. Hubel, SINGLE-CELL RESPONSES IN STRIATE CORTEX OF KITTENS DEPRIVED OF VISION IN ONE EYE. *J Neurophysiol* **26**, 1003-1017 (1963).

201. E. H. Boyd, D. N. Pandya, K. E. Bignall, Homotopic and nonhomotopic interhemispheric cortical projections in the squirrel monkey. *Exp Neurol* **32**, 256-274 (1971).

202. G. O. Ivy, H. P. Killackey, The ontogeny of the distribution of callosal projection neurons in the rat parietal cortex. *J Comp Neurol* **195**, 367-389 (1981).

203. C. Baranek *et al.*, Protooncogene Ski cooperates with the chromatin-remodeling factor Satb2 in specifying callosal neurons. *Proc Natl Acad Sci U S A* **109**, 3546-3551 (2012).

204. P. Rakic, P. I. Yakovlev, Development of the corpus callosum and cavum septi in man. *J Comp Neurol* **132**, 45-72 (1968).

205. S. E. Koester, D. D. O'Leary, Axons of early generated neurons in cingulate cortex pioneer the corpus callosum. *J Neurosci* **14**, 6608-6620 (1994).

206. D. Wahlsten, Prenatal schedule of appearance of mouse brain commissures. *Brain Res* **227**, 461-473 (1981).

207. H. S. Ozaki, D. Wahlsten, Prenatal formation of the normal mouse corpus callosum: a quantitative study with carbocyanine dyes. *J Comp Neurol* **323**, 81-90 (1992).

208. A. Chovsepian, L. Empl, D. Correa, F. M. Bareyre, Heterotopic Transcallosal Projections Are Present throughout the Mouse Cortex. *Front Cell Neurosci* **11**, 36 (2017).

209. T. Shu, V. Sundaresan, M. M. McCarthy, L. J. Richards, Slit2 guides both precrossing and postcrossing callosal axons at the midline in vivo. *J Neurosci* **23**, 8176-8184 (2003).

210. G. López-Bendito *et al.*, Robo1 and Robo2 cooperate to control the guidance of major axonal tracts in the mammalian forebrain. *J Neurosci* **27**, 3395-3407 (2007).

211. Y. Wang, J. Zhang, S. Mori, J. Nathans, Axonal growth and guidance defects in Frizzled3 knock-out mice: a comparison of diffusion tensor magnetic resonance imaging, neurofilament staining, and genetically directed cell labeling. *J Neurosci* **26**, 355-364 (2006).

212. T. Serafini *et al.*, Netrin-1 is required for commissural axon guidance in the developing vertebrate nervous system. *Cell* **87**, 1001-1014 (1996).

213. Y. Choe, J. A. Siegenthaler, S. J. Pleasure, A cascade of morphogenic signaling initiated by the meninges controls corpus callosum formation. *Neuron* **73**, 698-712 (2012).

214. J. Silver, S. E. Lorenz, D. Wahlsten, J. Coughlin, Axonal guidance during development of the great cerebral commissures: descriptive and experimental studies, in vivo, on the role of preformed glial pathways. *J Comp Neurol* **210**, 10-29 (1982).

215. J. Silver, M. A. Edwards, P. Levitt, Immunocytochemical demonstration of early appearing astroglial structures that form boundaries and pathways along axon tracts in the fetal brain. *J Comp Neurol* **328**, 415-436 (1993).

216. L. K. Paul *et al.*, Agenesis of the corpus callosum: genetic, developmental and functional aspects of connectivity. *Nat Rev Neurosci* **8**, 287-299 (2007).

217. K. M. Smith *et al.*, Midline radial glia translocation and corpus callosum formation require FGF signaling. *Nat Neurosci* **9**, 787-797 (2006).

218. T. Shu, L. J. Richards, Cortical axon guidance by the glial wedge during the development of the corpus callosum. *J Neurosci* **21**, 2749-2758 (2001).

219. T. Shu, A. C. Puche, L. J. Richards, Development of midline glial populations at the corticoseptal boundary. *J Neurobiol* **57**, 81-94 (2003).

220. M. Probst, Ueber den Bau des vollständig balkenlosen Gross-hirnes sowie über Mikrogyrie und Heterotopie der grauen Substanz. *Archiv für Psychiatrie und Nervenkrankheiten* **34**, 709-786 (1901).

221. G. M. Innocenti, L. Fiore, R. Caminiti, Exuberant projection into the corpus callosum from the visual cortex of newborn cats. *Neurosci Lett* **4**, 237-242 (1977).

222. C. J. Shatz, Anatomy of interhemispheric connections in the visual system of Boston Siamese and ordinary cats. *J Comp Neurol* **173**, 497-518 (1977).

223. E. M. Callaway, Prenatal development of layer-specific local circuits in primary visual cortex of the macaque monkey. *J Neurosci* **18**, 1505-1527 (1998).

224. F. Assal, G. M. Innocenti, Transient intra-areal axons in developing cat visual cortex. *Cereb Cortex* **3**, 290-303 (1993).

225. D. O. Frost, Y. P. Moy, D. C. Smith, Effects of alternating monocular occlusion on the development of visual callosal connections. *Exp Brain Res* **83**, 200-209 (1990).

226. G. O. Ivy, R. M. Akers, H. P. Killackey, Differential distribution of callosal projection neurons in the neonatal and adult rat. *Brain Res* **173**, 532-537 (1979).

227. D. D. O'Leary, B. B. Stanfield, W. M. Cowan, Evidence that the early postnatal restriction of the cells of origin of the callosal projection is due to the elimination of axonal collaterals rather than to the death of neurons. *Brain Res* **227**, 607-617 (1981).

228. A. S. LaMantia, P. Rakic, Axon overproduction and elimination in the corpus callosum of the developing rhesus monkey. *J Neurosci* **10**, 2156-2175 (1990).

229. D. Aggoun-Aouaoui, D. C. Kiper, G. M. Innocenti, Growth of callosal terminal arbors in primary visual areas of the cat. *Eur J Neurosci* **8**, 1132-1148 (1996).

230. R. Suárez *et al.*, Balanced interhemispheric cortical activity is required for correct targeting of the corpus callosum. *Neuron* **82**, 1289-1298 (2014).

231. M. Yasuda, S. Nagappan-Chettiar, E. M. Johnson-Venkatesh, H. Umemori, An activity-dependent determinant of synapse elimination in the mammalian brain. *Neuron* **109**, 1333-1349.e1336 (2021).

232. F. M. Rodríguez-Tornos *et al.*, Cux1 Enables Interhemispheric Connections of Layer II/III Neurons by Regulating Kv1-Dependent Firing. *Neuron* **89**, 494-506 (2016).

233. N. Antón-Bolaños *et al.*, Prenatal activity from thalamic neurons governs the emergence of functional cortical maps in mice. *Science* **364**, 987-990 (2019).

234. M. Pedraza, A. Hoerder-Suabedissen, M. A. Albert-Maestro, Z. Molnár, J. A. De Carlos, Extracortical origin of some murine subplate cell populations. *Proc Natl Acad Sci U S A* **111**, 8613-8618 (2014).

235. I. Bystron, C. Blakemore, P. Rakic, Development of the human cerebral cortex: Boulder Committee revisited. *Nat Rev Neurosci* **9**, 110-122 (2008).

236. S. Ramón y Cajal, *Beitrag zum Studium der Medulla oblongata, des Kleinhirns und des Ursprungs der Gehirnnerven* (Verlag von Johann Ambrosius Barth, 1896).

237. M. Judaš, G. Sedmak, M. Pletikos, Early history of subplate and interstitial neurons: from Theodor Meynert (1867) to the discovery of the subplate zone (1974). *J Anat* **217**, 344-367 (2010).

238. S. Hatai, Observations on the developing neurones of the cerebral cortex of foetal cats. *Journal of Comparative Neurology* **12**, 199-204 (1902).

239. I. Kostović, M. E. Molliver, A new interpretation of the laminar development of cerebral cortex: synaptogenesis in different layers of neopallium in the human fetus. *Anat Rec* **178**, 395 (1974).

240. I. Kostović, P. Rakic, Cytology and time of origin of interstitial neurons in the white matter in infant and adult human and monkey telencephalon. *J Neurocytol* **9**, 219-242 (1980).

241. J. R. Naegele, C. J. Barnstable, P. R. Wahle, Expression of a unique 56-kDa polypeptide by neurons in the subplate zone of the developing cerebral cortex. *Proc Natl Acad Sci U S A* **88**, 330-334 (1991).

242. D. J. Price, S. Aslam, L. Tasker, K. Gillies, Fates of the earliest generated cells in the developing murine neocortex. *J Comp Neurol* **377**, 414-422 (1997).

243. M. B. Luskin, C. J. Shatz, Studies of the earliest generated cells of the cat's visual cortex: cogeneration of subplate and marginal zones. *J Neurosci* **5**, 1062-1075 (1985).

244. F. Valverde, M. V. Facal-Valverde, Postnatal development of interstitial (subplate) cells in the white matter of the temporal cortex of kittens: a correlated Golgi and electron microscopic study. *J Comp Neurol* **269**, 168-192 (1988).

245. F. Valverde, M. V. Facal-Valverde, Transitory population of cells in the temporal cortex of kittens. *Brain Res* **429**, 283-288 (1987).

246. I. Kostović, P. Rakic, Developmental history of the transient subplate zone in the visual and somatosensory cortex of the macaque monkey and human brain. *J Comp Neurol* **297**, 441-470 (1990).

247. I. Ferrer, E. Bernet, E. Soriano, T. del Rio, M. Fonseca, Naturally occurring cell death in the cerebral cortex of the rat and removal of dead cells by transitory phagocytes. *Neuroscience* **39**, 451-458 (1990).

248. A. Duque, Z. Krsnik, I. Kostović, P. Rakic, Secondary expansion of the transient subplate zone in the developing cerebrum of human and nonhuman primates. *Proc Natl Acad Sci U S A* **113**, 9892-9897 (2016).

249. C. F. v. Economo, G. N. j. a. Koskinas, *Die cytoarchitektonik der hirnrinde des erwachsenen menschen* (J. Springer, Wien und Berlin, 1925), vol. Wien und Berlin.

250. M. Z. Ozair *et al.*, hPSC Modeling Reveals that Fate Selection of Cortical Deep Projection Neurons Occurs in the Subplate. *Cell Stem Cell* **23**, 60-73.e66 (2018).

251. M. A. Mostajo-Radji, A. A. Pollen, Postmitotic Fate Refinement in the Subplate. *Cell Stem Cell* **23**, 7-9 (2018).

252. D. L. Meinecke, P. Rakic, Expression of GABA and GABAA receptors by neurons of the subplate zone in developing primate occipital cortex: evidence for transient local circuits. *J Comp Neurol* **317**, 91-101 (1992).

253. N. Zecevic, A. Milosevic, Initial development of gamma-aminobutyric acid immunoreactivity in the human cerebral cortex. *J Comp Neurol* **380**, 495-506 (1997).

254. A. Cobas, A. Fairén, G. Alvarez-Bolado, M. P. Sánchez, Prenatal development of the intrinsic neurons of the rat neocortex: a comparative study of the distribution of GABA-immunoreactive cells and the GABAA receptor. *Neuroscience* **40**, 375-397 (1991).

255. D. D. Wang, A. R. Kriegstein, Defining the role of GABA in cortical development. *J Physiol* **587**, 1873-1879 (2009).

256. I. L. Hanganu, W. Kilb, H. J. Luhmann, Functional synaptic projections onto subplate neurons in neonatal rat somatosensory cortex. *J Neurosci* **22**, 7165-7176 (2002).

257. A. Hoerder-Suabedissen, Z. Molnár, Morphology of mouse subplate cells with identified projection targets changes with age. *J Comp Neurol* **520**, 174-185 (2012).

258. M. Marx *et al.*, Neocortical Layer 6B as a Remnant of the Subplate - A Morphological Comparison. *Cereb Cortex* **27**, 1011-1026 (2017).

259. I. Kostović , Z. Kelović , L. Mrzljak, I. Kračun, Distribution and morphology of interstitial acetylcholinesterase (AChE) reactive neurons in the fiber bundles of the human fetal telencephalon. *Neuroscience Letters*, S288 (1981).

260. E. Friauf, S. K. McConnell, C. J. Shatz, Functional synaptic circuits in the subplate during fetal and early postnatal development of cat visual cortex. *J Neurosci* **10**, 2601-2613 (1990).

261. M. E. Molliver, I. Kostović, H. van der Loos, The development of synapses in cerebral cortex of the human fetus. *Brain Res* **50**, 403-407 (1973).

262. I. Kostović, P. S. Goldman-Rakic, Transient cholinesterase staining in the mediodorsal nucleus of the thalamus and its connections in the developing human and monkey brain. *J Comp Neurol* **219**, 431-447 (1983).

263. I. Kostović, P. Rakic, Development of prestriate visual projections in the monkey and human fetal cerebrum revealed by transient cholinesterase staining. *J Neurosci* **4**, 25-42 (1984).

264. M. Marin-Padilla, Early prenatal ontogenesis of the cerebral cortex (neocortex) of the cat (Felis domestica). A Golgi study. I. The primordial neocortical organization. *Z Anat Entwicklungsgesch* **134**, 117-145 (1971).

265. M. Marin-Padilla, Dual origin of the mammalian neocortex and evolution of the cortical plate. *Anat Embryol (Berl)* **152**, 109-126 (1978).

266. G. R. Stewart, A. L. Pearlman, Fibronectin-like immunoreactivity in the developing cerebral cortex. *J Neurosci* **7**, 3325-3333 (1987).

267. M. Marin-Padilla, Structural organization of the human cerebral cortex prior to the appearance of the cortical plate. *Anatomy and embryology* **168**, 21-40 (1983).

268. M. Rickmann, J. Wolff, Differentiation of 'preplate' neurons in the pallium of the rat. *Bibliotheca Anatomica*, 142-146 (1981).

269. Z. Molnár, R. Adams, A. M. Goffinet, C. Blakemore, The role of the first postmitotic cortical cells in the development of thalamocortical innervation in the reeler mouse. *J Neurosci* **18**, 5746-5765 (1998).

270. S. Rakic, C. Davis, Z. Molnár, M. Nikolic, J. G. Parnavelas, Role of p35/Cdk5 in preplate splitting in the developing cerebral cortex. *Cereb Cortex* **16 Suppl 1**, i35-45 (2006).

271. A. K. Voss *et al.*, C3G regulates cortical neuron migration, preplate splitting and radial glial cell attachment. *Development* **135**, 2139-2149 (2008).

272. V. J. Caviness, Neocortical histogenesis in normal and reeler mice: a developmental study based upon [3H]thymidine autoradiography. *Brain Res* **256**, 293-302 (1982).

273. T. Lai *et al.*, SOX5 Controls the Sequential Generation of Distinct Corticofugal Neuron Subtypes. *Neuron* **57**, 232-247 (2008).

274. L. Ratie *et al.*, Loss of Dmrt5 Affects the Formation of the Subplate and Early Corticogenesis. *Cereb Cortex* (2019).

275. M. Yoshida, S. Assimacopoulos, K. R. Jones, E. A. Grove, Massive loss of Cajal-Retzius cells does not disrupt neocortical layer order. *Development* **133**, 537-545 (2006).

276. H. S. Ozaki, D. Wahlsten, Timing and origin of the first cortical axons to project through the corpus callosum and the subsequent emergence of callosal projection cells in mouse. *J Comp Neurol* **400**, 197-206 (1998).

277. A. Antonini, C. J. Shatz, Relation Between Putative Transmitter Phenotypes and Connectivity of Subplate Neurons During Cerebral Cortical Development. *Eur J Neurosci* **2**, 744-761 (1990).

278. J. J. Chun, M. J. Nakamura, C. J. Shatz, Transient cells of the developing mammalian telencephalon are peptide-immunoreactive neurons. *Nature* **325**, 617-620 (1987).

279. T. Ren *et al.*, Imaging, anatomical, and molecular analysis of callosal formation in the developing human fetal brain. *Anat Rec A Discov Mol Cell Evol Biol* **288**, 191-204 (2006).

280. S. Koester, D. O'Leary (1991) Subplate cells in medial cortex send the first axons across the corpus callosum. in *Soc. Neurosci. Abstr*, p 41.

281. M. L. Schwartz, P. S. Goldman-Rakic, Prenatal specification of callosal connections in rhesus monkey. *J Comp Neurol* **307**, 144-162 (1991).

282. L. C. deAzevedo, C. Hedin-Pereira, R. Lent, Callosal neurons in the cingulate cortical plate and subplate of human fetuses. *J Comp Neurol* **386**, 60-70 (1997).

283. S. K. McConnell, A. Ghosh, C. J. Shatz, Subplate neurons pioneer the first axon pathway from the cerebral cortex. *Science* **245**, 978-982 (1989).

284. J. A. De Carlos, D. D. O'Leary, Growth and targeting of subplate axons and establishment of major cortical pathways. *J Neurosci* **12**, 1194-1211 (1992).

285. S. McConnell, A. Ghosh, C. Shatz, Subplate pioneers and the formation of descending connections from cerebral cortex. *J Neurosci* **14**, 1892-1907 (1994).

286. F. Clascá, A. Angelucci, M. Sur, Layer-specific programs of development in neocortical projection neurons. *Proc Natl Acad Sci U S A* **92**, 11145-11149 (1995).

287. B. Miller, L. Chou, B. L. Finlay, The early development of thalamocortical and corticothalamic projections. *J Comp Neurol* **335**, 16-41 (1993).

288. C. Blakemore, Z. Molnar, Factors involved in the establishment of specific interconnections between thalamus and cerebral cortex. *Cold Spring Harb Symp Quant Biol* **55**, 491-504 (1990).

289. A. R. Bicknese, A. M. Sheppard, D. D. O'Leary, A. L. Pearlman, Thalamocortical axons extend along a chondroitin sulfate proteoglycan-enriched pathway coincident with the neocortical subplate and distinct from the efferent path. *J Neurosci* **14**, 3500-3510 (1994).

290. A. L. Pearlman, A. M. Sheppard, Extracellular matrix in early cortical development. *Prog Brain Res* **108**, 117-134 (1996).

291. A. M. Sheppard, S. K. Hamilton, A. L. Pearlman, Changes in the distribution of extracellular matrix components accompany early morphogenetic events of mammalian cortical development. *J Neurosci* **11**, 3928-3942 (1991).

292. I. Kostović, I. Išasegi, Ž. Krsnik, Sublaminar organization of the human subplate: developmental changes in the distribution of neurons, glia, growing axons and extracellular matrix. *J Anat* **235**, 481-506 (2019).

293. I. Kostović, M. Judas, M. Rados, P. Hrabac, Laminar organization of the human fetal cerebrum revealed by histochemical markers and magnetic resonance imaging. *Cereb Cortex* **12**, 536-544 (2002).

294. I. Kostović *et al.*, Perinatal and early postnatal reorganization of the subplate and related cellular compartments in the human cerebral wall as revealed by histological and MRI approaches. *Brain Struct Funct* **219**, 231-253 (2014).

295. B. Miller, A. M. Sheppard, A. R. Bicknese, A. L. Pearlman, Chondroitin sulfate proteoglycans in the developing cerebral cortex: the distribution of neurocan distinguishes forming afferent and efferent axonal pathways. *J Comp Neurol* **355**, 615-628 (1995).

296. K. Mackarehtschian, C. K. Lau, I. Caras, S. K. McConnell, Regional differences in the developing cerebral cortex revealed by ephrin-A5 expression. *Cereb Cortex* **9**, 601-610 (1999).

297. N. Sestan, P. Rakic, M. J. Donoghue, Independent parcellation of the embryonic visual cortex and thalamus revealed by combinatorial Eph/ephrin gene expression. *Curr Biol* **11**, 39-43 (2001).

298. C. Auladell, P. Perez-Sust, H. Super, E. Soriano, The early development of thalamocortical and corticothalamic projections in the mouse. *Anat Embryol (Berl)* **201**, 169-179 (2000).

299. A. Agmon, L. T. Yang, D. K. O'Dowd, E. G. Jones, Organized growth of thalamocortical axons from the deep tier of terminations into layer IV of developing mouse barrel cortex. *J Neurosci* **13**, 5365-5382 (1993).

300. E. Grant, A. Hoerder-Suabedissen, Z. Molnár, Development of the corticothalamic projections. *Front Neurosci* **6**, 53 (2012).

301. A. Alzu'bi, J. Homman-Ludiye, J. A. Bourne, G. J. Clowry, Thalamocortical Afferents Innervate the Cortical Subplate much Earlier in Development in Primate than in Rodent. *Cereb Cortex* **29**, 1706-1718 (2019).

302. D. Z. Doyle *et al.*, Chromatin remodeler Arid1a regulates subplate neuron identity and wiring of cortical connectivity. *Proc Natl Acad Sci U S A* **118** (2021).

303. A. Ghosh, A. Antonini, S. K. McConnell, C. J. Shatz, Requirement for subplate neurons in the formation of thalamocortical connections. *Nature* **347**, 179-181 (1990).

304. A. Ghosh, C. J. Shatz, Involvement of subplate neurons in the formation of ocular dominance columns. *Science* **255**, 1441-1443 (1992).

305. A. Ghosh, C. J. Shatz, A role for subplate neurons in the patterning of connections from thalamus to neocortex. *Development* **117**, 1031-1047 (1993).

306. D. Magnani, K. Hasenpusch-Theil, T. Theil, Gli3 controls subplate formation and growth of cortical axons. *Cereb Cortex* **23**, 2542-2551 (2013).

307. P. O. Kanold, P. Kara, R. C. Reid, C. J. Shatz, Role of subplate neurons in functional maturation of visual cortical columns. *Science* **301**, 521-525 (2003).

308. P. O. Kanold, C. J. Shatz, Subplate neurons regulate maturation of cortical inhibition and outcome of ocular dominance plasticity. *Neuron* **51**, 627-638 (2006).

309. S. Akbarian *et al.*, Distorted distribution of nicotinamide-adenine dinucleotide phosphate-diaphorase neurons in temporal lobe of schizophrenics implies anomalous cortical development. *Arch Gen Psychiatry* **50**, 178-187 (1993).

310. S. Akbarian *et al.*, Maldistribution of interstitial neurons in prefrontal white matter of the brains of schizophrenic patients. *Arch Gen Psychiatry* **53**, 425-436 (1996).

311. M. Serati *et al.*, The Role of the Subplate in Schizophrenia and Autism: A Systematic Review. *Neuroscience* **408**, 58-67 (2019).

312. I. Kostović, M. Judaš, G. Sedmak, Developmental history of the subplate zone, subplate neurons and interstitial white matter neurons: relevance for schizophrenia. *Int J Dev Neurosci* **29**, 193-205 (2011).

313. A. Hoerder-Suabedissen *et al.*, Expression profiling of mouse subplate reveals a dynamic gene network and disease association with autism and schizophrenia. *Proc Natl Acad Sci U S A* **110**, 3555-3560 (2013).

314. S. L. Eastwood, P. J. Harrison, Interstitial white matter neuron density in the dorsolateral prefrontal cortex and parahippocampal gyrus in schizophrenia. *Schizophr Res* **79**, 181-188 (2005).

315. J. J. Hutsler, T. Love, H. Zhang, Histological and magnetic resonance imaging assessment of cortical layering and thickness in autism spectrum disorders. *Biol Psychiatry* **61**, 449-457 (2007).

316. O. Ranke, Beiträge zur Kenntnis der normalen und pathologischen Hirnrindenbildung. *Beiträge zur pathologischen Anatomie und zur allgemeinen Pathologie* **47**, 51-125 (1910).

317. S. Akbarian *et al.*, Altered distribution of nicotinamide-adenine dinucleotide phosphate-diaphorase cells in frontal lobe of schizophrenics implies disturbances of cortical development. *Arch Gen Psychiatry* **50**, 169-177 (1993).

318. S. De Rubeis *et al.*, Synaptic, transcriptional and chromatin genes disrupted in autism. *Nature* **515**, 209-215 (2014).

319. M. Gabriele, A. Lopez Tobon, G. D'Agostino, G. Testa, The chromatin basis of neurodevelopmental disorders: Rethinking dysfunction along the molecular and temporal axes. *Prog Neuropsychopharmacol Biol Psychiatry* **84**, 306-327 (2018).

320. S. Iwase, D. M. Martin, Chromatin in nervous system development and disease. *Mol Cell Neurosci* **87**, 1-3 (2018).

321. S. J. Sanders *et al.*, Insights into Autism Spectrum Disorder Genomic Architecture and Biology from 71 Risk Loci. *Neuron* **87**, 1215-1233 (2015).

322. C. R. Clapier, B. R. Cairns, The biology of chromatin remodeling complexes. *Annu Rev Biochem* **78**, 273-304 (2009).

323. S. Li *et al.*, Origin recognition complex harbors an intrinsic nucleosome remodeling activity. *Proc Natl Acad Sci U S A* **119**, e2211568119 (2022).

324. M. L. Loupart, S. A. Krause, M. S. Heck, Aberrant replication timing induces defective chromosome condensation in Drosophila ORC2 mutants. *Curr Biol* **10**, 1547-1556 (2000).

325. B. Li, M. Carey, J. L. Workman, The role of chromatin during transcription. *Cell* **128**, 707-719 (2007).

326. M. F. Arlt, A. C. Ozdemir, S. R. Birkeland, T. E. Wilson, T. W. Glover, Hydroxyurea induces de novo copy number variants in human cells. *Proc Natl Acad Sci U S A* **108**, 17360-17365 (2011).

327. M. F. Arlt, S. Rajendran, S. R. Birkeland, T. E. Wilson, T. W. Glover, De novo CNV formation in mouse embryonic stem cells occurs in the absence of Xrcc4-dependent nonhomologous end joining. *PLoS Genet* **8**, e1002981 (2012).

328. T. E. Wilson *et al.*, Large transcription units unify copy number variants and common fragile sites arising under replication stress. *Genome Res* **25**, 189-200 (2015).

329. A. Piazza, W. D. Heyer, Homologous Recombination and the Formation of Complex Genomic Rearrangements. *Trends Cell Biol* **29**, 135-149 (2019).

330. M. Papamichos-Chronakis, C. L. Peterson, The Ino80 chromatin-remodeling enzyme regulates replisome function and stability. *Nat Struct Mol Biol* **15**, 338-345 (2008).

331. J. A. Vincent, T. J. Kwong, T. Tsukiyama, ATP-dependent chromatin remodeling shapes the DNA replication landscape. *Nat Struct Mol Biol* **15**, 477-484 (2008).

332. J. S. Runge, J. R. Raab, T. Magnuson, Identification of Two Distinct Classes of the Human INO80 Complex Genome-Wide. *G3 (Bethesda)* **8**, 1095-1102 (2018).

333. G. J. Gowans *et al.*, INO80 Chromatin Remodeling Coordinates Metabolic Homeostasis with Cell Division. *Cell Rep* **22**, 611-623 (2018).

334. Y. Cai *et al.*, YY1 functions with INO80 to activate transcription. *Nat Struct Mol Biol* **14**, 872-874 (2007).

335. M. Papamichos-Chronakis, S. Watanabe, O. J. Rando, C. L. Peterson, Global regulation of H2A.Z localization by the INO80 chromatin-remodeling enzyme is essential for genome integrity. *Cell* **144**, 200-213 (2011).

336. X. Shen, G. Mizuguchi, A. Hamiche, C. Wu, A chromatin remodelling complex involved in transcription and DNA processing. *Nature* **406**, 541-544 (2000).

337. A. M. Alazami *et al.*, Accelerating novel candidate gene discovery in neurogenetic disorders via whole-exome sequencing of prescreened multiplex consanguineous families. *Cell Rep* **10**, 148-161 (2015).

338. L. R. Goodwin, D. J. Picketts, The role of ISWI chromatin remodeling complexes in brain development and neurodevelopmental disorders. *Mol Cell Neurosci* **87**, 55-64 (2018).

339. N. Collins *et al.*, An ACF1-ISWI chromatin-remodeling complex is required for DNA replication through heterochromatin. *Nat Genet* **32**, 627-632 (2002).

340. R. A. Poot *et al.*, The Williams syndrome transcription factor interacts with PCNA to target chromatin remodelling by ISWI to replication foci. *Nat Cell Biol* **6**, 1236-1244 (2004).

341. D. Li *et al.*, Pathogenic variants in SMARCA5, a chromatin remodeler, cause a range of syndromic neurodevelopmental features. *Sci Adv* **7** (2021).

342. A. Zaghlool *et al.*, A Role for the Chromatin-Remodeling Factor BAZ1A in Neurodevelopment. *Hum Mutat* **37**, 964-975 (2016).

343. M. S. Huh *et al.*, Stalled replication forks within heterochromatin require ATRX for protection. *Cell Death Dis* **7**, e2220 (2016).

344. L. Villard *et al.*, XNP mutation in a large family with Juberg-Marsidi syndrome. *Nat Genet* **12**, 359-360 (1996).

345. C. Kadoch, G. R. Crabtree, Mammalian SWI/SNF chromatin remodeling complexes and cancer: Mechanistic insights gained from human genomics. *Sci Adv* **1**, e1500447 (2015).

346. S. He *et al.*, Structure of nucleosome-bound human BAF complex. *Science* **367**, 875-881 (2020).

347. N. Mashtalir *et al.*, Modular Organization and Assembly of SWI/SNF Family Chromatin Remodeling Complexes. *Cell* **175**, 1272-1288.e1220 (2018).

348. Y. Tsurusaki *et al.*, Mutations affecting components of the SWI/SNF complex cause Coffin-Siris syndrome. *Nat Genet* **44**, 376-378 (2012).

349. T. Kosho, N. Miyake, J. C. Carey, Coffin-Siris syndrome and related disorders involving components of the BAF (mSWI/SNF) complex: historical review and recent advances using next generation sequencing. *Am J Med Genet C Semin Med Genet* **166c**, 241-251 (2014).

350. M. Koga *et al.*, Involvement of SMARCA2/BRM in the SWI/SNF chromatin-remodeling complex in schizophrenia. *Hum Mol Genet* **18**, 2483-2494 (2009).

351. S. Matsumoto *et al.*, Brg1 is required for murine neural stem cell maintenance and gliogenesis. *Dev Biol* **289**, 372-383 (2006).

352. J. Lessard *et al.*, An essential switch in subunit composition of a chromatin remodeling complex during neural development. *Neuron* **55**, 201-215 (2007).

353. F. Gao *et al.*, Heterozygous Mutations in SMARCA2 Reprogram the Enhancer Landscape by Global Retargeting of SMARCA4. *Mol Cell* **75**, 891-904.e897 (2019).

354. T. C. Tuoc *et al.*, Chromatin regulation by BAF170 controls cerebral cortical size and thickness. *Dev Cell* **25**, 256-269 (2013).

355. T. C. Tuoc, R. Narayanan, A. Stoykova, BAF chromatin remodeling complex: cortical size regulation and beyond. *Cell Cycle* **12**, 2953-2959 (2013).

356. R. Narayanan *et al.*, Chromatin Remodeling BAF155 Subunit Regulates the Genesis of Basal Progenitors in Developing Cortex. *iScience* **4**, 109-126 (2018).

357. R. Narayanan *et al.*, Loss of BAF (mSWI/SNF) Complexes Causes Global Transcriptional and Chromatin State Changes in Forebrain Development. *Cell Rep* **13**, 1842-1854 (2015).

358. G. Sokpor *et al.*, Loss of BAF Complex in Developing Cortex Perturbs Radial Neuronal Migration in a WNT Signaling-Dependent Manner. *Front Mol Neurosci* **14**, 687581 (2021).

359. B. T. Staahl, G. R. Crabtree, Creating a neural specific chromatin landscape by npBAF and nBAF complexes. *Curr Opin Neurobiol* **23**, 903-913 (2013).

360. S. M. Braun *et al.*, The npBAF to nBAF Chromatin Switch Regulates Cell Cycle Exit in the Developing Mammalian Cortex. *bioRxiv*, 2020.2001.2017.910794 (2020).

361. S. M. G. Braun *et al.*, BAF subunit switching regulates chromatin accessibility to control cell cycle exit in the developing mammalian cortex. *Genes Dev* **35**, 335-353 (2021).

362. B. T. Staahl *et al.*, Kinetic analysis of npBAF to nBAF switching reveals exchange of SS18 with CREST and integration with neural developmental pathways. *J Neurosci* **33**, 10348-10361 (2013).

363. J. I. Wu *et al.*, Regulation of dendritic development by neuron-specific chromatin remodeling complexes. *Neuron* **56**, 94-108 (2007).

364. A. Vogel-Ciernia *et al.*, The neuron-specific chromatin regulatory subunit BAF53b is necessary for synaptic plasticity and memory. *Nat Neurosci* **16**, 552-561 (2013).

365. C. Wiegreffe *et al.*, Bcl11a (Ctip1) Controls Migration of Cortical Projection Neurons through Regulation of Sema3c. *Neuron* **87**, 311-325 (2015).

366. L. C. Greig, M. B. Woodworth, C. Greppi, J. D. Macklis, Ctip1 Controls Acquisition of Sensory Area Identity and Establishment of Sensory Input Fields in the Developing Neocortex. *Neuron* **90**, 261-277 (2016).

367. M. B. Woodworth *et al.*, Ctip1 Regulates the Balance between Specification of Distinct Projection Neuron Subtypes in Deep Cortical Layers. *Cell Rep* **15**, 999-1012 (2016).

368. H. Du *et al.*, Transcription factors Bcl11a and Bcl11b are required for the production and differentiation of cortical projection neurons. *Cereb Cortex* **32**, 3611-3632 (2022).

369. C. Hodges, J. G. Kirkland, G. R. Crabtree, The Many Roles of BAF (mSWI/SNF) and PBAF Complexes in Cancer. *Cold Spring Harb Perspect Med* **6** (2016).

370. X. Wang *et al.*, Two related ARID family proteins are alternative subunits of human SWI/SNF complexes. *Biochem J* **383**, 319-325 (2004).

371. P. B. Dallas *et al.*, The human SWI-SNF complex protein p270 is an ARID family member with non-sequence-specific DNA binding activity. *Mol Cell Biol* **20**, 3137-3146 (2000).

372. A. Patsialou, D. Wilsker, E. Moran, DNA-binding properties of ARID family proteins. *Nucleic Acids Res* **33**, 66-80 (2005).

373. G. W. Santen *et al.*, Mutations in SWI/SNF chromatin remodeling complex gene ARID1B cause Coffin-Siris syndrome. *Nat Genet* **44**, 379-380 (2012).

374. E. M. Jung *et al.*, Arid1b haploinsufficiency disrupts cortical interneuron development and mouse behavior. *Nat Neurosci* **20**, 1694-1707 (2017).

375. J. J. Moffat *et al.*, Differential roles of ARID1B in excitatory and inhibitory neural progenitors in the developing cortex. *Sci Rep* **11**, 3856 (2021).

376. C. Martins-Costa *et al.*, ARID1B controls transcriptional programs of axon projection in the human corpus callosum. *bioRxiv*, 2023.2005.2004.539362 (2023).

377. C. Celen *et al.*, Arid1b haploinsufficient mice reveal neuropsychiatric phenotypes and reversible causes of growth impairment. *Elife* **6** (2017).

378. M. Shibutani *et al.*, Arid1b Haploinsufficiency Causes Abnormal Brain Gene Expression and Autism-Related Behaviors in Mice. *Int J Mol Sci* **18** (2017).

379. M. Ka, D. A. Chopra, S. M. Dravid, W. Y. Kim, Essential Roles for ARID1B in Dendritic Arborization and Spine Morphology of Developing Pyramidal Neurons. *J Neurosci* **36**, 2723-2742 (2016).

380. N. C. Bramswig *et al.*, Heterozygosity for ARID2 loss-of-function mutations in individuals with a Coffin-Siris syndrome-like phenotype. *Hum Genet* **136**, 297-305 (2017).

381. L. He *et al.*, BAF200 is required for heart morphogenesis and coronary artery development. *PLoS One* **9**, e109493 (2014).

382. C. Kadoch *et al.*, Proteomic and bioinformatic analysis of mammalian SWI/SNF complexes identifies extensive roles in human malignancy. *Nat Genet* **45**, 592-601 (2013).

383. S. Jones *et al.*, Frequent mutations of chromatin remodeling gene ARID1A in ovarian clear cell carcinoma. *Science* **330**, 228-231 (2010).

384. R. L. Chandler *et al.*, Coexistent ARID1A-PIK3CA mutations promote ovarian clear-cell tumorigenesis through pro-tumorigenic inflammatory cytokine signalling. *Nat Commun* **6**, 6118 (2015).

385. X. Gao *et al.*, ES cell pluripotency and germ-layer formation require the SWI/SNF chromatin remodeling component BAF250a. *Proc Natl Acad Sci U S A* **105**, 6656-6661 (2008).

386. R. L. Chandler, T. Magnuson, The SWI/SNF BAF-A complex is essential for neural crest development. *Dev Biol* **411**, 15-24 (2016).

387. M. Trizzino *et al.*, The Tumor Suppressor ARID1A Controls Global Transcription via Pausing of RNA Polymerase II. *Cell Rep* **23**, 3933-3945 (2018).

388. T. W. R. Kelso *et al.*, Chromatin accessibility underlies synthetic lethality of SWI/SNF subunits in ARID1A-mutant cancers. *Elife* **6** (2017).

389. K. C. Helming *et al.*, ARID1B is a specific vulnerability in ARID1A-mutant cancers. *Nat Med* **20**, 251-254 (2014).

390. L. Pagliaroli *et al.*, Inability to switch from ARID1A-BAF to ARID1B-BAF impairs exit from pluripotency and commitment towards neural crest formation in ARID1B-related neurodevelopmental disorders. *Nat Commun* **12**, 6469 (2021).

391. B. H. Alver *et al.*, The SWI/SNF chromatin remodelling complex is required for maintenance of lineage specific enhancers. *Nat Commun* **8**, 14648 (2017).

392. R. Mathur *et al.*, ARID1A loss impairs enhancer-mediated gene regulation and drives colon cancer in mice. *Nat Genet* **49**, 296-302 (2017).

393. R. Lakshminarasimhan *et al.*, Down-regulation of ARID1A is sufficient to initiate neoplastic transformation along with epigenetic reprogramming in non-tumorigenic endometriotic cells. *Cancer Lett* **401**, 11-19 (2017).

394. C. N. Vallianatos *et al.*, Mutually suppressive roles of KMT2A and KDM5C in behaviour, neuronal structure, and histone H3K4 methylation. *Commun Biol* **3**, 278 (2020).

395. T. Kosho, N. Okamoto, Genotype-phenotype correlation of Coffin-Siris syndrome caused by mutations in SMARCB1, SMARCA4, SMARCE1, and ARID1A. *Am J Med Genet C Semin Med Genet* **166c**, 262-275 (2014).

396. M. Lek *et al.*, Analysis of protein-coding genetic variation in 60,706 humans. *Nature* **536**, 285-291 (2016).

397. J. A. Gorski *et al.*, Cortical excitatory neurons and glia, but not GABAergic neurons, are produced in the Emx1-expressing lineage. *J Neurosci* **22**, 6309-6314 (2002).

398. M. D. Muzumdar, B. Tasic, K. Miyamichi, L. Li, L. Luo, A global double-fluorescent Cre reporter mouse. *Genesis* **45**, 593-605 (2007).

399. I. Kostović, M. Judas, The development of the subplate and thalamocortical connections in the human foetal brain. *Acta Paediatr* **99**, 1119-1127 (2010).

400. S. Goebbels *et al.*, Genetic targeting of principal neurons in neocortex and hippocampus of NEX-Cre mice. *Genesis* **44**, 611-621 (2006).

401. L. Madisen *et al.*, A robust and high-throughput Cre reporting and characterization system for the whole mouse brain. *Nat Neurosci* **13**, 133-140 (2010).

402. S. K. Zaidi *et al.*, "Mitotic bookmarking of genes: a novel dimension to epigenetic control" in Nat Rev Genet. (England, 2010), vol. 11, pp. 583-589.

403. S. Kadam *et al.*, Functional selectivity of recombinant mammalian SWI/SNF subunits. *Genes Dev* **14**, 2441-2451 (2000).

404. Z. Zhu *et al.*, Mitotic bookmarking by SWI/SNF subunits. *Nature* (2023).

405. T. Lu *et al.*, Gene regulation and DNA damage in the ageing human brain. *Nature* **429**, 883-891 (2004).

406. R. Madabhushi *et al.*, Activity-Induced DNA Breaks Govern the Expression of Neuronal Early-Response Genes. *Cell* **161**, 1592-1605 (2015).

407. R. Watanabe *et al.*, SWI/SNF factors required for cellular resistance to DNA damage include ARID1A and ARID1B and show interdependent protein stability. *Cancer Res* **74**, 2465-2475 (2014).

408. K. L. Allendoerfer, C. J. Shatz, The subplate, a transient neocortical structure: its role in the development of connections between thalamus and cortex. *Annu Rev Neurosci* **17**, 185-218 (1994).

409. S. McConnell, A. Ghosh, C. Shatz, Subplate neurons pioneer the first axon pathway from the cerebral cortex. *Science* **245**, 978-982 (1989).

410. A. Hoerder-Suabedissen, Z. Molnár, Development, evolution and pathology of neocortical subplate neurons. *Nat Rev Neurosci* **16**, 133-146 (2015).

411. W. Z. Wang *et al.*, Subplate in the developing cortex of mouse and human. *J Anat* **217**, 368-380 (2010).

412. Z. Molnár, H. J. Luhmann, P. O. Kanold, Transient cortical circuits match spontaneous and sensory-driven activity during development. *Science* **370** (2020).

413. I. Kostović, The enigmatic fetal subplate compartment forms an early tangential cortical nexus and provides the framework for construction of cortical connectivity. *Prog Neurobiol* **194**, 101883 (2020).

414. Z. Molnár *et al.*, New insights into the development of the human cerebral cortex. *J Anat* **235**, 432-451 (2019).

415. P. O. Kanold, H. J. Luhmann, The subplate and early cortical circuits. *Annu Rev Neurosci* **33**, 23-48 (2010).

416. J. M. Wess, A. Isaiah, P. V. Watkins, P. O. Kanold, Subplate neurons are the first cortical neurons to respond to sensory stimuli. *Proc Natl Acad Sci U S A* **114**, 12602-12607 (2017).

417. C. Blakemore, Z. Molnár, Factors involved in the establishment of specific interconnections between thalamus and cerebral cortex. *Cold Spring Harb Symp Quant Biol* **55**, 491-504 (1990).

418. Z. Molnár, C. Blakemore, How do thalamic axons find their way to the cortex? *Trends Neurosci* **18**, 389-397 (1995).

419. Y. Chen, D. Magnani, T. Theil, T. Pratt, D. J. Price, Evidence that descending cortical axons are essential for thalamocortical axons to cross the pallial-subpallial boundary in the embryonic forebrain. *PLoS One* **7**, e33105 (2012).

420. F. M. Oeschger *et al.*, Gene expression analysis of the embryonic subplate. *Cereb Cortex* **22**, 1343-1359 (2012).

421. Y. Arai *et al.*, Evolutionary Gain of Dbx1 Expression Drives Subplate Identity in the Cerebral Cortex. *Cell Rep* **29**, 645-658.e645 (2019).

422. A. Routh, S. R. Head, P. Ordoukhanian, J. E. Johnson, ClickSeq: Fragmentation-Free Next-Generation Sequencing via Click Ligation of Adaptors to Stochastically Terminated 3'-Azido cDNAs. *J Mol Biol* **427**, 2610-2616 (2015).

423. M. D. Robinson, D. J. McCarthy, G. K. Smyth, edgeR: a Bioconductor package for differential expression analysis of digital gene expression data. *Bioinformatics* **26**, 139-140 (2010).

424. Y. Liu *et al.*, Myosin Vb controls biogenesis of post-Golgi Rab10 carriers during axon development. *Nat Commun* **4**, 2005 (2013).

425. A. E. Ayoub *et al.*, Transcriptional programs in transient embryonic zones of the cerebral cortex defined by high-resolution mRNA sequencing. *Proc Natl Acad Sci U S A* **108**, 14950-14955 (2011).

426. S. A. Yuzwa *et al.*, Developmental Emergence of Adult Neural Stem Cells as Revealed by Single-Cell Transcriptional Profiling. *Cell Rep* **21**, 3970-3986 (2017).

427. L. Loo *et al.*, Single-cell transcriptomic analysis of mouse neocortical development. *Nat Commun* **10**, 134 (2019).

428. S. M. Sunkin *et al.*, Allen Brain Atlas: an integrated spatio-temporal portal for exploring the central nervous system. *Nucleic Acids Res* **41**, D996-d1008 (2013).

429. M. V. Kuleshov *et al.*, Enrichr: a comprehensive gene set enrichment analysis web server 2016 update. *Nucleic Acids Res* **44**, W90-97 (2016).

430. A. Visel, C. Thaller, G. Eichele, GenePaint.org: an atlas of gene expression patterns in the mouse embryo. *Nucleic Acids Res* **32**, D552-556 (2004).

431. S. Gong *et al.*, A gene expression atlas of the central nervous system based on bacterial artificial chromosomes. *Nature* **425**, 917-925 (2003).

432. B. J. Molyneaux *et al.*, DeCoN: genome-wide analysis of in vivo transcriptional dynamics during pyramidal neuron fate selection in neocortex. *Neuron* **85**, 275-288 (2015).

433. F. M. Oeschger *et al.*, Gene expression analysis of the embryonic subplate. *Cereb Cortex* **22**, 1343-1359 (2012).

434. J. J. Chun, C. J. Shatz, The earliest-generated neurons of the cat cerebral cortex: characterization by MAP2 and neurotransmitter immunohistochemistry during fetal life. *J Neurosci* **9**, 1648-1667 (1989).

435. H. J. Luhmann, S. Kirischuk, W. Kilb, The Superior Function of the Subplate in Early Neocortical Development. *Front Neuroanat* **12**, 97 (2018).

436. Z. Molnár, S. Garel, G. López-Bendito, P. Maness, D. J. Price, Mechanisms controlling the guidance of thalamocortical axons through the embryonic forebrain. *Eur J Neurosci* **35**, 1573-1585 (2012).

437. Z. Molnár, C. Blakemore, Lack of regional specificity for connections formed between thalamus and cortex in coculture. *Nature* **351**, 475-477 (1991).

438. E. Jacobs *et al.*, Visualization of corticofugal projections during early cortical development in a tau-GFP-transgenic mouse. *Eur J Neurosci* **25**, 17-30 (2007).

439. M. C. Piñon, A. Jethwa, E. Jacobs, A. Campagnoni, Z. Molnár, Dynamic integration of subplate neurons into the cortical barrel field circuitry during postnatal development in the Golli-tau-eGFP (GTE) mouse. *J Physiol* **587**, 1903-1915 (2009).

440. M. Judas, N. J. Milosević, M. R. Rasin, M. Heffer-Lauc, I. Kostović, Complex patterns and simple architects: molecular guidance cues for developing axonal pathways in the telencephalon. *Prog Mol Subcell Biol* **32**, 1-32 (2003).

441. P. Malatesta *et al.*, Neuronal or glial progeny: regional differences in radial glia fate. *Neuron* **37**, 751-764 (2003).

442. A. Hoerder-Suabedissen, Z. Molnar, Development, evolution and pathology of neocortical subplate neurons. *Nat Rev Neurosci* **16**, 133-146 (2015).

443. L. Ratie *et al.*, Loss of Dmrt5 Affects the Formation of the Subplate and Early Corticogenesis. *Cereb Cortex* (2019).

444. S. Garel, J. L. Rubenstein, Intermediate targets in formation of topographic projections: inputs from the thalamocortical system. *Trends Neurosci* **27**, 533-539 (2004).

445. Z. Molnar, S. Garel, G. Lopez-Bendito, P. Maness, D. J. Price, Mechanisms controlling the guidance of thalamocortical axons through the embryonic forebrain. *Eur J Neurosci* **35**, 1573-1585 (2012).

446. I. Kostovic, P. Rakic, Developmental history of the transient subplate zone in the visual and somatosensory cortex of the macaque monkey and human brain. *J Comp Neurol* **297**, 441-470 (1990).

447. I. Kostovic, M. Judas, The development of the subplate and thalamocortical connections in the human foetal brain. *Acta Paediatr* **99**, 1119-1127 (2010).

448. C. S. Barros, S. J. Franco, U. Muller, Extracellular matrix: functions in the nervous system. *Cold Spring Harb Perspect Biol* **3**, a005108 (2011).

449. P. C. Letourneau, M. L. Condic, D. M. Snow, Interactions of developing neurons with the extracellular matrix. *J Neurosci* **14**, 915-928 (1994).

450. M. Inatani, F. Irie, A. S. Plump, M. Tessier-Lavigne, Y. Yamaguchi, Mammalian brain morphogenesis and midline axon guidance require heparan sulfate. *Science* **302**, 1044-1046 (2003).

451. M. Tessier-Lavigne, M. Placzek, A. G. Lumsden, J. Dodd, T. M. Jessell, Chemotropic guidance of developing axons in the mammalian central nervous system. *Nature* **336**, 775-778 (1988).

452. C. Benadiba *et al.*, The ciliogenic transcription factor RFX3 regulates early midline distribution of guidepost neurons required for corpus callosum development. *PLoS Genet* **8**, e1002606 (2012).

453. S. Timpano, D. J. Picketts, Neurodevelopmental Disorders Caused by Defective Chromatin Remodeling: Phenotypic Complexity Is Highlighted by a Review of ATRX Function. *Front Genet* **11**, 885 (2020).

454. J. L. Ronan, W. Wu, G. R. Crabtree, From neural development to cognition: unexpected roles for chromatin. *Nat Rev Genet* **14**, 347-359 (2013).

455. A. Dobin *et al.*, STAR: ultrafast universal RNA-seq aligner. *Bioinformatics* **29**, 15-21 (2013).

456. T. Smith, A. Heger, I. Sudbery, UMI-tools: modeling sequencing errors in Unique Molecular Identifiers to improve quantification accuracy. *Genome Res* **27**, 491-499 (2017).

457. S. Anders, P. T. Pyl, W. Huber, HTSeq-a Python framework to work with high-throughput sequencing data. *Bioinformatics* **31**, 166-169 (2015).

458. F. Pedregosa *et al.*, Scikit-learn: Machine learning in Python. *the Journal of machine Learning research* **12**, 2825-2830 (2011).

459. F. Wagner, Y. Yan, I. Yanai, K-nearest neighbor smoothing for high-throughput single-cell RNA-Seq data. *bioRxiv*, 217737 (2018).

460. C. R. Harris *et al.*, Array programming with NumPy. *Nature* **585**, 357-362 (2020).

461. M. Waskom, t. seaborn development team (2020) mwaskom/seaborn. (Zenodo).

462. O. M. Subach, P. J. Cranfill, M. W. Davidson, V. V. Verkhusha, An enhanced monomeric blue fluorescent protein with the high chemical stability of the chromophore. *PLoS One* **6**, e28674 (2011).

463. T. Matsuda, C. L. Cepko, Electroporation and RNA interference in the rodent retina in vivo and in vitro. *Proc Natl Acad Sci U S A* **101**, 16-22 (2004).

464. L. Zhuo *et al.*, hGFAP-cre transgenic mice for manipulation of glial and neuronal function in vivo. *Genesis* **31**, 85-94 (2001).

465. A. Slavotinek *et al.*, Prenatal presentation of multiple anomalies associated with haploinsufficiency for ARID1A. *Eur J Med Genet* **65**, 104407 (2022).

466. Z. Kozmik *et al.*, Characterization of mammalian orthologues of the Drosophila osa gene: cDNA cloning, expression, chromosomal localization, and direct physical interaction with Brahma chromatin-remodeling complex. *Genomics* **73**, 140-148 (2001).

467. A. Flores-Alcantar, A. Gonzalez-Sandoval, D. Escalante-Alcalde, H. Lomeli, Dynamics of expression of ARID1A and ARID1B subunits in mouse embryos and in cells during the cell cycle. *Cell Tissue Res* **345**, 137-148 (2011).

468. B. Guan, M. Gao, C. H. Wu, T. L. Wang, M. Shih Ie, Functional analysis of in-frame indel ARID1A mutations reveals new regulatory mechanisms of its tumor suppressor functions. *Neoplasia* **14**, 986-993 (2012).

469. E. C. Dykhuizen *et al.*, BAF complexes facilitate decatenation of DNA by topoisomerase IIα. *Nature* **497**, 624-627 (2013).

470. Y. L. Lyu, J. C. Wang, Aberrant lamination in the cerebral cortex of mouse embryos lacking DNA topoisomerase IIbeta. *Proc Natl Acad Sci U S A* **100**, 7123-7128 (2003).

471. L. R. Fenlon, R. Suarez, Z. Lynton, L. J. Richards, The evolution, formation and connectivity of the anterior commissure. *Semin Cell Dev Biol* **118**, 50-59 (2021).

472. P. Marcos-Mondejar *et al.*, The Ihx2 transcription factor controls thalamocortical axonal guidance by specific regulation of robo1 and robo2 receptors. *J Neurosci* **32**, 4372-4385 (2012).

473. S. Pal *et al.*, An Early Cortical Progenitor-Specific Mechanism Regulates Thalamocortical Innervation. *J Neurosci* **41**, 6822-6835 (2021).

474. C. Godfraind, M. Schachner, A. M. Goffinet, Immunohistological localization of cell adhesion molecules L1, J1, N-CAM and their common carbohydrate L2 in the embryonic cortex of normal and reeler mice. *Brain Res* **470**, 99-111 (1988).

475. S. Yoshinaga *et al.*, Comprehensive characterization of migration profiles of murine cerebral cortical neurons during development using FlashTag labeling. *iScience* **24**, 102277 (2021).

476. S. Rana *et al.*, The Subplate: A Potential Driver of Cortical Folding? *Cereb Cortex* **29**, 4697-4708 (2019).

477. K. E. Rhodes, J. W. Fawcett, Chondroitin sulphate proteoglycans: preventing plasticity or protecting the CNS? *J Anat* **204**, 33-48 (2004).

478. P. S. Goldman-Rakic, Neuronal development and plasticity of association cortex in primates. *Neurosci Res Program Bull* **20**, 520-532 (1982).

479. P. Rakic, Prenatal development of the visual system in rhesus monkey. *Philos Trans R Soc Lond B Biol Sci* **278**, 245-260 (1977).

480. S. Higashi, K. Hioki, T. Kurotani, N. Kasim, Z. Molnár, Functional thalamocortical synapse reorganization from subplate to layer IV during postnatal development in the reeler-like mutant rat (shaking rat Kawasaki). *J Neurosci* **25**, 1395-1406 (2005).

481. J. J. Chun, C. J. Shatz, Redistribution of synaptic vesicle antigens is correlated with the disappearance of a transient synaptic zone in the developing cerebral cortex. *Neuron* **1**, 297-310 (1988).

482. S. M. Catalano, C. J. Shatz, Activity-dependent cortical target selection by thalamic axons. *Science* **281**, 559-562 (1998).

483. E. Matsunaga, S. Nambu, M. Oka, A. Iriki, Complex and dynamic expression of cadherins in the embryonic marmoset cerebral cortex. *Dev Growth Differ* **57**, 474-483 (2015).

484. I. Martinez-Garay, Molecular Mechanisms of Cadherin Function During Cortical Migration. *Front Cell Dev Biol* **8**, 588152 (2020).

485. K. Oishi *et al.*, Identity of neocortical layer 4 neurons is specified through correct positioning into the cortex. *Elife* **5** (2016).

486. G. Ying *et al.*, The protocadherin gene Celsr3 is required for interneuron migration in the mouse forebrain. *Mol Cell Biol* **29**, 3045-3061 (2009).

487. J. Z. Tsien *et al.*, Subregion- and cell type-restricted gene knockout in mouse brain. *Cell* **87**, 1317-1326 (1996).

488. S. Gong *et al.*, Targeting Cre recombinase to specific neuron populations with bacterial artificial chromosome constructs. *J Neurosci* **27**, 9817-9823 (2007).

489. J. A. Harris *et al.*, Anatomical characterization of Cre driver mice for neural circuit mapping and manipulation. *Front Neural Circuits* **8**, 76 (2014).

490. C. R. Gerfen, R. Paletzki, N. Heintz, GENSAT BAC cre-recombinase driver lines to study the functional organization of cerebral cortical and basal ganglia circuits. *Neuron* **80** (2013).

491. A. Hoerder-Suabedissen *et al.*, Subset of Cortical Layer 6b Neurons Selectively Innervates Higher Order Thalamic Nuclei in Mice. *Cereb Cortex* **28**, 1882-1897 (2018).

492. N. Kessaris *et al.*, Competing waves of oligodendrocytes in the forebrain and postnatal elimination of an embryonic lineage. *Nat Neurosci* **9**, 173-179 (2006).

493. C. H. Chan *et al.*, Emx1 is a marker for pyramidal neurons of the cerebral cortex. *Cereb Cortex* **11**, 1191-1198 (2001).

494. J. J. Reske *et al.*, Co-existing TP53 and ARID1A mutations promote aggressive endometrial tumorigenesis. *PLoS Genet* **17**, e1009986 (2021).

495. R. R. Zhao *et al.*, Lentiviral vectors express chondroitinase ABC in cortical projections and promote sprouting of injured corticospinal axons. *J Neurosci Methods* **201**, 228-238 (2011).

496. P. Day *et al.*, Targeting chondroitinase ABC to axons enhances the ability of chondroitinase to promote neurite outgrowth and sprouting. *PLoS One* **15**, e0221851 (2020).

497. N. Kaneko *et al.*, ADAMTS2 regulates radial neuronal migration by activating TGF-β signaling at the subplate layer of the developing neocortex. *bioRxiv*, 2022.2008.2007.502954 (2022).